Adaptive tensor product wavelet methods for solving PDEs

Tammo Jan Dijkema

Adaptive tensor product wavelet methods for solving PDEs

The rectangles on the cover of this thesis illustrate the support of the 2221 wavelets that are used in the 26th iteration of the algorithm in Chapter 5 for solving the two-dimensional Poisson problem

$$
\begin{aligned}
\boldsymbol{\Delta} u &= 1 \quad \textit{on } (0,1) \times (0,1), \\
u &= 0 \quad \textit{on } (1,y),\ (x,1), \\
\tfrac{\partial u}{\partial x} &= 0 \quad \textit{on } (0,y), \\
\tfrac{\partial u}{\partial y} &= 0 \quad \textit{on } (x,0).
\end{aligned}
$$

2000 Mathematics Subject Classification: 35J05, 35J20, 41A25, 41A63, 65T60

ISBN 978-90-39350942

Adaptive tensor product wavelet methods for solving PDEs

Adaptieve tensorproductwaveletmethoden
voor het oplossen van
partiële differentiaalvergelijkingen

(met een samenvatting in het Nederlands)

Proefschrift

ter verkrijging van de graad van doctor aan de
Universiteit Utrecht op gezag van de rector magnificus,
prof. dr. J. C. Stoof, ingevolge het besluit van het college
voor promoties in het openbaar te verdedigen op
29 juni 2009 des middags te 2:30 uur door

Tammo Jan Dijkema

geboren op 4 januari 1981
te Oosterhesselen

Promotoren: Prof. dr. R. P. Stevenson
Prof. dr. H. A. van der Vorst

Dit proefschrift werd mede mogelijk gemaakt door financiële steun van NWO.

Contents

Chapter 1
Introduction

This thesis deals with the adaptive solution of partial differential equations in high space dimensions by means of tensor product wavelet methods. We will show that these methods converge with the best possible rate. Because of the tensor product construction, this rate is independent of the space dimension, while the computational cost scales linearly with the number of unknowns.

Well-posed linear operator equations

We will consider methods for solving, for an unknown $u \in H$, well-posed linear operator equations of the form

$$Au = f, \tag{1.1}$$

where H is a separable Hilbert space (over $\mathbb{R}$), $A\colon H \to H'$ is a boundedly invertible linear operator, and $f \in H'$ is given. With the bilinear form a on $H \times H$ defined by $a(u,v) = (Au)(v)$, an equivalent formulation reads as

$$a(u,v) = f(v), \quad \text{for all } v \in H. \tag{1.2}$$

We consider a to be symmetric and elliptic, although the methods we discuss can be generalized to situations where these conditions are violated.

Non-adaptive methods

A standard *non-adaptive* numerical method for solving (1.2) consists of selecting V_i from some a priori *given* sequence $V_0 \subset V_1 \subset \cdots \subset H$, and computing the *Galerkin solution* $u_i \in V_i$, which is defined as the solution of

$$a(u_i, v_i) = f(v_i), \quad \text{for all } v_i \in V_i.$$

Examples of such spaces V_i are finite element spaces with respect to an i times uniformly dyadically refined initial mesh, or when using wavelets, spans of all wavelets with levels up to i. In the model case of H being the Sobolev space $H^m(\Omega)$, relevant for elliptic boundary value problems of order $2m$ on a domain $\Omega \subset \mathbb{R}^n$, it is well-known that

$$\|u - u_i\|_{H^m(\Omega)} < C N_i^{-\frac{d-m}{n}} \|u\|_{H^d(\Omega)}, \tag{1.3}$$

where $N_i \coloneqq \dim V_i$, d is the order of the finite elements or wavelets, and C is some constant that does not depend on i. On an n-dimensional domain Ω and with a method of order d, a convergence rate $\frac{d-m}{n}$ in $H^m(\Omega)$ is the best that generally can be expected. The fact that this rate decreases with n, in particular that it is inversely proportional to n, is known as the *curse of dimensionality*.

The estimate (1.3) applies only when $u \in H^d(\Omega)$, a condition that is usually violated because of singularities in u caused by the shape of the boundary. In that case, the best possible rate can be retrieved by a proper refinement of the mesh or the wavelet index set towards the boundary, which, except in some model cases, is very hard to determine a priori. An automatic generation of suitable refinements is possible by the application of an *adaptive* method.

Adaptive wavelet-Galerkin method

Assume that we have available a Riesz basis or stable basis $\Psi = \{\psi_\lambda \colon \lambda \in \nabla\}$ for H, which means that there are constants $0 < C_1 \leq C_2 < \infty$ such that

$$C_1 \|\mathbf{c}\|^2_{\ell_2(\nabla)} \leq \|\sum_{\lambda\in\nabla} c_\lambda \psi_\lambda\|^2_H \leq C_2 \|\mathbf{c}\|^2_{\ell_2(\nabla)} \quad \text{for all } \mathbf{c} \coloneqq \{c_\lambda\}_{\lambda\in\nabla} \in \ell_2. \tag{1.4}$$

With such a basis, the problem (1.1) can be transformed into a bi-infinite matrix-vector problem involving the coefficients $\mathbf{u} = (\mathbf{u}_\lambda)_{\lambda\in\nabla}$ of the expansion $u = \mathbf{u}^\mathsf{T}\Psi \coloneqq \sum_{\lambda\in\nabla} \mathbf{u}_\lambda \psi_\lambda$ with respect to Ψ. Indeed, defining the bi-infinite stiffness matrix $\mathbf{A}$ by $\mathbf{A}_{\lambda,\mu} \coloneqq a(\psi_\mu, \psi_\lambda)$ and the right-hand side vector $\mathbf{f}$ by $\mathbf{f}_\lambda \coloneqq f(\psi_\lambda)$, the problem is equivalent to finding $\mathbf{u} \in \ell_2(\nabla)$ such that

$$\mathbf{A}\mathbf{u} = \mathbf{f}.$$

Given some finite index set $\Lambda_i \subset \nabla$, the Galerkin solution u_i from $\operatorname{span}\{\psi_\lambda \colon \lambda \in \Lambda_i\}$ can be written as $u_i = \mathbf{u}_i^\mathsf{T}\Psi$, where $\mathbf{u}_i$ is the solution of the finite-dimensional matrix–vector equation

$$\mathbf{A}|_{\Lambda_i\times\Lambda_i}\, \mathbf{u}_i = \mathbf{f}|_{\Lambda_i}.$$

The residual $\mathbf{r}_i \coloneqq \mathbf{A}\mathbf{u}_i - \mathbf{f}$ has its support outside Λ_i and can be used as an *a posteriori error estimator* known from finite element methods. As proposed in [CDD01], this estimator can be used to steer an adaptive method: Fixing some $\theta \in (0,1)$, the set Λ_i is expanded to a set Λ_{i+1} by collecting the locations of the largest entries (in modulus) of $\mathbf{r}_i$ until $\|\mathbf{r}_i|_{\Lambda_{i+1}}\| \geq \theta\|\mathbf{r}_i\|$. The resulting sequence $\mathbf{u}_0, \mathbf{u}_1, \ldots$ can now be shown to converge to $\mathbf{u}$. Moreover, as shown in [GHS07], if θ is selected to be sufficiently small, depending on the condition number of $\mathbf{A}$, then the convergence rate is equal to that of the sequence of *best N-term approximations* $(\mathbf{u}_N)_N$, where $\mathbf{u}_N$ is the vector that coincides with $\mathbf{u}$ on those N locations where the latter has its largest coefficients and is zero elsewhere. These best N-term approximations converge to $\mathbf{u}$ with the best possible rate – being equal to $\frac{d-m}{n}$ in the model case – under much milder conditions than the sequence of Galerkin approximations corresponding to the non-adaptive standard choice of $(\Lambda_i)_i$.

The algorithm outlined above cannot be executed in practice. Indeed, generally any column of $\mathbf{A}$ has infinitely many non-zeros (however, cf. Chapter 6), and

so has the vector $\mathbf{f}$. Thanks to the wavelets being smooth and having vanishing moments, the matrix $\mathbf{A}$ is, however, close to being sparse. It can be shown that by a suitable choice of the wavelets, $\mathbf{A}$ is sufficiently close to a sparse matrix that a scheme with inexact evaluations of the residuals and inexact solutions of the arising Galerkin systems converge with the same rate as the exact scheme. The computational cost now scales linearly with the support lengths of the iterands.

Isotropic vs. anisotropic wavelets

The construction of biorthogonal isotropic or multiresolution wavelets on $\Omega \subset \mathbb{R}^n$ starts with two nested sequences, called multiresolution analyses,

$$V_0 \subset V_1 \subset \cdots \subset L_2(\Omega),$$
$$\tilde{V}_0 \subset \tilde{V}_1 \subset \cdots \subset L_2(\Omega),$$

that have approximations orders d and $\tilde{d}$, respectively, are contained in the Sobolev spaces $H^s(\Omega)$ for any $s < \gamma$ or $s < \tilde{\gamma}$, respectively, and are such that the biorthogonal projector $Q_j \colon L_2(\Omega) \to L_2(\Omega)$ defined by $\operatorname{Im} Q_j = V_j$ and $\operatorname{Im}(I - Q_j) = \tilde{V}_j^\perp$ is bounded uniformly in j. When V_j and $\operatorname{Im}(Q_{j+1} - Q_j) = V_{j+1} \cap \tilde{V}_j^\perp$ are equipped with (uniform) Riesz bases $\Phi_j \coloneqq \{\varphi_{j,k} \colon k \in I_j \subset \mathbb{Z}\}$ and $\Psi_j \coloneqq \{\psi_{j,k} \colon k \in J_j \subset \mathbb{Z}\}$, respectively, the collection

$$\Psi \coloneqq \Phi_0 \cup \bigcup_{j=0}^{\infty} \Psi_j$$

forms a Riesz basis for $L_2(\Omega)$. With an appropriate scaling, it even forms a Riesz basis for $H^s(\Omega)$ for all $s \in (-\min(\tilde{\gamma}, \tilde{d}), \min(\gamma, d))$.

The construction of such multiresolution analyses on the interval $(0,1)$, where the primal spaces V_j are standard spline spaces, is well-known. We will revisit the construction from [DKU99] to end up with wavelets with highly improved quantitative properties.

When Ω is a product domain in n dimensions, e.g. $\Omega = (0,1)^n$, suitable multiresolution analyses can be constructed by tensorizing one-dimensional multiresolution analyses. In e.g. two dimensions, the resulting wavelets, i.e., the functions that span the resulting biorthogonal complement spaces $V_{j+1} \cap \tilde{V}_j^\perp$, will be of the form $\varphi_{j,k} \otimes \psi_{j,m}$, $\psi_{j,k} \otimes \varphi_{j,m}$ or $\psi_{j,k} \otimes \psi_{j,m}$, where thus the involved univariate wavelets and scaling functions are functions on the *same* level j. Such wavelets are called *isotropic*. Domain decomposition techniques allow to extend the construction of such wavelet bases to general, non-product domains (see e.g. [DS99a, DS99b]).

Based on the characterization

$$H^m(\Omega_1 \times \Omega_2) = H^m(\Omega_1) \otimes L_2(\Omega_2) \cap L_2(\Omega_1) \otimes H^m(\Omega_2), \tag{1.5}$$

a different option to construct wavelet bases on product domains is to tensorize one-dimensional wavelet bases. Indeed, if Ψ is a Riesz basis for both $L_2(0,1)$ and, after rescaling, for $H^m(0,1)$, then by applying (1.5) repeatedly, we infer that the n-fold tensor product $\Psi \otimes \cdots \otimes \Psi$ is, after a proper scaling, a Riesz basis

for $H^m(0,1)^n$. Now the basis elements are of type $\psi_{j_1,k_1} \otimes \cdots \otimes \psi_{j_n,k_n}$, where the j_i and k_i run independently over all levels and positions meaning that the supports of the basis functions can be arbitrarily *anisotropic*.

Non-adaptive and adaptive sparse grids

The expansion of a function u on $(0,1)^n$ with respect to a tensor product wavelet basis reads as $u = \sum_{j_i,k_i} \langle u, \tilde{\psi}_{j_1,k_1} \otimes \cdots \otimes \tilde{\psi}_{j_n,k_n} \rangle \, \psi_{j_1,k_1} \otimes \cdots \otimes \psi_{j_n,k_n}$. When u is *sufficiently smooth*, $|\langle u, \tilde{\psi}_{j_1,k_1} \otimes \cdots \otimes \tilde{\psi}_{j_n,k_n} \rangle| < C 2^{-(j_1+\cdots+j_n)d}$ for some C independent of all j_i and k_i, i.e., the coefficients decay as function of the *sum* of the levels.

In view of this, a sensible non-adaptive approach is to approximate u from the span of all those wavelets whose sum of their levels does not exceed some $L \in \mathbb{N}$. One can verify that the dimension N of this space is of order $L^{n-1}2^L$, while the error in the best approximation from this space decays as $L^{\frac{n-1}{2}} 2^{-dL} \eqsim (\log N)^{(n-1)(\frac{1}{2}+d)} N^{-d}$. When measuring the error in $H^m(\Omega)$ for $m \geq 1$, by slightly adapting the set of wavelets whose span define the approximation space, the logarithmic factors can even be removed; with an approximation space of dimension N, the error is of order $N^{-(d-m)}$. Surprisingly, this best possible rate $d-m$ is *independent of the space dimension* n, meaning that the curse of dimensionality, known from isotropic approximation, has complety disappeared.

The type of approximation outlined above is known as *sparse grid* ([Zen91]) or hyperbolic cross approximation, or, with the adaptation to get rid of the log-factor when measuring the error in a Sobolev norm with positive smoothness index, as *optimized sparse grid* approximation ([GK00]).

Obtaining the best possible rate $d-m$ in $H^m(0,1)^n$ requires that u is sufficiently smooth, in the sense that it should have $L_2(0,1)^n$-bounded mixed partial derivatives of a sufficiently high order. For the case of Poisson's problem on $(0,1)^n$, we will verify that this condition is generally *not* fulfilled regardless of the smoothness of the right-hand side f. In [DS09] (cf. also [Nit06, Nit05]) it is proven that if for this problem the sparse grid approach is combined with a proper local refinement of the wavelet index sets towards the boundary, then the best possible rate is retrieved. As with isotropic wavelets, such a refinement can be generated automatically by applying the adaptive wavelet-Galerkin scheme, now applied to the tensor product basis.

We conclude in Chapter 5 that this adaptive tensor product method does indeed converge with an optimal, dimension independent rate, where moreover the constants that are involved are independent of the dimension.

Thesis outline

In Chapter 2, we create wavelet bases for the interval $(0,1)$ for which the spaces V_j are standard spline spaces with respect to a uniform partition of the interval with mesh width 2^{-j}. This is done by adapting the construction from [DKU99]. The bases created in that work have the disadvantage of having prohibitively large condition numbers. It is altered by extending the primal space to the mentioned spline space, and adding corresponding dual boundary functions. The condition numbers of the resulting bases are much lower than those in comparable constructions such as [Pri06].

In Chapter 3 the optimal approximation rate in $H_0^1((0,1)^n)$ is derived, using sparse grids and optimized sparse grids approximations. It is shown that this approximation rate is independent of the space dimension n. We also analyze the smoothness conditions on the function that is approximated in order to obtain this rate. In Section 3.5, we show that the solution of Poisson's equation on $(0,1)^n$ does not satisfy these conditions when the right-hand side does not vanish near the boundary of the domain. This is a motivation to study adaptive methods in Chapter 5.

In Chapter 4, a divergence-free tensor-product wavelet basis is constructed, using the one-dimensional basis from Chapter 2. It is shown that when the velocity component of the solution of the Stokes equations is expressed in terms of this basis, it can be found as the solution of an elliptic problem. This problem can then be solved with either an non-adaptive or an adaptive method. In particular, it is shown that the sparse grid approximation results from Chapter 3 also hold for approximating vector-valued functions.

Chapter 5 is joint work with Christoph Schwab and Rob Stevenson and will appear as [DSS09]. In this chapter, an adaptive method for elliptic problems in high space dimensions is studied. We will verify that the stiffness matrix in tensor product wavelet coordinates is sufficiently close to a sparse matrix for the adaptive scheme to realize the same high, dimension independent rate as the best N-term approximations from this basis. Moreover, we carefully verify that the constant factor we may lose in the error bound compared to best N-term approximations is independent of n. Indeed, without precautions this factor easily grows exponentially with n, rendering the method useless in practice. The computational cost involved in computing these approximations may grow with n, but only linearly.

Chapter 6 is joint work with Rob Stevenson, and is under review for publication. It deals with the construction of a wavelet basis on the interval $(0,1)$ such that the representation of the Poisson equation on $(0,1)^n$, with respect to the n-fold tensor product of this basis, is a uniformly *sparse* matrix. The results extend to any second order partial differential operator with constant coefficients that defines a boundedly invertible operator.

Chapter 2
Well-conditioned biorthogonal spline wavelet bases on the interval

In [CDF92], biorthogonal wavelet bases were created for the line. These bases were adapted to the interval in [DKU99]. A problem of the latter construction is that it yields large condition numbers (which was partly remedied in [DKU97], [Bit06]). In [Pri06], the construction was dramatically improved. The main idea is to let the primal space be a spline space with respect to a uniform partition of the interval. The construction in this chapter does the same, but by choosing different boundary functions on the dual side. The resulting condition numbers are in most cases much better, and never significantly worse, than those in [Pri06].

2.1 Biorthogonal multiresolution analyses

Some notations

Let H be a separable Hilbert space with scalar product $\langle \cdot\,, \cdot \rangle_H$ and norm $\| \cdot \|_H$. Let $\Sigma := (\sigma_\lambda)_{\lambda\in\nabla}$ be a countable collection in H. Formally viewing Σ as a column vector, we will write $\mathbf{c}^T\Sigma$ for the sum $\sum_{\lambda\in\nabla} c_\lambda\sigma_\lambda$, with $\mathbf{c} = (c_\lambda)_{\lambda\in\nabla}$ being a vector of scalars. For any $x \in H$, by $\langle \Sigma, x\rangle$ and $\langle x, \Sigma\rangle$ we will mean the column and row vectors with elements $\langle \sigma_\lambda, x\rangle$, $\langle x, \sigma_\lambda\rangle$, respectively. More generally, for any two collections Σ_1, Σ_2, we define $\langle \Sigma_1, \Sigma_2\rangle_H$ as the (possibly infinite) matrix $\big(\langle \sigma_1, \sigma_2\rangle_H\big)_{\sigma_1\in\Sigma_1,\sigma_2\in\Sigma_2}$.

Riesz bases and biorthogonality

A countable collection $\Sigma \subset H$ is called a *Riesz system* when there are constants $0 < C_1 \le C_2 < \infty$ such that

$$C_1\|\mathbf{c}\|^2_{\ell_2(\nabla)} \le \big\|\mathbf{c}^T\Sigma\big\|^2_H \le C_2\|\mathbf{c}\|^2_{\ell_2(\nabla)} \quad \text{for all } \mathbf{c} := \{c_\lambda\}_{\lambda\in\nabla} \in \ell_2. \tag{2.1}$$

The best possible constants C_1, C_2 are called *Riesz constants*. If (and only if) the collection is orthogonal, $C_1 = C_2 = 1$. When Σ is dense in H, it is called a *Riesz basis*. We define the *condition number* of Σ as

$$\kappa(\Sigma) := \frac{C_2}{C_1}. \tag{2.2}$$

Note that C_1 and C_2 are the smallest and largest eigenvalues, respectively, of the *Gramian* or *mass matrix* $\langle \Sigma, \Sigma \rangle_H$. When comparing condition numbers from the literature, it is important to note that sometimes (e.g. in [DKU99, Pri06]) the condition number is defined as the fraction $\sqrt{C_1}/\sqrt{C_2}$.

When a Riesz system or basis depends on a parameter, we will speak about a *uniform Riesz system* or *basis* when its condition number is bounded uniformly over the range of values the parameter may assume.

Two collections $\Sigma, \tilde{\Sigma} \subset H$ are called *biorthogonal* if

$$\langle \Sigma, \tilde{\Sigma} \rangle_H = \mathbf{I}, \tag{2.3}$$

where $\mathbf{I}$ is the identity matrix of appropriate dimensions. In this case, the collections Σ and $\tilde{\Sigma}$ are called *dual* to each other.

By $f \lesssim g$ we mean that $f \leq C \cdot g$ with a constant that does not depend on parameters that f and g may depend on. Obviously $f \gtrsim g$ is defined as $g \lesssim f$, and $f \eqsim g$ as $f \lesssim g$ and $f \gtrsim g$. With this notation, (2.1) can be rewritten as $\|\mathbf{c}\|_{\ell_2(\nabla)} \eqsim \|\mathbf{c}^\mathsf{T}\Sigma\|_H$.

In the following, the Hilbert space H will be taken to be $L_2(\Omega)$. In this chapter, the domain Ω will be either $\mathbb{R}$ or $\mathrm{I} \coloneqq (0,1)$. For $s \geq 0$, let $\big(\mathcal{H}^s(\Omega)\big)_s$ and $\big(\tilde{\mathcal{H}}^s(\Omega)\big)_s$ denote scales of Sobolev spaces measuring s orders of smoothness in $L_2(\Omega)$. These two scales may only differ at the point whether and which essential boundary conditions are incorporated in their definition. $\mathcal{H}^0(\Omega) = \tilde{\mathcal{H}}^0(\Omega)$ will be denoted as $L_2(\Omega)$. For $s < 0$, $\mathcal{H}^s(\Omega) \coloneqq \big(\tilde{\mathcal{H}}^{-s}(\Omega)\big)'$ and $\tilde{\mathcal{H}}^s(\Omega) \coloneqq \big(\mathcal{H}^{-s}(\Omega)\big)'$. The scale of Sobolev spaces without essential boundary conditions will be denoted as $\big(H^s(\Omega)\big)_s$.

Uniformly local Riesz bases

A collection of functions $\Sigma_j \subset L_2(\Omega)$, depending on a parameter $j \in \mathbb{Z}$, will be called *uniformly local* when for $\sigma_j \in \Sigma_j$, $x \in \Omega$,

$$\operatorname{diam}(\operatorname{supp}\sigma_j) \lesssim 2^{-j} \text{ and } \#\big\{\sigma_j \in \Sigma_j \colon B(x; 2^{-j}) \cap \operatorname{supp}\sigma_j \neq \varnothing\big\} \lesssim 1, \tag{2.4}$$

where $B(x; 2^{-j})$ is the ball with radius 2^{-j} centered at x.

Lemma 2.1.1. *Let $\Sigma_j = (\sigma_{j,k})_k$ and $\tilde{\Sigma}_j = (\tilde{\sigma}_{j,k})_k \subset L_2(\Omega)$ be dual collections whose elements are uniformly bounded and uniformly local. Then Σ_j and $\tilde{\Sigma}_j$ are uniform Riesz systems.*

Proof. We will prove this lemma for Σ_j, the proof for $\tilde{\Sigma}_j$ is analogous. Because the primal functions are local and bounded, the mass matrix $\langle \Sigma_j, \Sigma_j \rangle_{L_2(\Omega)}$ is uniformly sparse, and its elements are uniformly bounded. Therefore, $\|\mathbf{c}^\mathsf{T}\Sigma_j\|^2_{L_2(\Omega)} = \langle \langle \Sigma_j, \Sigma_j \rangle_{L_2(\Omega)} \mathbf{c}, \mathbf{c} \rangle_{\ell_2(\nabla)} \lesssim \|\mathbf{c}\|^2_{\ell_2(\nabla)}$.

Let $u = \mathbf{c}^\mathsf{T}\Sigma_j$, for $\mathbf{c} = (c_k)_k$. By the duality between Σ_j and $\tilde{\Sigma}_j$, $c_k = \langle u, \tilde{\sigma}_{j,k} \rangle_{L_2(\Omega)}$. Because $\tilde{\sigma}_{j,k}$ is uniformly bounded, $c_k \lesssim \|u\|_{L_2(\operatorname{supp}\tilde{\sigma}_{j,k})}$. By the uniform localness of $\tilde{\Sigma}_j$, we conclude that $\|\mathbf{c}\|^2_{\ell_2(\nabla)} \lesssim \|u\|^2_{L_2(\Omega)}$. ◊

From this point, the subscript from the inner product $\langle \cdot, \cdot \rangle_{L_2(\Omega)}$ will be dropped. Closures are taken with respect to the $L_2(\Omega)$-norm, and $\perp$ will denote orthogonality with respect to that norm.

Direct and inverse estimates

We will look at *nested* sequences of subspaces $(V_j)_j$, $(\tilde{V}_j)_j$ of $L_2(\Omega)$, i.e.

$$\begin{aligned} &\cdots \subset V_j \subset V_{j+1} \subset \cdots \subset L_2(\Omega), \\ &\cdots \subset \tilde{V}_j \subset \tilde{V}_{j+1} \subset \cdots \subset L_2(\Omega). \end{aligned} \tag{2.5}$$

The primal sequence is said to satisfy a *Jackson* or *direct estimate* of order d if

$$\inf_{v_j \in V_j} \|v - v_j\|_{L_2(\Omega)} \lesssim 2^{-jd} \|v\|_{\mathcal{H}^d} \quad \text{for all } v \in \mathcal{H}^d(\Omega). \tag{2.6}$$

A direct estimate of order d is satisfied when all polynomials of order d satisfying the possibly essential boundary conditions are included in V_j (*exactness of order* d), and when, for example, V_j has a basis Σ_j with a dual collection $\tilde{\Sigma}_j \subset L_2(\Omega)$ that is uniformly local and bounded.

The primal sequence is said to satisfy a *Bernstein* or *inverse estimate* of order γ if for all $s < \gamma$,

$$\|v_j\|_{\mathcal{H}^s(\Omega)} \lesssim 2^{-js} \|v_j\|_{L_2(\Omega)} \quad \text{for all } v_j \in V_j. \tag{2.7}$$

An inverse estimate of order γ is known to hold with $\gamma = r + \frac{3}{2}$ when V_j is spanned by piecewise smooth, globally C^r-functions for some $r \in \{-1, 0, 1, \ldots\}$, where $r = -1$ means that no global continuity condition is satisfied.

The definition of Jackson or Bernstein estimates for the dual sequence is analogous, with $\left(\mathcal{H}^s(\Omega)\right)_s$ replaced by $\left(\tilde{\mathcal{H}}^s(\Omega)\right)_s$.

Biorthogonal space decompositions

Later in this chapter, we will create biorthogonal uniform $L_2(\Omega)$-Riesz systems Φ_j, $\tilde{\Phi}_j$ such that for sequences $(V_j)_j$, $(\tilde{V}_j)_j$ as above,

$$V_j = \operatorname{clos}_{\operatorname{span}} \Phi_j, \tag{2.8}$$

$$\tilde{V}_j = \operatorname{clos}_{\operatorname{span}} \tilde{\Phi}_j. \tag{2.9}$$

The elements of these bases will be called *primal* and *dual scaling functions*. For now, we assume these bases as given.

The nesting of the spaces V_j ($\tilde{V}_j$) implies that the functions in Φ_j ($\tilde{\Phi}_j$) are linear combinations of the functions in Φ_{j+1} ($\tilde{\Phi}_{j+1}$). This can be expressed as

$$\Phi_j^T = \Phi_{j+1}^T \mathbf{M}_{j,0}, \tag{2.10}$$

$$\tilde{\Phi}_j^T = \tilde{\Phi}_{j+1}^T \tilde{\mathbf{M}}_{j,0}, \tag{2.11}$$

where $\mathbf{M}_{j,0} := \langle \tilde{\Phi}_{j+1}, \Phi_j \rangle$ and $\tilde{\mathbf{M}}_{j,0} := \langle \Phi_{j+1}, \tilde{\Phi}_j \rangle$ are *refinement matrices* of appropriate (possibly infinite) dimensions. If Φ_j and $\tilde{\Phi}_j$ are uniformly local bases, these matrices are uniformly sparse.

The bases Φ_j, $\tilde{\Phi}_j$ are crucial ingredients for the following theorem, which states how Riesz bases for a range of Sobolev spaces can be created.

Theorem 2.1.2 ([DS99c]). *For some $j_0 \in \mathbb{N}_0$, let $V_{j_0} \subset V_{j_0+1} \subset V_{j_0+2} \subset \ldots$ and $\tilde{V}_{j_0} \subset \tilde{V}_{j_0+1} \subset \tilde{V}_{j_0+2} \subset \ldots$ be sequences of nested closed subspaces of $L_2(\Omega)$, equipped with biorthogonal uniform $L_2(\Omega)$-Riesz bases Φ_j, $\tilde{\Phi}_j$. Also assume that for $(V_j)_j$ ($(\tilde{V}_j)_j$)*

a Jackson estimate with parameter d ($\tilde{d}$) and a Bernstein inequality with parameter γ ($\tilde{\gamma}$) hold. Given some uniform $L_2(\Omega)$-Riesz bases Ψ_j for the spaces $V_{j+1} \cap \tilde{V}_j^\perp$, then for all $s \in \big(-\min(\tilde{\gamma}, \tilde{d}), \min(\gamma, d)\big)$, the collection $\Psi_{j_0,\infty,s}$ is a Riesz basis for $\mathcal{H}^s(\Omega)$, where for $j_{\max} \in \mathbb{N}_{\geq j_0} \cup \{\infty\}$ the multiscale basis $\Psi_{j_0,j_{\max},s}$ for $\mathcal{H}^s(\Omega)$ *is defined as*

$$\Psi_{j_0,j_{\max},s} := \Phi_{j_0} \cup \bigcup_{j=j_0}^{j_{\max}} 2^{-sj}\Psi_j.$$

We will also refer to such multiscale bases simply as *wavelet bases*.

Two sequences $(V_j)_j$, $(\tilde{V}_j)_j$ that satisfy the requirements of Theorem 2.1.2 will be called *biorthogonal multiresolution analyses* for Ω.

The following lemma will be used, among other things, to derive properties of a dual wavelet basis.

Lemma 2.1.3 ([Ste03])**.** *Let X, $\tilde{X}$ be closed subspaces of a separable Hilbert space H.*

1. *The following three statements are equivalent:*
   (a) *There exist Riesz bases Σ and $\tilde{\Sigma}$ for X and $\tilde{X}$ such that $\langle \Sigma, \tilde{\Sigma}\rangle$ is boundedly invertible.*
   (b) *There exists a unique bounded projector $Q\colon H \to H$ with $\operatorname{Im} Q = X$ and $\operatorname{Im}(I-Q) = \tilde{X}^\perp$.*
   (c) *To any Riesz basis for $\tilde{X}$ there corresponds a unique dual collection in X. Moreover, this collection is a Riesz basis for X.*
2. *Let any of the three equivalent conditions above be satisfied. Let Y, Z be subspaces of H such that $Y = X + Z$ and*

$$\cos\angle(Z,X) := \sup_{0\neq z\in Z, 0\neq x\in X} \frac{|\langle z,x\rangle|}{\|z\|_H\|x\|_H} < 1. \tag{2.12}$$

   Then $(I-Q)|_Z\colon Z \to Y \cap \tilde{X}^\perp$ is boundedly invertible.

The projector Q from this lemma can be computed as $Qx = \langle x, \tilde{\Sigma}\rangle\langle \Sigma, \tilde{\Sigma}\rangle^{-1}\Sigma$. Its adjoint $Q^*\colon H \to H$ satisfies $\operatorname{Im} Q^* = \tilde{X}$, $\operatorname{Im}(I-Q^*) = X^\perp$ and can be computed by $Q^*x = \langle x, \Sigma\rangle\langle \tilde{\Sigma}, \Sigma\rangle^{-1}\tilde{\Sigma}$.

This lemma still holds when the spaces X and $\tilde{X}$ are replaced by a pair of spaces X_j and $\tilde{X}_j$ that depend on a parameter j, and the conditions are replaced by corresponding conditions that hold uniformly in j.

The following proposition was also derived in [Ngu05]. We include a short proof. For ease of notation, we define $\Psi_{j_0-1} := \Phi_{j_0}$, $\tilde{\Psi}_{j_0-1} := \tilde{\Phi}_{j_0}$, $V_{j_0-1} := \tilde{V}_{j_0-1} := 0$, and $Q_{j_0-1} := 0$.

Proposition 2.1.4. *In the setting of Theorem 2.1.2, there is a unique dual Riesz basis for $L_2(\Omega)$, denoted by $\tilde{\Psi}_{j_0,\infty,0}$. This basis can be decomposed as*

$$\tilde{\Psi}_{j_0,\infty,0} = \bigcup_{j=j_0-1}^{\infty} \tilde{\Psi}_j, \tag{2.13}$$

where $\tilde{\Psi}_j$ is a basis for $\tilde{V}_{j+1} \cap V_j^\perp$. For $s \in (-\min(\gamma, d), \min(\tilde{\gamma}, \tilde{d}))$,

$$\tilde{\Psi}_{j_0,\infty,s} := \tilde{\Psi}_{j_0-1} \cup \bigcup_{j=j_0}^{\infty} 2^{-sj}\tilde{\Psi}_j.$$

is a Riesz basis for $\tilde{\mathcal{H}}^s(\Omega)$.

Proof. The existence of the dual Riesz basis $\tilde{\Psi}_{j_0,\infty,0}$ follows from Lemma 2.1.3. We split $\tilde{\Psi}_{j,\infty,0} = \bigcup_{j=j_0-1}^{\infty} \tilde{\Psi}_j$, where $\tilde{\Psi}_j$ is the collection of duals of Ψ_j. It remains to verify that $\tilde{\Psi}_j$ is a basis for $\tilde{V}_{j+1} \cap V_j^\perp$.

To this end, let $Q_j \colon L_2(\Omega) \to L_2(\Omega)$ denote the uniformly bounded projector such that $\operatorname{Im} Q_j = V_j$ and $\operatorname{Im}(I - Q_j) \perp \tilde{V}_j^\perp$. The existence and uniform boundedness of this projector follow from the existence of uniform $L_2(\Omega)$-Riesz bases Φ_j, $\tilde{\Phi}_j$ for V_j, $\tilde{V}_j$ and Lemma 2.1.3. From $V_j \subset V_{j+1}$ and $\tilde{V}_j \subset \tilde{V}_{j+1}$ it follows that $Q_{j+1}Q_j = Q_j$ and $Q_{j+1}^* Q_j^* = Q_j^*$, or (by taking adjoints) $Q_j Q_{j+1} = Q_j$. It follows that $Q_{j+1} - Q_j$ is a projector. Using $Q_{j+1} - Q_j = (I - Q_j)Q_{j+1}$ we see that $\operatorname{Im}(Q_{j+1} - Q_j) = V_{j+1} \cap \tilde{V}_j^\perp$. Analogously, $Q_{j+1}^* - Q_j^*$ is a projector onto $\tilde{V}_{j+1} \cap V_j^\perp$. Because $\Psi_{j_0,\infty,0}$ and $\tilde{\Psi}_{j_0,\infty,0}$ are Riesz bases for $L_2(\Omega)$, we have $I = \sum_{j=j_0-1}^{\infty}(Q_{j+1} - Q_j)$ and $I = \sum_{j=j_0-1}^{\infty}(Q_{j+1}^* - Q_j^*)$.

We will now show that $\operatorname{span} \tilde{\Psi}_j \subset \operatorname{Im}(Q_{j+1}^* - Q_j^*)$. To that end, let $w_j \in \operatorname{span} \tilde{\Psi}_j$, and write $w_j = \sum_i (Q_{i+1}^* - Q_i^*) w_j$. Now for all $z \in L_2(\Omega)$, we have

$$\big\langle z, (Q_{i+1}^* - Q_i^*) w_j \big\rangle = \big\langle (Q_{i+1} - Q_i) z, w_j \big\rangle.$$

Because $(Q_{i+1} - Q_i)z \in \operatorname{span} \Psi_i$ and $\Psi_i \perp \tilde{\Psi}_j$ for all $i \neq j$, this inner product vanishes for all $i \neq j$. It follows that $w_j = (Q_{j+1}^* - Q_j^*) w_j$, and thus $w_j \in \operatorname{Im}(Q_{j+1}^* - Q_j^*)$.

Because $\tilde{\Psi}_{j_0,\infty,0}$ is a basis for $L_2(\Omega)$, necessarily $\operatorname{span} \tilde{\Psi}_j = \operatorname{Im}(Q_j^* - Q_{j-1}^*) = \tilde{V}_{j+1} \cap V_j^\perp$. Applying Theorem 2.1.2 once more (with reversed role of primal and dual) shows the last statement of the proposition. ◊

Construction of wavelets

The next task will be to construct a suitable wavelet basis Ψ_j for $V_{j+1} \cap \tilde{V}_j^\perp$, as required by Theorem 2.1.2. To this end, suppose we have a uniformly local collection Ψ_j^{init} such that $\Phi_j \cup \Psi_j^{\text{init}}$ forms a uniform $L_2(\Omega)$-Riesz basis for V_{j+1}. We define the collection Ψ_j as

$$\Psi_j := (I - Q_j)\Psi_j^{\text{init}} = \Psi_j^{\text{init}} - \langle \Psi_j^{\text{init}}, \tilde{\Phi}_j \rangle \Phi_j. \tag{2.14}$$

The second statement of Lemma 2.1.3, with $X := V_j = \operatorname{clos}\operatorname{span} \Phi_j$, $\tilde{X} := \tilde{V}_j = \operatorname{clos}\operatorname{span} \tilde{\Phi}_j$, $Y := V_{j+1} = \operatorname{clos}\operatorname{span} \Phi_{j+1}$, $Z := \operatorname{clos}\operatorname{span} \Psi_j^{\text{init}}$, yields that the projector $(I - Q_j)|_Z \colon Z \to V_{j+1} \cap \tilde{V}_j^\perp$ is uniformly boundedly invertible. This shows that Ψ_j is a uniform $L_2(\Omega)$-Riesz basis for $V_{j+1} \cap \tilde{V}_j^\perp$. Since the matrix $\langle \Psi_j^{\text{init}}, \tilde{\Phi}_j \rangle$ is uniformly sparse, the set Ψ_j is moreover uniformly local.

We will call Ψ_j^{init} an *initial stable completion* and Ψ_j a *stable completion*. Since they are contained in $V_{j+1} = \operatorname{span} \Phi_{j+1}$, we can write

$$\begin{aligned} (\Psi_j^{\text{init}})^{\mathsf{T}} &= \Phi_{j+1}^{\mathsf{T}} \mathbf{M}_{j,1}^{\text{init}}, \\ \Psi_j^{\mathsf{T}} &= \Phi_{j+1}^{\mathsf{T}} \mathbf{M}_{j,1}, \end{aligned} \tag{2.15}$$

for some uniformly sparse matrices $\mathbf{M}_{j,1}^{\text{init}}$, $\mathbf{M}_{j,1}$ of appropriate (possibly infinite) dimensions.

Lemma 2.1.5. *The matrix* $\mathbf{M}_{j,1}$ *can be computed as* $\mathbf{M}_{j,1} = \big(\mathbf{I} - \mathbf{M}_{j,0}\tilde{\mathbf{M}}_{j,0}^{\mathsf{T}}\big)\mathbf{M}_{j,1}^{init}$.

Proof. Combining the definition of Ψ_j with (2.10) and (2.15), we have

$$\Psi_j = (\mathbf{M}_{j,1}^{\text{init}})^{\mathsf{T}}\Phi_{j+1} - \big\langle (\mathbf{M}_{j,1}^{\text{init}})^{\mathsf{T}}\Phi_{j+1}, \tilde{\mathbf{M}}_{j,0}^{\mathsf{T}}\tilde{\Phi}_{j+1}\big\rangle \mathbf{M}_{j,0}^{\mathsf{T}}\Phi_{j+1}.$$

The biorthogonality relation $\langle \Phi_{j+1}, \tilde{\Phi}_{j+1}\rangle = \mathbf{I}$ yields

$$\Psi_j = \big((\mathbf{M}_{j,1}^{\text{init}})^{\mathsf{T}} - (\mathbf{M}_{j,1}^{\text{init}})^{\mathsf{T}}\tilde{\mathbf{M}}_{j,0}\mathbf{M}_{j,0}^{\mathsf{T}}\big)\Phi_{j+1}.$$

Transposing both sides and comparing with (2.15) yields the result. ◊

The relations (2.10) and (2.15) can be combined to read

$$[\Phi_j^{\mathsf{T}} \;\; \Psi_j^{\mathsf{T}}] = \Phi_{j+1}^{\mathsf{T}}\mathbf{M}_j,$$

where $\mathbf{M}_j := [\mathbf{M}_{j,0} \;\; \mathbf{M}_{j,1}]$. Because $\operatorname{span}\tilde{\Phi}_j$, $\operatorname{span}\tilde{\Psi}_j \subset \operatorname{span}\tilde{\Phi}_{j+1}$, there exists a matrix $\tilde{\mathbf{M}}_j$ such that $[\tilde{\Phi}_j^{\mathsf{T}} \;\; \tilde{\Psi}_j^{\mathsf{T}}] = \tilde{\Phi}_{j+1}^{\mathsf{T}}\tilde{\mathbf{M}}_j$. The relations $\Psi_j \subset V_{j+1} \cap \tilde{V}_j^{\perp}$, $\tilde{\Psi}_j \subset \tilde{V}_{j+1} \cap V_j^{\perp}$, and the biorthogonality of $(\Phi_j, \tilde{\Phi}_j)$, $(\Psi_j, \tilde{\Psi}_j)$ and (Φ_{j+1}, Φ_{j+1}) show that

$$\mathbf{I} = \big\langle [\Phi_j^{\mathsf{T}} \;\; \Psi_j^{\mathsf{T}}]^{\mathsf{T}}, [\tilde{\Phi}_j^{\mathsf{T}} \;\; \tilde{\Psi}_j^{\mathsf{T}}]\big\rangle = \mathbf{M}_j^{\mathsf{T}}\tilde{\mathbf{M}}_j.$$

It follows that $\tilde{\mathbf{M}}_j$ is the inverse of $\mathbf{M}_j^{\mathsf{T}}$. Note that $\tilde{\mathbf{M}}_j$ can be written as $[\tilde{\mathbf{M}}_{j,0} \;\; \tilde{\mathbf{M}}_{j,1}]$, where $\tilde{\mathbf{M}}_{j,0}$ is as in (2.10), and $\tilde{\mathbf{M}}_{j,1}$ comprises the remaining columns of $\tilde{\mathbf{M}}_j$.

The construction of a uniformly local Ψ_j^{init} such that $\Phi_j \cup \Psi_j^{\text{init}}$ is a uniform $L_2(\Omega)$-Riesz basis for V_{j+1} amounts to finding $\mathbf{M}_{j,1}^{\text{init}}$ such that the matrix $[\mathbf{M}_{j,0} \;\; \mathbf{M}_{j,1}^{\text{init}}]$ is uniformly sparse and uniformly boundedly invertible. We will construct $\mathbf{M}_{j,1}^{\text{init}}$ such that, moreover, $[\mathbf{M}_{j,0} \;\; \mathbf{M}_{j,1}^{\text{init}}]^{-1}$ is uniformly sparse.

Writing, according to Lemma 2.1.5,

$$\mathbf{M}_j = \big[\mathbf{M}_{j,0} \;\; \mathbf{M}_{j,1}\big] = \big[\mathbf{M}_{j,0} \;\; \mathbf{M}_{j,1}^{\text{init}}\big]\begin{bmatrix} \mathbf{I} & -\tilde{\mathbf{M}}_{j,0}^{\mathsf{T}}\mathbf{M}_{j,1}^{\text{init}} \\ \mathbf{0} & \mathbf{I} \end{bmatrix},$$

we have

$$\tilde{\mathbf{M}}_j = \mathbf{M}_j^{-\mathsf{T}} = \big[\mathbf{M}_{j,0} \;\; \mathbf{M}_{j,1}^{\text{init}}\big]^{-\mathsf{T}}\begin{bmatrix} \mathbf{I} & \mathbf{0} \\ (\mathbf{M}_{j,1}^{\text{init}})^{\mathsf{T}}\tilde{\mathbf{M}}_{j,0} & \mathbf{I} \end{bmatrix}.$$

By assumption, all matrices occurring in this expression are uniformly sparse, which shows that the dual wavelets are uniformly local. Thus, the uniform sparsity of $[\mathbf{M}_{j,0} \;\; \mathbf{M}_{j,1}^{\text{init}}]^{-1}$ leads to uniformly local dual wavelets.

2.2 Biorthogonal multiresolution analyses on $\mathbb{R}$

In this section we will recall some facts about multiresolution analyses on $\mathbb{R}$. To distinguish this construction from other constructions, we will write $[\,\cdot\,]$ in the subscript of constructions on the line. We will construct the scaling functions as dilates and translates of one[1] function, called *mother scaling function*. All wavelets will be dilates and translates of one *mother wavelet*.

[1] In so-called multiwavelet constructions, scaling functions and wavelets are allowed to be dilates and translates of multiple functions.

To ensure nesting of the spaces $V_{[j]}$, $\tilde{V}_{[j]}$, we will demand that the mother scaling function is refinable. A function $\theta \in L_2(\mathbb{R})$ is called *refinable* if there exists a sequence $(a_k)_k$, also called *mask*, with $\sum_k a_k = 2$, such that the *two-scale relation*

$$\theta(x) = \sum_{k\in\mathbb{Z}} a_k \theta(2x-k) \tag{2.16}$$

holds. Because we want to construct uniformly local functions, we will be interested in mother scaling functions with compact support. The following proposition is well-known and can be verified easily.

Proposition 2.2.1. *When a function is refinable and its mask $(a_k)_k$ is nonzero only for $k \in \{\ell_1, \dots, \ell_2\}$ then the convex hull of its support (i.e. the smallest interval in which its support is contained) is $[\ell_1, \ell_2]$.*

Remark 2.2.2. The converse of Proposition 2.2.1 is not true: there are compactly supported functions that are refinable with an infinite mask, as noted in [SSZ99]. An example is the function $\chi_{[0,2)} + \chi_{[1,2)}$ with mask $a_0 = 1$, $a_1 = \frac{1}{2}$, $a_2 = \frac{1}{4}$, $a_k = (-1)^{k+1}3/2^k$ for $k \geq 3$.

Two functions θ, $\tilde{\theta}$ are called a *dual pair* if $\langle \theta(\cdot - k), \tilde{\theta}(\cdot - m)\rangle = \delta_{k,m}$.

In Section 2.3, multiresolution analyses on the interval will be created by adapting a multiresolution on $\mathbb{R}$ to $(0,1)$. It will be important to preserve the Jackson property of the primal and dual space, by retaining polynomial exactness. We will use the following lemma, of which we include the short proof.

Lemma 2.2.3. *[DM93b] Let φ, $\tilde{\varphi}$ be a dual pair, and let the space* $\operatorname{span}\{\varphi(\cdot - m) \colon m \in \mathbb{Z}\}$ *contain all polynomials of degree at most $d-1$. Then the coefficients $\tilde{\alpha}_{m,r}$ such that $x^r = \sum_m \tilde{\alpha}_{m,r}\varphi(x-m)$ can be computed recursively using the following identities:*

$$\tilde{\alpha}_{m,0} = \int \tilde{\varphi}(x)\,\mathrm{d}x, \qquad m \in \mathbb{Z},$$

$$\tilde{\alpha}_{m,r} = \sum_{i=0}^{r} \binom{r}{i} m^i \tilde{\alpha}_{0,r-i}, \qquad r = 1, \dots, d-1, m \in \mathbb{Z}\backslash\{0\},$$

$$\tilde{\alpha}_{0,r} = \frac{1}{2^{r+1}-2} \sum_{k=\ell_1}^{\ell_2} a_k \sum_{i=0}^{r-1} \binom{r}{i} k^{r-i} \tilde{\alpha}_{0,i}, \qquad r = 1, \dots, d-1.$$

Proof. Because φ and $\tilde{\varphi}$ form a dual pair we have $\tilde{\alpha}_{m,r} = \int x^r \tilde{\varphi}(x-m)\,\mathrm{d}x$. The statement for $\tilde{\alpha}_{m,0}$ follows immediately. The second statement follows from

$$\int x^r \tilde{\varphi}(x-m)\,\mathrm{d}x = \int (x+m)^r \tilde{\varphi}(x)\,\mathrm{d}x = \int \sum_{i=0}^{r} \binom{r}{i} m^i x^{r-i} \tilde{\varphi}(x)\,\mathrm{d}x.$$

The last statement follows from

$$\begin{aligned}\int x^r \tilde{\varphi}(x)\,\mathrm{d}x &= \sum_k a_k \int x^r \tilde{\varphi}(2x-k)\,\mathrm{d}x = 2^{-r-1} \sum_k a_k \int (x+k)^r \tilde{\varphi}(x)\,\mathrm{d}x \\ &= 2^{-r-1} \sum_k a_k \sum_{i=0}^{r} \binom{r}{i} k^{r-i} \int x^i \tilde{\varphi}(x)\,\mathrm{d}x.\end{aligned}$$

Using $\sum_k a_k = 2$, it follows that

$$\tilde{\alpha}_{0,r} = 2^{-r-1} \sum_k a_k \sum_{i=0}^{r-1} k^{r-i} \binom{r}{i} \tilde{\alpha}_{0,i} + 2^{-r} \tilde{\alpha}_{0,r}. \qquad \Diamond$$

In the following, we will take the mother scaling functions φ and $\tilde{\varphi}$ to be refinable functions, with finite masks $(a_k)_k$, $(\tilde{a}_k)_k$, that satisfy the conditions of Lemma 2.2.3. The collection $\Phi_{[j]}$ is defined as

$$\Phi_{[j]} := \{\varphi_{[j,k]} := 2^{j/2}\varphi(2^j \cdot - k) \colon k \in \mathbb{Z}\}. \tag{2.17}$$

The dual scaling functions $\tilde{\Phi}_{[j]}$ are created similarly from $\tilde{\varphi}$. The scaling $2^{j/2}$ is such that $\|\varphi_{[j,k]}\|_{L_2(\mathbb{R})} = \|\varphi\|_{L_2(\mathbb{R})}$, so that the resulting scaling functions are uniformly bounded. By construction, these collections are also uniformly local. Because φ and $\tilde{\varphi}$ form a dual pair, $\Phi_{[j]}$ and $\tilde{\Phi}_{[j]}$ are biorthogonal. An application of Lemma 2.1.1 shows that $\Phi_{[j]}$ and $\tilde{\Phi}_{[j]}$ are uniform $L_2(\mathbb{R})$-Riesz bases for their spans $V_{[j]}$ and $\tilde{V}_{[j]}$, respectively.

Refinability of the functions φ, $\tilde{\varphi}$ is equivalent to nesting of the spaces $V_{[j]}$, $\tilde{V}_{[j]}$. Using the two-scale relation of φ, we have

$$\varphi_{[j,m]} = \frac{1}{\sqrt{2}} \sum_{k=2m+\ell_1}^{2m+\ell_2} a_{k-2m} \varphi_{[j+1,k]}. \tag{2.18}$$

From Lemma 2.2.3 and the definition of $\varphi_{[j,m]}$ in (2.17) we obtain, by substituting $x = 2^j y$,

$$y^r = 2^{-jr} \sum_m \tilde{\alpha}_{m,r} \varphi(2^j y - m) = 2^{-j(r+1/2)} \sum_m \tilde{\alpha}_{m,r} \varphi_{[j,m]}(y). \tag{2.19}$$

In the current shift-invariant case, the refinement matrix $\mathbf{M}_{[j,0]}$ from (2.10) is given by $(\mathbf{M}_{[j,0]})_{p,q} = a_{p-2q}/\sqrt{2}$. A similar comment applies to $\tilde{\mathbf{M}}_{[j,0]}$.

Wavelets

To construct wavelets, we will first construct the mother wavelet ψ such that its integer shifts are orthogonal to all integer shifts of the mother scaling function $\tilde{\varphi}$. The following function satisfies this condition:

$$\psi(x) := \sum_{k\in\mathbb{Z}} (-1)^k \tilde{a}_{1-k} \varphi(2x - k). \tag{2.20}$$

Indeed, by using the two-scale relation (2.16) for $\tilde{\varphi}$ and the duality of φ and $\tilde{\varphi}$ we see that

$$\begin{aligned} \big\langle \psi(x-\ell), \tilde{\varphi}(x) \big\rangle &= \Big\langle \sum_{k\in\mathbb{Z}} (-1)^k \tilde{a}_{1-k} \varphi(2x - 2\ell - k), \sum_{m\in\mathbb{Z}} \tilde{a}_m \tilde{\varphi}(2x - m) \Big\rangle \\ &= \sum_{k\in\mathbb{Z}} (-1)^k \tilde{a}_{1-k} \tilde{a}_{k+2\ell} = \sum_{k\in 2\mathbb{Z}} \tilde{a}_{1-k} a_{k+2\ell} - \sum_{k\in 2\mathbb{Z}+1} \tilde{a}_{1-k} a_{k+2\ell} = 0, \end{aligned} \tag{2.21}$$

where in the last step the substitution $k' = 1 - 2\ell - k$ was made.

All wavelets are now defined by means of

$$\Psi_{[j]} := \{\psi_{[j,k]}(x) := 2^{j/2} \psi(2^j x - k) \colon k \in \mathbb{Z}\}.$$

Comparing this to the general setting in Section 2.1, we have skipped the step of choosing an initial stable completion by choosing a stable completion directly such that $\Psi_j \perp \tilde{\Phi}_j$. Equivalently, one could view this as taking the initial completion Ψ_j^{init} such that in (2.14), $(I - Q_j)\Psi_j^{\text{init}} = \Psi_j^{\text{init}}$. Obviously, $\Psi_{[j]} \subset \operatorname{span} \Phi_{[j+1]}$. The matrix $\mathbf{M}_{[j,1]} = \langle \Phi_{[j+1]}, \Psi_{[j]} \rangle$ satisfies $(\mathbf{M}_{[j,1]})_{p,q} = (-1)^k \tilde{a}_{1-p+2q}/\sqrt{2}$. It follows from (2.21) that $\psi_{[j,k]} \perp \tilde{\varphi}_{[j,k']}$ for all j, k, k', so that $\operatorname{span} \Psi_{[j]} \perp \operatorname{span} \tilde{\Phi}_{[j]}$. We note that, by an application of the Schur lemma, the two-scale matrix $\mathbf{M}_{[j]} = [\mathbf{M}_{[j,0]} \ \mathbf{M}_{[j,1]}]$ is uniformly bounded.

On the dual side, we *define* a dual wavelet $\tilde{\psi}$ as in (2.20), with the role of primal and dual interchanged. By interchanging the role of primal and dual in the above arguments, we have $\tilde{\Psi}_{[j]} \subset \operatorname{span} \tilde{\Phi}_{[j+1]}$ and $\operatorname{span} \tilde{\Psi}_{[j]} \perp \operatorname{span} \Phi_{[j]}$. Also, $\tilde{\mathbf{M}}_{[j]}$ is uniformly bounded.

It remains to be shown that $\Psi_{[j]}$ and $\tilde{\Psi}_{[j]}$ are biorthogonal, and that they are Riesz bases for $V_{[j+1]} \cap \tilde{V}_{[j]}^{\perp}$ and $\tilde{V}_{[j+1]} \cap V_{[j]}^{\perp}$, respectively. We will first verify the biorthogonality. From the duality of φ and $\tilde{\varphi}$ we have

$$\delta_{\ell,0} = \big\langle \varphi(x-\ell), \tilde{\varphi}(x) \big\rangle = \sum_{k,m\in\mathbb{Z}} a_k \tilde{a}_m \big\langle \varphi(2x-2\ell-k), \tilde{\varphi}(2x-m) \big\rangle = \sum_{k\in\mathbb{Z}} a_k \tilde{a}_{k+2\ell}.$$

This shows that

$$\begin{aligned} \big\langle \psi(x-\ell), \tilde{\psi}(x) \big\rangle &= \sum_{k,m\in\mathbb{Z}} (-1)^k (-1)^m \tilde{a}_{1-k} a_{1-m} \big\langle \varphi(2x-2\ell k), \tilde{\varphi}(2x-m) \big\rangle \\ &= \sum_{k\in\mathbb{Z}} \tilde{a}_{1-k} a_{1-(k+2\ell)} = \delta_{\ell,0}. \end{aligned}$$

We conclude that ψ and $\tilde{\psi}$ are dual, implying the biorthogonality of $\Psi_{[j]}$ and $\tilde{\Psi}_{[j]}$. Combining this with the biorthogonality of $\Phi_{[j]}$ and $\tilde{\Phi}_{[j]}$, and the orthogonality relations derived previously, we have

$$\begin{aligned} \mathbf{I} &= \big\langle [\Phi_{[j]}^{\mathsf{T}} \ \Psi_{[j]}^{\mathsf{T}}]^{\mathsf{T}}, [\tilde{\Phi}_{[j]}^{\mathsf{T}} \ \tilde{\Psi}_{[j]}^{\mathsf{T}}]^{\mathsf{T}} \big\rangle = \big\langle \mathbf{M}_{[j]}^{\mathsf{T}} \Phi_{[j+1]}, \tilde{\mathbf{M}}_{[j]}^{\mathsf{T}} \tilde{\Phi}_{[j+1]} \big\rangle \\ &= \mathbf{M}_{[j]}^{\mathsf{T}} \big\langle \Phi_{[j+1]}, \tilde{\Phi}_{[j+1]} \big\rangle \tilde{\mathbf{M}}_{[j]} = \mathbf{M}_{[j]}^{\mathsf{T}} \tilde{\mathbf{M}}_{[j]}. \end{aligned}$$

Analogously, it can be shown that $\mathbf{I} = \tilde{\mathbf{M}}_{[j]}^{\mathsf{T}} \mathbf{M}_{[j]}$. This shows that $\mathbf{M}_{[j]}^{-1} = \tilde{\mathbf{M}}_{[j]}^{\mathsf{T}}$, so that $\mathbf{M}_{[j]}$ and $\tilde{\mathbf{M}}_{[j]}$ are uniformly boundedly invertible. Because $\Phi_{[j+1]}$ and $\Phi_{[j+1]}$ are uniform $L_2(\mathbb{R})$-Riesz bases, this shows that also $\Phi_{[j]} \cup \Psi_{[j]}$ and $\tilde{\Phi}_{[j]} \cup \tilde{\Psi}_{[j]}$ are uniform $L_2(\mathbb{R})$-Riesz bases for $V_{[j+1]}$ and $\tilde{V}_{[j+1]}$, respectively. Therefore, Theorem 2.1.2 can be applied.

B-splines

In the following, we will take the primal mother scaling function φ to be a cardinal B-spline, which we will define now. Like in [dB01, IX.13], for $d \in \mathbb{N}$ and for some non-decreasing *knot sequence* $\mathbf{t} := (t_i)_{i=1}^N$ with $t_{k+d} > t_k$ for all $k \in \{1, \dots, N-d\}$ we define the k-th *B-spline* $B_{d,\mathbf{t}}^k$ of order d recursively through $B_{1,\mathbf{t}}^k = \chi_{[t_k, t_{k+1})}$, and for $d > 1$,

$$B_{d,\mathbf{t}}^k(x) := \frac{x - t_k}{t_{k+d-1} - t_k} B_{d-1,\mathbf{t}}^k(x) + \frac{t_{k+d} - x}{t_{k+d} - t_{k+1}} B_{d-1,\mathbf{t}}^{k+1}(x),$$

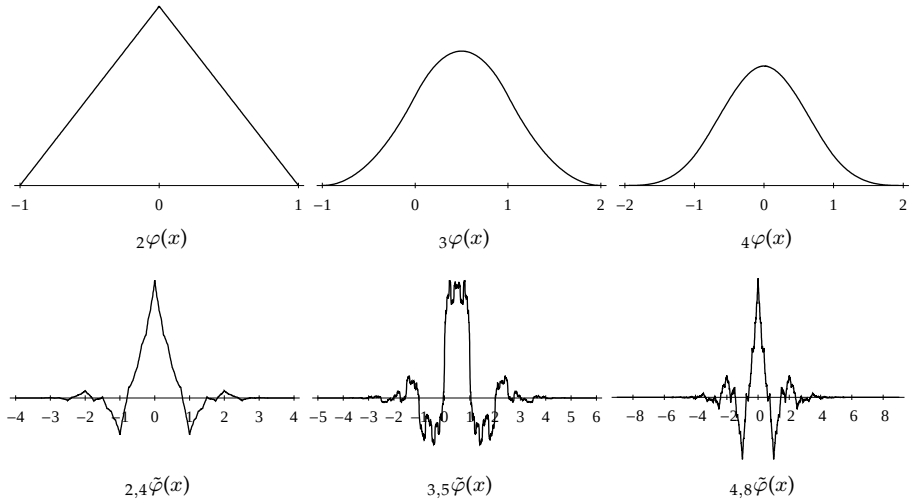

Figure 2.1: Biorthogonal spline wavelets and their duals from [CDF92].

with the convention that if $t_{k+d-1} = t_k$ or $t_{k+d} = t_{k+1}$ then the corresponding term should be discarded. When $\mathbf{t} = \mathbb{Z}$, we call these functions *cardinal B-splines*.

In view of the construction of multiresolution analyses on the interval in Section 2.3, we already collect some properties of B-splines on knot sequences on the interval. This knot sequence $\mathbf{t}$ will be allowed to have multiple knots 0 and 1, and knots with single multiplicity in between. For such sequences, the following properties hold (properties of B-splines for more general knot sequences can be found in [dB01]).

- For $d = 1$, $\operatorname{span}\{B^k_{1,\mathbf{t}} : k\}$ is the space of piecewise constant functions w.r.t. the pieces $[t_i, t_{i+1})$. Let $\Pi^d(\mathrm{I})$ denote the space of polynomials of degree d on the interval I. For $d > 1$, $\operatorname{span}\{B^k_{d,\mathbf{t}} : k\}$ is the space of functions in $C^{d-2}([t_1, t_N))$ whose restriction to $[t_i, t_{i+1})$ is in $\Pi^{d-1}([t_i, t_{i+1}))$, and whose derivatives up to order $d-1-m_L$ (resp. $d-1-m_R$) vanish at the left (resp. right) boundary, where the multiplicity of the knot at 0 is $m_L + 1$, and the multiplicity of the knot at 1 is $m_R + 1$.
- The support of $B^k_{d,\mathbf{t}}$ is $[t_k, t_{k+d}]$. For all $x \in (t_k, t_{k+d})$, $B^k_{d,\mathbf{t}}(x) > 0$.
- The set of B-splines of order d on $\mathbf{t}$ form a partition of unity on the interval $(t_{d-1}, t_{N-d+1}]$, i.e., $\sum_k B^k_{d,\mathbf{t}}(x) = 1$.

Construction from [CDF92]

For $d > 0$, with $[\ell_1, \ell_2] := [-\lfloor d/2 \rfloor, \lceil d/2 \rceil]$, the mother scaling function ${}_d\varphi$ is defined as the cardinal B-spline ${}_d\varphi(x) = B^1_{d,(\ell_1,\ell_1+1,\ldots,\ell_2)}(x)$. This function is refinable, and its two-scale relation is known (see, e.g., [TtMvD00, CT99]) to be

$$ {}_d\varphi(x) = \sum_{k=\ell_1}^{\ell_2} a_k \, {}_d\varphi(2x-k), \quad \text{with} \quad a_k = 2^{1-d} \binom{d}{k-\ell_1}. $$

Since ${}_d\varphi(x)$ is a cardinal B-spline, its integer translations form a partition of unity. It follows that

$$1 = \int_0^1 1 \,\mathrm{d}x = \int_0^1 \sum_{k=1-\ell_2}^{-\ell_1} {}_d\varphi(x-k)\,\mathrm{d}x = \sum_{k=1-\ell_2}^{-\ell_1} \int_{-k}^{-k+1} {}_d\varphi(x)\,\mathrm{d}x = \int_{\ell_1}^{\ell_2} {}_d\varphi(x)\,\mathrm{d}x.$$

Using that ${}_d\varphi \geq 0$, we conclude that $\|{}_d\varphi\|_{L_1(\Omega)} = 1$.

One can verify that the function ${}_d\varphi(x)$ is symmetric around $\mu(d)/2$, and $a_k = a_{\mu(d)-k}$, with $\mu(d) := d \bmod 2$.

The challenge is to find a refinable dual scaling function which also satisfies Jackson and Bernstein estimates. In [CDF92] it was shown that for $\tilde{d} > d$ sufficiently large, and such that $d + \tilde{d}$ is even, there exists a function ${}_{d,\tilde{d}}\tilde{\varphi} \in L_2(\mathbb{R})$ with the following properties:

- ${}_{d,\tilde{d}}\tilde{\varphi}$ has support $[\tilde{\ell}_1, \tilde{\ell}_2] := [\ell_1 - \tilde{d} + 1, \ell_2 + \tilde{d} - 1]$.
- ${}_{d,\tilde{d}}\tilde{\varphi}$ is refinable, with refinement coefficients denoted by $\big(\tilde{a}_k\big)_{k=\tilde{\ell}_1}^{\tilde{\ell}_2}$.
- ${}_{d,\tilde{d}}\tilde{\varphi}$ is exact of order $\tilde{d}$.
- ${}_{d,\tilde{d}}\tilde{\varphi}$ is symmetric around $\mu(d)/2$, and $\tilde{a}_k = \tilde{a}_{\mu(d)-k}$.
- ${}_{d,\tilde{d}}\tilde{\varphi}$ and ${}_d\varphi$ form a dual pair.
- The set $\{{}_{d,\tilde{d}}\tilde{\varphi}(\cdot - k) \colon k \in \mathbb{Z}\}$ is *locally linearly independent*, i.e. for any open set $G \subset \mathbb{R}$, the set

  $$\big\{ {}_{d,\tilde{d}}\varphi(\cdot - k)\big|_G \colon \operatorname{supp} {}_{d,\tilde{d}}\varphi(\cdot - k) \cap G \neq \varnothing \big\}$$

  is linearly independent (see, e.g., [Sun91]).

Figure 2.1 illustrates some primal and dual scaling functions from [CDF92].

Regularity of the dual scaling functions

We will now determine a $\tilde{\gamma} > 0$ such that the nested sequence of spaces $\tilde{V}_{[0]} \subset \tilde{V}_{[1]} \subset \cdots$ satisfies a Bernstein estimate with parameter $\tilde{\gamma}$. To that end, we will determine the Sobolev regularity of the function ${}_{d,\tilde{d}}\tilde{\varphi}$ (and therefore also of the functions ${}_{d,\tilde{d}}\tilde{\varphi}_{[j,k]}$).

Proposition 2.2.4 (e.g. [Dah95, Met02])**.** *Let ${}_{d,\tilde{d}}\tilde{\varphi}$ have a Sobolev regularity $\tilde{\gamma}(d,\tilde{d}) := \sup\{s \colon {}_{d,\tilde{d}}\tilde{\varphi} \in H^s(\mathbb{R})\} > 0$. Then the nested sequence of spaces $(\tilde{V}_j)_j$ satisfies a Bernstein estimate with parameter $\tilde{\gamma}(d,\tilde{d})$.*

The Sobolev regularity of a refinable function can be computed using an algorithm presented in [Vil94]. An implementation of this algorithm was presented in [BDM00, Thi04]. It was noted in [Thi04] that only the values of $\tilde{\gamma}(d,d)$ are necessary to compute the regularity of scaling functions ${}_{d,\tilde{d}}\tilde{\varphi}$ for $\tilde{d} \geq d$. Other values can be recovered using

$$\tilde{\gamma}(d,\tilde{d}) = \tilde{\gamma}\Big(\frac{d+\tilde{d}}{2}, \frac{d+\tilde{d}}{2}\Big) + \frac{\tilde{d}-d}{2}.$$

The Sobolev regularity of ${}_{d,d}\tilde{\varphi}$ is given in Table 2.1. For a range of d, $\tilde{d}$, the regularity is depicted in Figure 2.2. These results confirm that the scaling function ${}_{4,4}\tilde{\varphi}$ is not in $L_2(\mathbb{R})$, as conjectured in [Pri06]. Note that for higher primal

d	$\tilde\gamma(d,d)$	d	$\tilde\gamma(d,d)$	d	$\tilde\gamma(d,d)$	d	$\tilde\gamma(d,d)$
1	0.500	6	−1.138	11	−3.717	16	−6.415
2	0.441	7	−1.637	12	−4.250	17	−6.962
3	0.175	8	−2.147	13	−4.787	18	−7.511
4	−0.207	9	−2.665	14	−5.327	19	−8.062
5	−0.656	10	−3.189	15	−5.870	20	−8.614

Table 2.1: Sobolev regularity of the functions ${}_{d,d}\tilde\varphi(x)$ for $d = 1, \dots, 20$.

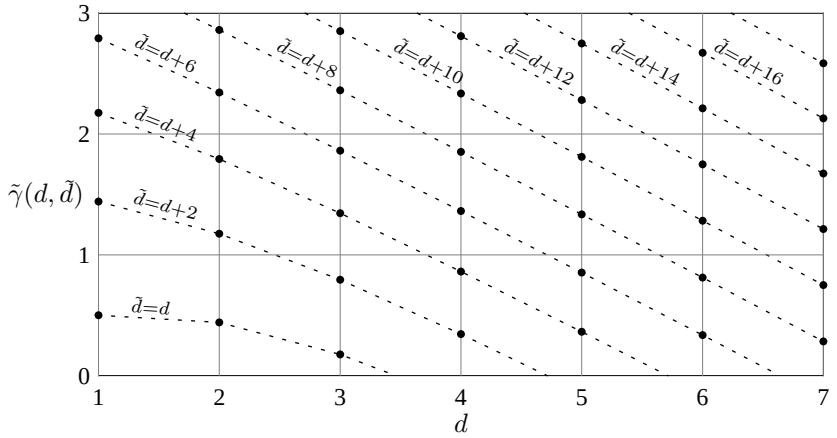

Figure 2.2: Sobolev regularity of the functions ${}_{d,\tilde d}\tilde\varphi(x)$ for $d \le 7$, $\tilde d$ such that $0 \le \tilde\gamma(d,\tilde d) \le 3$.

orders d, the dual order has to be increasingly large to retain even membership of $L_2(\mathbb{R})$ of the dual scaling functions.

In [CDF92], a lower bound for $\tilde\gamma(d,\tilde d)$ was constructed that for every d grows linearly with $\tilde d$. The results from Table 2.1 suggest that $\tilde\gamma(d,d) > 1.0524 - 0.5524d$ and thus $\gamma(d,\tilde d) > 1.0524 - 0.2762(d+\tilde d) + (\tilde d - d)/2$.

In the remainder of this chapter, we will take $d, \tilde d$ arbitrary but fixed (still such that $\tilde d \ge d \ge 1$, and $d+\tilde d$ is even), and we will drop them from the notation. The role of $\varphi_{[j,k]}$, $\tilde\varphi_{[j,k]}$ will be played by the functions from [CDF92].

2.3 Biorthogonal multiresolution analyses on $(0,1)$

In this section, we will construct a biorthogonal MRA for $L_2(\mathrm{I})$, where $\mathrm{I} := (0,1)$. We will try to maintain as many properties as possible from the construction on the line. On every level j, only a finite number of scaling functions will be defined: the set $\Phi_j = \{\varphi_{j,k} : k \in I_j\}$, for some finite *index set* I_j. Clearly, the requirement that each scaling function is a translate of a mother scaling function has to be dropped. Instead, we will require that, corresponding to (2.10), for some matrix $\mathbf{M}_{j,0} \in \mathbb{R}^{\#I_{j+1} \times \#I_j}$ such that

$$\Phi_j^{\mathsf T} = \Phi_{j+1}^{\mathsf T} \mathbf{M}_{j,0}.$$

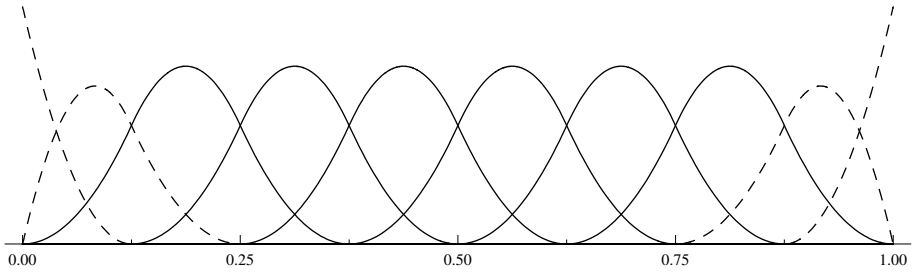

Figure 2.3: The spline basis Φ_3 for $d = 3$. The dashed functions are boundary functions.

2.3.1 Primal side

We choose the primal space to be the standard spline space with respect to the knot sequence

$$\mathbf{t}_j := \{\underbrace{0,\dots,0}_{d \text{ times}}, 2^{-j},\dots,1-2^{-j},\underbrace{1,\dots,1}_{d \text{ times}}\}.$$

Note that this spline space is the same space as the space that is obtained by restricting the primal space $V_{[j]} = \operatorname{span}\Phi_{[j]}$ from [CDF92] to the interval. In particular, the Jackson and Bernstein properties are conserved.

As a basis, we choose the primal basis Φ_j to be the B-spline basis:

$$\Phi_j := \{\varphi_{j,k}(x) := B^{k+\ell_2}_{d,\mathbf{t}_j}(x) \colon k \in I_j\},$$

where I_j is defined as $I_j := \{1-\ell_2,\dots,2^j-\ell_1-1\}$. This basis is illustrated in Figure 2.3. The cardinality of this set is $2^j + d - 1$. For those j,k for which the support of $\varphi_{[j,k]}$ is entirely contained in $[0,1]$, viz. $k \in \{-\ell_1,\dots,2^j-\ell_2\}$, it holds that $\varphi_{j,k} = \varphi_{[j,k]}$. Redefining $\Phi_{[j]}$ as $\Phi_{[j]} := \{\varphi_{[j,k]}|_{[0,1]} \colon k \in I_j\}$ we have

$$\Phi_j^{\mathsf{T}} = \Phi_{[j]}^{\mathsf{T}}\mathbf{R}_j, \tag{2.22}$$

where $\mathbf{R}_j$ is the invertible basis transformation from $\Phi_{[j]}$ to Φ_j. This matrix can be computed, for example, with the Oslo algorithm (see [dB01]).

Remark 2.3.1. In the construction of [DKU99], the primal space is the spline space w.r.t. the knot sequence

$$\{\underbrace{0,\dots,0}_{d \text{ times}}, r2^{-j}, (r+1)2^{-j},\dots,1-(r+1)2^{-j}, 1-r2^{-j},\underbrace{1,\dots,1}_{d \text{ times}}\}, \tag{2.23}$$

for some integer $r \geq d-1$. For $d > 2$, the dimension of this space is smaller than the dimension of the primal space of our construction. Away from the boundary, the functions obtained from both constructions coincide.

The scaling functions satisfy the symmetry

$$\varphi_{j,k}(x) = \varphi_{j,2^j-k-\mu(d)}(1-x). \tag{2.24}$$

With $(\cdot)^{\dotplus}$ denoting the operation of reversing the rows and columns of a matrix, i.e. for an $n \times m$ matrix $\mathbf{A}$, $\mathbf{A}^{\dotplus}_{p,q} := \mathbf{A}_{n-p,m-q}$, this leads to the symmetry $\mathbf{M}^{\dotplus}_{j,0} = \mathbf{M}_{j,0}$.

2.3.2 Dual side

We move on to the dual side. We will try to maintain as many as possible functions from the construction from [CDF92], that is, we will keep all functions $\varphi_{[j,k]}$ whose supports are contained in $[0,1]$. We will supplement these collections with linear combinations of functions $\varphi_{[j,k]}$ restricted to $(0,1)$ so that *nesting* and *polynomials exactness* are maintained. In the following $\tilde{\Phi}_{[j]}$ will denote the restrictions of dual CDF functions to the interval:

$$\tilde{\Phi}_{[j]} := \{\tilde{\varphi}_{[j,k]}|_{[0,1]} \colon k \in \{1-\tilde{\ell}_2, \dots, 2^j - \tilde{\ell}_1 - 1\}\}. \tag{2.25}$$

Because the translations of $\tilde{\varphi}$ are locally linearly independent, the collection $\tilde{\Phi}_{[j]}$ is linearly independent. This was first shown in [Mey91] and [LR91].

A naive approach to creating a dual basis on the interval could be to just take $\tilde{\Phi}_{[j]}$. However, the cardinality of $\tilde{\Phi}_{[j]}$ is larger than that of the set Φ_j that was constructed in the previous subsection. This is due to the fact that the supports of the dual functions on $\mathbb{R}$ are larger than those of the primal functions (cf. Figure 2.1).

Remark 2.3.2. A less naive approach would be to restrict all primal scaling functions to the interval, and also restrict the corresponding dual functions to the interval. Indeed, these sets now have the same cardinality and the functions have the desired regularity. However, this does not necessarily preserve the polynomial exactness on the dual side.

We follow a different approach. To distinguish boundary functions from functions whose support does not intersect a boundary, we will first create three index sets for the dual side, one for both sets of boundary functions, and one for all inner functions. Note that, because of the biorthogonality condition, the cardinality of the union of these sets needs to be that of I_j. For $d \geq 2$, we define $\tilde{I}_j := \tilde{I}_j^L \cup \tilde{I}_j^0 \cup \tilde{I}_j^R$, with

$$\begin{aligned}
\tilde{I}_j^L &:= \{1-\ell_2, \dots, -\tilde{\ell}_1 - 1\}, \\
\tilde{I}_j^0 &:= \{-\tilde{\ell}_1, \dots, 2^j + \tilde{\ell}_1 - \mu(d)\}, \\
\tilde{I}_j^R &:= \{2^j + \tilde{\ell}_1 - \mu(d) + 1, \dots, 2^j - \ell_1 - 1\}.
\end{aligned}$$

For $d = 1$ we define $\tilde{I}_j^L$ and $\tilde{I}_j^R$ to be empty, and use the same definition for the set $\tilde{I}_j^0$.

Using $\ell_2 = \mu(d) - \ell_1$, it is clear that $\#\tilde{I}_j^L = \#\tilde{I}_j^R$. Moreover, we have $\tilde{I}_j = I_j$. The cardinality of the sets $\tilde{I}_j^L$ and $\tilde{I}_j^R$ is fixed, only $\tilde{I}_j^0$ grows with j. As mentioned, the inner scaling functions will be those from [CDF92]:

$$\tilde{\varphi}_{j,k} = \tilde{\varphi}_{[j,k]} \quad \text{for } k \in \tilde{I}_j^0. \tag{2.26}$$

All of these functions are entirely supported in $[0,1]$. We will construct dual boundary scaling functions in such a way that the approximation properties of the constructed basis will be inherited from the corresponding dual scaling functions on $\mathbb{R}$.

We will construct a dual basis $\tilde{\Phi}_j^{\text{init}} := \{\tilde{\varphi}_{j,k}^{\text{init}} \colon k \in \tilde{I}_j\}$ of which the boundary functions will initially not be biorthogonal to the primal functions. However,

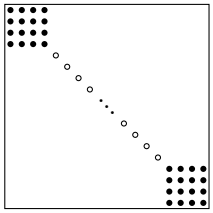

Matrix 2.1: Nonzero pattern of the matrix $\langle \Phi_j, \tilde{\Phi}_j^{\text{init}} \rangle$. Open dots represent ones.

$\tilde{\Phi}_j^{\text{init}}$ will be constructed to be uniformly local, in such a way that the nonzero structure of the *biorthogonalization matrix* $\langle \Phi_j, \tilde{\Phi}_j^{\text{init}} \rangle$ is as sketched in Matrix 2.1, where moreover the boundary blocks are *independent of* j (the size of the boundary blocks will depend on d and $\tilde{d}$, the order of polynomial exactness on the primal and dual side). The dual functions are now constructed as

$$\tilde{\Phi}_j := \langle \Phi_j, \tilde{\Phi}_j^{\text{init}} \rangle^{-1} \tilde{\Phi}_j^{\text{init}}. \tag{2.27}$$

Now the collections Φ_j and $\tilde{\Phi}_j$ are biorthogonal, and both collections are uniformly local and uniformly bounded, so that by Lemma 2.1.1 they form uniform Riesz bases.

In view of (2.27), it is necessary that the boundary blocks of $\langle \Phi_j, \tilde{\Phi}_j^{\text{init}} \rangle$ are uniformly *invertible*. In [DKU99], for a specific choice of boundary functions, it was proven to be so. Our construction has more boundary functions (cf. Remark 2.3.1). It is *a priori* not clear that the primal and dual boundary functions are not orthogonal. However, *a posteriori* the boundary blocks of the biorthogonalization matrix can easily be checked to be invertible. Since these blocks are independent of j, this needs to be checked only once. In subsection 2.3.4, we propose a way to compute these boundary blocks for the construction that follows. In all cases we have encountered, the boundary block of $\langle \Phi_j, \tilde{\Phi}_j^{\text{init}} \rangle$ was invertible.

We will, for now, only construct the boundary scaling functions near one boundary of the interval, and construct the ones near the other boundary by symmetry. In order to do this, the left and right boundary index sets should have an empty intersection. This leads to the requirement $-\tilde{\ell}_1 - 1 < 2^j + \tilde{\ell}_1 - \mu(d) + 1$, or equivalently

$$j \geq \lceil \log_2(-2\tilde{\ell}_1 - 1 + \mu(d)) \rceil =: j_0. \tag{2.28}$$

Remark 2.3.3. In earlier works, e.g. [DKU99, Pri06, BF03], it was required that constructed boundary functions do not overlap, which led to the requirement $j \geq \lceil \log_2(\ell_2 - \tilde{\ell}_1 - 1) + 1 \rceil$. The requirement we use, and which was also used in [Bur05], is less strict. The constructions in these earlier works can be improved by including lower levels.

The boundary functions $\{\tilde{\varphi}_{j,q}^{\text{init}} : q \in \tilde{I}_j^L\}$ will be created as linear combinations of the functions $\tilde{\varphi}_{[j,k]}$ whose support contains the point 0 in their interior, i.e. $k \in \{-\ell_2 + 1, -\tilde{\ell}_1 - 1\}$. That is, we look for certain c_{mq}, $q \in \tilde{I}_j^L$, independent of

the level j, such that

$$\tilde{\varphi}_{j,q}^{\text{init}} := \sum_{m=-\tilde{\ell}_2+1}^{-\tilde{\ell}_1-1} c_{mq}\tilde{\varphi}_{[j,m]}\big|_{[0,1]} \quad \text{for } q \in \tilde{I}_j^L. \tag{2.29}$$

For convenience, we will also state this in matrix notation. We define

$$\tilde{\boldsymbol{\Phi}}_{[j]}^L := \{\tilde{\varphi}_{[j,k]}\big|_{[0,\infty)} \colon -\tilde{\ell}_2+1 \le k \le -\tilde{\ell}_1-1\}, \tag{2.30}$$

$$\tilde{\boldsymbol{\Phi}}_j^L := \{\tilde{\varphi}_{j,k}^{\text{init}} \colon k \in \tilde{I}_j^L\}. \tag{2.31}$$

We also define the $(d+2\tilde{d}-3)\times(d+\tilde{d}-2)$ matrix $\tilde{\mathbf{C}}^L$, through $(\tilde{\mathbf{C}}^L)_{m,q} := c_{mq}$ for $m \in \{-\tilde{\ell}_2+1,\dots,-\tilde{\ell}_1-1\}$, $q \in \tilde{I}_j^L$. Now (2.29) can be stated as

$$(\tilde{\boldsymbol{\Phi}}_j^L)^{\mathsf{T}} = (\tilde{\boldsymbol{\Phi}}_{[j]}^L)^{\mathsf{T}}\tilde{\mathbf{C}}^L. \tag{2.32}$$

The following theorem tells how to choose the coefficients c_{mq} in such a way that the resulting boundary functions $\tilde{\boldsymbol{\Phi}}_j^L$ can be written as a linear combination of scaling functions on a higher level, so that the resulting spaces are nested.

Theorem 2.3.4. *Let the matrix $\tilde{\mathbf{A}} \in \mathbb{R}^{(d+2\tilde{d}-3)\times(d+2\tilde{d}-3)}$ be defined by*

$$(\tilde{\mathbf{A}})_{k,m} = \tilde{a}_{k-2m}, \qquad k,m \in \big\{-\tilde{\ell}_2+1,\dots,-\tilde{\ell}_1-1\big\}. \tag{2.33}$$

Then for $q \in \tilde{I}_j^L$, the function $\tilde{\varphi}_{j,q}^{\text{init}} := \sum_{m=-\tilde{\ell}_2+1}^{-\tilde{\ell}_1-1} c_{mq}\tilde{\varphi}_{[j,m]}\big|_{[0,1]}$ is in $\operatorname{span}\{\tilde{\varphi}_{j+1,k} \colon k \in \tilde{I}_{j+1}\}$ if and only if $\operatorname{span}\{c_{mk} \colon k \in \tilde{I}_j^L\}$ is an invariant subspace of $\tilde{\mathbf{A}}$.

Proof. Using the refinement equation (2.18) for the functions $\tilde{\varphi}_{[j,k]}$, we have

$$\tilde{\varphi}_{j,q}^{\text{init}} = 2^{-\frac{1}{2}} \sum_{m=-\tilde{\ell}_2+1}^{-\tilde{\ell}_1-1} c_{mq} \sum_{k=-\tilde{\ell}_2+1}^{\tilde{\ell}_2-2(\tilde{\ell}_1+1)} \tilde{a}_{k-2m}\tilde{\varphi}_{[j+1,k]}\big|_{[0,1]}.$$

The limits for the sum over k are found by summing only over those k for which $\tilde{a}_{k-2m} \neq 0$, and by using that $\tilde{\varphi}_{[j,k]}\big|_{[0,1]} = 0$ for $k < -\tilde{\ell}_2+1$. Reversing the order of summation and splitting the sum over k into two parts we get

$$\begin{aligned}\tilde{\varphi}_{j,q}^{\text{init}} = 2^{-\frac{1}{2}} \sum_{k=-\tilde{\ell}_2+1}^{-\tilde{\ell}_1-1} \tilde{\varphi}_{[j+1,k]}\big|_{[0,1]} \sum_{m=-\tilde{\ell}_2+1}^{-\tilde{\ell}_1-1} \tilde{a}_{k-2m}c_{mq} + \\ 2^{-\frac{1}{2}} \sum_{k=-\tilde{\ell}_1}^{\ell_2-2(\tilde{\ell}_1+1)} \tilde{\varphi}_{[j+1,k]} \sum_{m=-\tilde{\ell}_2+1}^{-\tilde{\ell}_1-1} \tilde{a}_{k-2m}c_{mq}.\end{aligned}$$

The second part is a linear combination of functions $\tilde{\varphi}_{[j+1,k]}$ with $k \in \tilde{I}_j^0$. By (2.26), these functions will be in $\operatorname{span}\{\tilde{\varphi}_{j+1,k} \colon k \in \tilde{I}_j^0\}$. Therefore, a sufficient and necessary condition for $\tilde{\varphi}_{j,q}$ to be in $\operatorname{span}\{\tilde{\varphi}_{j+1,k}^{\text{init}} \colon k \in \tilde{I}_{j+1}\}$ is that the first part is a linear combination of boundary scaling functions on level $j+1$. Denoting the q-th column of $\tilde{\mathbf{C}}^L$ by $\mathbf{c}_q$, with the matrix notation as above, this condition can be written as

$$2^{-\frac{1}{2}}\big(\tilde{\boldsymbol{\Phi}}_{[j+1]}^L\big)^{\mathsf{T}}\tilde{\mathbf{A}}\mathbf{c}_q \in \operatorname{span}\big\{\big(\tilde{\boldsymbol{\Phi}}_{[j+1]}^L\big)^{\mathsf{T}}\mathbf{c}_k \colon k \in \tilde{I}_j^L\big\}. \tag{2.34}$$

Since the elements of $\tilde{\Phi}^L_{[j+1]}$ are linearly independent, this is equivalent to

$$\tilde{\mathbf{A}}\mathbf{c}_q \in \operatorname{span}\{\mathbf{c}_k \colon k \in \tilde{I}^L_j\}, \quad \text{or } \operatorname{col}\tilde{\mathbf{A}}\tilde{\mathbf{C}}^L \subset \operatorname{col}\tilde{\mathbf{C}}^L,$$

where $\operatorname{col}(\,\cdot\,)$ denotes the column space. This corresponds to the space $\operatorname{col}\tilde{\mathbf{C}}^L = \operatorname{span}\{\tilde{\mathbf{c}}_k \colon k \in \tilde{I}^L_j\}$ being an invariant subspace of $\tilde{\mathbf{A}}$. ◊

We want to retain the polynomial exactness of the basis (so that Theorem 2.1.2 can be applied). To this end, we make a specific choice for some of the boundary functions, to ensure that $x^r \in \operatorname{span}\tilde{\Phi}^{\text{init}}_j$, for $r \in \{0,\dots,\tilde{d}-1\}$.

The following lemma was proven in [DKU99]. For convenience, we include a short proof.

Lemma 2.3.5. *For $0 \le r \le \tilde{d}-1$, and $\alpha_{m,r}$ as in Lemma 2.2.3, the vector $\boldsymbol{\alpha}^L_r := \{\alpha_{k,r} \colon k \in \{-\tilde{\ell}_2+1,\dots,-\tilde{\ell}_1-1\}\}$ is an eigenvector of $\tilde{\mathbf{A}}$, with corresponding eigenvalue 2^{-r}.*

Proof. Intuitively, this follows from the fact that monomials are included in the span of both $\tilde{\Phi}_{[j]}$ and $\tilde{\Phi}_{[j+1]}$. More precisely, analogously to (2.19) we have on the dual side

$$x^r = \sum_m 2^{-jr}2^{-j/2}\alpha_{m,r}\tilde{\varphi}_{[j,m]}(x).$$

Applying this on levels j and $j+1$, we have

$$x^r\big|_{[0,\infty)} = 2^{-j(r+1/2)} \quad \Big(\sum_{m=-\tilde{\ell}_2+1}^{-\tilde{\ell}_1-1} \alpha_{m,r}\tilde{\varphi}_{[j,m]}(x)\big|_{[0,\infty)} + \sum_{m>-\tilde{\ell}_1-1} \alpha_{m,r}\tilde{\varphi}_{[j,m]}(x)\Big), \tag{2.35}$$

$$x^r\big|_{[0,\infty)} = 2^{-(j+1)(r+1/2)}\Big(\sum_{k=-\tilde{\ell}_2+1}^{-\tilde{\ell}_1-1} \alpha_{k,r}\tilde{\varphi}_{[j+1,k]}(x)\big|_{[0,\infty)} + \sum_{k>-\tilde{\ell}_1-1} \alpha_{k,r}\tilde{\varphi}_{[j+1,k]}(x)\Big). \tag{2.36}$$

The first of these equations can be rewritten using the refinement equation (2.18):

$$\begin{aligned} x^r\big|_{[0,\infty)} = 2^{-j(r+1/2)}2^{-1/2}\Big(&\sum_{m=-\tilde{\ell}_2+1}^{-\tilde{\ell}_1-1} \alpha_{m,r} \sum_{k=-\tilde{\ell}_2+1}^{-\tilde{\ell}_1-1} \tilde{a}_{k-2m}\tilde{\varphi}_{[j+1,k]}\big|_{[0,\infty)} \\ &+ \sum_{m=-\tilde{\ell}_2+1}^{-\tilde{\ell}_1-1} \alpha_{m,r} \sum_{k>-\tilde{\ell}_1-1} \tilde{a}_{k-2m}\tilde{\varphi}_{[j+1,k]} + \sum_{m>-\tilde{\ell}_1-1} \alpha_{m,r} \sum_{k>-\tilde{\ell}_1-1} a_{k-2m}\tilde{\varphi}_{[j+1,k]}\Big). \end{aligned} \tag{2.37}$$

We now compare (2.36) with (2.37), and focus on the first summation in both equations. Because the functions $\{\tilde{\varphi}_{[j+1,k]}\big|_{[0,\infty)} \colon k > -\tilde{\ell}_2+1\}$ form an independent set, these summations must be equal element-wise. This means that for $k \in \{-\tilde{\ell}_2+1, -\tilde{\ell}_1-1\}$,

$$2^{-j(r+1/2)}2^{-1/2} \sum_{m=-\tilde{\ell}_2+1}^{-\tilde{\ell}_1-1} \tilde{a}_{k-2m}\alpha_{m,r} = 2^{-(j+1)(r+1/2)}\alpha_{k,r},$$

must hold. This is equivalent to $\tilde{\mathbf{A}}\boldsymbol{\alpha}^L_r = 2^{-r}\boldsymbol{\alpha}^L_r$. ◊

In [DKU99], the construction of dual scaling function ends here: the cardinality of the dual space is equal that of the primal space from Remark 2.3.1. Because the primal space of our construction is larger, we have to add some more boundary functions.

Remark 2.3.6. In [Pri06], the primal space is the same as in the present construction, and so also extra dual scaling functions had to be added to V_j. These were chosen from $\tilde{V}_{j+1}$ and higher levels to $\tilde{V}_j$. This way, the nesting remains intact. The extra functions in this construction were not restrictions of linear combinations of scaling functions on the line.

We will use Theorem 2.3.4 to create extra scaling functions. The total number of dual boundary functions to create near the left boundary is $\#\tilde{I}_j^L = d + \tilde{d} - 2$. We want to try every possible invariant subspace of $\tilde{\mathbf{A}}$ of this dimension which contains the vectors $\boldsymbol{\alpha}_r^L$. As there are $\tilde{d}$ such vectors, we need to add a space of dimension $d-2$. From this we conclude that for $d = 2$ no extra basis functions need to be added.

Remark 2.3.7. Also for $d = 1$ dual bases can be constructed on the interval. A problem there is that $\#\tilde{I}_j^L < \tilde{d}$. A solution is to expand $\tilde{I}_j^L$ with one index from $\tilde{I}_j^0$, i.e., to regard one function whose support is contained in $[0,1]$ as a boundary function. This increases the dimension of $\#\tilde{I}_j^L$ to $\tilde{d}$. Now the matrix $\tilde{\mathbf{A}}$ from Theorem 2.3.4 can be adapted to this situation by allowing k, m from (2.33) to be in the index set $\{-\ell_2+1,\dots,-\ell_1\}$. With this adapted matrix, the theorem still holds, and, with a corresponding modification, also Lemma 2.3.5 holds.

Every k-dimensional invariant subspace of a diagonalizable matrix is spanned by k eigenvectors. We have checked numerically that for all $2 < d \le \tilde{d} \le 100$, all eigenvalues of $\tilde{\mathbf{A}}$ are indeed simple. For $(d,\tilde{d}) = (2,2)$, an eigenvalue has double algebraic multiplicity, however for $d = 2$ there is no need to add additional boundary functions.

The matrix $\tilde{\mathbf{A}}$ has $d+2\tilde{d}-3$ eigenvectors, of which $\tilde{d}$ correspond to the vectors $\{\boldsymbol{\alpha}_r^L : 0 \le r \le \tilde{d}-1\}$. We have to choose $\#\tilde{I}_j - \tilde{d} = d-2$ other eigenvectors as columns of $\tilde{\mathbf{C}}^L$, leaving $\binom{d+\tilde{d}-3}{d-2}$ options. The freedom here can be used to optimize quantities such as the condition number.

Scaling functions near the right boundary are now constructed using the following lemma.

Lemma 2.3.8 ([DKU99])**.** *Let $\tilde{\boldsymbol{\Phi}}_j^R = \{\tilde{\varphi}_{j,k}^{\mathit{init}} : k \in I_j^{\mathbb{R}}\}$, the set of initial dual scaling functions near the right boundary, be defined by*

$$(\tilde{\boldsymbol{\Phi}}_j^R)^{\mathsf{T}} = (\tilde{\boldsymbol{\Phi}}_{[j]}^R)^{\mathsf{T}} \tilde{\mathbf{C}}^R, \quad \textit{with } \tilde{\mathbf{C}}^R := (\tilde{\mathbf{C}}^L)^{\dotplus},$$

where $\tilde{\boldsymbol{\Phi}}_{[j]}^R$ is defined analogously to (2.30)*. Then the dual scaling functions satisfy the same symmetry relation as the primal scaling functions, viz.* (2.24)*.*

The set of initial dual scaling functions $\tilde{\boldsymbol{\Phi}}_j^{\text{init}}$ is now defined as

$$(\tilde{\boldsymbol{\Phi}}_j^{\text{init}})^{\mathsf{T}} := \tilde{\boldsymbol{\Phi}}_{[j]}^{\mathsf{T}} \tilde{\mathbf{R}}_j^{\text{init}}, \tag{2.38}$$

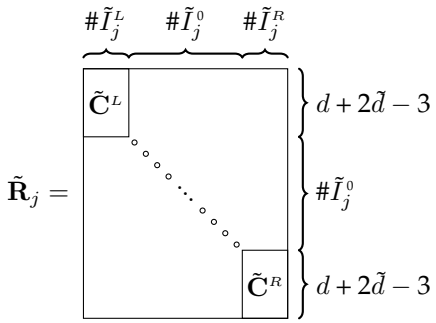

Figure 2.4: Nonzero pattern of the matrix $\tilde{\mathbf{R}}_j$. Open dots represent ones.

where the matrix $\tilde{\mathbf{R}}_j^{\text{init}}$ is formed as in Figure 2.4. With the biorthogonalization step (2.27), the dual scaling functions can be written as

$$\tilde{\Phi}_j^{\mathsf{T}} = \tilde{\Phi}_{[j]}^{\mathsf{T}} \tilde{\mathbf{R}}_j, \quad \text{with } \tilde{\mathbf{R}}_j := \tilde{\mathbf{R}}_j^{\text{init}} \langle \Phi_j, \tilde{\Phi}_j^{\text{init}} \rangle^{-\mathsf{T}}. \tag{2.39}$$

We have shown that the scaling functions $\tilde{\Phi}_j$ can be written as a linear combination of scaling functions on a higher level. In order to perform computations with this basis, it is necessary to have available the coefficients of this linear combination. These can be computed with the following lemma.

Lemma 2.3.9. *The dual refinement matrix $\tilde{\mathbf{M}}_{j,0}$ can be computed as*

$$\tilde{\mathbf{M}}_{j,0} = \mathbf{R}_{j+1} \langle \Phi_{[j+1]}, \tilde{\Phi}_{[j+1]} \rangle \tilde{\mathbf{M}}_{[j,0]} \tilde{\mathbf{R}}_j.$$

Proof. We use the relation $\tilde{\mathbf{M}}_{j,0} = \langle \Phi_{j+1}, \tilde{\Phi}_j \rangle$. Filling in (2.39) and its analogon on the primal side (2.22), we have

$$\tilde{\mathbf{M}}_{j,0} = \langle \mathbf{R}_{j+1}^{\mathsf{T}} \Phi_{[j+1]}, \tilde{\Phi}_{[j]} \rangle \tilde{\mathbf{R}}_j = \mathbf{R}_{j+1}^{\mathsf{T}} \langle \Phi_{[j+1]}, \tilde{\Phi}_{[j+1]} \rangle \tilde{\mathbf{M}}_{j,0} \tilde{\mathbf{R}}_j,$$

where we have used the refinement equation for $\tilde{\Phi}_{[j]}$. ◊

The following proposition concludes the construction of dual scaling functions.

Proposition 2.3.10. *Let the columns of $\tilde{\mathbf{C}}^L$ be eigenvectors of $\tilde{\mathbf{A}}$, including the vectors $\boldsymbol{\alpha}_r^L$, for $r = 0, \ldots, \tilde{d} - 1$. Then the spaces $\tilde{V}_j$ spanned by $\tilde{\Phi}_j^{init}$, or equivalently by $\tilde{\Phi}_j$, are nested, and exact of order $\tilde{d}$.*

2.3.3 Wavelets

In this section, we will construct uniformly local wavelets forming a basis for $V_{j+1} \cap \tilde{V}_j^{\perp}$, by creating a uniformly local initial stable completion, as discussed at the end of Section 2.1. We will make sure that these wavelets satisfy the same symmetry property as the scaling functions;

$$\psi_{j,k}(x) = \psi_{j,2^j - k}(1 - x). \tag{2.40}$$

Because the scaling functions Φ_{j+1} satisfy the symmetry (2.24), this symmetry is satisfied if $\mathbf{M}_{j,1}^{\dotplus} = \mathbf{M}_{j,1}$. Another restriction we impose is that for as many

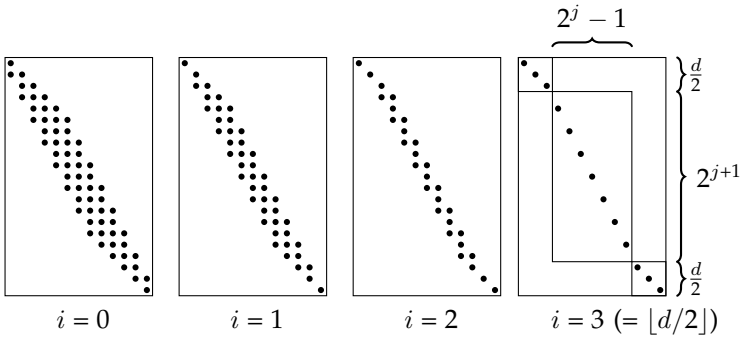

Figure 2.5: Nonzero structure of the matrix $\mathbf{M}_{3,0}^{(i)}$ for $d = 6$.

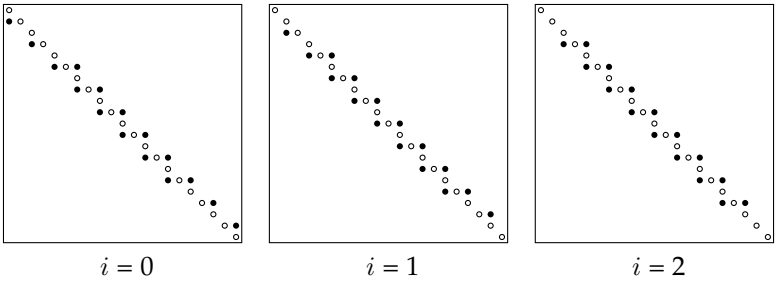

Figure 2.6: Nonzero structure of the matrix $\mathbf{H}_3^{(i)}$ and $\left(\mathbf{H}_3^{(i)}\right)^{-1}$ for $d = 6$. Open dots represent ones.

as possible wavelets, we have $\psi_{j,k} = \psi_{[j,k]}$, i.e., for wavelets that are entirely supported in $[0, 1]$, we want to reconstruct the wavelets from [CDF92].

The construction of an initial stable completion in this section follows the lines of [DM93a]. The general idea is to factorize the matrix $\mathbf{M}_{j,0}$ which will lead to a construction for $\mathbf{M}_{j,1}^{\text{init}}$. We briefly recall the main results from the last part of Section 2.1.

Proposition 2.3.11. *Given biorthogonal multiresolution analyses $(V_j)_j$, $(\tilde{V}_j)_j$, with bases Φ_j, $\tilde{\Phi}_j$, and a primal refinement matrix $\mathbf{M}_{j,0}$. Let $\mathbf{M}_{j,1}^{init}$ satisfy the following:*

- *$[\mathbf{M}_{j,0}\ \ \mathbf{M}_{j,1}^{init}]$ is uniformly bounded, invertible and uniformly sparse.*
- *$[\mathbf{M}_{j,0}\ \ \mathbf{M}_{j,1}^{init}]^{-1}$ is uniformly sparse.*

Furthermore, let the initial stable completion Ψ_j^{init} be defined through $(\Psi_j^{init})^\mathsf{T} := \tilde{\Phi}_{j+1}^\mathsf{T} \mathbf{M}_{j,1}^{init}$. Then the set $\Psi_j = \Psi_j^{init} - \langle \Psi_j^{init}, \tilde{\Phi}_j \rangle \Phi_j$, i.e. $\Psi_j^\mathsf{T} = \Phi_{j+1}^\mathsf{T} \mathbf{M}_{j,1}$, with $\mathbf{M}_{j,1} = (\mathbf{I} - \mathbf{M}_{j,0}\tilde{\mathbf{M}}_{j,0}^\mathsf{T})\mathbf{M}_{j,1}^{init}$, is a uniformly local uniform L_2(I)-Riesz basis for $V_{j+1} \cap \tilde{V}_j^\perp$, and the set $\tilde{\Psi}_j$ defined by $[\tilde{\Phi}_j\ \ \tilde{\Psi}_j] = \tilde{\Phi}_{j+1}^\mathsf{T}[\mathbf{M}_{j,0}\ \ \mathbf{M}_{j,1}]^{-1}$ is a uniformly local uniform Riesz basis for $\tilde{V}_{j+1} \cap V_j^\perp$.

For $i = 0, \ldots, \lfloor d/2 \rfloor$, we define the intermediate matrices $\mathbf{M}_j^{(i)}$ through $\mathbf{M}_j^{(0)} :=$

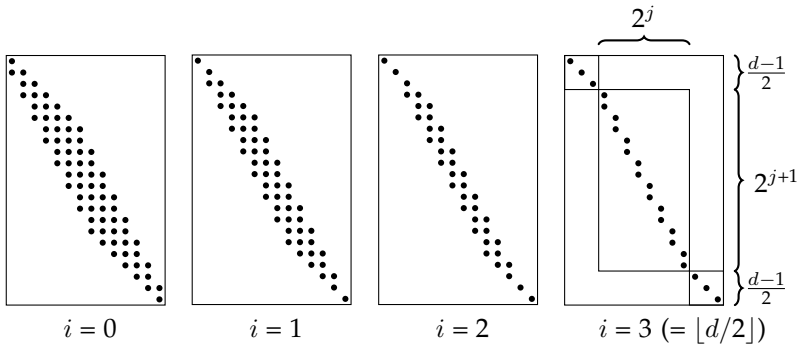

Figure 2.7: Nonzero structure of the matrix $\mathbf{M}_{3,0}^{(i)}$ for $d = 7$.

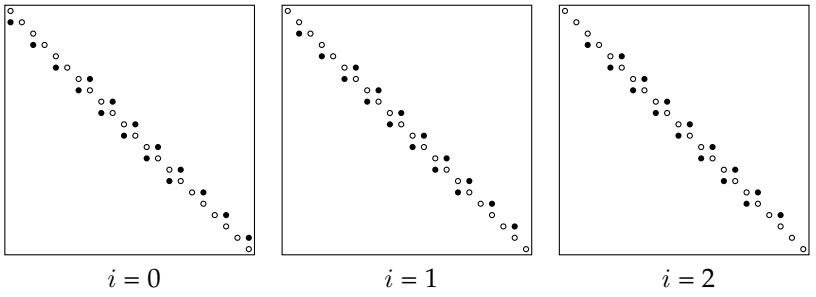

Figure 2.8: Nonzero structure of the matrix $\mathbf{H}_3^{(i)}$ and $\left(\mathbf{H}_3^{(i)}\right)^{-1}$ for $d = 7$. Open dots represent ones.

$\mathbf{M}_{j,0}$, $\mathbf{M}_j^{(i)} := \mathbf{H}_j^{(i-1)}\mathbf{M}_j^{(i-1)}$, where the matrices $\mathbf{H}_j^{(i)}$ will be constructed to reduce the number of nonzeros of $\mathbf{M}_j^{(i)}$ for increasing i (see Figure 2.5 and Figure 2.7). The following matrices $\mathbf{H}_j^{(i)}$ possess this property.

Definition 2.3.12. For $i = 0, \ldots, \lfloor d/2 \rfloor - 1$, we define the matrices $\mathbf{H}_j^{(i)} = (\mathbf{H}_j^{(i)})_{p,q}$ for $p, q \in I_{j+1}$, through

$$\begin{aligned}
\left(\mathbf{H}_j^{(i)}\right)_{p,p+1} &= \frac{(\mathbf{M}_j^{(i)})_{p,(p-\ell_2+i)/2}}{(\mathbf{M}_j^{(i)})_{p+1,(p-\ell_2+i)/2}} && \text{if } p - \ell_2 + i \text{ is even and} \\
& && p \in \{1 - \ell_2 + i, \ldots, 2^j - \ell_1 - d + i\}, \\
\left(\mathbf{H}_j^{(i)}\right)_{p+1,p} &= \frac{(\mathbf{M}_j^{(i)})_{p,(p-\ell_1-i)/2}}{(\mathbf{M}_j^{(i)})_{p-1,(p-\ell_1-i)/2}} && \text{if } p - \ell_1 - i \text{ is even and} \\
& && p \in \{d - \ell_2 - i, \ldots, 2^j - \ell_1 - 1 - i\}, \\
\left(\mathbf{H}_j^{(i)}\right)_{p,q} &= 1 && \text{if } p = q, \\
\left(\mathbf{H}_j^{(i)}\right)_{p,q} &= 0 && \text{otherwise.}
\end{aligned}$$

Away from the boundaries, this definition corresponds to the adaptation of the algorithm from [DM93a] introduced in [Har01]. The aim of this adaptation is to maintain the symmetry (2.40). We adopt this method, but have changed the

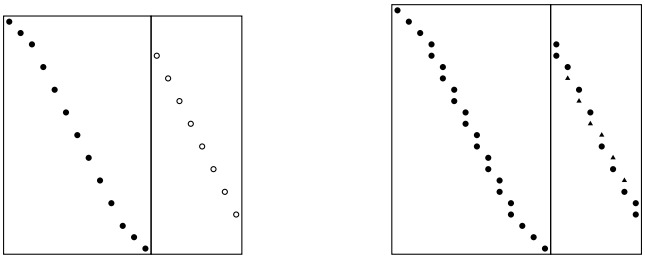

Figure 2.9: The matrix $\left[\mathbf{M}_j^{(\lfloor d/2 \rfloor)} \;\; \mathbf{F}_j\right]$ for even d (left) and odd d (right). Open dots represent ones, triangles represent minus the other nonzero in the column.

notation to unify the treatment of even and odd d. It was proven in [DM93a, Har01] that the procedure sketched above does not break down. An essential ingredient in this proof is that the matrices $\mathbf{M}_{j,0}^{(i)}$ are *totally positive*, meaning that the determinant of any square submatrix is nonnegative. Specifically, we have the following lemma.

Lemma 2.3.13. *The matrix $\mathbf{M}_j^{(i)}$ has a nonzero element at location (p, q) if and only if one of the following is true:*

- $q \in \{-\ell_2 + 1 + i, \ldots, 2^j - \ell_1 - 1 - i\}$ *and* $\max(\ell_1 + 2q + i, q) \le p \le \min(\ell_2 + 2q - i, q + 2^j)$,
- $q \notin \{-\ell_2 + 1 + i, \ldots, 2^j - \ell_1 - 1 - i\}$ *and* $p = q$.

The nonzero structure of $\mathbf{H}_j^{(i)}$ is sketched in Figure 2.6 and Figure 2.8, for even and odd d, respectively. In Figure 2.5 and Figure 2.7, the nonzero structure of the matrices $\mathbf{M}_j^{(i)}$ are sketched, for even and odd d, respectively.

As a consequence of Lemma 2.3.13, the matrices $\mathbf{H}_j^{(i)}$ introduced above are well-defined. These matrices satisfy the symmetry $\mathbf{H}_j^{(i)} = (\mathbf{H}_j^{(i)})^{\dagger\dagger}$. Their inverses have the same nonzero structure, specifically their inverses are uniformly sparse in j. Moreover, away from the boundaries, the matrices $\mathbf{H}_j^{(i)}$ are repetitive: all off-diagonal elements are equal. This follows from the structure of $\mathbf{M}_{j,0}$. As a consequence, for odd d, away from the boundaries, the two elements in the columns of $\mathbf{M}_{j,0}^{(\lfloor d/2 \rfloor)}$ are equal.

Note that

$$\mathbf{M}_{j,0} = \left(H_j^{(0)}\right)^{-1} \cdots \left(H_j^{(\lfloor d/2 \rfloor - 1)}\right)^{-1} \mathbf{M}_j^{(\lfloor d/2 \rfloor)},$$

which is the factorization announced earlier.

To construct an initial stable completion, we will construct a matrix $\mathbf{F}_j$ such that the properties of Proposition 2.3.11, with $\mathbf{M}_{j,0}$ replaced by $\mathbf{M}_j^{(\lfloor d/2 \rfloor)}$ and $\mathbf{M}_{j,1}^{\text{init}}$ replaced by $\mathbf{F}_j$, are satisfied. Because the matrix $\mathbf{M}_j^{(\lfloor d/2 \rfloor)}$ has very few nonzeros, it is easy to construct such a matrix.

For even d, we define the matrix $\mathbf{F}_j \in \mathbb{R}^{(2^{j+1}+d-1),2^j}$ through $(\mathbf{F}_j)_{p,q} := \delta_{p,2q}$, for $p \in I_{j+1}$, $q \in \{1, \ldots, 2^j\}$. With this definition, $[\mathbf{M}_{j,0}^{(d/2)} \;\; \mathbf{F}_j]$ is a permutation of a diagonal matrix, and thus satisfies all of the criteria of Proposition 2.3.11.

The structure of this matrix is illustrated in the left picture of Figure 2.9 (it also contains the matrix of the rightmost picture of Figure 2.5).

For odd d, the $(2^{j+1}+d-1)\times 2^j$ matrix $\mathbf{F}_j$ is defined through

$$\begin{aligned}
\big(\mathbf{F}_j\big)_{p,q} &= \big(\mathbf{M}_j^{(\frac{d-1}{2})}\big)_{p+1,q} && \text{if } p=2q \text{ and } q<2^j,\\
\big(\mathbf{F}_j\big)_{p,q} &= -\big(\mathbf{M}_j^{(\frac{d-1}{2})}\big)_{p-1,q} && \text{if } p=2q+1 \text{ and } q<2^j,\\
\big(\mathbf{F}_j\big)_{p,q} &= -\big(\mathbf{M}_j^{(\frac{d-1}{2})}\big)_{p+1,q} && \text{if } p=2q \text{ and } q\geq 2^j,\\
\big(\mathbf{F}_j\big)_{p,q} &= \big(\mathbf{M}_j^{(\frac{d-1}{2})}\big)_{p-1,q} && \text{if } p=2q+1 \text{ and } q\geq 2^j,
\end{aligned}$$

for $p\in I_{j+1}$ and $q\in\{0,\dots,2^j-1\}$. Because d is odd, the matrix $\mathbf{M}_j^{(\lfloor d/2\rfloor)}$ has an even number of columns. For any column in the first half of these columns containing only the elements $\left(\begin{smallmatrix}a\\b\end{smallmatrix}\right)$, there is a corresponding column $\left(\begin{smallmatrix}b\\-a\end{smallmatrix}\right)$ in the first half of the columns of $\mathbf{F}_j$. Similarly, for any column in the second half of columns of $\mathbf{M}_j^{(\lfloor d/2\rfloor)}$ containing only the elements $\left(\begin{smallmatrix}b\\a\end{smallmatrix}\right)$, there is a corresponding column with elements $\left(\begin{smallmatrix}-a\\b\end{smallmatrix}\right)$ in the second half of the columns of $\mathbf{F}_j$. The distinction between the first and second half of the columns is made to preserve the symmetry of $\mathbf{F}_j$. Now the matrix $[\mathbf{M}_{j,0}\ \mathbf{F}_j]$ is a permutation of a matrix consisting of invertible 2×2 blocks of the form $\left(\begin{smallmatrix}a&b\\b&-a\end{smallmatrix}\right)$ or $\left(\begin{smallmatrix}b&-a\\a&b\end{smallmatrix}\right)$ along the diagonal, and a small diagonal part near the boundaries (see the right picture in Figure 2.9). Thus, this matrix satisfies the conditions of Proposition 2.3.11.

The matrix $\mathbf{M}_{j,1}^{\text{init}}$ is now constructed as

$$\mathbf{M}_{j,1}^{\text{init}} := \big(\mathbf{H}_j^{(\lfloor d/2\rfloor-1)}\big)^{-1}\cdots\big(\mathbf{H}_j^{(0)}\big)^{-1}\mathbf{F}_j.$$

We now have

$$\big[\mathbf{M}_{j,0}\ \ \mathbf{M}_j^{\text{init}}\big] = \big(\mathbf{H}_j^{(0)}\big)^{-1}\cdots\big(\mathbf{H}_j^{(\lfloor d/2\rfloor-1)}\big)^{-1}\big[\mathbf{M}_j^{(\lfloor d/2\rfloor)}\ \ \mathbf{F}_j\big].$$

Because the matrices $\mathbf{H}_j^{(i)}$, $(\mathbf{H}_j^{(i)})^{-1}$ are all uniformly bounded and uniformly sparse, and the same holds for $[\mathbf{M}_j^{(\lfloor d/2\rfloor)}\ \ \mathbf{F}_j]$, the matrix on the left-hand side satisfies the conditions of Proposition 2.3.11. Thus, a stable completion can be constructed using Lemma 2.1.5. Because $\mathbf{F}_j=\mathbf{F}_j^{\perp}$, and the same symmetry holds for all of the $(\mathbf{H}_j^{(i)})^{-1}$, the resulting wavelets satisfy the symmetry (2.40).

Remark 2.3.14. In earlier works, e.g. [DKU99, Bar01, Har01], an initial stable completion was constructed in a similar fashion. However, only a certain submatrix of the primal refinement matrices in these works is totally positive (namely the submatrix obtained by disregarding the columns that correspond to boundary functions). This is circumvented by treating the boundary functions differently, leading to a more complicated factorization of $\mathbf{M}_{j,0}$. Away from the boundaries, the procedures coincide.

It was proven in [Har01, Pri06] that the internal wavelets are, up to scaling, the same as the wavelets from [CDF92].

2.3.4 Computation of biorthogonalization matrices

In order to create a biorthogonal basis, we assumed in subsection 2.3.2 (cf. (2.27)) the availability of the matrix $\langle \Phi_j, \tilde{\Phi}_j^{\text{init}} \rangle_{L_2(\mathrm{I})}$, with a structure as sketched in Matrix 2.1. In this section, we will present a method to compute this matrix. We assume that $j \geq j_0$, so that there is no function whose support contains both the left and right boundary in its interior.

Using the relations (2.22) and (2.39) we see that the biorthogonalization matrix can be computed as

$$\left\langle \Phi_j, \tilde{\Phi}_j^{\text{init}} \right\rangle_{L_2(\mathrm{I})} = \mathbf{R}_j \left\langle \Phi_{[j]}, \tilde{\Phi}_{[j]} \right\rangle_{L_2(\mathrm{I})} \tilde{\mathbf{R}}_j^{\text{init}}.$$

To construct the matrix $\langle \Phi_{[j]}, \tilde{\Phi}_{[j]} \rangle_{L_2(\mathrm{I})}$, it is necessary to compute the integrals $\int_0^1 \varphi(x)\tilde{\varphi}(x-k)\,\mathrm{d}x$. Because $j \geq j_0$, these integrals can be be reconstructed from the integrals $\int_0^\infty \varphi(x)\tilde{\varphi}(x-k)\,\mathrm{d}x$, which we will compute below.

By the duality between φ and $\tilde{\varphi}$ we already know $\int_{\mathbb{R}} \varphi(x-p)\tilde{\varphi}(x-q)\,\mathrm{d}x = \delta_{pq}$. However, by Remark 2.3.2, the matrix $\langle \Phi_{[j]}, \tilde{\Phi}_{[j]} \rangle_{L_2(\mathrm{I})}$ will differ from the identity matrix near the boundaries.

Remark 2.3.15. It was suggested in [DKU99] to write the integral $\int_0^1 \varphi(x)\tilde{\varphi}(x-k)\,\mathrm{d}x$ as $\int_{\mathbb{R}} \chi_{[0,1)}(x)\varphi(x)\tilde{\varphi}(x-k)\,\mathrm{d}x$. Because the indicator function $\chi_{[0,1)}$ is also refinable, the eigenvalue method of [DM93b] can also be used for this equation. The method we present below seems to be more efficient, because it only involves solving a linear system. In [Pri08], an alternative method to compute Gramian matrices for basis on an interval was suggested, which does not assume that these bases are linear combinations of restricted bases on the line.

For $1-\ell_2 \leq p \leq 1-\ell_1$, $1-\tilde{\ell}_2 \leq q \leq 1-\tilde{\ell}_1$, we define

$$c_{pq} := \int_0^\infty \varphi(x-p)\tilde{\varphi}(x-q)\,\mathrm{d}x. \tag{2.41}$$

Note that for all other values of p and q, this integral is known. We now use the two-scale relation (2.16) to obtain

$$\begin{aligned}
c_{pq} &= \sum_{k=\ell_1}^{\ell_2} \sum_{m=\tilde{\ell}_1}^{\tilde{\ell}_2} a_k \tilde{a}_m \int_0^\infty \varphi(2x-2p-k)\tilde{\varphi}(2x-2q-m)\,\mathrm{d}x \\
&= \frac{1}{2} \sum_{\tilde{k}=\ell_1+2p}^{\ell_2+2p} \sum_{\tilde{m}=\tilde{\ell}_1+2q}^{\tilde{\ell}_2+2q} a_{\tilde{k}-2p} \tilde{a}_{\tilde{m}-2q} \int_0^\infty \varphi(y-\tilde{k})\tilde{\varphi}(y-\tilde{m})\,\mathrm{d}y \\
&= \frac{1}{2} \sum_{k=-\ell_2+1}^{-\ell_1-1} \sum_{m=-\tilde{\ell}_2+1}^{-\tilde{\ell}_1-1} a_{k-2p} \tilde{a}_{m-2q} c_{km} \\
&\qquad + \frac{1}{2} \sum_{\substack{\text{other} \\ k,m}} a_{k-2p} \tilde{a}_{m-2q} \int_{\mathbb{R}} \varphi(y-k)\tilde{\varphi}(y-m)\,\mathrm{d}y.
\end{aligned} \tag{2.42}$$

where in the second step we have applied the substitutions $y = 2x$, $\tilde{k} = 2p+k$ and $\tilde{m} = 2q+m$. Note that the elements of the last summation are all known. We

now collect the scalars c_{pq} in a vector in the following way (with $p_{\min} := 1 - \ell_2$, $q_{\min} := 1 - \tilde{\ell}_2$, $p_{\max} := 1 - \ell_1$, $q_{\max} := 1 - \tilde{\ell}_1$):

$$\mathbf{c} := (c_{p_{\min},q_{\min}}, \dots, c_{p_{\min},q_{\max}}, \dots, c_{p_{\max},q_{\min}}, \dots, c_{p_{\max},q_{\max}})^{\mathsf{T}}.$$

The values of the last sum in (2.42), which are known, depend on p and q, and are put into the vector $\mathbf{f}$ in a similar way. Now we introduce the matrix $\mathbf{Z} \in \mathbb{R}^{(d+2\tilde{d}-3)\times(d+2\tilde{d}-3)}$ through

$$(\mathbf{Z})_{p(q_{\max}-q_{\min}+1)+q,\; k(m_{\max}-m_{\min}+1)+m} = \tfrac{1}{2} a_{k-2p} \tilde{a}_{m-2q},$$

with $k_{\max} := -\ell_1 - 1$, $m_{\min} := -\tilde{\ell}_2 + 1$. With this notation, we can write (2.42) as

$$\mathbf{c} = \mathbf{Z}\mathbf{c} + \mathbf{f}.$$

If $(\mathbf{I} - \mathbf{Z})$ is invertible, which it is in all cases we have encountered, this system can be solved for $\mathbf{c}$, yielding the values of c_{pq}.

Remark 2.3.16. The initial dual basis contains functions which, when restricted to $(0,(d-1)2^{-j})$, correspond to monomials. Monomials are known to form a poorly conditioned basis. As a result, the matrix $\langle \Phi_j, \tilde{\Phi}_j^{\text{init}} \rangle_{L_2(\mathrm{I})}$ is poorly conditioned. It was suggested in [DKU99, DKU97] to perform a basis change before performing the biorthogonalization. Since the dual basis is only used for the projection (2.14), we have not performed this change of basis. Instead, in our implementation, we have used high precision arithmetic to work with these poorly conditioned matrices.

2.3.5 Lower levels

So far we have assumed that the intersection between $\tilde{I}_j^L$ and $\tilde{I}_j^R$ was empty, so that the left and right boundary could be treated separately. This led to a minimum level j_0 for which the construction works, see (2.28). It may be desirable to extend the construction to include lower levels. This is motivated by the observation that the condition number of a wavelet basis is bounded from below by the condition number of scaling functions on the lowest level. It is known that B-splines are poorly conditioned in the H^1-norm: the condition number grows exponentially with the level j_0.

The lowest level on which scaling functions with polynomial exactness are conceivable, is determined by the degree of polynomial exactness on the dual side, which is $\tilde{d} \geq d$. There have to be at least $\tilde{d}$ degrees of freedom, which implies that $\#\tilde{I}_j \geq \tilde{d}$ should hold. Since $\#\tilde{I}_j = 2^j + d - 1$, this is satisfied only if

$$j \geq \lceil \log_2(\tilde{d} - d + 1) \rceil =: j_{\min}.$$

Note that the minimum level $j_{\min}$ is only determined by the difference in polynomial exactnesses $\tilde{d} - d$.

To construct the wavelets on lower levels, we consider the construction for level j_0 and upwards as given, and on levels $j_0 - 1$, $j_0 - 2$, down to $j_{\min}$ we again search the basis as a linear combination of CDF-wavelets restricted to the interval. On the primal side, this is easy: we can just take the B-spline basis with respect to the knot sequence

$$\{\underbrace{0,\dots,0}_{d \text{ times}}, 2^{-j}, \dots, 1 - 2^{-j}, \underbrace{1,\dots,1}_{d \text{ times}}\}.$$

We proceed to the dual side. As in subsection 2.3.2, we write the desired dual basis as $\tilde{\Phi}_j^{\text{init}}$, and require this basis to be spanned by linear combinations of functions from $\tilde{\Phi}_{[j]}$. Note that the functions $\tilde{\Phi}_{[j]}$ satisfy the refinement equation $\tilde{\Phi}_{[j]}^{\mathsf{T}} = \tilde{\Phi}_{[j+1]}^{\mathsf{T}} \mathbf{M}_{[j,0]}$.

In the following proposition we use the notation $\operatorname{col}(\cdot)$ to denote the column space of a matrix.

Proposition 2.3.17. *Let $\tilde{\mathbf{Q}}_j$ be a matrix such that $\operatorname{col}(\tilde{\mathbf{Q}}_j) \subseteq \operatorname{col}(\tilde{\mathbf{M}}_{[j,0]}) \cap \operatorname{col}(\tilde{\mathbf{R}}_{j+1})$, and let $\tilde{\Phi}_j^{init}$ be defined by $(\tilde{\Phi}_j^{init})^{\mathsf{T}} := \tilde{\Phi}_{[j+1]}^{\mathsf{T}} \tilde{\mathbf{Q}}_j$. Then $\operatorname{span} \tilde{\Phi}_j^{init} \subseteq \operatorname{span} \tilde{\Phi}_{j+1}$ and $\operatorname{span} \tilde{\Phi}_j^{init} \subseteq \operatorname{span} \tilde{\Phi}_{[j]}$.*

Proof. To show that $\operatorname{span} \tilde{\Phi}_j \subseteq \operatorname{span} \tilde{\Phi}_{[j]}$, let us write $\tilde{\mathbf{Q}}_j = \tilde{\mathbf{M}}_{[j,0]} \tilde{\mathbf{R}}_j^{\text{init}}$, for some matrix $\tilde{\mathbf{R}}_j^{\text{init}}$ (such a matrix exists because $\operatorname{col}(\tilde{\mathbf{Q}}) \subseteq \operatorname{col}(\tilde{\mathbf{M}}_{[j,0]})$ by assumption). We have:

$$(\tilde{\Phi}_j^{\text{init}})^{\mathsf{T}} = \tilde{\Phi}_{[j+1]}^{\mathsf{T}} \tilde{\mathbf{M}}_{[j,0]} \tilde{\mathbf{R}}_j^{\text{init}} = \tilde{\Phi}_{[j]}^{\mathsf{T}} \tilde{\mathbf{R}}_j^{\text{init}}.$$

Similarly, let us write $\tilde{\mathbf{Q}}_j = \tilde{\mathbf{R}}_{j+1} \tilde{\mathbf{M}}_{j,0}^{\text{init}}$, for some matrix $\tilde{\mathbf{M}}_{j,0}$ (which exists because $\operatorname{col}(\tilde{\mathbf{Q}}) \subseteq \operatorname{col}(\tilde{\mathbf{R}}_{j+1})$ by assumption). We have

$$(\tilde{\Phi}_j^{\text{init}})^{\mathsf{T}} = \tilde{\Phi}_{[j+1]}^{\mathsf{T}} \tilde{\mathbf{R}}_{j+1} \tilde{\mathbf{M}}_{j,0}^{\text{init}} = \tilde{\Phi}_{j+1} \tilde{\mathbf{M}}_{j,0}^{\text{init}}. \qquad \Diamond$$

To maintain a Jackson estimate of order $\tilde{d}$, we will construct $\tilde{\Phi}_j$ such that it contains all polynomials of degree $\tilde{d}-1$. By Lemma 2.2.3, we have the following result.

Lemma 2.3.18. *For $r \in \{0, \dots, \tilde{d}-1\}$, let $\boldsymbol{\alpha}_r$ be defined as*

$$\boldsymbol{\alpha}_r := \{\alpha_{k,r} : k \in \{1-\tilde{\ell}_2, \dots, 2^j - \tilde{\ell}_1 - 1\}.$$

Then the collection $\tilde{\Phi}_j$ spans all polynomials of degree $\tilde{d}-1$ if and only if $\boldsymbol{\alpha}_r \in \operatorname{col} \tilde{\mathbf{Q}}_j$ for all $r \in \{0, \dots, \tilde{d}-1\}$.

Lemma 2.3.19. *The dimension of $\operatorname{col}(\tilde{\mathbf{M}}_{[j,0]}) \cap \operatorname{col}(\tilde{\mathbf{R}}_{j+1})$ is at least $2^j + d - 1$.*

Proof. Because $\tilde{\Phi}_{[j]}$, $\tilde{\Phi}_{[j+1]}$ and $\tilde{\Phi}_{j+1}$ are independent sets, both $\tilde{\mathbf{M}}_{[j,0]}$ and $\tilde{\mathbf{R}}_{j+1}$ have full column rank. Taking the union of the columns of $\tilde{\mathbf{M}}_{[j,0]}$ and $\tilde{\mathbf{R}}_{j+1}$ yields $(2^j + d + 2\tilde{d} - 3) + (2^{j+1} + d - 1)$ columns in $\mathbb{R}^{2^{j+1}+d+2\tilde{d}-3}$. At most $2^{j+1} + d + 2\tilde{d} - 3$ can be independent, so there is a dependent set of dimension at least $(2^j + d + 2\tilde{d} - 3) + (2^{j+1} + d - 1) - (2^{j+1} + d + 2\tilde{d} - 3) = 2^j + d - 1$. $\Diamond$

Lemma 2.3.20. *For every $j \geq j_{\min}$, the basis $\tilde{\Phi}_j$ can be chosen such that its span contains $\Pi^{\tilde{d}-1}(\mathrm{I})$.*

Proof. By induction on j. For $j \geq j_0$, the statement holds by Lemma 2.3.5. Also, for every $j \in \mathbb{Z}$, $\operatorname{span} \tilde{\Phi}_{[j]}$ contains all polynomials of degree $\tilde{d}-1$. Now assume, by the induction hypothesis, that $\Pi^{\tilde{d}-1}(\mathrm{I}) \subset \operatorname{span} \tilde{\Phi}_{j+1}$. Then $\Pi^{\tilde{d}-1}(\mathrm{I})$ is a subspace of $\operatorname{span} \tilde{\Phi}_{[j]} \cap \operatorname{span} \tilde{\Phi}_{j+1}$, and $\tilde{\Phi}_j$ can be chosen to contain it. $\Diamond$

For $j < j_{\min}$ the cardinality of $\tilde{\Phi}_j$ is too small to span the polynomials.

Remark 2.3.21. To perform the biorthogonalization (2.27), it is necessary to compute the matrix $\langle \Phi_j, \tilde{\Phi}_j^{\text{init}} \rangle^{-1}$. The method presented in subsection 2.3.4 can not be applied for $j < j_0$. However the refinement matrices $\mathbf{M}_{j,0}$, $\tilde{\mathbf{M}}_{j,0}^{\text{init}}$ can be used to compute this matrix. Indeed,

$$\langle \Phi_j, \tilde{\Phi}_j^{\text{init}} \rangle = \mathbf{M}_{j,0}^{\mathsf{T}} \langle \Phi_{j+1}, \tilde{\Phi}_{j+1} \rangle \tilde{\mathbf{M}}_{j,0} = \mathbf{M}_{j,0}^{\mathsf{T}} \tilde{\mathbf{M}}_{j,0}^{\text{init}},$$

where the biorthogonality of Φ_{j+1} and $\tilde{\Phi}_{j+1}$ was used.

2.3.6 Boundary conditions

In this section, we will sketch how to construct multiresolution analyses for spaces with homogeneous boundary conditions. Defining the space $H^m_{0,\{x\}}(\mathrm{I})$, for $x \in \{0,1\}$, through $H^m_{0,\{x\}}(\mathrm{I}) := \{u \in H^m(\mathrm{I})\colon u(x) = \cdots = u^{(m-1)}(x) = 0\}$, we will construct wavelet bases for the spaces

$$\mathcal{H}^s(\mathrm{I}) := \left[L_2(\mathrm{I}), H^d(\mathrm{I}) \cap H^{m_L}_{0,\{0\}}(\mathrm{I}) \cap H^{m_R}_{0,\{1\}}(\mathrm{I})\right]_{s/d} \qquad s \in [0,\gamma),$$

$$\tilde{\mathcal{H}}^s(\mathrm{I}) := \left[L_2(\mathrm{I}), H^{\tilde{d}}(\mathrm{I}) \cap H^{\tilde{m}_L}_{0,\{0\}}(\mathrm{I}) \cap H^{\tilde{m}_R}_{0,\{1\}}(\mathrm{I})\right]_{s/\tilde{d}} \qquad s \in [0,\tilde{\gamma}),$$

where m_L, $m_R \le d$ ($\tilde{m}_L$, $\tilde{m}_R \le \tilde{d}$) denote the order of the boundary conditions at the primal (dual) side on the left and right boundary. Since, for $s \notin \mathbb{N} + \frac{1}{2}$,

$$\begin{aligned}\mathcal{H}^s(\mathrm{I}) = \big\{u \in H^s(\mathrm{I})\colon\ & u(0) = \ldots = u^{(\min(m_L, \lfloor s+\frac{1}{2}\rfloor)-1)}(0) = 0,\\ & u(1) = \ldots = u^{(\min(m_R, \lfloor s+\frac{1}{2}\rfloor)-1)}(1) = 0\big\},\end{aligned}$$

and similarly for the dual side, it is sufficient to consider

$$m_L, m_R \le \sup_{s<\gamma} \lfloor s + \tfrac{1}{2} \rfloor = d - 1,$$

$$\tilde{m}_L, \tilde{m}_R \le \sup_{s<\tilde{\gamma}} \lfloor s + \tfrac{1}{2} \rfloor,$$

where $\tilde{\gamma}$ can be found in Table 2.1 or Figure 2.2. Note that generally $\tilde{\gamma} \notin \mathbb{N} + \frac{1}{2}$, so that we can safely take $\lfloor \tilde{\gamma} + \frac{1}{2} \rfloor$ as an upper bound for $\tilde{m}_L$, $\tilde{m}_R$.

We will use Theorem 2.1.2, and adapt the construction from earlier sections to match the boundary conditions.

As the primal space V_j, we will again use a spline space (equipped with the B-spline basis), with respect to the knot sequence

$$\{\underbrace{0,\ldots,0}_{d-m_L \text{ times}}, 2^{-j}, \ldots, 1-2^{-j}, \underbrace{1,\ldots,1}_{d-m_R \text{ times}}\}.$$

Indeed, all functions in this space satisfy the boundary conditions. Moreover, the sequence of spaces satisfies a Jackson estimate (see (2.6)) of order d, and a Bernstein estimate (see (2.7)) of order $\gamma = d - 1/2$ with respect to the scale of Sobolev spaces $\mathcal{H}^s(\mathrm{I})$. The dimension of V_j is $2^j + d - 1 - m_L - m_R$.

On the dual side, we modify the basis from subsection 2.3.2. This basis can be modified so that for every $m \in \{1,\ldots,\lfloor \tilde{\gamma} - \frac{1}{2} \rfloor\}$, there is only one scaling function $\tilde{\varphi}_{j,k}$ whose $(m-1)$-th derivative does not vanish at zero or one. In fact, it seems that this is already true for the initial collection $\tilde{\Phi}_j^{\text{init}}$ as constructed

in Proposition 2.3.10. A modified set is now obtained by discarding the $\tilde{m}_L + \tilde{m}_R$ functions from $\tilde{\Phi}_j^{\text{init}}$ that do not satisfy the boundary conditions. However, generally this set does not have the same cardinality as I_j.

Note that the spaces spanned by this modified set still satisfy a Jackson estimate of order $\tilde{d}$ and a Bernstein estimate of order $\tilde{\gamma}$ with respect to $\tilde{\mathcal{H}}^s(\mathrm{I})$.

Let us for the moment consider only the left boundary, and assume $m_L \geq \tilde{m}_L$. Since on the primal side m_L functions are discarded, to get the right number of functions on the dual side, also there m_L functions have to be dropped. Recall that in subsection 2.3.2 we have constructed $d-2$ extra boundary functions on the dual side that were not necessary for polynomial exactness. Having already dropped $\tilde{m}_L$ functions on the dual side that do not satisfy the boundary conditions, we can safely drop $m_L - \tilde{m}_L$ from these $d-2$ extra boundary functions. When $m_L - \tilde{m}_L > d-2$, we encounter the situation as in Remark 2.3.7. In this case, $m_L - \tilde{m}_L - d + 2$ indices from $\tilde{I}_j^0$ have to be moved to $\tilde{I}_j^L$ to further reduce the cardinality of $\tilde{I}_j$.

When $m_L < \tilde{m}_L$, one could proceed in a similar fashion and drop functions on the primal side, obtaining a knot sequence like (2.23). Indeed, this was proposed in [DS98]. We will instead create more dual scaling functions that satisfy the boundary conditions, thereby making the cardinality of I_j and $\tilde{I}_j$ equal. To this end, we again write $(\tilde{\Phi}^L)^{\mathsf{T}} = (\tilde{\Phi}_{[j]}^L)^{\mathsf{T}} \tilde{\mathbf{C}}^L$ (cf. (2.32)), where $\tilde{d} - \tilde{m}_L$ of the columns of $\tilde{\mathbf{C}}^L$ are given by the vectors $\boldsymbol{\alpha}_r^L$, for $r = \tilde{m}_L, \ldots, \tilde{d}-1$. To get the right cardinality for $\tilde{I}_j$, $d - 2 - m_L + \tilde{m}_L$ extra eigenvectors of $\tilde{\mathbf{A}}$ have to be added to $\tilde{\mathbf{C}}^L$. Since there are $d + \tilde{d} - 3$ eigenvectors of $\tilde{\mathbf{A}}$ that do not correspond to any of the $\boldsymbol{\alpha}_r^L$, we need

$$d - 2 - m_L + \tilde{m}_L \leq d + \tilde{d} - 3, \quad \text{or} \quad \tilde{m}_L - m_L \leq \tilde{d} - 1.$$

Since, for all $\tilde{d} > 1$, $\tilde{m}_L < \tilde{\gamma} < \tilde{d} - 1$ (cf. Figure 2.2) this holds for any m_L.

As in subsection 2.3.2, the created bases are not biorthogonal but have to be biorthogonalized. In all cases we have tested, this was indeed possible.

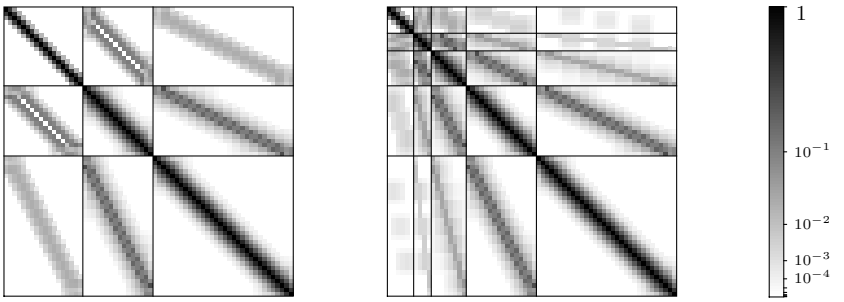

Figure 2.10: Mass matrix for $(d, \tilde{d}) = (3, 5)$, $j_{\max} = 6$, on the left without added lower levels (i.e., the mass matrix of $\Psi_{j_0,6,0}$) and on the right with lower levels (i.e., the mass matrix of $\Psi_{j_{\min},6,0}$). For these values of d and $\tilde{d}$, $j_{\min} = 3$, $j_0 = 5$.
Note the unusual color scale: elements far away from the main diagonal are very small.

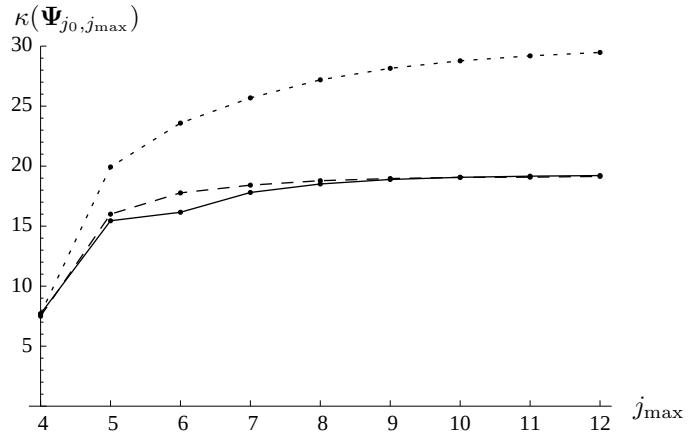

Figure 2.11: Convergence of the condition number of the mass matrix (without lower levels added) as a function of $j_{\max}$, for $(d, \tilde{d}) = (3, 5)$. The solid line represents the new construction, the dotted line that from [Pri06] and the dashed line represents the basis with periodic boundary conditions.

2.4 Conclusions and numerical results

In this chapter we have constructed a biorthogonal spline wavelet basis for the interval by adapting such a basis on the whole line. This construction was performed by taking linear combinations of restrictions of the latter basis to the interval. A key feature of our construction is that the primal space is spanned by the B-splines with respect to a uniform partition of the interval. The dual basis functions near the boundaries of the interval are initially not biorthogonal to the primal basis functions, however it was verified numerically that they can be modified to be so. This verification involves checking the invertibility of a matrix of bounded dimensions.

The construction is such that scaling functions and wavelets on $\mathbb{R}$ that are supported entirely in $[0, 1]$ will also be part of the wavelets for the interval.

The aim of this construction was to make a well-conditioned wavelet basis $\mathbf{\Psi}_{j_0,\infty,0}$, which is the union of scaling functions on level j_0 and wavelets on levels $j_0, \ldots, \infty$. The last index 0 indicates that the wavelets are scaled to form a basis for $L_2(\mathrm{I})$. The lowest level j_0 is chosen such that the boundary adaptation on the left boundary does not interfere with that on the right boundary.

For $d > 2$, there is a choice to make for the extra boundary functions to add. We have used this freedom to minimize the condition numbers with respect to $L_2(\mathrm{I})$, see Table 2.2. This condition number is given by the ratio of the largest and the smallest eigenvalue of the mass matrix $\langle \mathbf{\Psi}_{j_0,\infty,0}, \mathbf{\Psi}_{j_0,\infty,0} \rangle_{L_2(\mathrm{I})}$. Theorem 2.1.2 shows that this condition number is bounded.

In practice, it is of course impossible to compute eigenvalues of the bi-infinite mass matrix. Instead, a maximum level $j_{\max}$ is set, leading to finite-dimensional mass matrices (Figure 2.10). Figure 2.11 shows the convergence of the condition number as a function of the maximum level $j_{\max}$. This figure shows that the

condition number of the smaller basis $\Psi_{j_0,10,0}$ can be expected to give a good approximation to the condition number of the full basis. In all our experiments, we have set $j_{\max} = 10$.

In Table 2.3, conditions numbers are given for the basis $\Psi_{j_0,10,0}$ with no boundary conditions imposed (i.e., $m_{\scriptscriptstyle L} = \tilde{m}_{\scriptscriptstyle L} = m_{\scriptscriptstyle R} = \tilde{m}_{\scriptscriptstyle R} = 0$). This basis was scaled to be normalized in L_2(I).

We compare the condition numbers of our construction with those of [Pri06], and with those of a basis with periodic boundary conditions. The latter basis is defined through $\varphi_{j,k}^{\text{per}} := \sum_{m\in\mathbb{Z}} \varphi_{[j,k+2^j m]}\big|_{[0,1]}$, for $j \geq j_0$ and $k \in \{0,\dots,2^j-1\}$. As proven in [Pri06, Remark 2.19], the condition numbers of this periodic basis are the same as that of the basis on $\mathbb{R}$ from Section 2.2.

From Table 2.3, it can be concluded that our construction yields better condition numbers than the construction of [Pri06], except for the case $d = 3$, $\tilde{d} = 5$, for which the difference is marginal. For larger values of d, $\tilde{d}$, the difference grows.

The condition number of the multiscale basis $\Psi_{j_0,\infty,s}$ is bounded from below by the condition number of the scaling function basis on level j_0. For $s = 1$, it is known that the B-splines form a poorly conditioned basis. Indeed, because Φ_{j_0} is a locally supported basis, its condition number $\kappa(\Phi_{j_0})$ w.r.t. H^1(I) grows exponentionally in j_0. Therefore, we have reduced the lowest level to $j_{\min}$, which is generally smaller that j_0. The condition on $j_{\min}$ is only determined by $\tilde{d} - d$, the difference of the order of polynomial exactness on the dual and primal side.

In Table 2.4, condition numbers are presented for the basis $\Psi_{j_0,10,1}$, where so-called *complementary boundary conditions* are imposed, i.e., $m_{\scriptscriptstyle L} = m_{\scriptscriptstyle R} = 1$, $\tilde{m}_{\scriptscriptstyle L} = \tilde{m}_{\scriptscriptstyle R} = 0$. With the homogeneous boundary conditions on the primal side, the H^1(I)-norm is equivalent to the H^1(I)-seminorm. The basis was scaled to be normalized in the H^1(I)-seminorm. From the table, it is clear that reducing the lowest level is very advantageous for lowering the condition number, since the condition number of the scaling functions on the lowest level is already high.

d	$\tilde{d}$	$m_{\scriptscriptstyle L} = 0$	$m_{\scriptscriptstyle L} = 1$
1	$*$	$1,\dots,\tilde{d}$	$1,\dots,\tilde{d}$
2	$*$	$1,\dots,\tilde{d}$	$1,\dots,\tilde{d}$
3	3	$2,4,\underline{5},6$	$2,4,6$
3	5	$1,3,\underline{4},6,8,10$	$1,3,6,8,10$
3	7	$1,2,5,\underline{7},8,10,12,14$	$1,2,5,8,10,12,14$
3	9	$1,2,\underline{3},5,7,10,12,14,15,18$	$1,2,5,7,10,12,14,15,18$
4	6	$1,\underline{3},4,7,\underline{8},9,11,13$	$1,4,\underline{6},7,9,11,13$
4	8	$1,\underline{3},4,\underline{5},6,9,11,13,14,17$	$1,\underline{2},4,6,9,11,13,14,17$
4	10	$1,2,5,\underline{7},8,\underline{9},10,13,16,17,18,21$	$1,2,5,8,10,\underline{12},13,16,17,18,21$
5	9	$1,\underline{3},4,\underline{5},7,9,\underline{11},12,15,16,17,20$	$1,\underline{2},4,7,9,12,\underline{13},15,16,17,20$

Table 2.2: Indication of the eigenvectors om $\tilde{\mathbf{A}}$ to take to get optimal L_2(I) condition numbers. The numbers indicate which eigenvectors to take, when sorted in decreasing absolute value of the corresponding eigenvalue. The non-underlined numbers correspond to the eigenvectors $\boldsymbol{\alpha}_r^L$ for $r \in \{0,\dots,\tilde{d}\}$.

d	$\tilde{d}$	j_0	new	Primbs	periodic
1	1	0	1.00	1.00	1.00
1	3	3	12.5	-	3.04
1	5	4	57.9	-	4.38
2	2	2	8.71	8.71	8.37
2	4	3	5.54	5.54	4.14
2	6	4	9.21	9.21	4.03
2	8	4	36.3	36.3	4.09
3	3	3	69.8	51.1	56.2
3	5	4	19.1	28.8	19.1
3	7	4	17.1	74.9	16.3
3	9	5	18.6	645.2	16.0
4	6	4	159.8	$> 10^4$	101.9
4	8	5	67.9	$> 10^4$	68.4
4	10	5	64.5	$> 10^5$	64.7
5	9	5	622.4	$> 10^6$	311.1

Table 2.3: L_2-condition numbers for the multiscale wavelet bases $\Psi_{j_0,10,0}$. The numbers for the periodic basis also appear in [Bit05].

		without reduced lowest level				with reduced lowest level		
d	$\tilde{d}$	j_0	new	Primbs	$\kappa(\Phi_{j_0})$	$j_{\min}$	new	$\kappa(\Phi_{j_{\min}})$
2	2	3	33.1	33.1	25.3	2	14.7	5.83
2	4	4	165.2	165.2	103.1	3	72.6	25.3
3	3	3	12.9	12.9	10.0	2	5.43	2.78
3	5	4	55.2	55.2	39.2	3	14.5	10.0
3	7	4	71.9	71.9	39.2	3	47.6	10.0
4	6	4	51.9	53.9	41.4	3	16.3	10.9
4	8	5	209.3	253.3	164.0	3	19.0	10.9
5	9	5	201.6	3853.	191.5	3	64.5	13.1

Table 2.4: Condition numbers for the multiscale wavelet bases $\Psi_{j_0,10,1}$ w.r.t. the H^1 seminorm.

2.5 Examples

In the following we present examples of the construction from of this chapter. The ideas presented earlier were implemented in *Mathematica*. Full refinement matrices can be downloaded from http://www.tammo80.nl/thesis but may also be included in this PDF-file. (mats.zip)

For $(d, \tilde{d}) = (3, 5)$, and without boundary conditions (i.e. $m_L = m_R = \tilde{m}_L = \tilde{m}_R = 0$), the minimum level for which the left and right boundary can be treated separately, is given by $j_0 = 4$ (cf. (2.28)). The matrix $\tilde{\mathbf{R}}_{j_0}$ from (2.38) is given in Matrix 2.2. The column that does not correspond to a monomial (cf. Lemma 2.3.5), is only given as an eigenvector of a matrix, and therefore, can not be expected to have rational coefficients. The non-rational entries of the matrix are given in Table 2.5. Illustrations of the dual boundary scaling functions before and after biorthogonalization are given in Figure 2.12 and Figure 2.13, respectively. In Figure 2.12, the monomials to which the scaling functions correspond, can clearly be recognized. The resulting primal wavelets are illustrated in Figure 2.14.

To illustrate the construction on lower levels from subsection 2.3.5 we consider the construction for $(d, \tilde{d}) = (3, 5)$ with the complementary boundary conditions $m_L = m_R = 1$, $\tilde{m}_L = \tilde{m}_R = 0$. For these parameters, $j_0 = 4$ and $j_{\min} = 3$. In this case, the dimension of $\operatorname{span} \tilde{\Phi}_{[j_{\min}]} \cap \operatorname{span} \tilde{\Phi}_{j_{\min}+1}$ is exactly $\#\tilde{I}_{j_{\min}}$. This means that there is no choice for the space $\tilde{V}_{j_{\min}} = \operatorname{span} \tilde{\Phi}_{j_{\min}}$. The functions $\tilde{\Phi}_{j_{\min}}$ are fixed by the biorthogonality relation $\langle \Phi_{j_{\min}}, \tilde{\Phi}_{j_{\min}} \rangle = \mathbf{I}$. These functions are illustrated in Figure 2.15. By Lemma 2.3.20, $\tilde{V}_{j_{\min}}$ is exact of order $\tilde{d}$. The resulting primal wavelets are given in Figure 2.16. Note that away from the boundaries, the wavelets still correspond to CDF-wavelets. The refinement matrix $\mathbf{M}_{j_{\min}}$ is given in Matrix 2.4, and the matrix $\tilde{\mathbf{R}}_{j_{\min}}$ is given in Matrix 2.3.

The case $(d, \tilde{d}) = (1, 3)$ may be useful for solving integral equations. Dual boundary functions before and after biorthogonalization are given in Figure 2.17 and Figure 2.18, respectively. Primal wavelets are illustrated in Figure 2.19. The matrices $\tilde{\mathbf{R}}_{j_0}^{\text{init}}$ and $\tilde{\mathbf{R}}_{j_0}$ are given in Matrix 2.5, and the matrix $\mathbf{M}_{j_0}$ is given in Matrix 2.6.

$$\tilde{\mathbf{R}}^{\text{init}}_{j_0} = \begin{pmatrix}
1 & 1 & 1 & 1 & 1 & 1 & & & & & & & & & & & & \\
1 & \frac{7}{9} & \frac{25}{41} & \frac{13}{27} & \frac{843}{2203} & c_1 & & & & & & & & & & & & \\
1 & \frac{5}{9} & \frac{13}{41} & \frac{5}{27} & \frac{243}{2203} & c_2 & & & & & & & & & & & & \\
1 & \frac{1}{3} & \frac{5}{41} & \frac{1}{21} & \frac{43}{2203} & c_3 & & & & & & & & & & & & \\
1 & \frac{1}{9} & \frac{1}{41} & \frac{1}{189} & \frac{3}{2203} & c_4 & & & & & & & & & & & & \\
1 & -\frac{1}{9} & \frac{1}{41} & -\frac{1}{189} & \frac{3}{2203} & c_4 & & & & & & & & & & & & \\
1 & -\frac{1}{3} & \frac{5}{41} & -\frac{1}{21} & \frac{43}{2203} & c_3 & & & & & & & & & & & & \\
1 & -\frac{5}{9} & \frac{13}{41} & -\frac{5}{27} & \frac{243}{2203} & c_2 & & & & & & & & & & & & \\
1 & -\frac{7}{9} & \frac{25}{41} & -\frac{13}{27} & \frac{843}{2203} & c_1 & & & & & & & & & & & & \\
1 & -1 & 1 & -1 & 1 & 1 & & & & & & & & & & & & \\
 & & & & & & 1 & & & & & & & & & & & \\
 & & & & & & & 1 & & & & & & & & & & \\
 & & & & & & & & 1 & & & & & & & & & \\
 & & & & & & & & & 1 & & & & & & & & \\
 & & & & & & & & & & 1 & & & & & & & \\
 & & & & & & & & & & & 1 & & & & & & \\
 & & & & & & & & & & & & 1 & 1 & -1 & 1 & -1 & 1 \\
 & & & & & & & & & & & & c_1 & $\frac{843}{2203}$ & $-\frac{13}{27}$ & $\frac{25}{41}$ & $-\frac{7}{9}$ & 1 \\
 & & & & & & & & & & & & c_2 & $\frac{243}{2203}$ & $-\frac{5}{27}$ & $\frac{13}{41}$ & $-\frac{5}{9}$ & 1 \\
 & & & & & & & & & & & & c_3 & $\frac{43}{2203}$ & $-\frac{1}{21}$ & $\frac{5}{41}$ & $-\frac{1}{3}$ & 1 \\
 & & & & & & & & & & & & c_4 & $\frac{3}{2203}$ & $-\frac{1}{189}$ & $\frac{1}{41}$ & $-\frac{1}{9}$ & 1 \\
 & & & & & & & & & & & & c_4 & $\frac{3}{2203}$ & $\frac{1}{189}$ & $\frac{1}{41}$ & $\frac{1}{9}$ & 1 \\
 & & & & & & & & & & & & c_3 & $\frac{43}{2203}$ & $\frac{1}{21}$ & $\frac{5}{41}$ & $\frac{1}{3}$ & 1 \\
 & & & & & & & & & & & & c_2 & $\frac{243}{2203}$ & $\frac{5}{27}$ & $\frac{13}{41}$ & $\frac{5}{9}$ & 1 \\
 & & & & & & & & & & & & c_1 & $\frac{843}{2203}$ & $\frac{13}{27}$ & $\frac{25}{41}$ & $\frac{7}{9}$ & 1 \\
 & & & & & & & & & & & & 1 & 1 & 1 & 1 & 1 & 1
\end{pmatrix}.$$

Matrix 2.2: The matrix $\tilde{\mathbf{R}}^{\text{init}}_{j_0}$ for $(d, \tilde{d}) = (3, 5)$. The values of $c_1, \ldots, c_4$ are given in Table 2.5.

$$\begin{aligned}
c_1 &= (\ 3076204655\ -\ 28043495a\ )/\ b\ \approx -0.11427500310446548 \\
c_2 &= (12271605600 - 235866183a)/16b \approx -0.41409991825769983 \\
c_3 &= (\ 4057172000\ -\ 23585755a\ )/16b \approx\ \ 0.03225405475974428 \\
c_4 &= (\ \ 300213000\ -\ \ \ 99333a\ \ )/\ 8b\ \approx\ \ 0.01501044948711200 \\
a &= 43 + \sqrt{5849} \\
b &= 2401200719
\end{aligned}$$

Table 2.5: Values of $c_1, \ldots, c_4$ in Matrix 2.2, with a machine-precision approximation.

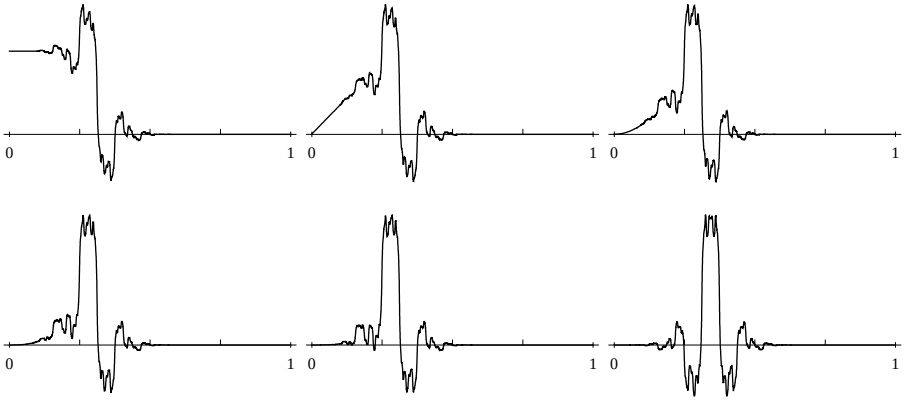

Figure 2.12: Dual boundary scaling functions for $(d, \tilde{d}) = (3, 5)$, before biorthogonalization.

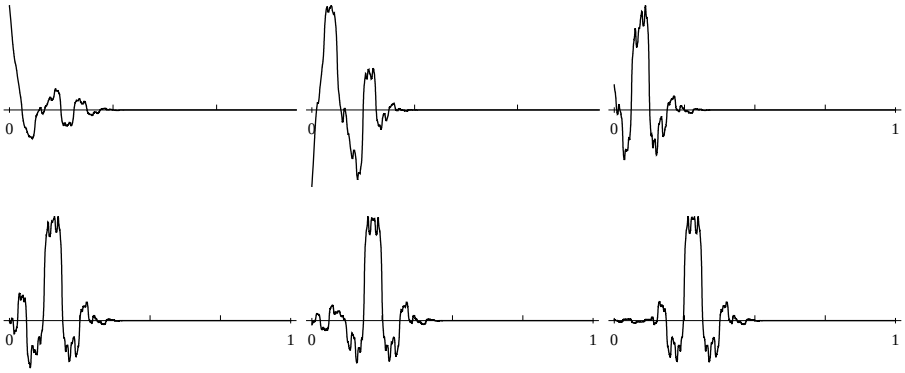

Figure 2.13: Dual boundary scaling functions for $(d, \tilde{d}) = (3, 5)$, after biorthogonalization.

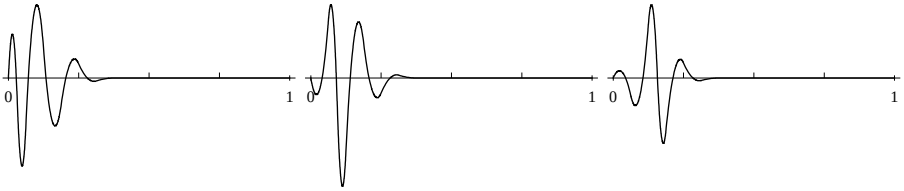

Figure 2.14: Primal boundary wavelets for $(d, \tilde{d}) = (3, 5)$.

$$\tilde{\mathbf{R}}_{j_{\min}} = \begin{pmatrix}
441 & -\frac{7539}{10} & \frac{7983}{10} & -\frac{2142}{5} & 91 & & & \\
245 & -\frac{819}{2} & \frac{847}{2} & -223 & \frac{140}{3} & & & \\
\frac{245}{2} & -\frac{791}{4} & \frac{791}{4} & -\frac{203}{2} & \frac{125}{6} & & & \\
\frac{105}{2} & -\frac{319}{4} & \frac{303}{4} & -\frac{75}{2} & \frac{15}{2} & & & \\
\frac{35}{2} & -\frac{93}{4} & \frac{81}{4} & -\frac{19}{2} & \frac{11}{6} & & & \\
\frac{7}{2} & -\frac{53}{20} & \frac{41}{20} & -\frac{9}{10} & \frac{1}{6} & & & \\
 & 1 & & & & & & \\
 & & 1 & & & & & \\
 & & & 1 & & & & \\
 & & & & 1 & & & \\
 & & & & & 1 & & \\
 & & & & & & 1 & \\
 & & & \frac{1}{6} & -\frac{9}{10} & \frac{41}{20} & -\frac{53}{20} & \frac{7}{2} \\
 & & & \frac{11}{6} & -\frac{19}{2} & \frac{81}{4} & -\frac{93}{4} & \frac{35}{2} \\
 & & & \frac{15}{2} & -\frac{75}{2} & \frac{303}{4} & -\frac{319}{4} & \frac{105}{2} \\
 & & & \frac{125}{6} & -\frac{203}{2} & \frac{791}{4} & -\frac{791}{4} & \frac{245}{2} \\
 & & & \frac{140}{3} & -223 & \frac{847}{2} & -\frac{819}{2} & 245 \\
 & & & 91 & -\frac{2142}{5} & \frac{7983}{10} & -\frac{7539}{10} & 441
\end{pmatrix}.$$

Matrix 2.3: The matrix $\tilde{\mathbf{R}}_{j_{\min}}$ for $(d, \tilde{d}) = (3, 5)$ with complementary boundary conditions.

$$\mathbf{M}_{j_{\min}} = \begin{pmatrix}
\frac{1}{2} & & & & & & & & \frac{1925}{4096} & -\frac{63}{512} & \frac{35}{512} & & & & & & \\
\frac{3}{4} & \frac{1}{4} & & & & & & & -\frac{11165}{16384} & \frac{147}{10240} & \frac{21}{2048} & \frac{5}{512} & & & & & \\
\frac{1}{4} & \frac{3}{4} & & & & & & & \frac{11915}{49152} & \frac{5481}{10240} & -\frac{497}{2048} & \frac{15}{512} & & & & & \\
 & \frac{3}{4} & \frac{1}{4} & & & & & & \frac{3455}{8192} & -\frac{3969}{5120} & -\frac{7}{1024} & -\frac{19}{512} & -\frac{5}{512} & & & & \\
 & \frac{1}{4} & \frac{3}{4} & & & & & & -\frac{1175}{8192} & \frac{85}{1024} & \frac{735}{1024} & -\frac{97}{512} & -\frac{15}{512} & & & & \\
 & & \frac{3}{4} & \frac{1}{4} & & & & & -\frac{13675}{49152} & \frac{699}{2048} & -\frac{1295}{2048} & \frac{13}{256} & \frac{19}{512} & -\frac{25}{3072} & \frac{7}{1024} & -\frac{175}{24576} & \\
 & & \frac{1}{4} & \frac{3}{4} & & & & & \frac{285}{16384} & -\frac{3}{10240} & -\frac{117}{2048} & \frac{175}{256} & \frac{97}{512} & -\frac{25}{1024} & \frac{21}{1024} & -\frac{175}{8192} & \\
 & & & \frac{3}{4} & \frac{1}{4} & & & & \frac{1435}{12288} & -\frac{311}{2560} & \frac{253}{1536} & -\frac{175}{256} & -\frac{13}{256} & \frac{17}{512} & -\frac{57}{2560} & \frac{245}{12288} & \\
 & & & \frac{1}{4} & \frac{3}{4} & & & & \frac{245}{12288} & -\frac{57}{2560} & \frac{17}{512} & -\frac{13}{256} & -\frac{175}{256} & \frac{253}{1536} & -\frac{311}{2560} & \frac{1435}{12288} & \\
 & & & & \frac{3}{4} & \frac{1}{4} & & & -\frac{175}{8192} & \frac{21}{1024} & -\frac{25}{1024} & \frac{97}{512} & \frac{175}{256} & -\frac{117}{2048} & -\frac{3}{10240} & \frac{285}{16384} & \\
 & & & & \frac{1}{4} & \frac{3}{4} & & & -\frac{175}{24576} & \frac{7}{1024} & -\frac{25}{3072} & \frac{19}{512} & \frac{13}{256} & -\frac{1295}{2048} & \frac{699}{2048} & -\frac{13675}{49152} & \\
 & & & & & \frac{3}{4} & \frac{1}{4} & & & & & -\frac{15}{512} & -\frac{97}{512} & \frac{735}{1024} & \frac{85}{1024} & -\frac{1175}{8192} & \\
 & & & & & \frac{1}{4} & \frac{3}{4} & & & & & -\frac{5}{512} & -\frac{19}{512} & -\frac{7}{1024} & -\frac{3969}{5120} & \frac{3455}{8192} & \\
 & & & & & & \frac{3}{4} & \frac{1}{4} & & & & & \frac{15}{512} & -\frac{497}{2048} & \frac{5481}{10240} & \frac{11915}{49152} & \\
 & & & & & & \frac{1}{4} & \frac{3}{4} & & & & & \frac{5}{512} & \frac{21}{2048} & \frac{147}{10240} & -\frac{11165}{16384} & \\
 & & & & & & & \frac{1}{2} & & & & & & \frac{35}{512} & -\frac{63}{512} & \frac{1925}{4096} &
\end{pmatrix}.$$

Matrix 2.4: The matrix $\mathbf{M}_{j_{\min}}$ for $(d, \tilde{d}) = (3, 5)$ with complementary boundary conditions.

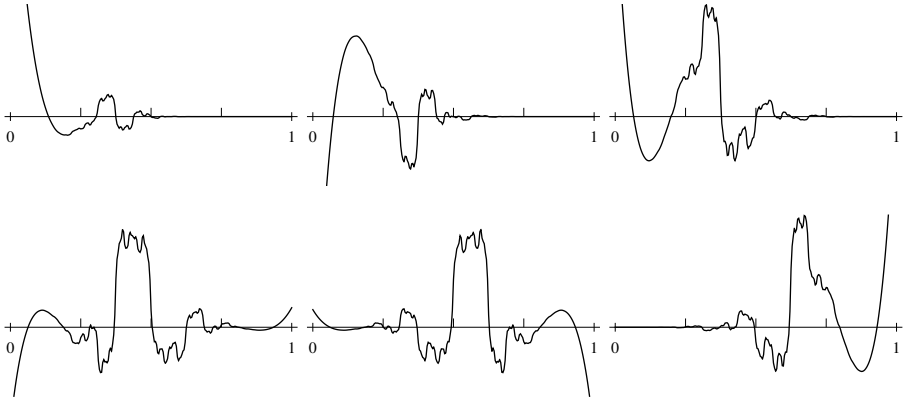

Figure 2.15: Dual scaling functions for $(d, \tilde{d}) = (3, 5)$ on level $j_{\min} = 3 = j_0 - 1$.
Two functions are omitted but can be found by the symmetry (2.24).

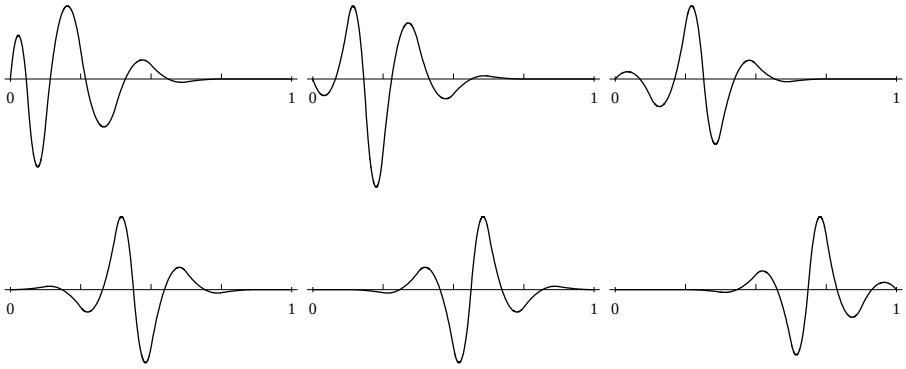

Figure 2.16: Primal wavelets for $(d, \tilde{d}) = (3, 5)$ on level $j_{\min} = 3 = j_0 - 1$.
Two functions are omitted but can be found by the symmetry (2.40).

$$\tilde{\mathbf{R}}_{j_0}^{\text{init}} = \begin{pmatrix} 1 & 1 & 1 & & & & & & \\ 1 & \frac{1}{3} & \frac{1}{7} & & & & & & \\ 1 & -\frac{1}{3} & \frac{1}{7} & & & & & & \\ 1 & -1 & 1 & & & & & & \\ 1 & -\frac{5}{3} & \frac{19}{7} & & & & & & \\ & & & 1 & & & & & \\ & & & & 1 & & & & \\ & & & & & \frac{19}{7} & -\frac{5}{3} & 1 \\ & & & & & 1 & -1 & 1 \\ & & & & & \frac{1}{7} & -\frac{1}{3} & 1 \\ & & & & & \frac{1}{7} & \frac{1}{3} & 1 \\ & & & & & 1 & 1 & 1 \end{pmatrix}, \quad \tilde{\mathbf{R}}_{j_0} = \begin{pmatrix} 6 & -8 & 3 & & & & & & \\ 3 & -3 & 1 & & & & & & \\ 1 & & & & & & & & \\ & 1 & & & & & & & \\ & & 1 & & & & & & \\ & & & 1 & & & & & \\ & & & & 1 & & & & \\ & & & & & 1 & & & \\ & & & & & & 1 & & \\ & & & & & & & 1 & \\ & & & & & & & & 1 \\ & & & & & & 1 & -3 & 3 \\ & & & & & & 3 & -8 & 6 \end{pmatrix}.$$

Matrix 2.5: The matrices $\tilde{\mathbf{R}}_{j_0}^{\text{init}}$ and $\tilde{\mathbf{R}}_{j_0}$ for $(d, \tilde{d}) = (1, 3)$.

$$\mathbf{M}_{j_0} = \begin{pmatrix} 1 & & & & & & \frac{5}{8} & -\frac{1}{8} & & & & & & & \\ 1 & & & & & & -\frac{11}{8} & -\frac{1}{8} & & & & & & & \\ & 1 & & & & & \frac{1}{2} & 1 & -\frac{1}{8} & & & & & & \\ & 1 & & & & & \frac{1}{2} & -1 & -\frac{1}{8} & & & & & & \\ & & 1 & & & & -\frac{1}{8} & \frac{1}{8} & 1 & -\frac{1}{8} & & & & & \\ & & 1 & & & & -\frac{1}{8} & \frac{1}{8} & -1 & -\frac{1}{8} & & & & & \\ & & & 1 & & & & & \frac{1}{8} & 1 & \frac{1}{8} & & & & \\ & & & 1 & & & & & \frac{1}{8} & -1 & \frac{1}{8} & & & & \\ & & & & 1 & & & & & \frac{1}{8} & -1 & \frac{1}{8} & & & \\ & & & & 1 & & & & & \frac{1}{8} & 1 & \frac{1}{8} & & & \\ & & & & & 1 & & & & & -\frac{1}{8} & -1 & \frac{1}{8} & -\frac{1}{8} & \\ & & & & & 1 & & & & & -\frac{1}{8} & 1 & \frac{1}{8} & -\frac{1}{8} & \\ & & & & & & 1 & & & & & -\frac{1}{8} & -1 & \frac{1}{2} & \\ & & & & & & 1 & & & & & -\frac{1}{8} & 1 & \frac{1}{2} & \\ & & & & & & & 1 & & & & & -\frac{1}{8} & -\frac{11}{8} & \\ & & & & & & & 1 & & & & & -\frac{1}{8} & \frac{5}{8} & \end{pmatrix}.$$

Matrix 2.6: The matrix $\mathbf{M}_{j_0}$ for $(d, \tilde{d}) = (1, 3)$.

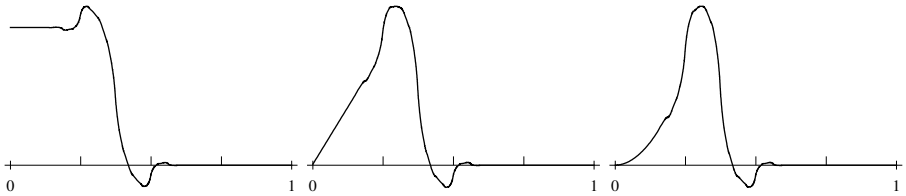

Figure 2.17: Dual boundary scaling functions for $(d, \tilde{d}) = (1, 3)$, before biorthogonalization.

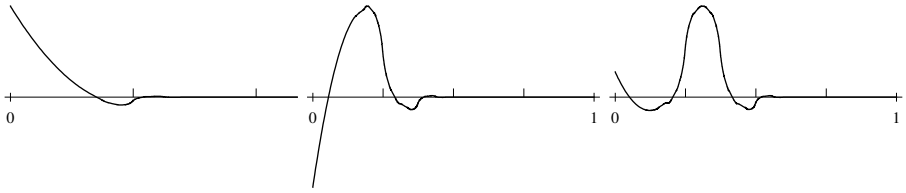

Figure 2.18: Dual boundary scaling functions for $(d, \tilde{d}) = (1, 3)$, after biorthogonalization.

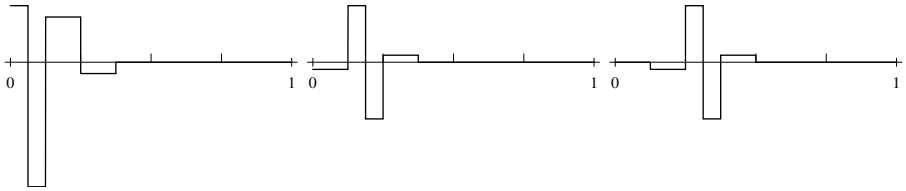

Figure 2.19: Primal wavelets for $(d, \tilde{d}) = (1, 3)$ (only one wavelet is a boundary wavelet).

Chapter 3
Sparse grids

In this chapter we will derive the best possible rate of approximation in $H_0^1(\mathrm{I}^n)$ that can be obtained by using a sequence of so-called *sparse grid* or *hyperbolic cross approximations* with respect to a tensor product wavelet basis. The use of sparse grids yields an almost-optimal rate, apart from some some log-factors. We will show that these factors can be removed by the use of *optimized sparse grids*. For general references on sparse grids, we refer to [BG04, GK00, Zen91]. Optimized sparse grids have attracted quite some attention recently, see e.g. [GK08, Tod09].

The optimal rate will require a sufficient regularity of the function u that is approximated. In the last section we study this issue for u being the solution of the n-dimensional Poisson equation. We will conclude that the required regularity condition to get the optimal rate is generally not fulfilled. This is the motivation to study *adaptive* tensor product approximations in Chapter 5.

As a side project, we will also study sparse grid approximation rates based on Fourier expansions.

Since we study merely approximation *rates*, in this chapter we will ignore dependence of "constants" on the space dimension n.

3.1 Some general results

3.1.1 Some properties of Riesz bases

Lemma 3.1.1. *Let $\Sigma := \{\sigma_k : k \in \mathbb{N}\}$, possibly after a suitable scaling, be a Riesz basis for a Hilbert space H. For $i \in \mathbb{N}$, let $A_i \subset \mathbb{N}$ be such that $\mathbb{N} = \cup_i A_i$ and $A_i \cap A_j = \varnothing$ for $i \neq j$. Then $\|\sum_{k\in\mathbb{N}} c_k\sigma_k\|_H^2 \eqsim \sum_i \|\sum_{k\in A_i} c_k\sigma_k\|_H^2$. This holds uniformly in the splitting $\mathbb{N} = \cup_i A_i$ and the sequence $(c_k) \in \ell_2$.*

Proof. This is a direct consequence of Σ being a Riesz basis. ◊

Lemma 3.1.2 (Lebesgue's lemma)**.** *Let $\Sigma = \{\sigma_k : k \in \mathbb{N}\}$ be a Riesz basis of H. Then, for $A \subset \mathbb{N}$ and $u = \sum_{k\in\mathbb{N}} u_k\sigma_k \in H$, we have*

$$\inf_{v\in\operatorname{span}\{\sigma_k :\, k\in A\}} \big\|u - v\big\|_H \eqsim \big\|u - \sum_{k\in A} u_k\sigma_k\big\|_H$$

uniformly in A and u.

Proof. Of course, $\inf_{v\in\operatorname{span}\{\sigma_k\colon k\in A\}}\|u-v\|_H \le \|u-\sum_{k\in A}u_k\sigma_k\|_H$. To see the converse inequality, define the projector $P_A\colon H\to\operatorname{span}\{\sigma_k\colon k\in A\}\colon u\mapsto\sum_{k\in A}u_k\sigma_k$. By Lemma 3.1.1 (with the splitting $(A,\mathbb{N}\setminus A)$), the norm of P_A is bounded, uniformly in A. This implies that for any $v\in\operatorname{span}\{\sigma_k\colon k\in A\}$,

$$\begin{aligned}\|u-P_Au\|_H &= \|u-v-P_A(u-v)\|_H\\ &\le \|u-v\|_H+\|P_A\|_{H\to\operatorname{span}\{\sigma_k\colon k\in A\}}\|u-v\|_H\lesssim\|u-v\|_H.\end{aligned}\qquad\Diamond$$

3.1.2 One-dimensional setting

In the following, we assume the availability of a Riesz basis

$$\Psi\coloneqq\{\psi_\lambda\colon\lambda\in\nabla\}$$

of wavelet type for $L_2(\mathrm{I})$. This basis should be taken such that the set

$$\{2^{-|\lambda|}\psi_\lambda\colon\lambda\in\nabla\}$$

is a Riesz basis for $H_0^1(\mathrm{I})$. Here $|\lambda|\in\mathbb{N}_0$ denotes the *level* of ψ_λ. The support of ψ_λ should scale proportionally to $2^{-|\lambda|}$. With the notation $\lambda=(j,k)$, $|\lambda|=j$, the bases constructed in Chapter 2 with $d>1$ and $m_{\scriptscriptstyle L}=m_{\scriptscriptstyle R}=1$ satisfy these conditions.

Because Ψ is a Riesz basis, every $u\in L_2(\mathrm{I})$ has a unique expansion $u=\sum_{\lambda\in\nabla}u_\lambda\psi_\lambda$, with $(u_\lambda)_{\lambda\in\nabla}\in\ell_2$. For $\ell\in\mathbb{N}_0$, we define the projector Q_ℓ as

$$Q_\ell\colon L_2(\mathrm{I})\to L_2(\mathrm{I})\colon u\mapsto\sum_{\{\lambda\in\nabla\colon|\lambda|\le\ell\}}u_\lambda\psi_\lambda.$$

In the following, we will use the notation

$$u|_\Lambda\coloneqq\sum_{\lambda\in\Lambda}u_\lambda\psi_\lambda,\tag{3.1}$$

for $\Lambda\subset\nabla$. With this notation we could have equivalently defined Q_ℓ as $Q_\ell u=u|_{\{\lambda\in\nabla\colon|\lambda|\le\ell\}}$.

We will assume that the wavelet basis Ψ satisfies a *Jackson estimate* of order $d\in\mathbb{N}$, in the sense that

$$\|I-Q_\ell\|_{H^d(\mathrm{I})\cap H_0^1(\mathrm{I})\to L_2(\mathrm{I})}\lesssim 2^{-\ell d}.\tag{3.2}$$

For any $s\in[0,d]$, we define the interpolation space

$$\mathcal{H}^s(\mathrm{I})\coloneqq\big[L_2(\mathrm{I}),H^d(\mathrm{I})\cap H_0^1(\mathrm{I})\big]_{\frac{s}{d},2}.\tag{3.3}$$

It is known (see e.g. [Coh03, LM72]) that for $s\notin\mathbb{N}+\frac12$,

$$\mathcal{H}^s(\mathrm{I})=\begin{cases}H_0^s(\mathrm{I}) & \text{for } s\in[0,1),\\ H^s(\mathrm{I})\cap H_0^1(\mathrm{I}) & \text{for } s\in[1,d].\end{cases}\tag{3.4}$$

By interpolation between $L_2(\mathrm{I})$ and $\mathcal{H}^d(\mathrm{I})$, a result of (3.2) and the uniform $L_2(\mathrm{I})$-boundedness of Q_ℓ is that, for all $s\in[0,d]$, we have

$$\|I-Q_\ell\|_{\mathcal{H}^s(\mathrm{I})\to L_2(\mathrm{I})}\lesssim 2^{-\ell s}.\tag{3.5}$$

In the following lemma the corresponding error estimate in $H^1(\mathrm{I})$ is given.

Lemma 3.1.3. *For all $s \in [0, d-1]$ we have $\|I - Q_\ell\|_{\mathcal{H}^{s+1}(\mathrm{I}) \to H_0^1(\mathrm{I})} \lesssim 2^{-\ell s}$.*

Proof. Because the set $\{2^{-|\lambda|}\psi_\lambda \colon \lambda \in \nabla\}$ is a Riesz basis for $H_0^1(\mathrm{I})$, the result is immediate for $s = 0$ by Lemma 3.1.1. Also, for $u \in H_0^1(\mathrm{I})$, we have $\|(I - Q_\ell)u\|_{H^1(\mathrm{I})}^2 \eqsim \sum_{\{\lambda \in \nabla \colon |\lambda| > \ell\}} 4^{|\lambda|}|u_\lambda|^2$. By Lemma 3.1.1,

$$\sum_{\{\lambda \in \nabla \colon |\lambda| = k\}} |u_\lambda|^2 \eqsim \Big\| \sum_{\{\lambda \in \nabla \colon |\lambda| = k\}} u_\lambda \psi_\lambda \Big\|_{L_2(\mathrm{I})}^2 = \|(Q_k - Q_{k-1})u\|_{L_2(\mathrm{I})}^2.$$

With the Jackson estimate (3.5), for $s \in [0, d-1]$ we have $\|Q_k - Q_{k-1}\|_{\mathcal{H}^{s+1}(\mathrm{I}) \to L_2(\mathrm{I})} \lesssim 2^{-(s+1)k}$, so that for $s \in (0, d]$, $u \in \mathcal{H}^{s+1}(\mathrm{I})$,

$$\begin{aligned}\|(I - Q_\ell)u\|_{H^1(\mathrm{I})}^2 &\eqsim \sum_{k=\ell+1}^{\infty} \sum_{\{\lambda \in \nabla \colon |\lambda| = k\}} 4^{|\lambda|}|u_\lambda|^2 \eqsim \sum_{k=\ell+1}^{\infty} 4^k \|(Q_k - Q_{k-1})u\|_{L_2(\mathrm{I})}^2 \\ &\lesssim \sum_{k=\ell+1}^{\infty} 4^k 4^{-(s+1)k} \|u\|_{\mathcal{H}^{s+1}(\mathrm{I})}^2 \lesssim 4^{-\ell s} \|u\|_{\mathcal{H}^{s+1}(\mathrm{I})}^2. \qquad \lozenge\end{aligned}$$

3.1.3 Tensor product setting

In order to approximate functions in more than one space dimension, we use a tensor product basis. We first recall some basic properties of tensor products. The following lemma was proven in e.g. [LC85]. We refer to that book also for more information on tensor products.

Lemma 3.1.4. *Let H_1, H_2, K_1, K_2 be Hilbert spaces, and let $A \colon H_1 \to K_1$, $B \colon H_2 \to K_2$ be bounded linear operators. Then $v_1 \otimes v_2 \mapsto Av_1 \otimes Bv_2$ extends to a bounded linear operator from $H_1 \otimes H_2$ to $K_1 \otimes K_2$, that we denote as $A \otimes B$. We have $\|A \otimes B\|_{H_1 \otimes H_2 \to K_1 \otimes K_2} = \|A\|_{H_1 \to K_1} \|B\|_{H_2 \to K_2}$.*

From the definition of a tensor product of separable Hilbert spaces (see, e.g., [LC85]), we have the following lemma.

Lemma 3.1.5. *For $i \in \{1, \dots, n\}$, let $H^{(i)}$ be a Hilbert space with Riesz basis Σ_i. Then $\bigotimes_{i=1}^n \Sigma_i := \{\bigotimes_{i=1}^n \sigma_i \colon \sigma_i \in \Sigma_i\}$ forms a Riesz basis for the tensor product space $\bigotimes_{i=1}^n H^{(i)}$.*

We will now recall some facts about tensor product bases for product domains. We define $\square := \mathrm{I}^n$. The following lemma is well-known.

Lemma 3.1.6. *We have $L_2(\square) = \bigotimes_{m=1}^n L_2(\mathrm{I})$.*

Proof. Because this lemma is used frequently, we include a short argument. The Haar basis (coinciding with the wavelet basis from Chapter 2 with $(d, \tilde{d}) = (1, 1)$) forms an orthonormnal basis for $L_2(\mathrm{I})$. By Lemma 3.1.5, the tensor products of Haar basis functions form a Riesz basis for $L_2(\mathrm{I}) \otimes \cdots \otimes L_2(\mathrm{I})$. It remains to be shown that these tensor product functions are also a Riesz basis for $L_2(\square)$. These functions form an orthogonal collection with respect to the norm on $L_2(\square)$. It is clear that they span all functions that are piecewise constant with respect to a uniform partition of $\square$ with mesh width 2^{-j} for any $j \in \mathbb{N}$. The fact that the latter functions are dense in $L_2(\square)$ completes the argument. $\lozenge$

We can now construct a wavelet basis for $L_2(\square)$:

Lemma 3.1.7. *The following set forms a Riesz basis for $L_2(\square)$:*

$$\boldsymbol{\Psi} := \Psi \otimes \cdots \otimes \Psi := \left\{ \psi_{\boldsymbol{\lambda}} := \psi_{\lambda_1} \otimes \cdots \otimes \psi_{\lambda_n} : \psi_{\lambda_1}, \ldots, \psi_{\lambda_n} \in \Psi \right\},$$

where $\boldsymbol{\lambda} := (\lambda_1, \ldots, \lambda_n) \in \boldsymbol{\nabla} := \nabla^n$.

Proof. This is a consequence of Ψ being a Riesz basis for $L_2(\mathrm{I})$, Lemma 3.1.5 and Lemma 3.1.6. ◊

Analogous to (3.1), we define, for $\boldsymbol{\Lambda} \in \boldsymbol{\nabla}$,

$$u|_{\boldsymbol{\Lambda}} := \sum_{\boldsymbol{\lambda} \in \boldsymbol{\Lambda}} u_{\boldsymbol{\lambda}} \psi_{\boldsymbol{\lambda}}.$$

To construct a wavelet basis for $H_0^1(\square)$, we recall the following lemma, which was proven in [GO95, Proposition 2]. For convenience, we include the short proof.

Lemma 3.1.8. *Let $\Sigma := \{\sigma_\lambda : \lambda \in \nabla\}$ be a Riesz basis for a Hilbert space H such that for $i = 1, \ldots, n$ and some nonzero scalars $d_\lambda^{(i)}$, the set $\Sigma^{(i)} := \{(d_\lambda^{(i)})^{-1} \sigma_\lambda\}$ forms a Riesz basis for $H^{(i)} \subseteq H$, with Riesz constants $C_1^{(i)}$, $C_2^{(i)}$ (as defined in (2.1)). Then the collection*

$$\left\{ \sigma_\lambda \Big/ \sqrt{\textstyle\sum_{i=1}^n \left(d_\lambda^{(i)}\right)^2} : \lambda \in \nabla \right\}$$

forms a Riesz basis for $\bigcap_{i=1}^n H^{(i)}$ with (squared) norm $\|\cdot\|^2_{\bigcap_{i=1}^n H^{(i)}} := \sum_{i=1}^n \|\cdot\|^2_{H^{(i)}}$. The condition number of this basis is not larger than $C_2^{(\max)}/C_1^{(\min)}$, where $C_1^{(\min)} := \min_i C_1^{(i)}$, $C_2^{(\max)} := \max_i C_2^{(i)}$.

Proof. It suffices to prove this fact for $n = 2$. Let $u \in H^{(1)} \cap H^{(2)}$, and write $u = \sum_\lambda c_\lambda \psi_\lambda$. Because $\Sigma^{(1)}$ and $\Sigma^{(2)}$ are Riesz bases for $H^{(1)}$ and $H^{(2)}$, respectively,

$$\frac{1}{C_2^{(\max)}} \|u\|^2_{H^{(1)}} \le \frac{1}{C_2^{(1)}} \|u\|^2_{H^{(1)}} \le \sum_{\lambda \in \nabla} \left(d_\lambda^{(1)}\right)^2 c_\lambda^2 \le \frac{1}{C_1^{(1)}} \|u\|^2_{H^{(1)}} \le \frac{1}{C_1^{(\min)}} \|u\|^2_{H^{(1)}},$$

$$\frac{1}{C_2^{(\max)}} \|u\|^2_{H^{(2)}} \le \frac{1}{C_2^{(2)}} \|u\|^2_{H^{(2)}} \le \sum_{\lambda \in \nabla} \left(d_\lambda^{(2)}\right)^2 c_\lambda^2 \le \frac{1}{C_1^{(2)}} \|u\|^2_{H^{(2)}} \le \frac{1}{C_1^{(\min)}} \|u\|^2_{H^{(2)}}.$$

By summing these inequalities, we have

$$\frac{1}{C_2^{\max}} \|u\|^2_{H^{(1)} \cap H^{(2)}} \le \sum_{\lambda \in \nabla} \left(\left(d_\lambda^{(1)}\right)^2 + \left(d_\lambda^{(2)}\right)^2 \right) c_\lambda^2 \le \frac{1}{C_1^{\min}} \|u\|^2_{H^{(1)} \cap H^{(2)}},$$

which concludes the proof. ◊

The following observation from [GO95, Example 3] is crucial for constructing a basis for $H_0^1(\square)$.

Lemma 3.1.9. *We have $H_0^1(\square) = H_0^1(\mathrm{I}) \otimes L_2(\mathrm{I}) \otimes \cdots \otimes L_2(\mathrm{I}) \cap \ldots \cap L_2(\mathrm{I}) \otimes \cdots \otimes L_2(\mathrm{I}) \otimes H_0^1(\mathrm{I})$*

Proposition 3.1.10. *The set $\left\{ \left(\sum_{i=1}^n 4^{|\lambda_i|}\right)^{-1} \psi_{\boldsymbol{\lambda}} : \boldsymbol{\lambda} \in \boldsymbol{\nabla} \right\}$ forms a Riesz basis for $H_0^1(\square)$.*

Proof. This follows from Lemma 3.1.9, Lemma 3.1.8, and the fact that Ψ is a Riesz basis for $L_2(\mathrm{I})$ and $\{2^{-|\lambda|}\psi_\lambda : \lambda \in \nabla\}$ is a Riesz basis for $H_0^1(\square)$. ◊

Before proving approximation properties of this basis, we introduce some more notation.

For $s_1, \dots, s_n \in [0, d]$ we define the space $\mathcal{H}^{(s_1,\dots,s_n)}(\square) := \bigotimes_{i=1}^n \mathcal{H}^{s_i}(\mathrm{I})$. For $s, t \in [0, d]$, we define

$$\mathscr{H}_{s,t}(\square) := \mathcal{H}^{(s,t,\dots,t)}(\square) \cap \mathcal{H}^{(t,s,t,\dots,t)}(\square) \cdots \cap \mathcal{H}^{(t,\dots,t,s)}(\square). \tag{3.6}$$

The norm on $\mathscr{H}_{s,t}(\square)$ is given by

$$\|u\|_{\mathscr{H}_{s,t}(\square)} := \sqrt{\|u\|^2_{\mathcal{H}^{(s,t,\dots,t)}(\square)} + \|u\|^2_{\mathcal{H}^{(t,s,t,\dots,t)}(\square)} + \cdots + \|u\|^2_{\mathcal{H}^{(t,\dots,t,s)}(\square)}}.$$

With this definition, the statement of Lemma 3.1.9 can be reformulated as $H_0^1(\square) = \mathscr{H}_{1,0}(\square)$.

3.2 Approximation errors

To motivate the remainder of this chapter, let us consider the n-dimensional Poisson problem of finding $u \in H_0^1(\square)$ such that

$$\big(\operatorname{grad} u, \operatorname{grad} v\big)_{L_2(\square)} = f\big(v\big) \qquad \big(v \in H_0^1(\square)\big), \tag{3.7}$$

for some given $f \in H^{-1}(\square) := (H_0^1(\square))'$. Since $\boldsymbol{\Psi}$ is a basis for $H_0^1(\square)$, we can write $u = \sum_{\boldsymbol{\lambda}\in\boldsymbol{\nabla}} c_{\boldsymbol{\lambda}}\psi_{\boldsymbol{\lambda}}$. For any $\boldsymbol{\Lambda} \subset \boldsymbol{\nabla}$, the *Galerkin solution* $\bar{u} \in \bar{V} := \operatorname{span}\{\psi_{\boldsymbol{\lambda}} : \boldsymbol{\lambda} \in \boldsymbol{\Lambda}\}$ of the problem

$$\big(\operatorname{grad} \bar{u}, \operatorname{grad} \bar{v}\big)_{L_2(\square)} = f\big(\bar{v}\big) \qquad \big(\bar{v} \in \bar{V}\big)$$

satisfies $\|u - \bar{u}\|_{H^1(\square)} \eqsim \inf_{\bar{w}\in\bar{V}} \|u - \bar{w}\|_{H^1(\square)} \eqsim \|u - u|_{\boldsymbol{\Lambda}}\|_{H^1(\square)}$, by Cea's lemma and Lebesgue's lemma (Lemma 3.1.2), respectively.

Seeking a good approximation to u, we will try to find a good set $\boldsymbol{\Lambda} \in \boldsymbol{\nabla}$, in the sense that $\|u - u|_{\boldsymbol{\Lambda}}\|$ is small (w.r.t. the $L_2(\square)$- or $H^1(\square)$-norm) compared to $\#\boldsymbol{\Lambda}$. This set shall only depend on the levels $|\boldsymbol{\lambda}| := (|\lambda_1|, \dots, |\lambda_n|)$.

A choice for $\boldsymbol{\Lambda}$ is the *full grid space* $\boldsymbol{\nabla}_J^{\mathrm{full}} := \{\boldsymbol{\lambda} \in \boldsymbol{\nabla} : \|\boldsymbol{\lambda}\|_\infty \le J\}$ (illustrated in Figure 3.1(a)). Assuming that $u \in H_0^1(\square) \cap H^d(\square)$, it is well-known that $\|u - u|_{\boldsymbol{\nabla}_J^{\mathrm{full}}}\|_{L_2(\square)} \lesssim 2^{-Jd}\|u\|_{\mathcal{H}^d(\square)}$ (this can be deduced from Lemma 3.1.3 and the forthcoming Proposition 3.2.3). It is easy to see that $\#\boldsymbol{\nabla}_J^{\mathrm{full}} \eqsim 2^{Jn}$. With $N := \#\boldsymbol{\nabla}_J^{\mathrm{full}}$ denoting the number of basis functions needed to represent the approximate solution $u|_{\boldsymbol{\nabla}_J^{\mathrm{full}}}$, this leads to $\|u - u|_{\boldsymbol{\nabla}_J^{\mathrm{full}}}\|_{L_2(\square)} \lesssim N^{-d/n}$. The fact that this rate is inversely proportional to the space dimension n is known as the *curse of dimensionality*.

The methods described below are meant to circumvent this curse of dimensionality on product domains. In this section, for the choice of $\boldsymbol{\Lambda}$ corresponding to sparse grid or optimized sparse grid index sets, we will derive estimates for $\|u - u|_{\boldsymbol{\Lambda}}\|_{L_2(\square)}$ and $\|u - u|_{\boldsymbol{\Lambda}}\|_{H^1(\square)}$, while in Section 3.3 we will give bounds for $\#\boldsymbol{\Lambda}$.

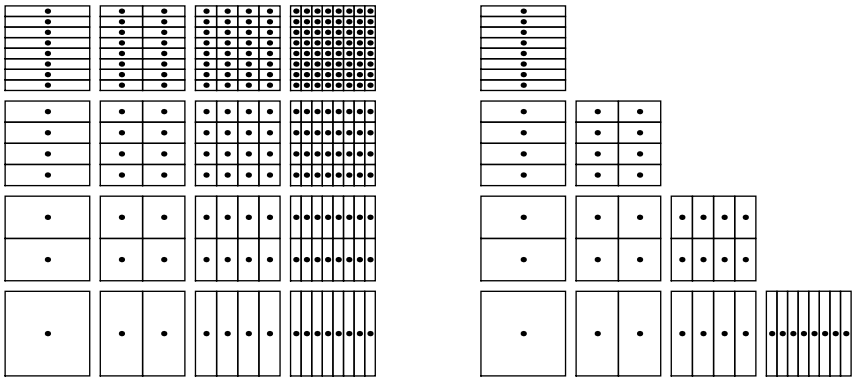

(a) Full grid (b) Sparse grid

Figure 3.1: Illustration of the full grid set $\boldsymbol{\nabla}_3^{\text{full}}$ and the sparse grid set $\boldsymbol{\nabla}_3^{(0)}$. The rectangles indicate the supports of the functions $\psi_{\boldsymbol{\lambda}}$ for $\boldsymbol{\lambda}$ in the corresponding index set.

3.2.1 Sparse grid approximation error in $L_2(\square)$

For $\boldsymbol{\ell} \in \mathbb{N}_0^n$, we define the projector $P_{\boldsymbol{\ell}}$ as

$$P_{\boldsymbol{\ell}} \colon L_2(\square) \to \operatorname{span}\{\psi_{\boldsymbol{\lambda}} \colon |\boldsymbol{\lambda}| = \boldsymbol{\ell}\} \colon u \mapsto \bigotimes_{i=1}^{n} (Q_{\ell_i} - Q_{\ell_i - 1})\, u,$$

with $Q_{-1} \coloneqq 0$. Note that $P_{\boldsymbol{\ell}} \psi_{\boldsymbol{\lambda}} = \psi_{\boldsymbol{\lambda}}$ if $|\boldsymbol{\lambda}| = \boldsymbol{\ell}$ and $P_{\boldsymbol{\ell}} \psi_{\boldsymbol{\lambda}} = 0$ for $|\boldsymbol{\lambda}| \neq \boldsymbol{\ell}$, which shows that $P_{\boldsymbol{\ell}}$ is indeed a projector.

Lemma 3.2.1. *For all $s \in [0, d]$ we have $\|P_{\boldsymbol{\ell}}\|_{\mathcal{H}^{(s,\dots,s)}(\square) \to L_2(\square)} \lesssim 2^{-\|\boldsymbol{\ell}\|_1 s}$.*

Proof. Using Lemma 3.1.4, we can write

$$\begin{aligned} \|P_{\boldsymbol{\ell}}\, u\|_{L_2(\square)} &= \|\textstyle\bigotimes_{i=1}^{n} (Q_{\ell_i} - Q_{\ell_i - 1})\, u\|_{L_2(\square)} \\ &\leq \textstyle\prod_{i=1}^{n} \|Q_{\ell_i} - Q_{\ell_i - 1}\|_{\mathcal{H}^s(\mathrm{I}) \to L_2(\mathrm{I})}\, \|u\|_{\mathcal{H}^{(s,\dots,s)}(\square)}. \end{aligned}$$

We now use the Jackson estimate (3.5) to obtain

$$\|P_{\boldsymbol{\ell}}\, u\|_{L_2(\square)} \lesssim \textstyle\prod_{i=1}^{n} 2^{-\ell_i s} \|u\|_{\mathcal{H}^{(s,\dots,s)}(\square)} = 2^{-\|\boldsymbol{\ell}\|_1 s} \|u\|_{\mathcal{H}^{(s,\dots,s)}(\square)}. \qquad \lozenge$$

Because the bound from the previous lemma only depends on $\|\boldsymbol{\ell}\|_1$ (and not on $\|\boldsymbol{\ell}\|_\infty$), we define the set $I_J^{(0)} \coloneqq \{\boldsymbol{\ell} \in \mathbb{N}_0^n \colon \|\boldsymbol{\ell}\|_1 \leq J\}$ and correspondingly the *sparse grid index set* $\boldsymbol{\nabla}_J^{(0)} \coloneqq \{\boldsymbol{\lambda} \in \nabla \colon |\boldsymbol{\lambda}| \in I_J^{(0)}\}$, where $|\boldsymbol{\lambda}| \coloneqq (|\lambda_1|, \dots, |\lambda_n|)$. This set is illustrated in Figure 3.1(b). The following lemma will be useful for proving statements involving this sparse grid index set.

Lemma 3.2.2. *For $\rho > 1$, $J \in \mathbb{N}$ we have $\sum_{\boldsymbol{\ell} \in \mathbb{N}_0^n \setminus I_J^{(0)}} \rho^{-\|\boldsymbol{\ell}\|_1} \eqsim \rho^{-J} J^{n-1}$.*

Proof. We have

$$\sum_{\boldsymbol{\ell} \in \mathbb{N}_0^n \setminus I_J^{(0)}} \rho^{-\|\boldsymbol{\ell}\|_1} = \sum_{m=J+1}^{\infty} \sum_{\{\boldsymbol{\ell} \in \mathbb{N}_0^n \colon \|\boldsymbol{\ell}\|_1 = m\}} \rho^{-m} = \sum_{m=J+1}^{\infty} \rho^{-m}\, \#\{\boldsymbol{\ell} \in \mathbb{N}_0^n \colon \|\boldsymbol{\ell}\|_1 = m\}.$$

The cardinality $\#\{\boldsymbol{\ell} \in \mathbb{N}^n \colon \|\boldsymbol{\ell}\|_1 = m\}$ can be viewed as the number of ways to group m objects into n groups. Thinking of this as choosing $n-1$ separators among $m+n-1$ objects, we infer that this number is $\binom{m+n-1}{n-1}$.

Neglecting dependence of constants on the space dimension n, we have

$$\binom{m+n-1}{n-1} \leq \frac{(m+n-1)^{n-1}}{(n-1)!} \eqsim m^{n-1}. \tag{3.8}$$

Similarly, also $\binom{m+n-1}{n-1} \geq \frac{m^{n-1}}{(n-1)!} \eqsim m^{n-1}$. Using this, we can estimate

$$\sum_{\boldsymbol{\ell} \in \mathbb{N}_0^n \setminus I_J^{(0)}} \rho^{-\|\boldsymbol{\ell}\|_1} \eqsim \sum_{m=J+1}^{\infty} \rho^{-m} m^{n-1} \eqsim \rho^{-J} J^{n-1},$$

because $\rho^{-1} < 1$. ◊

The following proposition states that by the use of the sparse grid index set, the rate of decrease of the approximation error $\|u - u|_{\boldsymbol{\nabla}_J^{(0)}}\|_{L_2(\square)}$ is, up to a logarithmic factor, *independent* of the space dimension n.

Proposition 3.2.3. *For $s \in [0,d]$, whenever $u \in \mathcal{H}^{(s,\ldots,s)}(\square)$, the error in $L_2(\square)$ of the sparse grid approximation $u|_{\boldsymbol{\nabla}_J^{(0)}}$ satisfies*

$$\|u - u|_{\boldsymbol{\nabla}_J^{(0)}}\|_{L_2(\square)} \lesssim 2^{-sJ} J^{(n-1)/2} \|u\|_{\mathcal{H}^{(s,\ldots,s)}(\square)}.$$

Proof. By Lemma 3.2.1,

$$\|u - u|_{\boldsymbol{\nabla}_J^{(0)}}\|_{L_2(\square)}^2 \eqsim \sum_{\boldsymbol{\ell} \in \mathbb{N}_0^n \setminus I_J^{(0)}} \|P_{\boldsymbol{\ell}} u\|_{L_2(\square)}^2 \lesssim \sum_{\boldsymbol{\ell} \in \mathbb{N}_0^n \setminus I_J^{(0)}} 4^{-\|\boldsymbol{\ell}\|_1 s} \|u\|_{\mathcal{H}^{(s,\ldots,s)}(\square)}^2.$$

Applying Lemma 3.2.2 and taking square roots yields the result. ◊

3.2.2 Sparse grid approximation error in $H_0^1(\square)$

We will now look at the sparse grid approximation error in $H_0^1(\square)$. In view of Lemma 3.1.9, it is sufficient to consider only the error in $\mathcal{H}^{(1,0,\ldots,0)}(\square)$.

Lemma 3.2.4. *For all $s \in [0, d-1]$, $t \in [0,d]$, we have $\|P_{\boldsymbol{\ell}}\|_{\mathcal{H}^{(s+1,t\ldots,t)}(\square) \to \mathcal{H}^{(1,0,\ldots,0)}(\square)} \lesssim 2^{-\ell_1 s} 2^{-t(\|\boldsymbol{\ell}\|_1 - \ell_1)}$.*

Proof. The proof is similar to that of Lemma 3.2.1, except we now have to distinguish the first coordinate direction from the others. We have

$$\begin{aligned}\|P_{\boldsymbol{\ell}} u\|_{\mathcal{H}^{(1,0,\ldots,0)}(\square)} &\leq \|Q_{\ell_1} - Q_{\ell_1 - 1}\|_{\mathcal{H}^{s+1}(\mathrm{I}) \to H^1(\mathrm{I})} \times \\ &\qquad \prod_{i=2}^{n} \|Q_{\ell_i} - Q_{\ell_i - 1}\|_{\mathcal{H}^t(\mathrm{I}) \to L_2(\mathrm{I})} \|u\|_{\mathcal{H}^{(s+1,t,\ldots,t)}(\mathrm{I})} \\ &\lesssim 2^{-\ell_1 s} 2^{-t(\sum_{k=2}^n \ell_k)} \|u\|_{\mathcal{H}^{(s+1,t,\ldots,t)}(\square)},\end{aligned}$$

by the Jackson assumption (3.5) and Lemma 3.1.3. ◊

This lemma allows us to prove the following proposition.

Proposition 3.2.5. *For $s \in [0, d-1]$, whenever $u \in \mathscr{H}_{s+1,s}(\square)$, the error in $H_0^1(\square)$ of the sparse grid approximation $u|_{\boldsymbol{\nabla}_J^{(0)}}$ satisfies*

$$\|u - u|_{\boldsymbol{\nabla}_J^{(0)}}\|_{H^1(\square)} \lesssim 2^{-Js} J^{(n-1)/2} \|u\|_{\mathscr{H}_{s+1,s}(\square)}.$$

Proof. For $s = 0$, this follows, even without the factor $J^{(n-1)/2}$, from the fact that $\boldsymbol{\Psi}$ forms a Riesz basis for $H_0^1(\square)$ (cf. Lemma 3.1.9). For $s \in (0, d-1]$,

$$\begin{aligned}\|u - u|_{\boldsymbol{\nabla}_J^{(0)}}\|^2_{\mathcal{H}^{(1,0,\dots,0)}(\square)} &\eqsim \sum_{\boldsymbol{\ell} \in \mathbb{N}_0^n \setminus I_J^{(0)}} \|P_{\boldsymbol{\ell}} u\|^2_{\mathcal{H}^{(1,0,\dots,0)}(\square)} \\ &\lesssim \sum_{\boldsymbol{\ell} \in \mathbb{N}_0^n \setminus I_J^{(0)}} 4^{-\|\boldsymbol{\ell}\|_1 s} \|u\|^2_{\mathcal{H}^{(s+1,s,\dots,s)}(\square)},\end{aligned}$$

by Lemma 3.2.4 with $t = s$.
Lemma 3.2.2 with $\rho = 4^s$ yields $\|u - u|_{\boldsymbol{\nabla}_J^{(0)}}\|^2_{\mathcal{H}^{(1,0,\dots,0)}(\square)} \lesssim 4^{-J} J^{n-1} \|u\|_{\mathcal{H}^{(s+1,s,\dots,s)}(\square)}$. Similarly, $\|u - u|_{\boldsymbol{\nabla}_J^{(0)}}\|^2_{\mathcal{H}^{(0,1,0,\dots,0)}(\square)} \lesssim 4^{-J} J^{n-1} \|u\|_{\mathcal{H}^{(s,s+1,s,\dots,s)}(\square)}$, and so on. The proof is completed by Lemma 3.1.9 and the definition of $\|\cdot\|_{\mathscr{H}_{s+1,s}(\square)}$ from (3.6). ◊

In the remainder of this subsection, we will show that the factor $J^{(n-1)/2}$ from the upper bound for $\|u - u|_{\boldsymbol{\nabla}_J^{(0)}}\|_{\mathcal{H}^{(1,0,\dots,0)}(\square)}$ can be removed assuming slightly stronger regularity of u.

For future reference we formulate the following easy result as a lemma.

Lemma 3.2.6. *For $\rho > 1$, $m \in \mathbb{N}$, $\sum_{k=0}^{J} \rho^k (J-k)^m \eqsim \rho^{J-1}$.*

We will also use the following lemma.

Lemma 3.2.7. *For all $s \geq 0$, $t > s$ we have $\sum_{\boldsymbol{\ell} \in \mathbb{N}_0^n \setminus I_J^{(0)}} 4^{-s\ell_1} 4^{-t(\|\boldsymbol{\ell}\|_1 - \ell_1)} \eqsim 4^{-Js}$.*

Proof. We split the sum into two sums, one with $\ell_1 > J$, and one with $\ell_1 \leq J$. The first sum can be written as

$$\sum_{\ell_1 > J} \sum_{\boldsymbol{\ell}' \in \mathbb{N}_0^{n-1}} 4^{-\ell_1 s} 4^{-t\|\boldsymbol{\ell}'\|_1} \eqsim \sum_{\ell_1 > J} 4^{-\ell_1 s} \eqsim 4^{-Js}$$

since s, $t > 0$. The second sum reads as

$$\sum_{\ell_1 \leq J} 4^{-\ell_1 s} \sum_{\{\boldsymbol{\ell}' \in \mathbb{N}_0^{n-1} \colon \|\boldsymbol{\ell}'\|_1 > J - \ell_1\}} 4^{-t\|\boldsymbol{\ell}'\|_1}.$$

Since $t > 0$, by Lemma 3.2.2, we have

$$\sum_{\{\boldsymbol{\ell}' \in \mathbb{N}_0^{n-1} \colon \|\boldsymbol{\ell}'\|_1 > J - \ell_1\}} 4^{-t\|\boldsymbol{\ell}'\|_1} \eqsim 4^{-(J-\ell_1)t} (J - \ell_1)^{n-2},$$

so that

$$\begin{aligned}\sum_{\ell_1 \leq J} 4^{-\ell_1 s} \sum_{\{\boldsymbol{\ell}' \in \mathbb{N}_0^{n-1} \colon \|\boldsymbol{\ell}'\|_1 > J - \ell_1\}} 4^{-t\|\boldsymbol{\ell}'\|_1} &\eqsim 4^{-Jt} \sum_{\ell_1 \leq J} 4^{\ell_1 (t-s)} (J - \ell_1)^{(n-2)} \\ &\eqsim 4^{-Jt} 4^{J(t-s)} = 4^{-Js},\end{aligned}$$

where the last equivalence follows from Lemma 3.2.6 and $t > s$. ◊

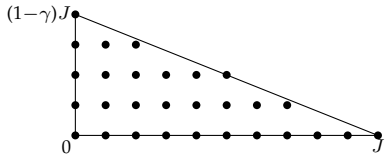

Figure 3.2: Sketch of the set $I_{J,1}^{(\gamma)}$ for $n = 2$.

Proposition 3.2.8. *For $s \in [0, d-1]$, $t \in (s, d]$, whenever $u \in \mathscr{H}_{s+1,t}(\square)$, the error in $H_0^1(\square)$ of the sparse grid approximation $u\big|_{\boldsymbol{\nabla}_J^{(0)}}$ satisfies*

$$\|u - u_{\boldsymbol{\nabla}_J^{(0)}}\|_{H^1(\square)} \lesssim 2^{-Js}\|u\|^2_{\mathscr{H}_{s+1,t}(\square)}.$$

Proof. As in the proof of Proposition 3.2.5 it suffices to consider $s > 0$. We have

$$\begin{aligned}\|u - u|_{\boldsymbol{\nabla}_J^{(0)}}\|^2_{\mathcal{H}^{(1,0,\dots,0)}(\square)} &\eqsim \sum_{\boldsymbol{\ell}\in\mathbb{N}_0^n\setminus I_J^{(0)}} \|P_{\boldsymbol{\ell}}u\|^2_{\mathcal{H}^{(1,0,\dots,0)}(\square)} \\ &\lesssim \|u\|^2_{\mathcal{H}^{(s+1,t,\dots,t)}(\square)} \sum_{\boldsymbol{\ell}\in\mathbb{N}_0^n\setminus I_J^{(0)}} 4^{-\ell_1 s}4^{-t(\|\boldsymbol{\ell}\|_1-\ell_1)}\end{aligned}$$

by Lemma 3.2.4. Lemma 3.2.7 yields the result. ◊

This improved version of Proposition 3.2.5 shows that indeed the factor $J^{(n-1)/2}$ from that proposition can be removed. However, as we will show in Section 3.3, the cardinality of the set $\boldsymbol{\nabla}_J^{(0)}$ will also contain a similar factor, leading to logarithmic terms in the approximation rate. Therefore, we turn to optimized sparse grids.

3.2.3 Approximation error in $H_0^1(\square)$ for optimized sparse grids

In this section, we will show that the same approximation rate in $H_0^1(\square)$ can be achieved with a set that has an even lower cardinality than the sparse grid index set defined previously. This idea was introduced in [GK00].

We define the set $I_{J,k}^{(\gamma)} \coloneqq \{\boldsymbol{\ell} \in \mathbb{N}_0^n \colon \|\boldsymbol{\ell}\|_1 - \gamma\ell_k \le (1-\gamma)J\}$, for $\gamma \in (0,1)$, $k \in \{1,\dots,n\}$. Correspondingly, we define $\boldsymbol{\nabla}_{J,k}^{(\gamma)} \coloneqq \{\boldsymbol{\lambda} \in \boldsymbol{\nabla} \colon |\boldsymbol{\lambda}| \in I_{J,k}^{(\gamma)}\}$. A sketch of the former set is shown in Figure 3.2.

Lemma 3.2.9. *For any $s \in [0, d-1]$, $t \in (s, d]$, $\gamma \in [0, 1 - s/t)$,*

$$\big\|u - u|_{\boldsymbol{\nabla}_{J,1}^{(\gamma)}}\big\|_{\mathcal{H}^{(1,0,\dots,0)}(\square)} \lesssim 2^{-Js}\|u\|_{\mathcal{H}^{(s+1,t,\dots,t)}(\square)}.$$

Proof. It is sufficient to consider the case $s > 0$. We have

$$\begin{aligned}\big\|u - u|_{\boldsymbol{\nabla}_{J,1}^{(\gamma)}}\big\|^2_{\mathcal{H}^{(1,0,\dots,0)}(\square)} &\eqsim \sum_{\boldsymbol{\ell}\in\mathbb{N}_0^n\setminus I_{J,1}^{(\gamma)}} \|P_{\boldsymbol{\ell}}u\|^2_{\mathcal{H}^{(1,0,\dots,0)}(\square)} \\ &\lesssim \|u\|^2_{\mathcal{H}^{(s+1,t,\dots,t)}(\square)} \sum_{\boldsymbol{\ell}\in\mathbb{N}_0^n\setminus I_{J,1}^{(\gamma)}} 4^{-\ell_1 s}4^{-(\|\boldsymbol{\ell}\|_1-\ell_1)t},\end{aligned}$$

by Lemma 3.2.4. This sum can be split into two parts, a part where $\ell_1 > J$ and a part where $\ell_1 \le J$. For the first part we have, with $\boldsymbol{\ell}' \coloneqq (\ell_2, \dots, \ell_n) \in \mathbb{N}_0^{n-1}$,

$$\sum_{\{\boldsymbol{\ell} \in \mathbb{N}_0^n \setminus I_{J,1}^{(\gamma)} \colon \ell_1 > J\}} 4^{-\ell_1 s} 4^{-(\|\boldsymbol{\ell}\|_1 - \ell_1)t} = \sum_{\ell_1 > J} 4^{-\ell_1 s} \sum_{\boldsymbol{\ell}' \in \mathbb{N}_0^{n-1}} 4^{-\|\boldsymbol{\ell}'\|_1 t} \tag{3.9}$$

$$\eqsim \sum_{\ell_1 > J} 4^{-\ell_1 s} \lesssim 4^{-Js}, \tag{3.10}$$

because s, $t > 0$.

For the second part we have

$$\sum_{\{\boldsymbol{\ell} \in \mathbb{N}_0^n \setminus I_{J,1}^{(\gamma)} \colon \ell_1 \le J\}} 4^{-\ell_1 s} 4^{-(\|\boldsymbol{\ell}\|_1 - \ell_1)t} = \sum_{\ell_1 = 0}^{J} 4^{-\ell_1 s} \sum_{\boldsymbol{\ell}' \in G_J(\ell_1)} 4^{-\|\boldsymbol{\ell}'\|_1 t},$$

with $G_J(\ell_1) \coloneqq \{\boldsymbol{\ell}' \in \mathbb{N}_0^{n-1} \colon \|\boldsymbol{\ell}'\|_1 > (1-\gamma)(J - \ell_1)\}$. Lemma 3.2.2 shows that

$$\sum_{\boldsymbol{\ell}' \in G_J(\ell_1)} 4^{-\|\boldsymbol{\ell}'\|_1 t} \lesssim 4^{-(1-\gamma)(J-\ell_1)t} ((1-\gamma)(J-\ell_1))^{n-2}.$$

This shows that

$$\sum_{\ell_1 = 0}^{J} 4^{-\ell_1 s} \sum_{\boldsymbol{\ell}' \in G_J(\ell_1)} 4^{-\|\boldsymbol{\ell}'\|_1 t} \lesssim \sum_{\ell_1 = 0}^{J} 4^{-\ell_1 s} 4^{-(1-\gamma)(J-\ell_1)t} ((1-\gamma)(J-\ell_1))^{n-2}$$

$$\eqsim 4^{-(1-\gamma)Jt} \sum_{\ell_1 = 0}^{J} 4^{-\ell_1 (s - (1-\gamma)t)} (J - \ell_1)^{n-2}.$$

Using $\gamma < 1 - s/t$, we have $s - (1-\gamma)t < 0$ so that by Lemma 3.2.6 the sum can be bounded by some multiple of $4^{-J(s-(1-\gamma)t)}$. This leads to

$$\sum_{\{\boldsymbol{\ell} \in \mathbb{N}_0^n \setminus I_{J,1}^{(\gamma)} \colon \ell_1 \le J\}} 4^{-\ell_1 s} 4^{-\|\boldsymbol{\ell}'\|_1 t} \lesssim 4^{-(1-\gamma)Jt - Js + (1-\gamma)Jt} = 4^{-Js}. \tag{3.11}$$

Combining (3.10) and (3.11), we get

$$\big\| u - u|_{\boldsymbol{\nabla}_{J,1}^{(\gamma)}} \big\|_{\mathcal{H}^{(1,0,\dots,0)}(\square)}^2 \lesssim 4^{-Js} \|u\|_{\mathcal{H}^{(s+1,t,\dots,t)}(\square)}^2.$$

The result follows by taking square roots. ◊

With $I_J^{(\gamma)} \subset \mathbb{N}^n$ denoting the union of all $I_{J,k}^{(\gamma)}$, i.e.

$$I_J^{(\gamma)} \coloneqq \bigcup_{k=1}^{n} I_{J,k}^{(\gamma)} = \{\boldsymbol{\ell} \colon \|\boldsymbol{\ell}\|_1 - \gamma \|\boldsymbol{\ell}\|_\infty \le (1-\gamma)J\},$$

we define the *concave* or *optimized sparse grid index set* $\boldsymbol{\nabla}_J^{(\gamma)} \coloneqq \{\boldsymbol{\lambda} \in \boldsymbol{\nabla} \colon |\boldsymbol{\lambda}| \in I_J^{(\gamma)}\}$. This set is illustrated in Figure 3.3(a). For this set, we have the same approximation rate as in Proposition 3.2.8:

Proposition 3.2.10. *For any $s \in [0, d-1]$, $t \in (s, d]$, $\gamma \in [0, 1 - \frac{s}{t})$, whenever $u \in \mathscr{H}_{s+1,t}(\square)$, we have*

$$\|u - u|_{\boldsymbol{\nabla}_J^{(\gamma)}}\|_{H^1(\square)} \lesssim 2^{-Js} \|u\|_{\mathscr{H}_{s+1,t}(\square)}.$$

Proof. Again, it is sufficient to consider the case $s > 0$. For $s \in (0, d]$, obviously, $\boldsymbol{\nabla}_J^{(\gamma)}$ is larger than $\boldsymbol{\nabla}_{J,1}^{(\gamma)}$, so

$$\begin{aligned}\|u - u|_{\boldsymbol{\nabla}_J^{(\gamma)}}\|^2_{\mathcal{H}^{(1,0,\ldots,0)}(\square)} &\eqsim \sum_{\boldsymbol{\ell}\in\mathbb{N}^n\setminus I_J^{(\gamma)}} \|P_{\boldsymbol{\ell}}u\|^2_{\mathcal{H}^{(1,0,\ldots,0)}(\square)} \leq \sum_{\boldsymbol{\ell}\in\mathbb{N}^n\setminus I_{J,1}^{(\gamma)}} \|P_{\boldsymbol{\ell}}u\|^2_{\mathcal{H}^{(1,0,\ldots,0)}(\square)} \\ &\eqsim \big\|u - u|_{\boldsymbol{\nabla}_{J,1}^{(\gamma)}}\big\|^2_{\mathcal{H}^{(1,0,\ldots,0)}(\square)} \lesssim 4^{-Js}\|u\|^2_{\mathcal{H}^{(s+1,t,\ldots,t)}(\square)},\end{aligned}$$

by Lemma 3.2.9. ◊

3.3 Cardinality of sparse grid index sets

Lemma 3.3.1. *The cardinality of the set $\boldsymbol{\nabla}_J^{(0)}$ is proportional to $2^J J^{n-1}$.*

Proof. Note that $\#\{\boldsymbol{\lambda} \in \boldsymbol{\nabla}\colon |\boldsymbol{\lambda}| = \boldsymbol{\ell}\} \eqsim 2^{\|\boldsymbol{\ell}\|_1}$ (since in one dimension we have $\#\{\lambda\colon |\lambda| = \ell\} \eqsim 2^\ell$). This leads to

$$\#\boldsymbol{\nabla}_J^{(0)} = \sum_{m=0}^{J} \sum_{\{\boldsymbol{\ell}\colon \|\boldsymbol{\ell}\|_1 = m\}} 2^m = \sum_{m=0}^{J} 2^m \cdot \#\{\boldsymbol{\ell}\colon \|\boldsymbol{\ell}\|_1 = m\} \eqsim \sum_{m=0}^{J} 2^m m^{n-1} \eqsim 2^J J^{n-1}.$$

The third step follows from (3.8). ◊

Proposition 3.3.2. *For $\gamma \in (0, 1]$, the cardinality of the set $\boldsymbol{\nabla}_J^{(\gamma)}$ is proportional to 2^J.*

Proof. The cardinality of the the set $\boldsymbol{\nabla}_{J,k}^{(\gamma)}$ is

$$\begin{aligned}\#\boldsymbol{\nabla}_{J,k}^{(\gamma)} &= \#\{\boldsymbol{\lambda}\colon \||\boldsymbol{\lambda}|\|_1 - \gamma|\lambda_k| \leq (1-\gamma)J\} \\ &= \sum_{\ell_k=0}^{J} \#\big\{\lambda_k\colon |\lambda_k| = \ell_k\big\} \cdot \#\Big\{\{\lambda_j\colon j \neq k\}\colon \sum_{j\neq k}|\lambda_j| \leq (1-\gamma)(J-\ell_k)\Big\} \\ &\eqsim \sum_{\ell_k=0}^{J} 2^{\ell_k} \#\Big\{\{\lambda_j\colon j \neq k\}\colon \sum_{j\neq k}|\lambda_j| \leq \lfloor(1-\gamma)(J-\ell_k)\rfloor\Big\}.\end{aligned}$$

The set $\{\{\lambda_j\colon j \neq k\}\colon \sum_{j\neq k}|\lambda_j| \leq \lfloor(1-\gamma)(J-\ell_k)\rfloor\}$ can be seen as the $(n-1)$-dimensional sparse grid space with level $\lfloor(1-\gamma)(J-\ell_k)\rfloor$, whose cardinality we have proved in Lemma 3.3.1 to be proportional to $2^{\lfloor(1-\gamma)(J-\ell_k)\rfloor}\lfloor(1-\gamma)(J-\ell_k)\rfloor^{n-2}$. This leads to

$$\begin{aligned}\#\boldsymbol{\nabla}_{J,k}^{(\gamma)} &\eqsim \sum_{\ell_k=0}^{J} 2^{\ell_k} 2^{\lfloor(1-\gamma)(J-\ell_k)\rfloor}\lfloor(1-\gamma)(J-\ell_k)\rfloor^{n-2} \\ &\eqsim 2^{(1-\gamma)J} \sum_{\ell_k=0}^{J} 2^{\gamma\ell_k}(J-\ell_k)^{n-2} \eqsim 2^{(1-\gamma)J}2^{\gamma J} = 2^J\end{aligned}$$

The last step follows from Lemma 3.2.6. The cardinality of $\boldsymbol{\nabla}_J^{(\gamma)}$ is proportional to $\sum_{k=1}^n \#\boldsymbol{\nabla}_{J,k}^{(\gamma)} \eqsim 2^J$ (where again we note that we discard dependence of constants on the space dimension n). ◊

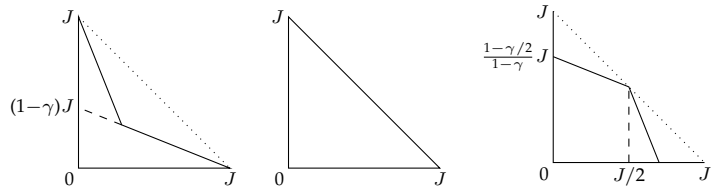

(a) $I_J^{(\gamma)}, \gamma \in (0,1]$ (b) $I_J^{(0)}$ (c) $I_J^{(\gamma)}, \gamma < 0$

Figure 3.3: Illustration of the sparse grid index set $I_J^{(\gamma)}$ in two dimensions.

For later reference, we also derive the cardinality of a *convex sparse grid space*, which is defined below and illustrated in Figure 3.3(c).

Definition 3.3.3. For $\gamma < 0$, the *convex sparse grid index set* $\boldsymbol{\nabla}_J^{(\gamma)}$ is defined as $\boldsymbol{\nabla}_J^{(\gamma)} := \{\boldsymbol{\lambda} \in \boldsymbol{\nabla} \colon |\boldsymbol{\lambda}| \in I_J^{(\gamma)}\}$ where $I_J^{(\gamma)} := \{\boldsymbol{\ell} \in \mathbb{N}_0^n \colon \|\boldsymbol{\ell}\|_1 - \gamma\|\boldsymbol{\ell}\|_\infty \le (1-\gamma/n)J\}$.

Proposition 3.3.4. *For $\gamma < 0$, the cardinality of $\boldsymbol{\nabla}_J^{(\gamma)}$ is proportional to 2^J.*

Proof. By induction on the space dimension n. For $n = 1$ the result is clear: $\sum_{\{\ell \in \mathbb{N}_0 \colon (1-\gamma)\ell \le (1-\gamma)J\}} 2^\ell \le 2^J$. Now let $n > 1$ and assume the statement holds for $n-1$. It is sufficient to consider those $\boldsymbol{\ell} \in I_J^{(\gamma)}$ with $\ell_1 \le \ell_2, \dots, \ell_n$, since the total cardinality will be at most n time as large (which dependency on n we ignore). From $\ell_1 \le \ell_2, \dots, \ell_n$ and $\boldsymbol{\ell} \in \boldsymbol{\nabla}_J^{(\gamma)}$, we have $\ell_1 \le J/n$ and $\|\boldsymbol{\ell}\|_\infty = \max_{i \ge 2} \ell_i$, and so we have

$$\begin{aligned}
\#\boldsymbol{\nabla}_J^{(\gamma)} &\lesssim \sum_{\ell_1=0}^{J/n} 2^{\ell_1} \sum_{\substack{\boldsymbol{\ell}' \in \mathbb{N}_0^{n-1} \colon \|\boldsymbol{\ell}'\|_1 - \gamma\|\boldsymbol{\ell}'\|_\infty \le (1-\frac{\gamma}{n})J - \ell_1, \\ \ell_1 \le \min(\ell_2, \dots, \ell_n)}} 2^{\|\boldsymbol{\ell}'\|_1} \\
&< \sum_{\ell_1=0}^{J/n} 2^{\ell_1} \sum_{\left\{\boldsymbol{\ell}' \in \mathbb{N}_0^{n-1} \colon \|\boldsymbol{\ell}'\|_1 - \gamma\|\boldsymbol{\ell}'\|_\infty \le \left(1-\frac{\gamma}{n-1}\right)\frac{(1-\gamma/n)J-\ell_1}{1-\gamma/(n-1)}\right\}} 2^{\|\boldsymbol{\ell}'\|_1} \\
&\lesssim \sum_{\ell_1=0}^{J/n} 2^{\ell_1} 2^{\frac{(1-\gamma/n)J-\ell_1}{1-\gamma/(n-1)}},
\end{aligned}$$

by the induction hypothesis. Rewriting this and using $\gamma < 0$ yields

$$\#\boldsymbol{\nabla}_J^{(\gamma)} \lesssim \sum_{\ell_1=0}^{J/n} 2^{\frac{(1-\gamma/n)J-(\gamma/(n-1))\ell_1}{1-\gamma/(n-1)}} \eqsim 2^{\frac{(1-\gamma/n)J-(\gamma/(n-1))J/n}{1-\gamma/(n-1)}} = 2^J. \qquad \lozenge$$

3.4 Rate of convergence

In this section we conclude the results of the previous sections by showing that sparse grids lead to a convergence rate that is, up to logarithmic factors, independent of the space dimension n. The last theorem in this section shows that when measuring the error in the $H^1(\square)$-norm, optimized sparse grids even lead to an optimal convergence rate, independent of n.

Lemma 3.4.1. *If for some functions f, g, we have $f(M) \lesssim M^{-s}(\log_2 M)^{\mu}$ and $g(M) = (\log_2 M)^{\nu} M =: N$, then*

$$(f \circ g^{-1})(N) \lesssim N^{-s}(\log_2 N)^{\mu+\nu s}.$$

This estimate is sharp.

Proof. We have

$$\begin{aligned}(f \circ g^{-1})(N) = f(M) &\lesssim M^{-s}(\log_2 M)^{\mu} \\ &= N^{-s}(\log_2 M)^{\nu s}(\log_2 M)^{\mu} \lesssim N^{-s}(\log_2 N)^{\nu s+\mu}\end{aligned}$$

To see that the estimate is sharp, assume that also $f(M) \gtrsim M^{-s}(\log_2 M)^{\mu}$. Now note that $M \gtrsim N^{1/2}$. This shows that $f(M) \gtrsim N^{-s}(\log_2 M)^{\nu s}(\log_2 M)^{\mu} \gtrsim N^{-s}(\log_2 N^{1/2})^{\nu s+\mu} \eqsim N^{-s}(\log_2 N)^{\nu s+\mu}$. ◊

Theorem 3.4.2. *If for some $s \in [0,d]$, $u \in \mathcal{H}^{(s,\dots,s)}(\square)$, then with $N := \#\boldsymbol{\nabla}_J^{(0)}$, being the cardinality of the sparse grid index set $\boldsymbol{\nabla}_J^{(0)}$, we have the estimate*

$$\|u - u|_{\boldsymbol{\nabla}_J^{(0)}}\|_{L_2(\square)} \lesssim N^{-s}(\log N)^{(n-1)(1/2+s)}\|u\|_{\mathcal{H}^{(s,\dots,s)}(\square)}.$$

Proof. We use Lemma 3.3.1 which states that $N \eqsim J^{n-1}2^J$. Proposition 3.2.3 states that $\|u - u|_{\boldsymbol{\nabla}_J^{(0)}}\|_{L_2(\square)}/\|u\|_{\mathcal{H}^{(s,\dots,s)}(\square)} \lesssim J^{(n-1)/2}2^{-Js}$. We are now in the situation of Lemma 3.4.1, with $M = 2^J$, $\nu = (n-1)$, $\mu = (n-1)/2$. ◊

Theorem 3.4.3. *If for some $s \in [0, d-1]$, $t \in (s,d]$, $u \in \mathscr{H}_{s+1,t}(\square)$, then with $N := \#\boldsymbol{\nabla}_J^{(0)}$, we have the estimate $\|u - u|_{\boldsymbol{\nabla}_J^{(0)}}\|_{H^1(\square)} \lesssim N^{-s}(\log N)^{(n-1)s}\|u\|_{\mathscr{H}_{s+1,t}(\square)}$.*

Proof. From Lemma 3.3.1 we have $N \eqsim J^{n-1}2^J$, and Proposition 3.2.8 shows

$$\|u - u|_{\boldsymbol{\nabla}_J^{(0)}}\|_{H^1(\square)}/\|u\|_{\mathscr{H}_{s+1,t}(\square)} \lesssim 2^{-Js}.$$

We are now in the setting of Lemma 3.4.1, with $M = 2^J$, $\nu = n-1$, $\mu = 0$. ◊

Theorem 3.4.4. *In the setting of Theorem 3.4.3, but with $t = s$, we have the estimate $\|u - u|_{\boldsymbol{\nabla}_J^{(0)}}\|_{H^1(\square)} \lesssim N^{-s}(\log N)^{(n-1)(s+\frac{1}{2})}\|u\|_{\mathscr{H}_{s+1,s}(\square)}$.*

Proof. As in Theorem 3.4.3, we have $N \eqsim J^{n-1}2^J$. Now Proposition 3.2.5 states that $\|u - u|_{\boldsymbol{\nabla}_J^{(0)}}\|_{H^1(\square)}/\|u\|_{\mathscr{H}_{s+1,s}(\square)} \lesssim J^{(n-1)/2}2^{-Js}$. The result follows by an application of Lemma 3.4.1, with $\nu = n-1$, $\mu = (n-1)/2$. ◊

Theorem 3.4.5. *If for some $s \in [0, d-1]$, $t \in (s,d]$, $u \in \mathscr{H}_{s+1,t}(\square)$, then with $N := \#\boldsymbol{\nabla}_J^{(\gamma)}$, $\gamma \in (0, 1-s/t)$, we have the estimate*

$$\|u - u|_{\boldsymbol{\nabla}_J^{(\gamma)}}\|_{H^1(\square)} \lesssim N^{-s}\|u\|_{\mathscr{H}_{s+1,t}(\square)}.$$

Proof. Proposition 3.3.2 shows that for $\gamma \in (0,1]$, $N \eqsim 2^J$. Proposition 3.2.10 shows that for $\gamma \in [0, 1-s/t)$, we have $\|u - u|_{\boldsymbol{\nabla}_J^{(\gamma)}}\|_{H^1(\square)}/\|u\|_{\mathscr{H}_{s+1,t}(\square)} \lesssim 2^{-Js}$. We are again in the setting of Lemma 3.4.1, with $\nu = \mu = 0$. ◊

3.5 Regularity of the solution of the Poisson problem on $\square$

We have shown in Theorem 3.4.5 that the sequence of optimized sparse grid approximations converges in $H_0^1(\square)$ with the optimal, dimension independent rate $d-1$, where d is the order of the basis. To get this rate, the function u that is approximated has to possess a certain regularity. In this section, we will study whether the solution of the Poisson equation on $\square$, i.e. the solution u of (3.7), fulfils these regularity conditions.

Using a Fourier basis, we can get an expression for the solution. To this end, for all $\ell \in \mathbb{N}$, let $\varphi_\ell(x) \coloneqq \sqrt{2}\sin(\ell\pi x)$, $\psi_\ell(x) \coloneqq \sqrt{2}\cos(\ell\pi x)$, and $\psi_0 = 1$.

Lemma 3.5.1. *The sets $\{\varphi_\ell \colon \ell \in \mathbb{N}\}$ and $\{\psi_\ell \colon \ell \in \mathbb{N}_0\}$ are orthonormal bases for $L_2(\mathrm{I})$.*

Proof. Orthonormality can be checked easily. It is known from Fourier theory that $\{\frac{1}{2}\sqrt{2}\varphi_\ell(x) \colon \ell \in \mathbb{N}\} \cup \{\frac{1}{2}\sqrt{2}\psi_\ell(x) \colon \ell \in \mathbb{N}_0\}$ is a basis for $L_2(-1,1)$. Given $f \in L_2(\mathrm{I})$, define $\tilde{f}$ by $\tilde{f}(x) = f(x)$ for $x \geq 0$, $\tilde{f}(x) = -f(-x)$ for $x < 0$. Now expand $\tilde{f}$ in the basis for $L_2(-1,1)$. Because f is odd, the coefficients in front of the even basis functions (the ψ_ℓ) are zero. Taking the restriction of $\tilde{f}$ to I, we see that the set $\{\frac{1}{2}\sqrt{2}\varphi_\ell \colon \ell \in \mathbb{N}\}$ is an orthogonal basis for $L_2(\mathrm{I})$. By normalization $\{\varphi_\ell \colon \ell \in \mathbb{N}\}$ is an orthonormal basis. The proof for $\{\psi_\ell \colon \ell \in \mathbb{N}_0\}$ follows the same route, but takes the symmetric extension for f. ◊

The following proposition states that the set $\{\frac{\varphi_\ell}{\ell\pi} \colon \ell \in \mathbb{N}\}$ is an orthonormal basis for $H_0^1(\mathrm{I})$ equipped with $|\cdot|_{H^1(\mathrm{I})}$.

Proposition 3.5.2. *Let $u = \sum_{\ell\in\mathbb{N}} c_\ell\varphi_\ell \in L_2(\mathrm{I})$, i.e., $(c_\ell)_\ell \in \ell_2$. Then*

$$(\ell c_\ell)_\ell \in \ell_2 \iff u' \in L_2(\mathrm{I}) \text{ and } u(0) = u(1) = 0.$$

In this case, $u' = \sum_{\ell\in\mathbb{N}} \ell c_\ell \pi\psi_\ell$, and so $\{\frac{\varphi_\ell}{\pi\ell} \colon \ell \in \mathbb{N}\}$ is an orthonormal basis of $H_0^1(\mathrm{I})$ equipped with $|\cdot|_{H^1(\mathrm{I})}$.

Proof. Let $(\ell c_\ell)_\ell \in \ell_2$. Then for any test function $\varphi \in C_0^\infty(\mathrm{I})$,

$$\int_0^1 u\varphi' = \int_0^1 \sum_{\ell\in\mathbb{N}} c_\ell\varphi_\ell\varphi' = -\sum_{\ell\in\mathbb{N}} c_\ell \int_0^1 \varphi_\ell'\varphi = -\sum_{\ell\in\mathbb{N}} c_\ell\ell\pi \int_0^1 \psi_\ell\varphi = -\int_0^1 \sum_{\ell\in\mathbb{N}} c_\ell\ell\pi\psi_\ell\varphi,$$

or $u' = \sum_{\ell\in\mathbb{N}} c_\ell\ell\pi\psi_\ell$, by definition of weak derivative. Since apparently $u = \sum_{\ell\in\mathbb{N}} c_\ell\varphi_\ell$ holds in $H^1(\mathrm{I})$ sense, by the Sobolev embedding theorem, equality holds also in $L_\infty(\mathrm{I})$ sense, and so $u(0) = u(1) = 0$.

Conversely, let $u' \in L_2(\mathrm{I})$ and $u(0) = u(1) = 0$. Then $\ell c_\ell = \ell\int_0^1 u\varphi_\ell = -\frac{1}{\pi}\int_0^1 u\psi_\ell' = \frac{1}{\pi}\int_0^1 u'\psi_\ell$, and thus $(\ell c_\ell)_\ell \in \ell_2$. ◊

Analogously, a basis can be created for $H^1(\square)$.

Proposition 3.5.3. *Let $u = \sum_{\ell\in\mathbb{N}_0} d_\ell\psi_\ell \in L_2(\mathrm{I})$, i.e., $(d_\ell)_\ell \in \ell_2$. Then*

$$(\ell d_\ell)_\ell \in \ell_2 \iff u' \in L_2(\mathrm{I}).$$

In this case $u' = -\sum_{\ell\in\mathbb{N}} d_\ell\ell\pi\varphi_\ell$, and the set $\{\frac{\psi_\ell}{\sqrt{1+\pi^2\ell^2}} \colon \ell \in \mathbb{N}_0\}$ forms an orthonormal basis of $H^1(\mathrm{I})$.

Proof. Similar to the proof of Proposition 3.5.2. In this case, $\ell d_\ell = -\frac{1}{\pi}\int_0^1 u'\varphi_\ell$ since φ_ℓ vanishes at the boundary. ◊

Because $L_2(\square) = L_2(\mathrm{I})\otimes\cdots\otimes L_2(\mathrm{I})$ (Lemma 3.1.6), we have the following lemma.

Lemma 3.5.4. *The collection* $\{\boldsymbol{\varphi}_{\boldsymbol{\ell}} \coloneqq \bigotimes_{i=1}^n \varphi_{\ell_i} : \boldsymbol{\ell}\in\mathbb{N}^n\}$ *is an orthonormal basis of* $L_2(\square)$.

Lemma 3.5.5. *The collection* $\{\frac{\boldsymbol{\varphi}_{\boldsymbol{\ell}}}{\pi\|\boldsymbol{\ell}\|_2} : \boldsymbol{\ell}\in\mathbb{N}^n\}$ *is an orthonormal basis of* $H_0^1(\square)$ *when this space is equipped with the norm* $|\cdot|_{H^1(\square)}$.

Proof. Lemma 3.5.1 and Proposition 3.5.2 state that $\{\varphi_\ell : \ell\in\mathbb{N}\}$, possibly after scaling, is a Riesz basis for $L_2(\mathrm{I})$ and for $H_0^1(\mathrm{I})$. This implies that after appropriate scaling, the set $\{\boldsymbol{\varphi}_{\boldsymbol{\ell}} : \boldsymbol{\ell}\in\mathbb{N}^n\}$ forms a Riesz basis of $\mathcal{H}^{(1,0,\dots,0)}(\square)$ up to $\mathcal{H}^{(0,\dots,0,1)}(\square)$. By Lemma 3.1.9, and Lemma 3.1.8, when properly scaled, the set forms a Riesz basis for $H_0^1(\square)$. Orthonormality of $\left\{\frac{\boldsymbol{\varphi}_{\boldsymbol{\ell}}}{\pi\|\boldsymbol{\ell}\|_2} : \boldsymbol{\ell}\in\mathbb{N}^n\right\}$ is verified easily. ◊

We can now write down the solution to the Poisson problem in terms of the basis $\{\boldsymbol{\varphi}_{\boldsymbol{\ell}} : \boldsymbol{\ell}\in\mathbb{N}^n\}$.

Proposition 3.5.6. *For* $f\in H_0^1(\square)'$, *the solution* u *of the Poisson problem is given by* $u = \sum_{\boldsymbol{\ell}\in\mathbb{N}^n} f(\frac{\boldsymbol{\varphi}_{\boldsymbol{\ell}}}{\pi\|\boldsymbol{\ell}\|_2})\frac{\boldsymbol{\varphi}_{\boldsymbol{\ell}}}{\pi\|\boldsymbol{\ell}\|_2}$.

Proof. Using the tensor product basis from Lemma 3.5.5, the stiffness matrix resulting from the variational variation of the Poisson problem is the identity. ◊

Theorem 3.4.5 states that for any $s\in[0,d-1]$, $t\in(s,d]$, whenever $u\in\mathscr{H}_{s+1,t}(\square)$, the optimized sparse grid approximation converges with rate s. Because of the sharpness of the Jackson estimate (3.5), and thus of the estimate from Lemma 3.2.1, this rate will generally not be possible for u being only a member of $\mathscr{H}_{s'+1,t'}(\square)$ for $s'<s$ or $t'<t$.

We will now investigate whether $u\in\mathscr{H}_{s+1,s}(\square)$ for some $s\in[0,d-1]$, which thus guarantees a rate $s-\varepsilon$, for any $\varepsilon>0$.

Lemma 3.5.7. *For* $s\in[0,d-1]$ *we have* $\mathscr{H}_{s+1,s}(\square) = \bigcap_{i=1}^n\bigotimes_{m=1}^n \mathcal{H}^{s+\delta_{im}}(\mathrm{I}) = H_0^1(\square)\cap\bigcap_{i=1}^n\bigotimes_{m=1}^n H^{s+\delta_{im}}(\mathrm{I})$.

Proof. It was shown in [HKZ00, Theorem 3] that $\bigcap_{i=1}^n\bigotimes_{m=1}^n \mathcal{H}^{d-1+\delta_{im}}(\mathrm{I}) = H_0^1(\square)\cap\bigcap_{i=1}^n\bigotimes_{m=1}^n H^{d-1+\delta_{im}}(\mathrm{I})$. From (3.4) and Lemma 3.1.9 we have that $\bigcap_{i=1}^n\bigotimes_{m=1}^n \mathcal{H}^{\delta_{im}}(\mathrm{I}) = H_0^1(\square)$. The result follows by interpolation on these spaces. ◊

Knowing that the solution u of the Poisson problem is in $H_0^1(\square)$, we now search for the largest s for which $u\in\bigcap_i\bigotimes_m H^{s+\delta_{im}}(\mathrm{I})$, or equivalently $\partial_i u\in H^{(s,\dots,s)}(\square) \coloneqq H^s(\mathrm{I})\otimes\cdots\otimes H^s(\mathrm{I})$, for all $i\in 1,\dots,n$.

Using the expression for the solution u of the Poisson problem from Proposition 3.5.6, we have

$$\partial_i u(\boldsymbol{x}) = \sum_{\boldsymbol{\ell}\in\mathbb{N}^n}\frac{\ell_i}{\|\boldsymbol{\ell}\|_2} f\big(\frac{\boldsymbol{\varphi}_{\boldsymbol{\ell}}}{\pi\|\boldsymbol{\ell}\|_2}\big)\psi_{\ell_i}(x_i)\prod_{j\neq i}\varphi_{\ell_j}(x_j).$$

Lemma 3.5.8. *For $s \in [0,1]$, $v = \sum_{\boldsymbol{\ell} \in \mathbb{N}^n} c_{\boldsymbol{\ell}} \varphi_{\boldsymbol{\ell}}$, we have*

$$\|v\|_{H^{(s,\dots,s)}(\square)} = \Big\| \Big(\Big(\prod_{j=1}^{n} \sqrt{1+\pi^2 \ell_j^2} \Big)^s c_{\boldsymbol{\ell}} \Big)_{\boldsymbol{\ell}} \Big\|_{\ell_2(\mathbb{N}^n)}.$$

The same holds when one or more components φ_{ℓ_j} in $\varphi_{\boldsymbol{\ell}}$ are replaced by ψ_{ℓ_j}.

Proof. We have $\|v\|_{L_2(\square)} = \|\boldsymbol{c}\|_{\ell_2(\mathbb{N}^n)}$. Furthermore, in one dimension, $\|v\|^2_{H^1(\mathrm{I})} = \|v\|^2_{L_2(\mathrm{I})} + \|v'\|^2_{L_2(\mathrm{I})} = \big\|\big((1+\pi^2\ell^2) c_\ell\big)_\ell\big\|^2_{\ell_2(\mathbb{N})}$, so the set $\big\{ \frac{\varphi_\ell}{\sqrt{1+\pi^2\ell^2}} : \ell \in \mathbb{N} \big\}$ forms an orthonormal basis for $H^1(\mathrm{I})$. By definition of a tensor product,

$$\Big\{ \frac{\varphi_{\boldsymbol{\ell}}}{\prod_{j=1}^n \sqrt{1+\pi^2\ell_j^2}} : \boldsymbol{\ell} \in \mathbb{N}^n \Big\}$$

forms an orthonormal basis for $H^{(1,\dots,1)}(\square)$. This means that

$$\|v\|_{H^{(1,\dots,1)}(\square)} = \Big\| \Big(\Big(\prod_{j=1}^{n} \sqrt{1+\pi^2 \ell_j^2} \Big) c_{\boldsymbol{\ell}} \Big)_{\boldsymbol{\ell}} \Big\|_{\ell_2(\mathbb{N}^n)}$$

The result follows by interpolation. ◊

We conclude that for any $i \in \{1,\dots,n\}$,

$$\partial_i u \in H^{(s,\dots,s)}(\square) \;\Leftrightarrow\; \Big(\Big(\prod_{j=1}^{n} \sqrt{1+\pi^2\ell_j^2} \Big)^s \frac{\ell_i}{\|\boldsymbol{\ell}\|_2} f\big(\frac{\varphi_{\boldsymbol{\ell}}}{\pi \|\boldsymbol{\ell}\|_2} \big) \Big)_{\boldsymbol{\ell}} \in \ell_2(\mathbb{N}^n).$$

In order to estimate the decay of the entries of this sequence when $\|\boldsymbol{\ell}\|_2 \to \infty$, we note that in one dimension

$$\int_0^1 g(x) \varphi_\ell(x)\,\mathrm{d}x = -g(x) \frac{\psi_\ell(x)}{\ell\pi}\Big|_0^1 + \int_0^1 g'(x) \frac{\psi_\ell(x)}{\ell\pi}\,\mathrm{d}x.$$

So when $g \in W_1^1(\mathrm{I}) \subset H^1(\mathrm{I})$, then $\int_0^1 g(x)\varphi_\ell(x)\,\mathrm{d}x = \mathcal{O}(1/\ell)$. Faster decay can be expected only if g vanishes at the boundary.

Therefore, for $f \in \bigotimes_{i=1}^n W_1^1(\mathrm{I})$ we have

$$\big| f\big(\frac{\varphi_{\boldsymbol{\ell}}}{\pi\|\boldsymbol{\ell}\|_2} \big) \big| \lesssim \frac{1}{\|\boldsymbol{\ell}\|_2} \frac{1}{\prod_{j=1}^n \ell_j}. \tag{3.12}$$

Generally, this estimate is sharp (noting that we ignore dependency on n): for example for the function $f = 1$ we have

$$f\big(\frac{\varphi_{\boldsymbol{\ell}}}{\pi\|\boldsymbol{\ell}\|_2} \big) = \begin{cases} \frac{1}{\pi\|\boldsymbol{\ell}\|_2} \big(\frac{2\sqrt{2}}{\pi}\big)^n \frac{1}{\prod_{j=1}^n \ell_j} & \text{when } \boldsymbol{\ell} \in (2\mathbb{N}+1)^n, \\ 0 & \text{otherwise.} \end{cases}$$

It follows from (3.12) that

$$\begin{aligned} \Big(\prod_{j=1}^{n} \sqrt{1+\pi^2\ell_j^2} \Big)^s \frac{\ell_i}{\|\boldsymbol{\ell}\|_2} f\Big(\frac{\varphi_{\boldsymbol{\ell}}}{\pi\|\boldsymbol{\ell}\|_2} \Big) &\lesssim \Big(\prod_{j=1}^{n} \sqrt{1+\pi^2\ell_j^2} \Big)^s \frac{\ell_i}{\|\boldsymbol{\ell}\|_2^2} \frac{1}{\prod_{j=1}^n \ell_j} \\ &\eqsim \frac{\ell_i}{\|\boldsymbol{\ell}\|_2^2} \Big(\prod_{j=1}^{n} \ell_j \Big)^{s-1} \end{aligned}$$

We claim that the right hand side is in $\ell_2(\mathbb{N}^n)$ if and only if $s < \frac{1}{2} + \frac{1}{n}$. Indeed,

$$\frac{\ell_i}{\|\boldsymbol{\ell}\|_2^2} \Big(\prod_{j=1}^{n} \ell_j \Big)^{s-1} \le \frac{1}{\|\boldsymbol{\ell}\|_2} \Big(\prod_{j=1}^{n} \ell_j \Big)^{s-1} < \Big(\prod_{j=1}^{n} \ell_j \Big)^{s-1-\frac{1}{n}}, \tag{3.13}$$

since $\ell_j \leq \|\boldsymbol{\ell}\|_2$ for all $j \in \{1,\dots,n\}$. Now

$$\sum_{\ell_1\in\mathbb{N}} \cdots \sum_{\ell_n\in\mathbb{N}} \Big(\prod_{j=1}^n \ell_j\Big)^{2(s-1-\frac{1}{n})} = \sum_{\ell_1\in\mathbb{N}} \ell_1^{2(s-1-\frac{1}{n})} \cdots \sum_{\ell_n\in\mathbb{N}} \ell_n^{2(s-1-\frac{1}{n})},$$

so that the right hand side from (3.13) is in $\ell_2(\mathbb{N}^n)$ iff $2(s-1-\frac{1}{n}) < -1$ or $s < \frac{1}{2} + \frac{1}{n}$.

We claim that the estimates from (3.13) are sharp, up to a constant factor (that may depend on n), for all $\boldsymbol{\ell}$ in the sector $\mathbb{N}^n_< := \{\boldsymbol{\ell} \in \mathbb{N}^n \colon \max_j \ell_j \leq 2\min_j \ell_j\}$. For those $\boldsymbol{\ell}$, $\prod_{j=1}^n \ell_j \eqsim \|\boldsymbol{\ell}\|_2^n \eqsim \max_j \ell_j^n$ so that $\big(\prod_{j=1}^n \ell_j\big)^{s-1-1/n} \eqsim \|\boldsymbol{\ell}\|_2^{n(s-1)-1}$. Clearly, $\sum_{\boldsymbol{\ell}\in\mathbb{N}^n_<} \|\boldsymbol{\ell}\|_2^{(n(s-1)-1)2} < \infty$ if and only if $\sum_{\boldsymbol{\ell}\in\mathbb{N}^n} \|\boldsymbol{\ell}\|_2^{(n(s-1)-1)2} < \infty$. The latter is the case if and only if $2(s-1)n - 2 + n - 1 < -1$, or $s < \frac{1}{2} + \frac{1}{n}$. This proves the claim.

We have now proven the following theorem.

Theorem 3.5.9. *For general, smooth right-hand sides f, the solution u of the Poisson equation* (3.7) *is in $\mathcal{H}^{(s,\dots,s)}(\square)$ for $s < \frac{1}{2} + \frac{1}{n}$, whereas it is generally not in $\mathcal{H}^{(s,\dots,s)}(\square)$ for $s > \frac{1}{2} + \frac{1}{n}$ (unless f vanishes at the boundary).*

In view of the bound for the approximation error we have derived in Theorem 3.4.5, the rate of approximation of the optimized sparse grid approximations in $H^1_0(\square)$ cannot be expected to be better than $\frac{1}{2} + \frac{1}{n}$, regardless of the order of the wavelets used.

In [DS09] it was shown that the use optimized sparse grids with local refinement near the boundaries does give rise to an optimal method (near-optimality was already shown in [Nit05]).

3.6 Rate of convergence for Fourier approximation

In Proposition 3.5.6 we have shown that the solution u of the Poisson problem is given by $u = \sum_{\boldsymbol{\ell}\in\mathbb{N}^n} f(\frac{\boldsymbol{\varphi}_{\boldsymbol{\ell}}}{\pi\|\boldsymbol{\ell}\|_2})\frac{\boldsymbol{\varphi}_{\boldsymbol{\ell}}}{\pi\|\boldsymbol{\ell}\|_2}$. Instead of using sparse grid approximations, one could also choose to approximate u by a subset of all Fourier basis functions, i.e. by $u|_{B_K} := \sum_{\boldsymbol{\ell}\in B_K} f(\frac{\boldsymbol{\varphi}_{\boldsymbol{\ell}}}{\pi\|\boldsymbol{\ell}\|_2})\frac{\boldsymbol{\varphi}_{\boldsymbol{\ell}}}{\pi\|\boldsymbol{\ell}\|_2}$, for some set $B_K \subset \mathbb{N}^n$. Because the set $\big\{\frac{\boldsymbol{\varphi}_{\boldsymbol{\ell}}}{\pi\|\boldsymbol{\ell}\|_2} \colon \boldsymbol{\ell} \in \mathbb{N}^n\big\}$ is an orthonormal basis for $H^1_0(\square)$ equipped with the $H^1(\square)$-seminorm, the error in such an approximation is given by

$$\big|u - u|_{B_K}\big|^2_{H^1(\square)} = \sum_{\boldsymbol{\ell}\in\mathbb{N}^n\setminus B_K} \big|f\big(\frac{\boldsymbol{\varphi}_{\boldsymbol{\ell}}}{\pi\|\boldsymbol{\ell}\|_2}\big)\big|^2.$$

From (3.12) we have $\big|f\big(\frac{\boldsymbol{\varphi}_{\boldsymbol{\ell}}}{\pi\|\boldsymbol{\ell}\|_2}\big)\big| \lesssim \frac{1}{\|\boldsymbol{\ell}\|_2}\frac{1}{\prod_{j=1}^n \ell_j}$, where the inequality is generally sharp. In view of this, we take

$$B_K := \big\{\boldsymbol{\ell} \in \mathbb{N}^n \colon \|\boldsymbol{\ell}\|_2 \prod_{j=1}^n \ell_j \leq K\big\}.$$

In the following lemma, we estimate the cardinality of B_K, which we will use to estimate the rate of convergence that can be expected when approximating with Fourier basis functions.

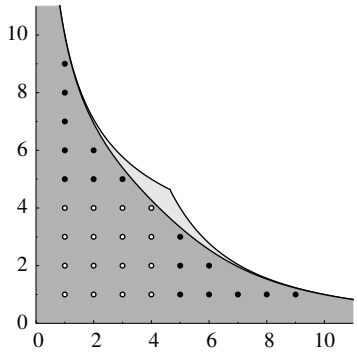

Figure 3.4: The set B_K for $K = 100$. Open dots indicate the set $\{\boldsymbol{\ell} \in \mathbb{N}^n \colon \sqrt{n}\|\boldsymbol{\ell}\|_\infty^{n+1} \le K\}$. Also indicated are the regions $\{\mathbf{x} \in \mathbb{R}^2 \colon \|\mathbf{x}\|_2 \prod_{j=1}^n x_i \le K\}$ (dark gray) and $\{\mathbf{x} \in \mathbb{R}^2 \colon \|\mathbf{x}\|_\infty \prod_{j=1}^n x_i \le K\}$ (light gray).

Lemma 3.6.1. *We have* $\#B_K \eqsim K^{\frac{n}{n+1}}$.

Proof. Since $\|\boldsymbol{\ell}\|_2 \le \sqrt{n}\|\boldsymbol{\ell}\|_\infty$, we have $B_K \supset \{\boldsymbol{\ell} \in \mathbb{N}^n \colon \sqrt{n}\|\boldsymbol{\ell}\|_\infty^{n+1} \le K\}$ (see Figure 3.4), and thus

$$\#B_K \ge \#\big\{\boldsymbol{\ell} \in \mathbb{N}^n \colon \|\boldsymbol{\ell}\|_\infty \le (K/\sqrt{n})^{\frac{1}{n+1}}\big\} \eqsim (K/\sqrt{n})^{\frac{n}{n+1}} \eqsim K^{\frac{n}{n+1}}.$$

To see that also $\#B_K \lesssim K^{\frac{n}{n+1}}$, note that the function $x \mapsto \|x\|_2 \prod_{j=1}^n x_j$ is increasing in all coordinate directions, so that

$$\#B_K \le \mathrm{vol}\big\{\mathbf{x} \in \mathbb{R}^n_{\ge 0} \colon \|\mathbf{x}\|_2 \textstyle\prod_{j=1}^n x_i \le K\big\} \le \mathrm{vol}\big\{\mathbf{x} \in \mathbb{R}^n_{\ge 0} \colon \|\mathbf{x}\|_\infty \textstyle\prod_{j=1}^n x_i \le K\big\},$$

since $\|\cdot\|_\infty \le \|\cdot\|_2$ (see Figure 3.4). Substituting $x_j = e^{y_j}$, $K = e^L$, this volume becomes

$$\int_{\{\mathbf{y} \in \mathbb{R}^n \colon \|\mathbf{y}\|_\infty + y_1 + \cdots + y_n \le L\}} e^{y_1 + \cdots + y_n} \,\mathrm{d}\mathbf{y}.$$

We claim that this integral is smaller than $C(n) e^{\frac{Ln}{1+n}}$, for some $C(n) > 0$. We will prove this by induction. For $n = 1$, we have $\int_0^{L/2} e^{y_1} \,\mathrm{d}y_1 = e^{L/2}$. Now assume that the statement holds for $n - 1$. Considering the volume in n dimensions, it suffices to consider only the region with $y_1 \le \min(y_2, \ldots, y_n)$: this region forms at most $1/n$ of the total volume, which dependence on n we ignore. In this region, we have $y_1 \le \frac{L}{n+1}$, so that the volume is bounded from above by

$$\int_{-\infty}^{\frac{L}{n+1}} e^{y_1} \int_{\{(y_2,\ldots,y_n) \in \mathbb{R}^{n-1} \colon \max(y_2,\ldots,y_n) + y_2 + \cdots + y_n \le L - y_1\}} e^{y_2 + \cdots + y_n} \,\mathrm{d}y_2 \cdots \mathrm{d}y_n,$$

which by the induction hypothesis is bounded by

$$\int_{-\infty}^{\frac{L}{n+1}} e^{y_1} C(n-1) e^{\frac{L - y_1}{1 + 1/(n-1)}} \,\mathrm{d}y_1 = nC(n-1) e^{\frac{Ln}{n+1}}.$$

This proves the claim. ◊

Theorem 3.6.2. *For u being the solution of the Poisson problem, the error in $H_0^1(\square)$ of the approximation $u|_{B_K}$ behaves as $N^{-(\frac{1}{2}+\frac{1}{n})}$, where $N := \#B_K$.*

Proof. Lemma 3.6.1 states that $\#B_K \eqsim K^{\frac{n}{n+1}}$. This means that there exist constants $c_2 \geq c_1 > 0$ independent of K such that

$$c_1 K^{\frac{n}{n+1}} \leq \#B_K \leq c_2 K^{\frac{n}{n+1}}.$$

We now claim that for $\rho > 1$ sufficiently large, we have $\#(B_{\rho K} \backslash B_K) \eqsim K^{\frac{n}{n+1}}$. More specifically, we will show that there exist $\tilde{c}_2 \geq \tilde{c}_1 > 0$, independent of K, such that

$$\tilde{c}_1 K^{\frac{n}{n+1}} \leq \#(B_{\rho K} \backslash B_K) \leq \tilde{c}_2 K^{\frac{n}{n+1}}.$$

Since $\#(B_{\rho K} \backslash B_K) \leq \#B_{\rho K}$ we can take $\tilde{c}_2 = \rho^{\frac{n}{n+1}} c_2$. Furthermore, we can take $\tilde{c}_1 = \rho^{\frac{n}{n+1}} c_1 - c_2$, which for ρ sufficiently large (but fixed), is greater than 0. This proves the claim. It follows that also $\#(B_{\rho^m K} \backslash B_{\rho^{m-1} K}) \eqsim (\rho^{m-1} K)^{\frac{n}{n+1}}$.

On $B_{\rho K} \backslash B_K$ we have $\|\boldsymbol{\ell}\|_2 \prod_{j=1}^n \ell_j \eqsim \rho^m K$, so that

$$\begin{aligned} \left|u - u|_{B_K}\right|^2_{H^1(\square)} &= \sum_{\boldsymbol{\ell} \in \mathbb{N}^n \backslash B_K} \left| f\left(\tfrac{\boldsymbol{\varphi}_{\boldsymbol{\ell}}}{\pi \|\boldsymbol{\ell}\|_2}\right)\right|^2 = \sum_{m=1}^{\infty} \sum_{\boldsymbol{\ell} \in B_{\rho^m K} \backslash B_{\rho^{m-1} K}} \frac{1}{\|\boldsymbol{\ell}\|_2^2 \prod_{j=1}^n \ell_j^2} \\ &\eqsim \sum_{m=1}^{\infty} (\rho^{m-1} K)^{\frac{n}{n+1}} (\rho^m K)^{-2} = K^{-\frac{n+2}{n+1}} \sum_{m=1}^{\infty} \rho^{m(\frac{n}{n+1}-2)} \rho^{-\frac{n}{n+1}}. \end{aligned}$$

Now since $\frac{n}{n+1} - 2 < 0$, the sum over m can be bounded by a constant that does not depend on K.

Writing $N = \#B_K \eqsim K^{\frac{n}{n+1}}$, we can now estimate the rate of convergence as

$$\left|u - u|_{B_K}\right|_{H^1(\square)} \eqsim K^{-\frac{n+2}{2(n+1)}} \eqsim N^{-(\frac{1}{2}+\frac{1}{n})}. \qquad \lozenge$$

Note that for the solution of Poisson's equation, the rate of approximation that can be achieved with optimized sparse grids is the same as the rate that can be achieved with a partial Fourier expansion. However, due to the global support of the Fourier basis functions $\boldsymbol{\varphi}_{\boldsymbol{\ell}}$, $\boldsymbol{\psi}_{\boldsymbol{\ell}}$, the computation of all coefficients in the partial Fourier expansion is is not possible in $\mathcal{O}(N)$ operations. In the (optimized) sparse grid methods based on a wavelet basis this is possible, due to the property that those basis functions have local support.

Chapter 4
Divergence-free wavelets on $(0,1)^n$

In [Ste08], a general framework was given for the construction of divergence-free wavelets on the hypercube. In this chapter, we give an alternative, hopefully more easily accessible presentation of the main results from that paper. Moreover, we will use the wavelets on the interval created in Chapter 2 as a building block to actually realize such divergence-free wavelets. With such wavelets at hand, the solution of the Stokes problem is reduced to the solution of an elliptic problem. Applications of divergence-free wavelets for solving Navier-Stokes equations can be found in [DP06, Urb02, SF98].

We will consider the space of vector-valued functions $L_2(\mathbb{R}^n)^n$ with norm

$$\|\mathbf{u}\|^2_{L_2(\mathbb{R}^n)^n} = \sum_{m=1}^{n} \|u_m\|^2_{L_2(\mathbb{R}^n)}, \quad \text{for } \mathbf{u} \coloneqq (u_1, \dots, u_n) \in L_2(\mathbb{R}^n)^n. \tag{4.1}$$

We are interested in functions whose divergence is in $L_2(\mathbb{R}^n)$, i.e., functions in the space $\mathbf{H}(\operatorname{div}; \mathbb{R}^n) \coloneqq \{\mathbf{u} \in L_2(\mathbb{R}^n)^n \colon \operatorname{div} \mathbf{u} \in L_2(\mathbb{R}^n)\}$. This is a closed linear subspace of $L_2(\mathbb{R}^n)$. Its norm is given by

$$\|\mathbf{u}\|^2_{\mathbf{H}(\operatorname{div};\mathbb{R}^n)} = \|\mathbf{u}\|^2_{L_2(\mathbb{R}^n)^n} + \|\operatorname{div} \mathbf{u}\|^2_{L_2(\mathbb{R}^n)}.$$

More specifically, we will look at the space of divergence-free functions, i.e., functions in $\mathbf{H}(\operatorname{div} 0; \mathbb{R}^n) \coloneqq \{\mathbf{u} \in \mathbf{H}(\operatorname{div}; \mathbb{R}^n) \colon \operatorname{div} \mathbf{u} = 0\}$, whose norm is given by

$$\|\mathbf{u}\|^2_{\mathbf{H}(\operatorname{div} 0;\mathbb{R}^n)} = \sum_{m=1}^{n} \|u_m\|^2_{L_2(\mathbb{R}^n)}. \tag{4.2}$$

Before creating Riesz bases for the above spaces, we recall some general properties about Riesz bases.

Lemma 4.0.1. *Let $\Sigma^{(1)} = \{\sigma^{(1)}_\lambda \colon \lambda \in \nabla\}$ be a Riesz basis for a Hilbert space H_1, with Riesz constants C_1, C_2. Let $A \colon H_1 \to H_2$ be a linear, boundedly invertible operator. Then $\Sigma^{(2)} \coloneqq \{\sigma^{(2)}_\lambda \colon \lambda \in \nabla\}$ with $\sigma^{(2)}_\lambda \coloneqq A\sigma^{(1)}_\lambda$ is a Riesz basis for H_2, with Riesz constants $C_1/\|A^{-1}\|_{H_2 \to H_1}$, $C_2\|A\|_{H_1 \to H_2}$.*

Proof. Let $u \in H_2$. Then $A^{-1}u \in H_1$, and because $\Sigma^{(1)}$ is a basis for H_1, there exists a unique sequence $\{c_\lambda \colon \lambda \in \nabla\}$ such that $A^{-1}u = \sum_{\lambda \in \nabla} c_\lambda \sigma^{(1)}_\lambda$. Now

$$u = AA^{-1}u = A\Big(\sum_{\lambda \in \nabla} c_\lambda \sigma^{(1)}_\lambda\Big) = \sum_{\lambda \in \nabla} c_\lambda A\sigma^{(1)}_\lambda = \sum_{\lambda \in \nabla} c_\lambda \sigma^{(2)}_\lambda,$$

where we have used the boundedness and linearity of A. Because A is invertible, the coefficients $\{c_\lambda : \lambda \in \nabla\}$ with respect to the basis $\Sigma^{(2)}$ are unique. This shows that $\Sigma^{(2)}$ is a basis. To show that it is a Riesz basis, note that we have, by assumption,

$$C_1 \sum_{\lambda\in\nabla} |c_\lambda|^2 \le \left\|A^{-1}u\right\|_{H_1}^2 \le C_2 \sum_{\lambda\in\nabla} |c_\lambda|^2,$$

so that

$$\|u\|_{H_2}^2 = \|AA^{-1}u\|_{H_2}^2 \le \|A\|_{H_1\to H_2}\|A^{-1}u\|_{H_1}^2 \le C_2\|A\|_{H_1\to H_2}\sum_{\lambda\in\nabla}|c_\lambda|^2,$$
$$\|u\|_{H_2}^2 \ge \frac{1}{\|A^{-1}\|_{H_2\to H_1}}\|A^{-1}u\|_{H_2}^2 \ge \frac{C_1}{\|A^{-1}\|_{H_2\to H_1}}\sum_{\lambda\in\nabla}|c_\lambda|^2. \qquad \Diamond$$

The following lemma is an easy corollary of Lemma 2.1.3 from Chapter 2:

Lemma 4.0.2. *Let Σ be a Riesz basis for a Hilbert space H. Let $\tilde\Sigma \subset H$ be such that $\langle\Sigma,\tilde\Sigma\rangle_H = \mathbf{I}$. Then also $\tilde\Sigma$ is a Riesz basis for H.*

4.1 Divergence-free wavelets on $\mathbb{R}^2$

To introduce the underlying ideas behind the construction of divergence-free wavelets, from the literature we recall the construction of divergence-free wavelets on $\mathbb{R}^2$. The construction of divergence-free wavelets on the unit cube in Section 4.3 will follow the same lines.

Let ψ, $\tilde\psi$ be compactly supported mother wavelets belonging to a biorthogonal multiresolution analysis for $L_2(\mathbb{R})$, where moreover $\tilde\psi \in H^1(\mathbb{R})$. It was shown in [LR92] that another pair of biorthogonal wavelets ψ^+, $\tilde\psi^-$ can be constructed in such a way that

$$\begin{aligned} \dot\psi^+ &= \psi, \\ \dot{\tilde\psi}^- &= -\dot{\tilde\psi}. \end{aligned} \tag{4.3}$$

Here, and throughout this chapter, a dot on top of a univariate function denotes its derivative.

As in Chapter 2, we define $\theta_{[j,m]} := 2^{-j/2}\theta(2^j x - m)$, for $\theta \in \{\psi, \tilde\psi, \psi^+, \tilde\psi^-\}$. With this notation, the collections $\{\psi_{[j,k]} : j,k \in \mathbb{Z}\}$, $\{\tilde\psi_{[j,k]} : j,k \in \mathbb{Z}\}$, $\{\psi^+_{[j,k]} : j,k \in \mathbb{Z}\}$, $\{\tilde\psi^-_{[j,k]} : j,k \in \mathbb{Z}\}$ are Riesz bases for $L_2(\mathbb{R})$.

As a consequence of (4.3) we have

$$\dot\psi^+_{[j,m]} = \quad 2^j\psi_{[j,m]} \tag{4.4}$$
$$\dot{\tilde\psi}_{[j,m]} = -2^j\tilde\psi^-_{[j,m]} \tag{4.5}$$

These relations were used in [DP06] for constructing a tensor product basis for $\mathbf{H}(\operatorname{div} 0;\mathbb{R}^n)$. We briefly present this method for $n = 2$. Since $L_2(\mathbb{R}^2) = L_2(\mathbb{R}) \otimes L_2(\mathbb{R})$ (see Lemma 3.1.6), the collection

$$\left\{ \begin{bmatrix} \psi^+_{[i,k]} \otimes \psi_{[j,m]} \\ 0 \end{bmatrix}, \begin{bmatrix} 0 \\ \psi_{[i,k]} \otimes \psi^+_{[j,m]} \end{bmatrix} : i,j,k,m \in \mathbb{Z} \right\} \tag{4.6}$$

forms a Riesz basis for $L_2(\mathbb{R}^2)^2$, with dual basis

$$\left\{ \begin{bmatrix} \tilde\psi^-_{[i,k]} \otimes \tilde\psi_{[j,m]} \\ 0 \end{bmatrix}, \begin{bmatrix} 0 \\ \tilde\psi_{[i,k]} \otimes \tilde\psi^-_{[j,m]} \end{bmatrix} : i,j,k,m \in \mathbb{Z} \right\}. \tag{4.7}$$

The next step is to modify this basis to get a basis for the space of divergence-free functions, and a basis for a complement space of functions that are not divergence-free. By applying the orthogonal matrix transformation $\frac{1}{\sqrt{4^i+4^j}} \left(\begin{smallmatrix} 2^j & -2^i \\ 2^i & 2^j \end{smallmatrix}\right)$ to the pair of basis functions $\left[\begin{smallmatrix} \psi^+_{[i,k]} \otimes \psi_{[j,m]} \\ 0 \end{smallmatrix}\right]$, $\left[\begin{smallmatrix} 0 \\ \psi_{[i,k]} \otimes \psi^+_{[j,m]} \end{smallmatrix}\right]$, we see that also the collection

$$\boldsymbol{\Psi}_{L_2(\mathbb{R}^2)^2} := \left\{ \frac{1}{\sqrt{4^i+4^j}} \begin{bmatrix} 2^j \psi^+_{[i,k]} \otimes \psi_{[j,m]} \\ -2^i \psi_{[i,k]} \otimes \psi^+_{[j,m]} \end{bmatrix}, \frac{1}{\sqrt{4^i+4^j}} \begin{bmatrix} 2^i \psi^+_{[i,k]} \otimes \psi_{[j,m]} \\ 2^j \psi_{[i,k]} \otimes \psi^+_{[j,m]} \end{bmatrix} : i,j,k,m \in \mathbb{Z} \right\}$$

constitutes a Riesz basis for $L_2(\mathbb{R}^2)^2$, with dual basis

$$\tilde{\boldsymbol{\Psi}}_{L_2(\mathbb{R}^2)^2} := \left\{ \frac{1}{\sqrt{4^i+4^j}} \begin{bmatrix} 2^j \tilde\psi^-_{[i,k]} \otimes \tilde\psi_{[j,m]} \\ -2^i \tilde\psi_{[i,k]} \otimes \tilde\psi^-_{[j,m]} \end{bmatrix}, \frac{1}{\sqrt{4^i+4^j}} \begin{bmatrix} 2^i \tilde\psi^-_{[i,k]} \otimes \tilde\psi_{[j,m]} \\ 2^j \tilde\psi_{[i,k]} \otimes \tilde\psi^-_{[j,m]} \end{bmatrix} : i,j,k,m \in \mathbb{Z} \right\}.$$

Proposition 4.1.1. *The collection*

$$\boldsymbol{\Psi}^{\mathrm{df}}_{\mathbf{H}(\mathbb{R}^2)} := \left\{ \begin{bmatrix} 2^j \psi^+_{[i,k]} \otimes \psi_{[j,m]} \\ -2^i \psi_{[i,k]} \otimes \psi^+_{[j,m]} \end{bmatrix} : i,j,k,m \in \mathbb{Z} \right\}$$

is a Riesz basis for $\mathbf{H}(\operatorname{div} 0; \mathbb{R}^2)$.

Proof. We first show that all functions in $\boldsymbol{\Psi}^{\mathrm{df}}_{L_2(\mathbb{R}^2)^2}$ are divergence-free. By (4.4),

$$\operatorname{div} \begin{bmatrix} 2^j \psi^+_{[i,k]} \otimes \psi_{[j,m]} \\ -2^i \psi_{[i,k]} \otimes \psi^+_{[j,m]} \end{bmatrix} = 2^j \dot\psi^+_{[i,k]} \otimes \psi_{[j,m]} - 2^i \psi_{[i,k]} \otimes \dot\psi^+_{[j,m]} = 0.$$

To see that $\boldsymbol{\Psi}^{\mathrm{df}}_{L_2(\mathbb{R}^2)^2}$ spans all divergence-free functions in $L_2(\mathbb{R}^2)^2$, take some $\mathbf{u} \in \mathbf{H}(\operatorname{div} 0; \mathbb{R}^2)$. Then by integration by parts we have, using (4.5),

$$\begin{aligned} \left\langle \mathbf{u}, \begin{bmatrix} 2^i \tilde\psi^-_{[i,k]} \otimes \tilde\psi_{[j,m]} \\ 2^j \tilde\psi_{[i,k]} \otimes \tilde\psi^-_{[j,m]} \end{bmatrix} \right\rangle_{L_2(\mathbb{R}^2)^2} &= -\left\langle \mathbf{u}, \mathbf{grad}\, \tilde\psi_{[i,k]} \otimes \tilde\psi_{[j,m]} \right\rangle_{L_2(\mathbb{R}^2)^2} \\ &= \left\langle \operatorname{div} \mathbf{u},\ \tilde\psi_{[i,k]} \otimes \tilde\psi_{[j,m]} \right\rangle_{L_2(\mathbb{R}^2)} = 0, \end{aligned}$$

which shows that the coefficients of $\mathbf{u}$ in front of basis functions in the complement $\boldsymbol{\Psi}_{L_2(\mathbb{R}^2)^2} \setminus \boldsymbol{\Psi}^{\mathrm{df}}_{L_2(\mathbb{R}^2)^2}$ vanish. ◊

4.2 Construction of auxiliary bases

The construction of divergence-free wavelets on $\square := \mathrm{I}^n$ will follow the same lines as the construction above. It relies on the availability of biorthogonal Riesz bases Ψ, $\tilde\Psi$ and Ψ^+, $\tilde\Psi^-$ for $L_2(\mathrm{I})$ that satisfy

$$\begin{aligned} \dot\Psi^+ &= \mathbf{D}\Psi, \\ \dot{\tilde\Psi} &= -\mathbf{D}\tilde\Psi^-, \end{aligned} \tag{4.8}$$

where $\mathbf{D}$ is an invertible diagonal matrix. These equations can be seen as a harmless generalization of (4.4) and (4.5).

Using (4.8) and the biorthogonality relations $\langle \Psi, \tilde{\Psi} \rangle_{L_2(\mathrm{I})} = \mathbf{I}$ and $\langle \Psi^+, \tilde{\Psi}^- \rangle_{L_2(\mathrm{I})} = \mathbf{I}$, integration by parts shows that necessarily

$$\begin{aligned}
&\mathbf{D}^{-1}\Psi^+(1)\tilde{\Psi}(1)^\mathsf{T} - \mathbf{D}^{-1}\Psi^+(0)\tilde{\Psi}(0)^\mathsf{T} \\
&= \big\langle \mathbf{D}^{-1}\dot{\Psi}^+, \tilde{\Psi} \big\rangle_{L_2(\mathrm{I})} + \big\langle \Psi^+, \mathbf{D}^{-1}\dot{\tilde{\Psi}} \big\rangle_{L_2(\mathrm{I})} \\
&= \big\langle \Psi, \tilde{\Psi} \big\rangle_{L_2(\mathrm{I})} - \big\langle \Psi^+, \tilde{\Psi}^- \big\rangle_{L_2(\mathrm{I})} = \mathbf{I} - \mathbf{I} = 0.
\end{aligned}$$

To satisfy this condition, we will construct bases such that the elements of $\tilde{\Psi}$ vanish at 1 and the elements of Ψ^+ vanish at 0.

Remark 4.2.1. Since, in view of (4.8),

$$\int_0^1 \Psi(y)\,\mathrm{d}y = \int_0^1 \mathbf{D}^{-1}\dot{\Psi}^+(y)\,\mathrm{d}y = \mathbf{D}^{-1}\big(\Psi^+(1) - \Psi^+(0)\big),$$

it is not possible to choose the elements of Ψ^+ to vanish at both 0 and 1. Indeed, if they would vanish at both boundaries, every function from Ψ would have zero mean and thus Ψ could not form a basis for $L_2(\mathrm{I})$. Following a similar argument, the elements of $\tilde{\Psi}$ cannot all vanish at both 0 and 1.

We will assume the availability of two collections Ψ, $\tilde{\Psi} \subset L_2(\mathrm{I})$ such that:

- Ψ and $\tilde{\Psi}$ are Riesz bases for $L_2(\mathrm{I})$.
- Ψ and $\tilde{\Psi}$ are biorthogonal, i.e. $\langle \Psi, \tilde{\Psi} \rangle_{L_2(\mathrm{I})} = \mathbf{I}$.
- The elements of $\tilde{\Psi}$ vanish at 1.
- There exists an invertible diagonal matrix $\mathbf{D}$ such that $\mathbf{D}^{-1}\tilde{\Psi}$ forms a Riesz basis for $H^1_{0,\{1\}}(\mathrm{I})$.

Remark 4.2.2. The bases created in Chapter 2 satisfy these conditions when $m_L = m_R = 0$, $\tilde{m}_R \geq 1$ and $\min(\tilde{\gamma}(d,\tilde{d}),\tilde{d}) \geq 1$.

We now define Ψ^+ and $\tilde{\Psi}^-$ by

$$\Psi^+ := x \mapsto \mathbf{D}\textstyle\int_0^x \Psi(y)\,\mathrm{d}y, \tag{4.9}$$

$$\tilde{\Psi}^- := -\mathbf{D}^{-1}\dot{\tilde{\Psi}}. \tag{4.10}$$

Lemma 4.2.3. *The collections Ψ^+ and $\tilde{\Psi}^-$ are biorthogonal.*

Proof. By integration by parts, we have

$$\langle \Psi^+, \tilde{\Psi}^- \rangle_{L_2(\mathrm{I})} = \big(\Psi^+(0)\tilde{\Psi}(0)^\mathsf{T} - \Psi^+(1)\tilde{\Psi}(1)^\mathsf{T}\big)\mathbf{D}^{-\mathsf{T}} + \mathbf{D}\langle \Psi, \tilde{\Psi} \rangle_{L_2(\mathrm{I})}\mathbf{D}^{-\mathsf{T}}.$$

By assumption, $\tilde{\Psi}(1) = 0$, and by construction, $\Psi^+(0) = 0$. The result now follows from the biorthogonality between Ψ and $\tilde{\Psi}$. ◊

Theorem 4.2.4. *The collections Ψ^+ and Ψ^- are Riesz bases for $L_2(\mathrm{I})$.*

Proof. We first show the statement for $\tilde{\Psi}^-$, by using Lemma 4.0.1. Differentiation is a linear, boundedly invertible operator from $H^1_{0,\{1\}}(\mathrm{I}) \to L_2(\mathrm{I})$. Indeed, its inverse is given by $f \mapsto (x \mapsto -\int_x^1 f(y)\,\mathrm{d}y)$. Since, by assumption, $\tilde{\Psi}$ is a Riesz basis for $H^1_{0,\{1\}}(\mathrm{I})$, this shows that the collection $\tilde{\Psi}^-$ forms a Riesz basis for $L_2(\mathrm{I})$. The statement for Ψ^+ follows from the biorthogonality between Ψ^+ and $\tilde{\Psi}^-$, and Lemma 4.0.2. ◊

Figure 4.1 summarizes the properties of the involved bases.

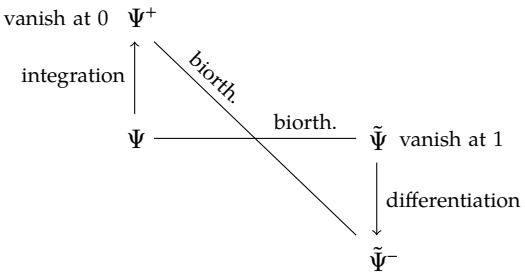

Figure 4.1: Schematic relation between Ψ, $\tilde{\Psi}$, Ψ^+ and $\tilde{\Psi}^-$.

4.3 Divergence-free wavelets on □

In this section we assume that the bases Ψ, $\tilde{\Psi}$, Ψ^+ and $\tilde{\Psi}^-$ are labelled with an index λ from some index set ∇. We set $d_\lambda := (\mathbf{D})_{\lambda\lambda}$.

Moving to higher dimensions, we set $\boldsymbol{\lambda} := (\lambda_1, \ldots, \lambda_n)$, $\boldsymbol{\nabla} := \nabla^n$. Because $L_2(\square) = L_2(\mathrm{I}) \otimes \cdots \otimes L_2(\mathrm{I})$ (see Lemma 3.1.6), we have the following proposition.

Proposition 4.3.1. *For $1 \le m \le n$, the collections*

$$\Psi^{(m)} := \{\psi^{(m)}_{\boldsymbol{\lambda}} := \psi_{\lambda_1} \otimes \cdots \otimes \psi^+_{\lambda_m} \otimes \cdots \otimes \psi_{\lambda_n} : \boldsymbol{\lambda} \in \boldsymbol{\nabla}\},$$
$$\tilde{\Psi}^{(m)} := \{\tilde{\psi}^{(m)}_{\boldsymbol{\lambda}} := \tilde{\psi}_{\lambda_1} \otimes \cdots \otimes \tilde{\psi}^-_{\lambda_m} \otimes \cdots \otimes \psi_{\lambda_n} : \boldsymbol{\lambda} \in \boldsymbol{\nabla}\}$$

are biorthogonal Riesz bases for $L_2(\square)$.

We will create a basis for the space of vector-valued functions $L_2(\square)^n$. To that end, we define the vector-valued functions

$$\underline{\boldsymbol{\Psi}} := \{\underline{\boldsymbol{\psi}}^{(m)}_{\boldsymbol{\lambda}} := \psi^{(m)}_{\boldsymbol{\lambda}} \mathbf{e}_m : 1 \le m \le n, \boldsymbol{\lambda} \in \boldsymbol{\nabla}\}, \tag{4.11}$$
$$\underline{\tilde{\boldsymbol{\Psi}}} := \{\underline{\tilde{\boldsymbol{\psi}}}^{(m)}_{\boldsymbol{\lambda}} := \tilde{\psi}^{(m)}_{\boldsymbol{\lambda}} \mathbf{e}_m : 1 \le m \le n, \boldsymbol{\lambda} \in \boldsymbol{\nabla}\}, \tag{4.12}$$

where $\mathbf{e}_m$ denotes the unit vector in the m-th coordinate direction.

Note that $\underline{\boldsymbol{\Psi}} \subset \mathbf{H}(\mathrm{div}; \square)$: for all $\underline{\boldsymbol{\psi}}^{(m)}_{\boldsymbol{\lambda}} \in \underline{\boldsymbol{\Psi}}$ we have

$$\mathrm{div}\, \underline{\boldsymbol{\psi}}^{(m)}_{\boldsymbol{\lambda}} = \partial_m \psi_{\lambda_1} \otimes \cdots \otimes \psi^+_{\lambda_m} \otimes \cdots \otimes \psi_{\lambda_n} = d_{\lambda_m} \psi_{\lambda_1} \otimes \cdots \otimes \psi_{\lambda_n}, \tag{4.13}$$

so that $\|\mathrm{div}\, \underline{\boldsymbol{\psi}}^{(m)}_{\boldsymbol{\lambda}}\|_{\mathbf{H}(\mathrm{div};\square)} = |d_{\lambda_m}| \prod_{k=1}^n \|\psi_{\lambda_k}\|_{L_2(\mathrm{I})} < \infty$.

As a consequence of Proposition 4.3.1, we have the following lemma (cf. (4.6), (4.7)).

Lemma 4.3.2. *The collections $\underline{\boldsymbol{\Psi}}$ and $\underline{\tilde{\boldsymbol{\Psi}}}$ are biorthogonal Riesz bases for $L_2(\square)^n$.*

To create divergence-free wavelet bases, we transform the functions from $\underline{\boldsymbol{\Psi}}$, $\underline{\tilde{\boldsymbol{\Psi}}}$ using an orthogonal matrix $\mathbf{A}^{\boldsymbol{\lambda}} \in \mathbb{R}^{n \times n}$ whose last row is given by $\boldsymbol{\alpha}^{\mathsf{T}}_{\boldsymbol{\lambda}}$, defined as

$$\boldsymbol{\alpha}_{\boldsymbol{\lambda}} := \big(d_{\lambda_1}, \ldots, d_{\lambda_n}\big)^{\mathsf{T}} \Big/ \sqrt{\textstyle\sum_{m=1}^n d^2_{\lambda_m}}.$$

Such matrices can be constructed from the Householder transformation

$$\mathbf{A}^{\boldsymbol{\lambda}} = \mathbf{I} - \frac{2(\boldsymbol{\alpha}_{\boldsymbol{\lambda}} - \mathbf{e}_n)(\boldsymbol{\alpha}_{\boldsymbol{\lambda}} - \mathbf{e}_n)^{\mathsf{T}}}{(\boldsymbol{\alpha}_{\boldsymbol{\lambda}} - \mathbf{e}_n)^{\mathsf{T}}(\boldsymbol{\alpha}_{\boldsymbol{\lambda}} - \mathbf{e}_n)}.$$

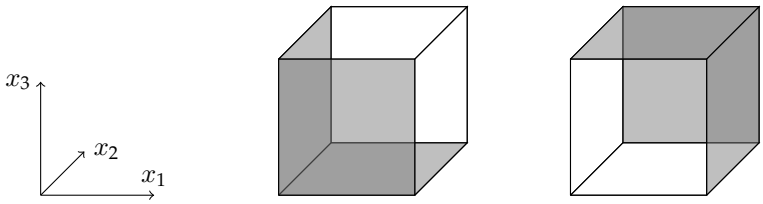

Figure 4.2: The boundaries Γ and $\tilde{\Gamma}$

For $n = 2$ and $n = 3$ the latter matrix is equal to

$$\begin{bmatrix} -\alpha_2 & \alpha_1 \\ \alpha_1 & \alpha_2 \end{bmatrix}, \quad \begin{bmatrix} 1-\frac{\alpha_1^2}{1-\alpha_3} & -\frac{\alpha_1\alpha_2}{1-\alpha_3} & \alpha_1 \\ -\frac{\alpha_1\alpha_2}{1-\alpha_3} & 1-\frac{\alpha_2^2}{1-\alpha_3} & \alpha_2 \\ \alpha_1 & \alpha_2 & \alpha_3 \end{bmatrix},$$

respectively.

The bases $\boldsymbol{\Psi} := \{\boldsymbol{\psi}_{\boldsymbol{\lambda}}^{(k)} : \boldsymbol{\lambda} \in \boldsymbol{\nabla}, 1 \le k \le n\}$ and $\tilde{\boldsymbol{\Psi}} := \{\tilde{\boldsymbol{\psi}}_{\boldsymbol{\lambda}}^{(k)} : \boldsymbol{\lambda} \in \boldsymbol{\nabla}, 1 \le k \le n\}$ are now defined by orthogonally transforming the basis functions from $\underline{\boldsymbol{\Psi}}$, $\underline{\tilde{\boldsymbol{\Psi}}}$, n at a time, using the matrices $\mathbf{A}^{\boldsymbol{\lambda}}$:

$$\begin{bmatrix} \boldsymbol{\psi}_{\boldsymbol{\lambda}}^{(1)} \\ \vdots \\ \boldsymbol{\psi}_{\boldsymbol{\lambda}}^{(n)} \end{bmatrix} := \mathbf{A}^{\boldsymbol{\lambda}} \begin{bmatrix} \underline{\boldsymbol{\psi}}_{\boldsymbol{\lambda}}^{(1)} \\ \vdots \\ \underline{\boldsymbol{\psi}}_{\boldsymbol{\lambda}}^{(n)} \end{bmatrix}, \quad \begin{bmatrix} \tilde{\boldsymbol{\psi}}_{\boldsymbol{\lambda}}^{(1)} \\ \vdots \\ \tilde{\boldsymbol{\psi}}_{\boldsymbol{\lambda}}^{(n)} \end{bmatrix} := \mathbf{A}^{\boldsymbol{\lambda}} \begin{bmatrix} \underline{\tilde{\boldsymbol{\psi}}}_{\boldsymbol{\lambda}}^{(1)} \\ \vdots \\ \underline{\tilde{\boldsymbol{\psi}}}_{\boldsymbol{\lambda}}^{(n)} \end{bmatrix}.$$

Because this transformation is orthogonal, it is boundedly invertible, with unit norm. By Lemma 4.0.1, the collection $\boldsymbol{\Psi}$ also forms a basis for $L_2(\square)^n$, with the same Riesz constants as $\underline{\boldsymbol{\Psi}}$. Moreover $\boldsymbol{\Psi}$ and $\tilde{\boldsymbol{\Psi}}$ are biorthogonal.

Using (4.13), we have

$$\operatorname{div} \boldsymbol{\psi}_{\boldsymbol{\lambda}}^{(k)} = \sum_{m=1}^{n} \mathbf{A}_{km}^{\boldsymbol{\lambda}} \operatorname{div} \underline{\boldsymbol{\psi}}_{\boldsymbol{\lambda}}^{(m)} = \big(\sum_{m=1}^{n} \mathbf{A}_{km}^{\boldsymbol{\lambda}} d_{\lambda_m}\big) \psi_{\lambda_1} \otimes \cdots \otimes \psi_{\lambda_n}. \tag{4.14}$$

For $1 \le k \le n-1$, this is zero, because by definition the first $n-1$ rows of $\mathbf{A}^{\boldsymbol{\lambda}}$ are orthogonal to the last.

We are now ready to create a basis for some spaces of divergence-free functions. To that end, let us define the boundary $\Gamma \subset \partial\square$ as the union of all faces of the unit n-cube that contain the point $(0, \dots, 0)$, and its complement $\tilde{\Gamma} = \partial\square \backslash \Gamma$, as illustrated in Figure 4.2.

Furthermore, we define the spaces

$$\mathbf{H}_{0,\Gamma}(\operatorname{div}; \square) := \big\{\mathbf{u} \in \mathbf{H}(\operatorname{div}; \square) : \mathbf{u} \cdot \mathbf{n} = 0 \text{ on } \Gamma\big\},$$
$$\mathbf{H}_{0,\Gamma}(\operatorname{div} 0; \square) := \big\{\mathbf{u} \in \mathbf{H}_{0,\Gamma}(\operatorname{div}; \square) : \operatorname{div} \mathbf{u} = 0\big\},$$

where $\mathbf{n}$ denotes an outward normal.

Lemma 4.3.3. *For all $\boldsymbol{\lambda} \in \boldsymbol{\nabla}$, $1 \le k \le n$, we have $\boldsymbol{\psi}_{\boldsymbol{\lambda}}^{(k)} \cdot \mathbf{n} = 0$ on Γ.*

Proof. We first show that the functions from $\underline{\boldsymbol{\Psi}}$ have vanishing normal components on Γ. To that end, let $\Gamma_k := \{\mathbf{x} \in \square : x_k = 0\}$, so that $\Gamma = \cup_{k=1}^{n} \Gamma_k$. On Γ_k we

have $\mathbf{n} = -\mathbf{e}_k$. For $m \neq k$, we have $\underline{\boldsymbol{\psi}}_{\boldsymbol{\lambda}}^{(m)} \cdot \mathbf{e}_k = \psi_{\boldsymbol{\lambda}}^{(m)} \mathbf{e}_m \cdot \mathbf{e}_k = 0$. Furthermore, we have $\Psi^+(0) = 0$ and thus for $\mathbf{x} \in \Gamma_k$,

$$\underline{\boldsymbol{\psi}}_{\boldsymbol{\lambda}}^{(k)}(\mathbf{x}) \cdot \mathbf{e}_k = \psi_{\boldsymbol{\lambda}}^{(k)}(\mathbf{x}) = \psi_{\lambda_1}(x_1) \cdots \psi_{\lambda_k}^+(0) \cdots \psi_{\lambda_n}(x_n) = 0.$$

Since $\mathbf{A}^{\boldsymbol{\lambda}}$ is linear, we also have $\boldsymbol{\psi}_{\boldsymbol{\lambda}}^{(k)} \cdot \mathbf{n} = 0$ on Γ, for all $\boldsymbol{\lambda} \in \boldsymbol{\nabla}$, $1 \leq k \leq n$. ◊

Lemma 4.3.4. *For* $\mathbf{u} \in \mathbf{H}_{0,\Gamma}(\operatorname{div} 0; \square)$, *we have* $\langle \mathbf{u}, \tilde{\boldsymbol{\psi}}_{\boldsymbol{\lambda}}^{(n)} \rangle_{L_2(\square)^n} = 0$.

Proof. We have

$$\begin{aligned}
\big\langle \mathbf{u}, \tilde{\boldsymbol{\psi}}_{\boldsymbol{\lambda}}^{(n)} \big\rangle_{L_2(\square)^n} &= \sum_{m=1}^{n} \mathbf{A}_{nm}^{\boldsymbol{\lambda}} \big\langle \mathbf{u}, \tilde{\psi}_{\lambda_1} \otimes \cdots \otimes \tilde{\psi}_{\lambda_m}^- \otimes \cdots \otimes \tilde{\psi}_{\lambda_n} \mathbf{e}_m \big\rangle_{L_2(\square)^n} \\
&= -\sum_{m=1}^{n} \mathbf{A}_{nm}^{\boldsymbol{\lambda}} d_{\lambda_m}^{-1} \big\langle \mathbf{u}, \tilde{\psi}_{\lambda_1} \otimes \cdots \otimes \dot{\tilde{\psi}}_{\lambda_m} \otimes \cdots \otimes \tilde{\psi}_{\lambda_n} \mathbf{e}_m \big\rangle_{L_2(\square)^n}, \\
&= -\sum_{m=1}^{n} \big\langle u_m \, \tilde{\psi}_{\lambda_1} \otimes \cdots \otimes \dot{\tilde{\psi}}_{\lambda_m} \otimes \cdots \otimes \tilde{\psi}_{\lambda_n} \big\rangle_{L_2(\square)} \Big/ \sqrt{\textstyle\sum_{m=1}^{n} d_{\lambda_m}^2} \\
&= -\Big[\int_{\partial\square} \mathbf{u} \cdot \mathbf{n} \; \tilde{\psi}_{\lambda_1} \otimes \cdots \otimes \tilde{\psi}_{\lambda_n} - \\
&\qquad \big\langle \operatorname{div} \mathbf{u}, \tilde{\psi}_{\lambda_1} \otimes \cdots \otimes \tilde{\psi}_{\lambda_n} \big\rangle_{L_2(\square)} \Big] \Big/ \sqrt{\textstyle\sum_{m=1}^{n} d_{\lambda_m}^2} = 0,
\end{aligned}$$

where we have used that on Γ, $\mathbf{u} \cdot \mathbf{n} = 0$ by the boundary conditions, and on $\tilde{\Gamma}$, $\tilde{\psi}_{\lambda_1} \otimes \cdots \otimes \tilde{\psi}_{\lambda_n} = 0$ by the assumption $\tilde{\psi}_\lambda(1) = 0$. ◊

Proposition 4.3.5. *The collection* $\boldsymbol{\Psi}^{\mathrm{df}} := \{\boldsymbol{\psi}_{\boldsymbol{\lambda}}^{(k)} : 1 \leq k \leq n-1, \boldsymbol{\lambda} \in \boldsymbol{\nabla}\}$ *is a Riesz basis for* $\mathbf{H}_{0,\Gamma}(\operatorname{div} 0; \square)$.

Proof. Lemma 4.3.4 shows that for $\mathbf{u} \in \mathbf{H}_{0,\Gamma}(\operatorname{div} 0; \square) \subset L_2(\square)^n$, the coefficients in front of the functions in $\boldsymbol{\Psi} \backslash \boldsymbol{\Psi}^{\mathrm{df}}$ vanish. By (4.14), the elements $\boldsymbol{\psi}_{\boldsymbol{\lambda}}^{(k)}$ of $\boldsymbol{\Psi}^{\mathrm{df}}$ have zero divergence, and by Lemma 4.3.3 they satisfy $\boldsymbol{\psi}_{\boldsymbol{\lambda}}^{(k)} \cdot \mathbf{n} = 0$ on Γ. ◊

In view of Remark 4.2.2, it is easy to construct an actual basis for $\mathbf{H}_{0,\Gamma}(\operatorname{div} 0; \square)$. We have chosen $d = 3$, $\tilde{d} = 5$ for the construction in Chapter 2, and impose the boundary conditions $m_L = m_R = 0$, $\tilde{m}_R = 1$. Figure 4.3 shows some of the resulting divergence-free wavelets. Note that on the left and on the lower boundary, the normal component of the wavelets vanishes, while this is not the case at the upper and right boundary.

4.4 Approximation properties

Let Ψ satisfy a Jackson estimate of order d. Then Ψ^+ satisfies a Jackson estimate of order $d+1$, and in particular also of order d. With this in mind, it is easy to verify that the approximation results from Proposition 3.2.3 from Chapter 3 hold for the bases $\Psi^{(m)}$. We will show that also, sparse grid approximation is possible for vector-valued functions. Indeed, with $\boldsymbol{\nabla}_J^{(0)}$ as in Chapter 3, i.e.

$$\boldsymbol{\nabla}_J^{(0)} := \{\boldsymbol{\lambda} \in \boldsymbol{\nabla} : |\boldsymbol{\lambda}|_1 \leq J\},$$

the following approximation result holds.

Proposition 4.4.1. *For $1 \le m \le n$, let $\Psi^{(m)}$ satisfy a Jackson estimate of order d, and let $\underline{\psi}^{(m)}_{\boldsymbol{\lambda}}$ be as defined in* (4.11)*. Then, for $s \in [0,d]$, $\mathbf{u} \in \mathbf{H}_{0,\Gamma}(\operatorname{div};\square)$,*

$$\inf_{\mathbf{v}\in\operatorname{span}\{\underline{\psi}^{(m)}_{\boldsymbol{\lambda}}\colon \boldsymbol{\lambda}\in\boldsymbol{\nabla}^{(0)}_J, 1\le m\le n\}} \|\mathbf{u}-\mathbf{v}\|_{L_2(\square)^n} \lesssim J^{\frac{n-1}{2}} 2^{-Js} \sqrt{\sum\nolimits_{k=1}^{n} \|u_m\|^2_{\mathcal{H}^{(s,\dots,s)}(\square)}} \tag{4.15}$$

whenever the right-hand side is bounded.

Proof. For each of the components u_m of $\mathbf{u}$, the error estimate

$$\inf_{v_m\in\operatorname{span}\{\psi^{(m)}_{\boldsymbol{\lambda}}\colon \boldsymbol{\lambda}\in\boldsymbol{\nabla}^{(0)}_J\}} \|u_m - v_m\|^2_{L_2(\square)} \lesssim J^{n-1}2^{-2Js}\|u_m\|^2_{\mathcal{H}^{(s,\dots,s)}(\square)} \tag{4.16}$$

holds by Proposition 3.2.3. The result follows by summing over $m = 1,\dots,n$ and taking square roots. ◊

A similar estimate holds when the basis $\underline{\boldsymbol{\Psi}}$ is replaced by $\boldsymbol{\Psi}$, since

$$\operatorname{span}\{\underline{\psi}^{(m)}_{\boldsymbol{\lambda}}\colon \boldsymbol{\lambda}\in\boldsymbol{\nabla}^{(0)}_J, 1\le m\le n\} = \operatorname{span}\{\psi^{(m)}_{\boldsymbol{\lambda}}\colon \boldsymbol{\lambda}\in\boldsymbol{\nabla}^{(0)}_J, 1\le m\le n\}.$$

Denoting the expansion of $\mathbf{u}$ in terms of the $\boldsymbol{\Psi}$ by

$$\mathbf{u} = \sum_{\substack{\boldsymbol{\lambda}\in\boldsymbol{\nabla}\\ 1\le m\le n}} u^{(m)}_{\boldsymbol{\lambda}}\psi^{(m)}_{\boldsymbol{\lambda}},$$

Lebesgue's lemma (Lemma 3.1.2) shows that the estimate (4.15) with $\underline{\boldsymbol{\Psi}}$ replaced by $\boldsymbol{\Psi}$ is equivalent to

$$\Big\|u - \sum_{\substack{\boldsymbol{\lambda}\in\boldsymbol{\nabla}^{(0)}_J\\ 1\le m\le n}} u^{(m)}_{\boldsymbol{\lambda}}\psi^{(m)}_{\boldsymbol{\lambda}}\Big\|_{L_2(\square)^n} \lesssim J^{\frac{n-1}{2}}2^{-Js}\sqrt{\sum\nolimits_{k=1}^{n}\|u_m\|^2_{\mathcal{H}^{(s,\dots,s)}(\square)}}. \tag{4.17}$$

Now for $\mathbf{u} \in \mathbf{H}_{0,\Gamma}(\operatorname{div} 0;\square)$, we know that $u^{(n)}_{\boldsymbol{\lambda}} = 0$, which shows that for divergence-free $\mathbf{u}$, the estimate (4.17) also holds for the basis $\boldsymbol{\Psi}^{\mathrm{df}}$.

We quote without proof the following proposition from [Ste08]:

Proposition 4.4.2. *The collection*

$$\boldsymbol{\Psi}^{\mathrm{df}}_{\mathbf{H}^1} := \Big\{\Big(\sum_{m=1}^{n} 4^{-\lambda_m}\Big)^{-\frac{1}{2}}\psi^{(k)}_{\boldsymbol{\lambda}}\colon 1\le k\le n-1, \boldsymbol{\lambda}\in\boldsymbol{\nabla}\Big\}$$

forms a Riesz basis for $\mathbf{H}_{0,\Gamma}(\operatorname{div} 0;\square)\cap H^1(\square)^n$.

Also for $\boldsymbol{\Psi}_{\mathbf{H}^1}$ a sparse grid approximation result can be derived. For $\gamma\in(0,1)$, recall the optimized sparse grid index set $\boldsymbol{\nabla}^{(\gamma)}_J$:

$$\boldsymbol{\nabla}^{(\gamma)}_J := \{\boldsymbol{\lambda}\in\boldsymbol{\nabla}\colon |\boldsymbol{\lambda}|_1 - \gamma|\boldsymbol{\lambda}|_\infty \le (1-\gamma)J\}.$$

With this set, an approximation result similar to Proposition 3.2.10 in Chapter 3 holds. The derivation of this result runs analogous to that of Proposition 4.4.1.

Proposition 4.4.3. *For any $s\in[0,d-1]$, $t\in(s,d]$, $\gamma\in[0,1-\frac{s}{t})$, $\mathbf{u}\in\mathbf{H}_{0,\Gamma}(\operatorname{div} 0;\square)\cap H^1(\square)^n$,*

$$\inf_{\mathbf{v}\in\operatorname{span}\{\psi^{(m)}_{\boldsymbol{\lambda}}\colon \boldsymbol{\lambda}\in\boldsymbol{\nabla}^{(\gamma)}_J, 1\le m\le n-1\}} \|\mathbf{u}-\mathbf{v}\|_{H^1(\square)^n} \eqsim 2^{-Js}\sqrt{\sum\nolimits_{k=1}^{n}\|u_m\|^2_{\mathscr{H}_{s+1,t}(\square)}}$$

whenever the right-hand side is bounded.

4.5 Stokes problem

In [Ste08], it was described how the constructed bases can be used for solving the following Stokes problem. Given $\mathbf{f} \in (\prod_{m=1}^{n} H^1_{0,\Gamma_k}(\square))'$, find $\mathbf{u} \in \prod_{m=1}^{n} H^1_{0,\Gamma_k}(\square)$ and $p \in L_2(\square)$ such that

$$\begin{aligned} -\boldsymbol{\Delta}\mathbf{u} + \mathbf{grad}\, p &= \mathbf{f} && \text{on } \square, \\ \operatorname{div} \mathbf{u} &= 0 && \text{on } \square, \\ \mathbf{u} &= 0 && \text{on } \Gamma, \\ p + \tfrac{\partial \mathbf{u}}{\partial \mathbf{n}} \cdot \mathbf{n} &= h && \text{on } \tilde{\Gamma}, \\ \tfrac{\partial \mathbf{u}}{\partial \mathbf{n}} \cdot \boldsymbol{\tau}_k &= g_k && \text{on } \partial\square,\ 1 \le k \le n-1, \end{aligned}$$

where $\boldsymbol{\tau}_1, \ldots, \boldsymbol{\tau}_{n-1}$ is an orthonormal set of tangent vectors.

With $a(\mathbf{u}, \mathbf{v}) \coloneqq \int_\square \mathbf{grad}\, \mathbf{u} : \mathbf{grad}\, \mathbf{v}$, $b(\mathbf{v}, q) \coloneqq \int_\square q \operatorname{div} \mathbf{v}$, for any sufficiently test function $\mathbf{v}$ that satisfies the essential boundary condition $\mathbf{v} \cdot \mathbf{n} = 0$ on Γ, integration by parts yields

$$\begin{aligned} &\int_\square -\boldsymbol{\Delta}\mathbf{u} \cdot \mathbf{v} - \int_\square \mathbf{grad}\, p \cdot \mathbf{v} \\ &= a(\mathbf{u}, \mathbf{v}) - \int_{\partial\square} \mathbf{v} \cdot \tfrac{\partial \mathbf{u}}{\partial \mathbf{n}} + b(\mathbf{v}, p) - \int_{\partial\square} p\, \mathbf{v} \cdot \mathbf{n} \\ &= a(\mathbf{u}, \mathbf{v}) + b(\mathbf{v}, p) - \int_{\partial\square \setminus \Gamma} (\mathbf{v} \cdot \mathbf{n}) h - \int_{\partial\square} \sum_{k=1}^{n-1} (\mathbf{v} \cdot \boldsymbol{\tau}_k) g_k. \end{aligned}$$

We collect all terms that do not involve the unknowns $\mathbf{u}$ and p in a source term $\mathbf{F}(\mathbf{v}) \coloneqq \mathbf{f}(\mathbf{v}) + \int_{\partial\square\setminus\Gamma} (\mathbf{v} \cdot \mathbf{n}) h + \int_{\partial\gamma} \sum_{k=1}^{n-1} (\mathbf{v} \cdot \boldsymbol{\tau}_k) g_k$. The problem now reduces to finding $\mathbf{u} \in \prod_{m=1}^{n} H^1_{0,\Gamma_k}(\square)$, $p \in L_2(\square)$ such that

$$a(\mathbf{u}, \mathbf{v}) + b(\mathbf{v}, p) = \mathbf{F}(\mathbf{v}) \quad \text{for all } \mathbf{v} \in \mathbf{H}_{0,\Gamma}(\operatorname{div}; \square), \tag{4.18}$$

$$b(\mathbf{u}, q) = 0 \quad \text{for all } q \in L_2(\square). \tag{4.19}$$

This saddle point problem was proven in [Ste08] to define a boundedly invertible mapping between $\prod_{m=1}^{n} H^1_{0,\Gamma_k}(\square) \times L_2(\square)$ and its dual, meaning that the variational problem is well-posed.

The velocity field $\mathbf{u} \in \mathbf{H}_{0,\Gamma}(\operatorname{div} 0; \square) \cap H^1(\square)^n$ solves the elliptic problem

$$a(\mathbf{u}, \mathbf{v}) = \mathbf{F}(\mathbf{v}) \quad \text{for all } \mathbf{v} \in \mathbf{H}_{0,\Gamma}(\operatorname{div} 0; \square) \cap H^1(\square)^n.$$

A result of Proposition 4.4.2 is that we may expand $\mathbf{u}$ in terms of the basis $\boldsymbol{\Psi}^{\mathrm{df}}_{\mathbf{H}^1}$. We write $\mathbf{u} = \vec{\mathbf{u}}^{\mathsf{T}} \boldsymbol{\Psi}^{\mathrm{df}}_{\mathbf{H}^1}$. An equivalent formulation of (4.18) is now given by the bi-infinite matrix-vector equation

$$a(\boldsymbol{\Psi}^{\mathrm{df}}_{\mathbf{H}^1}, \boldsymbol{\Psi}^{\mathrm{df}}_{\mathbf{H}^1}) \vec{\mathbf{u}} = \mathbf{F}(\boldsymbol{\Psi}^{\mathrm{df}}_{\mathbf{H}^1}),$$

where $a(\boldsymbol{\Psi}^{\mathrm{df}}_{\mathbf{H}^1}, \boldsymbol{\Psi}^{\mathrm{df}}_{\mathbf{H}^1})$ is a bounded, symmetric and positive definite bi-infinite matrix. To solve this problem, one could restrict the basis to a sparse grid index set and find a Galerkin solution. Alternatively, an adaptive method can be used to solve the problem.

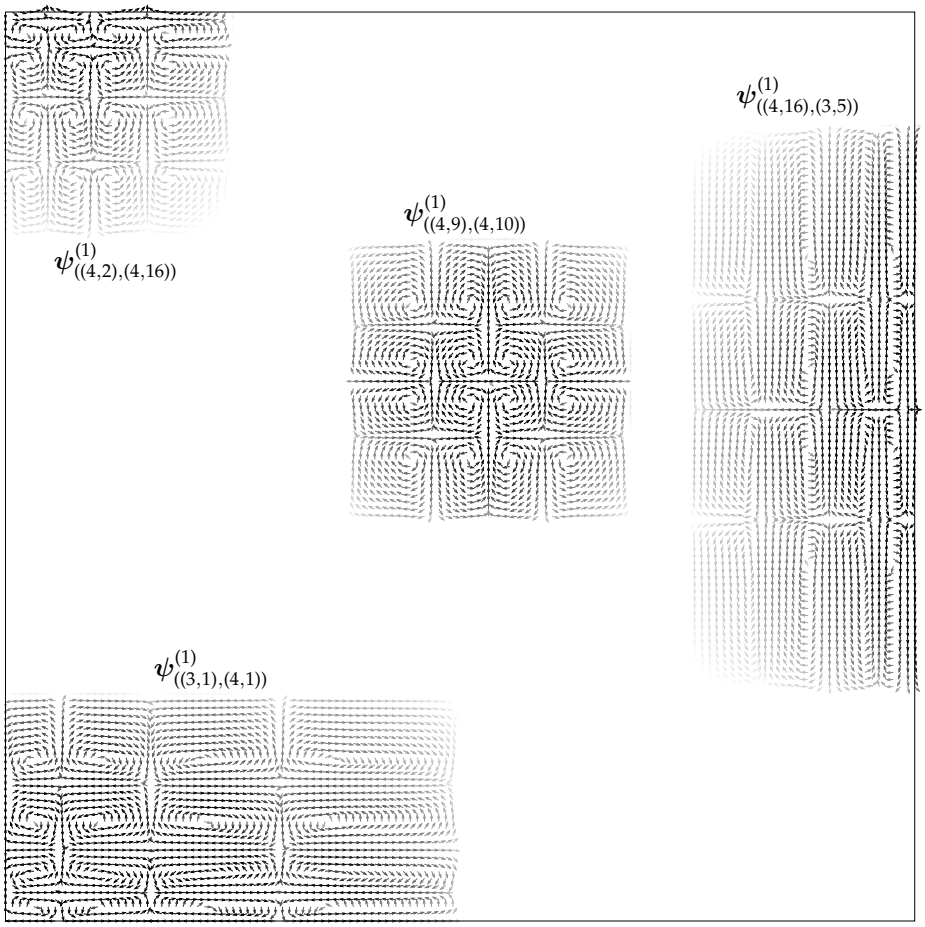

Figure 4.3: Some of the basis functions $\psi^{(1)}_{\boldsymbol{\lambda}} = \psi^{(1)}_{(j_1,k_1),(j_2,k_2)}$ from $\boldsymbol{\Psi}^{\mathrm{df}}$ on the unit square. The norm of each vector is indicated by its blackness.

Chapter 5
An adaptive wavelet method for solving high-dimensional elliptic PDEs

Adaptive tensor product wavelet methods are applied for solving Poisson's equation, as well as anisotropic generalizations, in high space dimensions. It will be demonstrated that the resulting approximations converge in energy norm with the same rate as the best approximations from the span of the best N tensor product wavelets, where moreover the constant factor that we may lose is independent of the space dimension n. The cost of producing these approximations will be proportional to their length with a constant factor that may grow with n, but only linearly.

5.1 Introduction

On $\Omega = (0,1)^n$, and with Γ_D the union of one or more $(n-1)$-dimensional faces of $\partial\Omega$, for given $f \in \left(H^1_{0,\Gamma_D}(\Omega)\right)'$, we study the numerical solution of the problem of finding $u \in H^1_{0,\Gamma_D}(\Omega)$ such that

$$a(u,v) := \int_\Omega c_0 uv + \sum_{m=1}^{n} c_m \partial_m u \partial_m v = f(v) \qquad (v \in H^1_{0,\Gamma_D}(\Omega)) \tag{5.1}$$

where $c_0 \geq 0$ and $c_m > 0$ $(m = 1,\dots,n)$ are constants.

PDEs such as (5.1) in spatial domains of high dimension arise in numerous areas. We only mention mathematical finance (valuation of derivative contracts on large baskets), elliptic homogenization problems with multiple separated length scales (e.g. [HS05]), deterministic methods for stochastic PDEs ([TS07]), the N-electron Schrödinger equation in molecular dynamics ([Yse05]) and problems from molecular biology.

Since the work of R. Feynman ([FH65]) (strong) solutions $u(x)$ at a point $x \in \Omega$ of the Dirichlet Problem (5.1) are well-known to be characterized by the first exit-time of the n-dimensional Wiener process W_t^x started at $t = 0$ in $x \in \Omega$ (see, e.g., [Fre85] and the references therein for a detailed account). For large dimension n, this probabilistic characterization of $u(x)$ can be used, in

conjunction with the Monte Carlo simulation of sample paths of W_t^x, to obtain numerical approximations to $u(x)$ *in a single point* $x \in \Omega$ of accuracy $O(1/\sqrt{m})$ where m denotes the number of sample paths; the work for generating m paths in $\mathbb{R}^n$ scales linearly with n.

Here, our aim is to develop deterministic approximations of $u(x)$ *at all points* $x \in (0,1)^n$ that are efficient for large n. With a standard, piecewise polynomial approximation procedure in $(0,1)^n$, the error in energy norm

$$|\!|\!| \cdot |\!|\!| := a(\,\cdot\,,\,\cdot\,)^{\frac{1}{2}} \tag{5.2}$$

on $H_0^1(\Omega)$ behaves at best as $\sim N^{-(d-1)/n}$, where $d \geq 2$ is the polynomial order and N is the number of degrees of freedom. The rate $(d-1)/n$ being inversely proportional to the space dimension n is known as *curse of dimensionality*.

Using that $\Omega = (0,1)^n$ is a tensor product domain, the curse of dimensionality can be circumvented by applying hyperbolic cross approximation or sparse grids ([Zen91, BG04]). With this approach, for any fixed n the error behaves as $\sim (\log N)^{(n-1)(d-1)} N^{-(d-1)}$, or, with some small modification (see [GK00]), even as $\sim N^{-(d-1)}$, *assuming* that $u \in \bigcap_{k=1}^n \bigotimes_{m=1}^n H^{d-1+\delta_{km}}(0,1)$ or, for some $\varepsilon > 0$, $u \in \bigcap_{k=1}^n \bigotimes_{m=1}^n H^{d-1+\delta_{km}+(1-\delta_{km})\varepsilon}(0,1)$, respectively. It can be shown that these regularity conditions are satisfied for smooth f that satisfy homogeneous Dirichlet boundary conditions of a sufficiently high order (for $n \geq 2$, an order larger than $d - \frac{5}{2} - \frac{1}{n}$ suffices). In Chapter 3 of this thesis it was shown that for $n \geq 2$, $\Gamma_D = \partial\Omega$ and general smooth f that do not vanish at the boundary, the solution $u \in \bigcap_{k=1}^n \bigotimes_{m=1}^n H^{s+\delta_{km}}(0,1)$ if and only if $s < \frac{1}{2} + \frac{1}{n}$, essentially thus being the rate of these sparse approximations regardless of d.

The key to overcome regularity restrictions is to apply *nonlinear approximation*. Let us write the Dirichlet boundary as

$$\Gamma_D := \bigcup_{m=1}^n [0,1]^{m-1} \times z_m \times [0,1]^{n-m},$$

where for $1 \leq m \leq n$, $z_m \subseteq \{0,1\}$ with $\bigcup_{m=1}^n z_m \neq \varnothing$. For $z \subseteq \{0,1\}$, let $\{\psi_\lambda^{(z)} \colon \lambda \in \nabla_z\}$ be a Riesz basis for $L_2(0,1)$ consisting of *wavelets* of order d, such that $\{2^{-|\lambda|}\psi_\lambda^{(z)} \colon \lambda \in \nabla_z\}$ is a Riesz basis for $H_{0,z}^1(0,1)$. As usual, here $|\lambda| \in \mathbb{N}_0$ denotes the *level* of $\psi_\lambda^{(z)}$, and for $\ell \in \mathbb{N}_0$, $\#\{\lambda \in \nabla_z \colon |\lambda| = \ell\}$ is of the order of 2^ℓ. Now for any n, the normalized *tensor product basis*

$$\boldsymbol{\Psi} := \Big\{ \boldsymbol{\psi}_{\boldsymbol{\lambda}} := \bigotimes_{m=1}^n \psi_{\lambda_m}^{(z_m)} \Big/ |\!|\!| \bigotimes_{m=1}^n \psi_{\lambda_m}^{(z_m)} |\!|\!| \colon \boldsymbol{\lambda} \in \boldsymbol{\nabla} := \prod_{m=1}^n \nabla_{z_m} \Big\} \tag{5.3}$$

is a Riesz basis for $H_{0,\Gamma_D}^1(0,1)^n$, even uniformly in $c_0 \geq 0$ and $c_m > 0$ ($m = 1,\dots,n$) when this space is equipped with norm $|\!|\!| \cdot |\!|\!|$. This means that *the condition number of* $\boldsymbol{\Psi}$ *with respect to* $|\!|\!| \cdot |\!|\!|$, being the quotient

$$\sup_{0 \neq \mathbf{v} \in \ell_2(\boldsymbol{\nabla})} \frac{|\!|\!| \sum_{\boldsymbol{\lambda} \in \boldsymbol{\nabla}} \mathbf{v}_{\boldsymbol{\lambda}} \boldsymbol{\psi}_{\boldsymbol{\lambda}} |\!|\!|^2}{\|\mathbf{v}\|_{\ell_2(\boldsymbol{\nabla})}^2} \Big/ \inf_{0 \neq \mathbf{v} \in \ell_2(\boldsymbol{\nabla})} \frac{|\!|\!| \sum_{\boldsymbol{\lambda} \in \boldsymbol{\nabla}} \mathbf{v}_{\boldsymbol{\lambda}} \boldsymbol{\psi}_{\boldsymbol{\lambda}} |\!|\!|^2}{\|\mathbf{v}\|_{\ell_2(\boldsymbol{\nabla})}^2} \tag{5.4}$$

is bounded, uniformly in $c_0 \geq 0$ and $c_m > 0$ ($m = 1,\dots,n$). With $|\boldsymbol{\lambda}| := (|\lambda_1|,\dots,|\lambda_n|)$, for any $\ell \in \mathbb{N}_0$, $\{\boldsymbol{\psi}_{\boldsymbol{\lambda}} \colon \boldsymbol{\lambda} \in \boldsymbol{\nabla}, \||\boldsymbol{\lambda}|\|_1 \leq \ell\}$ spans the corresponding sparse grid space of dimension N being of the order of $2^\ell \ell^{n-1}$.

Instead of restricting ourselves to sparse-grid approximation, we consider approximations to u from the span of $\{\psi_{\boldsymbol{\lambda}}\colon \boldsymbol{\lambda} \in \boldsymbol{\Lambda}_N\}$, where $\boldsymbol{\Lambda}_N \subset \boldsymbol{\nabla}$ is *any* subset with $\#\boldsymbol{\Lambda}_N = N$. Because of the boundedness of the condition number, approximating u by $\sum_{\boldsymbol{\lambda}\in\boldsymbol{\Lambda}_N} \mathbf{v}_{\boldsymbol{\lambda}}\psi_{\boldsymbol{\lambda}}$ in $\|\!|\!| \cdot |\!|\!|$ is equivalent to approximating its representation $\mathbf{u}$ with respect to $\boldsymbol{\Psi}$ by $(\mathbf{v}_{\boldsymbol{\lambda}})_{\boldsymbol{\lambda}\in\boldsymbol{\Lambda}_N}$ in $\|\cdot\|_{\ell_2(\boldsymbol{\nabla})}$. We have $\inf_{\{\mathbf{v}\in\ell_2(\boldsymbol{\nabla})\colon \operatorname{supp}\mathbf{v}\subset\boldsymbol{\Lambda}_N\}}\|\mathbf{u}-\mathbf{v}\|_{\ell_2(\boldsymbol{\nabla})} = \|\mathbf{u}-\mathbf{u}|_{\boldsymbol{\Lambda}_N}\|_{\ell_2(\boldsymbol{\nabla})}$, where $\mathbf{u}|_{\boldsymbol{\Lambda}_N}$ is the vector in $\ell_2(\boldsymbol{\nabla})$ that coincides with $\mathbf{u}$ on its support being $\boldsymbol{\Lambda}_N$. For approximating $\mathbf{u}$ in $\|\cdot\|_{\ell_2(\boldsymbol{\nabla})}$, a best choice for $\boldsymbol{\Lambda}_N$ is one such that $\mathbf{u}|_{\boldsymbol{\Lambda}_N}$ is a *best N-term approximation* to $\mathbf{u}$, denoted as $\mathbf{u}_N$, meaning that it contains the N largest coefficients in modulus of $\mathbf{u}$.

The class

$$\mathcal{A}^s_\infty := \{\mathbf{v}\in\ell_2(\boldsymbol{\nabla})\colon \|\mathbf{v}\|_{\mathcal{A}^s_\infty} := \sup_{\varepsilon>0}\varepsilon\times[\min\{N\in\mathbb{N}_0\colon \|\mathbf{v}-\mathbf{v}_N\|_{\ell_2(\boldsymbol{\nabla})}\le\varepsilon\}]^s<\infty\}^1$$

gathers under one roof all $\mathbf{v}$ whose best N-term approximations converge to $\mathbf{v}$ with rate $s>0$. Note that $\|\mathbf{v}\|_{\mathcal{A}^s_\infty} \ge \sup_{\varepsilon\ge\|\mathbf{v}\|_{\ell_2(\boldsymbol{\nabla})}}\varepsilon = \|\mathbf{v}\|_{\ell_2(\boldsymbol{\nabla})}$. Although $\mathcal{A}^s_\infty$ is non-empty for any s, as it contains any finitely supported vector, in view of the order d of polynomial reproduction being applied, the representation $\mathbf{v}$ of an arbitrarily smooth v cannot be expected to be in $\mathcal{A}^s_\infty$ for $s>d-1$. On the other hand, in [Nit06], Nitsche showed that for sufficiently smooth wavelets, e.g., spline wavelets, for $0<s<d-1$ and with $\tau=(s+\frac12)^{-1}$,

$$\mathbf{v}\in\mathcal{A}^s_\tau \iff v\in\bigcap_{k=1}^n\bigotimes_{m=1}^n{}_\tau B^{s+\delta_{mk}}_\tau(L_\tau(0,1))$$

where $\mathcal{A}^s_\tau := \{\mathbf{v}\in\ell_2(\boldsymbol{\nabla})\colon \sum_{N\in\mathbb{N}}(N^s\|\mathbf{v}-\mathbf{v}_N\|_{\ell_2(\boldsymbol{\nabla})})^\tau N^{-1}<\infty\}$, $B^t_p(L_p(0,1))$ is a Besov space measuring "t orders of smoothness in L_p", and $\bigotimes_\tau$ denotes the so-called "τ tensor product". Note that $\mathcal{A}^s_\tau$ is even (slightly) smaller than $\mathcal{A}^s_\infty$.

The upshot of this result is that $\bigcap_{k=1}^n\bigotimes_\tau{}_{m=1}^n B^{s+\delta_{mk}}_\tau(L_\tau(0,1))$ is much larger than $\bigcap_{k=1}^n\bigotimes_{m=1}^n H^{s+\delta_{km}}(0,1)$, with an increasing difference when s and n get larger, membership of which space is needed to guarantee the same rate with sparse grid approximation.

In particular, for two and three space dimensions, in [Nit05] it was shown that for general, sufficiently smooth f, the solution u of (5.1) is in $\mathcal{A}^s_\infty$ for any $s<d-1$, and actually even that the best N-term approximations converge with rate $d-1$ up to some log-factors (in [DS09] it is even shown that $u\in\mathcal{A}^{d-1}_\infty$). The proof in [Nit05] makes use of the splitting of u into known singular functions and a smooth remainder, which is also available for (5.1) in more than three dimensions in [Dau88b]. It indicates the potential of best N-term approximation in tensor product bases. For background on nonlinear approximation, we refer for example to [DeV98, Coh03].

Above considerations concern best N-term approximations that, however, are not feasible in practice, already because $\mathbf{u}$ is not given explicitly. It can be found as the solution of the infinite matrix-vector problem

$$\mathbf{A}\mathbf{u}=\mathbf{f}, \tag{5.5}$$

[1] We have $2^{-s}\|\!|\!|\cdot|\!|\!|_{\mathcal{A}^s_\infty}\le\|\cdot\|_{\mathcal{A}^s_\infty}\le\|\!|\!|\cdot|\!|\!|_{\mathcal{A}^s_\infty}$, where $\|\!|\!|\mathbf{v}|\!|\!|_{\mathcal{A}^s_\infty} := \sup_{N\in\mathbb{N}_0}(N+1)^s\|\mathbf{v}-\mathbf{v}_N\|_{\ell_2(\boldsymbol{\nabla})}$ is the common definition of the (quasi) norm on $\mathcal{A}^s_\infty$.

with "stiffness matrix" $\mathbf{A} = [a(\psi_\mu, \psi_\lambda)]_{\lambda,\mu\in\nabla}$ and $\mathbf{f} = [f(\psi_\lambda)]_{\lambda\in\nabla}$. This infinite matrix problem is equivalent to (5.1).

In [CDD01, CDD02], optimal *adaptive* algorithms were introduced for solving (5.5). It was shown that whenever for some $s > 0$, $\mathbf{u}$ happens to belong to $\mathcal{A}^s_\infty$, then, under two assumptions discussed below, the sequence of approximations produced by these algorithms converge to $\mathbf{u}$ with *this rate* s, requiring a number of operations equivalent to their length. The first assumption is that one has available a routine RHS that given an $\varepsilon > 0$ produces an approximation $\mathbf{f}_\varepsilon := \text{RHS}[\varepsilon]$ with $\|\mathbf{f} - \mathbf{f}_\varepsilon\| \le \varepsilon$ and

$$\mathbf{rhs}_s := \sup_{0<\varepsilon<\|\mathbf{f}\|_{\ell_2(\nabla)}} \varepsilon \times \big[\#\text{ operations required by the call RHS}[\varepsilon]\big]^s < \infty. \quad (5.6)$$

The second assumption is that for some $s^* > s$, $\mathbf{A}$ is s^*-computable, which is a quantitative measure of how well $\mathbf{A}$ can be approximated by computable sparse matrices. This assumption implies that $\mathbf{A}\colon \mathcal{A}^s_\infty \to \mathcal{A}^s_\infty$ is bounded ([CDD01]), and thus that $\|\mathbf{f}\|_{\mathcal{A}^s_\infty} \lesssim \|\mathbf{u}\|_{\mathcal{A}^s_\infty}$, where the $\lesssim$ symbol has its usual definition recalled at the end of this introduction. So in any case if we could realize (quasi-) best N-term approximations for $\mathbf{f}$ in $\mathcal{O}(N)$ operations, then the resulting routine RHS would satisfy $\mathbf{rhs}_s < \infty$, in particular with $\mathbf{rhs}_s \lesssim \|\mathbf{u}\|_{\mathcal{A}^s_\infty}$.

In the tensor product basis setting, applying as a building block univariate biorthogonal spline wavelets, in [SS08] it was proven that $\mathbf{A}$ is s^*-computable for some $s^* > d-1$, which s^* is thus larger than any s for which $\mathbf{u} \in \mathcal{A}^s_\infty$ might be expected. This result was shown in a more general setting than we consider here. Most importantly, in that work general, i.e., non-separable, smooth variable coefficients were allowed in the differential operator, meaning that a quadrature scheme had to be designed and analyzed. The results imply that for any n, and $s \in [0, d-1]$, the adaptive wavelet schemes produce an approximation to $\mathbf{u} \in \mathcal{A}^s_\infty$ within any given *tolerance* $0 < \varepsilon \lesssim \|\mathbf{f}\|_{\ell_2(\nabla)}$ in $\|\cdot\|_{\ell_2(\nabla)}$ with a *support length* not exceeding

$$D_1 \varepsilon^{-1/s} |\mathbf{u}|^{1/s}_{\mathcal{A}^s_\infty},$$

taking a *number of operations* not exceeding

$$D_2 \varepsilon^{-1/s} |\mathbf{u}|^{1/s}_{\mathcal{A}^s_\infty} + D_3 \varepsilon^{-1/s} \mathbf{rhs}_s^{1/s},$$

where D_1, D_2 and D_3 are some constants, independent of $c_0 \ge 0$ and $c_m > 0$ $(m = 1, \dots, n)$. Only knowing that $\mathbf{u} \in \mathcal{A}^s_\infty$, up to the factors D_1 or $D_2 + D_3[\mathbf{rhs}_s/|\mathbf{u}|_{\mathcal{A}^s_\infty}]^{1/s}$, this length or number of operations is indeed the best that generally can be expected.

What was not analyzed in [SS08], however, is the

dependence of the constants D_1, D_2, D_3 and the condition number of $\mathbf{\Psi}$ with respect to $|||\cdot|||$ on the space dimension n.

Concerning the latter, note that instead of approximating $\mathbf{u}$, our ultimate goal is to approximate u in $|||\cdot|||$ within some given tolerance with, up to some constant factor, the smallest linear combination of wavelets.

The condition number of $\mathbf{\Psi}$ with respect to $|||\cdot|||$ is equal to the spectral condition number $\kappa(\mathbf{A})$ of $\mathbf{A}$, which for biorthogonal wavelets can be expected

to grow exponentially with n. Since in any case also D_2 is an increasing function of $\kappa(\mathbf{A})$, it may be that, although optimal for any fixed n, the method has only practical value for relatively small values of n.

In view of this, in the current chapter we apply univariate $L_2(0,1)$-*orthonormal, piecewise polynomial* wavelets as introduced in [DGH96, DGH99, Goo03]. In this case, $\kappa(\mathbf{A})$ is bounded *uniformly in* n, and $c_0 \geq 0$ and $c_m > 0$ $(m = 1, \ldots, n)$. Thanks to both the L_2-orthonormality, and the fact that the wavelets are piecewise polynomial, the stiffness matrix $\mathbf{A}$ appears to be very close to a sparse matrix. We give a detailed description of an adaptive wavelet algorithm for which aforementioned statements are valid with

$$D_1, \tfrac{D_2}{n}, D_3 \text{ constants, } \textit{independent of } n \text{ and } c_0 \geq 0,\ c_m > 0 \ \ (m = 1, \ldots, n).$$

So only the constant involved in the operation count may grow with the space dimension, but only linearly.

The algorithm we use is a modification developed in [GHS07] of the adaptive wavelet method from [CDD01]. With this modification, the recurrent coarsening of the iterands is avoided, which yields a quantitatively better performing algorithm. In this chapter, an additional quantitative improvement will be obtained by the use of a modified approximate matrix vector routine **APPLY** that will use a posteriori information to optimize the accuracies with which the columns of the infinite stiffness matrix are approximated.

The remainder of this chapter is organized as follows. In Section 5.2, from [DGH96] we recall the construction of $L_2(0,1)$-orthonormal, piecewise polynomial wavelets. We show that, as a consequence of the $L_2(0,1)$-orthonormality, the stiffness matrix $\mathbf{A}$ of the n-dimensional Laplacian in tensor product wavelet coordinates is well-conditioned uniformly in n.

In Section 5.3, we construct sparse approximations to $\mathbf{A}$. Using that the wavelets are $L_2(0,1)$-orthonormal and piecewise polynomial, we construct approximations that with a multiple of jn non-zeros per column have an error of order $2^{-j/2}$.

Section 5.4 deals with adaptive wavelet schemes for solving general bi-infinite matrix-vector equations with symmetric positive definite system matrices. The construction and the theory behind these schemes from [CDD01, GHS07] is summarized. The most time consuming ingredient of such schemes is the approximate matrix-vector routine **APPLY**. We develop a new version of this routine that performs an optimization based on a posteriori optimization, and which has strongly improved quantitative properties.

In Section 5.5, we specialize the results about adaptive wavelet schemes to the application of solving problem (5.1) in high space dimensions.

Finally, in Section 5.6 we discuss the implementation of the scheme and present numerical results.

In this chapter, unless explicitly stated otherwise, by $C \lesssim D$ we will mean that C can be bounded by a multiple of D, independently of parameters which C and D may depend on, in particular the space dimension n or the coefficients c_m $(0 \leq m \leq n)$. Obviously, $C \gtrsim D$ is defined as $D \lesssim C$, and $C \eqsim D$ as $C \lesssim D$ and $C \gtrsim D$.

We use notations like $\vec{v}$ or $\vec{B}$ to indicate vectors in $\ell_2(\nabla_z)$ or linear mappings $\ell_2(\nabla_z) \to \ell_2(\nabla_z)$, respectively, and $\mathbf{v}$ or $\mathbf{B}$ to indicate vectors in $\ell_2(\boldsymbol{\nabla})$ or linear mappings $\ell_2(\boldsymbol{\nabla}) \to \ell_2(\boldsymbol{\nabla})$. We use the notation $\|\cdot\|$ to abbreviate all of $\|\cdot\|_{L_2(0,1)}$, $\|\cdot\|_{L_2(0,1)^n}$, $\|\cdot\|_{\ell_2(\nabla_z)}$, $\|\cdot\|_{\ell_2(\nabla_z)\to\ell_2(\nabla_z)}$, $\|\cdot\|_{\ell_2(\nabla)}$ and $\|\cdot\|_{\ell_2(\boldsymbol{\nabla})\to\ell_2(\boldsymbol{\nabla})}$. We write $\langle\cdot,\cdot\rangle$ instead of $\langle\cdot,\cdot\rangle_{\ell_2(\nabla_z)}$ or $\langle\cdot,\cdot\rangle_{\ell_2(\boldsymbol{\nabla})}$. We use the notation $|\!|\!|\cdot|\!|\!|$, earlier defined as $a(\cdot,\cdot)^{\frac{1}{2}}$, also to denote $\langle\mathbf{A}\cdot,\cdot\rangle^{\frac{1}{2}}$. Note that for any $\mathbf{v}\in\ell_2(\boldsymbol{\nabla})$, $|\!|\!|\mathbf{v}|\!|\!| = |\!|\!|\sum_{\boldsymbol{\lambda}\in\boldsymbol{\nabla}}\mathbf{v}_{\boldsymbol{\lambda}}\boldsymbol{\psi}_{\boldsymbol{\lambda}}|\!|\!|$.

5.2 Univariate $L_2(0,1)$-orthonormal, piecewise polynomial wavelets

For $z\subseteq\{0,1\}$, let $\{\psi_\lambda^{(z)}\colon \lambda\in\nabla_z\}$ be a Riesz basis for $L_2(0,1)$, normalized with respect to $\|\cdot\|$, such that $\{2^{-|\lambda|}\psi_\lambda^{(z)}\colon\lambda\in\nabla_z\}$ is a Riesz basis for $H^1_{0,z}(0,1)$. Let $\lambda_{\min}^{(0,z)}$, $\lambda_{\max}^{(1,z)}$ (≥ 1) and $\lambda_{\min}^{(0,z)}$, $\lambda_{\min}^{(1,z)}$ (≤ 1) be the smallest or largest constants such that

$$\lambda_{\min}^{(0,z)} \leq \|\sum_{\lambda\in\nabla_z}\vec{v}_\lambda\psi_\lambda^{(z)}\|^2/\|\vec{v}\|^2 \leq \lambda_{\max}^{(0,z)},\quad (\vec{v}\in\ell_2(\nabla_z)),$$
$$\lambda_{\min}^{(1,z)} \leq \|\sum_{\lambda\in\nabla_z}\vec{v}_\lambda\dot{\psi}_\lambda^{(z)}\|^2/\sum_{\lambda\in\nabla_z}|\vec{v}_\lambda|^2\|\dot{\psi}_\lambda^{(z)}\|^2 \leq \lambda_{\max}^{(1,z)},\quad ((2^{|\lambda|}\vec{v}_\lambda)_\lambda\in\ell_2(\nabla_z)). \tag{5.7}$$

(Throughout this chapter, a dot on top of a univariate function denotes its derivative.) Then, with $\boldsymbol{\nabla}:=\prod_{m=1}^n\nabla_{z_m}$, by a tensor product argument we have

$$\prod_{m=1}^n\lambda_{\min}^{(0,z_m)} \leq \|\sum_{\boldsymbol{\lambda}\in\boldsymbol{\nabla}}\mathbf{v}_{\boldsymbol{\lambda}}\bigotimes_{k=1}^n\psi_{\lambda_k}^{(z_k)}\|^2/\|\mathbf{v}\|^2 \leq \prod_{m=1}^n\lambda_{\max}^{(0,z_m)},\quad (\mathbf{v}\in\ell_2(\boldsymbol{\nabla})),$$

$$\lambda_{\min}^{(1,z_m)}\prod_{k\neq m}\lambda_{\min}^{(0,z_k)} \leq \|\sum_{\boldsymbol{\lambda}\in\boldsymbol{\nabla}}\mathbf{v}_{\boldsymbol{\lambda}}\partial_m\bigotimes_{k=1}^n\psi_{\lambda_k}^{(z_k)}\|^2/\sum_{\boldsymbol{\lambda}\in\boldsymbol{\nabla}}|\mathbf{v}_{\boldsymbol{\lambda}}|^2\|\dot{\psi}_{\lambda_m}^{(z_m)}\|^2 \leq \lambda_{\max}^{(1,z_m)}\prod_{k\neq m}\lambda_{\max}^{(0,z_k)}$$

($1\leq m\leq n$, $(2^{|\lambda_m|}\mathbf{v}_{\boldsymbol{\lambda}})_{\boldsymbol{\lambda}\in\boldsymbol{\nabla}}\in\ell_2(\boldsymbol{\nabla})$), with bounds that cannot be improved. By summing over these inequalities, multiplied by c_0 or c_m ($1\leq m\leq n$), we infer that

$$\min_m\min(\lambda_{\min}^{(0,z_m)},\lambda_{\min}^{(1,z_m)})\prod_{k\neq m}\lambda_{\min}^{(0,z_k)} \leq$$
$$\frac{|\!|\!|\sum_{\boldsymbol{\lambda}\in\boldsymbol{\nabla}}\mathbf{v}_{\boldsymbol{\lambda}}\bigotimes_{k=1}^n\psi_{\lambda_k}^{(z_k)}|\!|\!|^2}{\sum_{\boldsymbol{\lambda}\in\boldsymbol{\nabla}}[c_0+\sum_{m=1}^n c_m\|\dot{\psi}_{\lambda_m}^{(z_m)}\|^2]|\mathbf{v}_{\boldsymbol{\lambda}}|^2} \leq \max_m\max(\lambda_{\max}^{(0,z_m)},\lambda_{\max}^{(1,z_m)})\prod_{k\neq m}\lambda_{\max}^{(0,z_k)}$$

($([c_0+\sum_{m=1}^n c_m 4^{|\lambda_m|}]^{\frac{1}{2}}\mathbf{v}_{\boldsymbol{\lambda}})_{\boldsymbol{\lambda}}\in\ell_2(\boldsymbol{\nabla})$). In view of the definition of $\boldsymbol{\Psi}$ in (5.3) and that of the stiffness matrix $\mathbf{A}$, using that $|\!|\!|\bigotimes_{m=1}^n\psi_{\lambda_m}^{(z_m)}|\!|\!|^2 = c_0+\sum_{m=1}^n c_m\|\dot{\psi}_{\lambda_m}^{(z_m)}\|^2$, we arrive at

$$\min_m\min(\lambda_{\min}^{(0,z_m)},\lambda_{\min}^{(1,z_m)})\prod_{k\neq m}\lambda_{\min}^{(0,z_k)} \leq$$
$$\frac{\langle\mathbf{A}\mathbf{v},\mathbf{v}\rangle}{\|\mathbf{v}\|^2} = \frac{|\!|\!|\sum_{\boldsymbol{\lambda}\in\boldsymbol{\nabla}}\mathbf{v}_{\boldsymbol{\lambda}}\boldsymbol{\psi}_{\boldsymbol{\lambda}}|\!|\!|^2}{\|\mathbf{v}\|^2} \leq \max_m\max(\lambda_{\max}^{(0,z_m)},\lambda_{\max}^{(1,z_m)})\prod_{k\neq m}\lambda_{\max}^{(0,z_k)},$$

where moreover $\mathbf{\Psi}$ is a basis for $H^1_{0,\Gamma_D}(0,1)^n$ (cf. [GO95]).

So *if* for all $z \subseteq \cup_{m=1}^n z_m$, $\lambda_{\max}^{(0,z)} = \lambda_{\min}^{(0,z)}$, i.e., $\{\psi_\lambda^{(z)} \colon \lambda \in \nabla_z\}$ is an orthonormal basis for $L_2(0,1)$, *then*

$$\|\mathbf{A}\| \leq \max_z \lambda_{\max}^{(1,z)}, \quad \|\mathbf{A}^{-1}\| \leq \max_z 1/\lambda_{\min}^{(1,z)}, \tag{5.8}$$

which bounds are thus independent of n, $c_0 \geq 0$ and $c_m > 0$ $(1 \leq m \leq n)$. On the other hand, if for some $z \subseteq \bigcup_{m=1}^n z_m$, $\lambda_{\max}^{(0,z)} > \lambda_{\min}^{(0,z)}$, then one may verify that $\kappa(\mathbf{A}) \coloneqq \|\mathbf{A}\|\|\mathbf{A}^{-1}\|$ grows exponentially with the number of coordinate directions that have these Dirichlet boundaries. So in order to be able to obtain satisfactory results for large n, there is no option other than to start with *univariate $L_2(0,1)$-orthonormal wavelet bases*.

In view of obtaining a stiffness matrix that can be sufficiently well approximated by sparse matrices, in addition we need *compactly supported wavelets*. Examples of orthonormal compactly supported wavelet bases are given by those from the Daubechies family ([Dau88a]). With those wavelets, $\int_0^1 \psi_\mu^{(z)} \psi_\lambda^{(z)}$ can only be expected to be zero when the supports have empty intersection. In contrast, for compactly supported, orthonormal *piecewise polynomial* wavelets, say of order d, $\int_0^1 \psi_\mu^{(z)} \psi_\lambda^{(z)}$ is already zero when the singular support of one wavelet, say $\psi_\lambda^{(z)}$, has empty intersection with the interior of the convex hull of the support of the other. Indeed, in that case $\int_0^1 \dot{\psi}_\mu^{(z)} \psi_\lambda^{(z)} = -\int_0^1 \psi_\mu^{(z)} \ddot{\psi}_\lambda^{(z)} = 0$, since on the convex hull of $\operatorname{supp} \psi_\mu^{(z)}$, $\ddot{\psi}_\lambda^{(z)} \in P_{d-3}$, and $\psi_\mu^{(z)}$ has $d \geq d-2$ *vanishing moments*, i.e., $\psi_\mu^{(z)} \perp P_{d-1}$ (when $\operatorname{supp} \psi_\mu^{(z)}$ has non-empty intersection with the Dirichlet boundary z, the latter, and thus $\int \dot{\psi}_\mu^{(z)} \psi_\lambda^{(z)} = 0$, is not necessarily valid).

Compactly supported, orthonormal, piecewise polynomial (multi-) wavelets were constructed in [DGH96, DGH99, Goo03]. In [DGH96], it was shown that if $\cdots \subset V_{-1} \subset V_0 \subset V_1 \subset \cdots$ is a multiresolution analysis with finitely many generators (scaling functions), then for some m, $q \in \mathbb{N}_0$, there exists a multiresolution analysis $\cdots \subset \check{V}_{-1} \subset \check{V}_0 \subset \check{V}_1 \subset \cdots$ with $V_q \subset \check{V}_0 \subset V_{q+m}$ that has finitely many *orthogonal* generators. From those, finitely many orthogonal generators (wavelets) for the orthogonal complements $\check{V}_\ell \ominus^{\perp_{L_2(\mathbb{R})}} \check{V}_{\ell-1}$ can be constructed. In [DGH99], explicit constructions were given for V_ℓ being the spline space

$$\{u \in L_2(\mathbb{R}) \cap C^r(\mathbb{R}) \colon u|_{[i2^{-\ell},(i+1)2^{-\ell}]} \in P_{d-1},\ i \in \mathbb{Z}\}$$

for $r \in \{0,1\}$ and $d \geq r+2$, as well as some examples for $r = 2$.

For $r = 0$ and $d = 2$, i.e., *continuous piecewise linears*, (q,m) can be taken to be $(1,1)$, i.e., $V_1 \subset \check{V}_0 \subset V_2$, with generating orthonormal scaling functions and wavelets illustrated in Figure 5.1. For $\ell \in \mathbb{Z}$, the collections $\{\varphi_{j,\ell,i} \coloneqq 2^{\ell/2}\varphi_j(2^\ell \cdot - i) \colon j \in \{1,2,3\},\ i \in \mathbb{Z}\}$ and $\{\psi_{j,\ell,i} \coloneqq 2^{(\ell-1)/2}\psi_j(2^{\ell-1} \cdot - i) \colon j \in \{1,2,3\},\ i \in \mathbb{Z}\}$ are orthonormal bases for $\check{V}_\ell$ and $\check{V}_\ell \ominus^{\perp_{L_2(\mathbb{R})}} \check{V}_{\ell-1}$, respectively.

These scaling functions and wavelets on the line can be used to construct such functions on the interval. With $\check{V}_\ell^{(z)} \coloneqq \check{V}_\ell|_{[0,1]} \cap H^1_{0,z}(0,1)$, for the choice $z = \{1\}$, i.e., homogeneous Dirichlet boundary conditions at the right boundary, $L_2(0,1)$-orthonormal bases for $\check{V}_0^{(z)}$ and $\check{V}_\ell^{(z)} \ominus^{\perp_{L_2(0,1)}} \check{V}_{\ell-1}^{(z)}$ are given by $\{\varphi_1^{(z)}, \varphi_2^{(z)}, \varphi_3^{(z)}\}$,

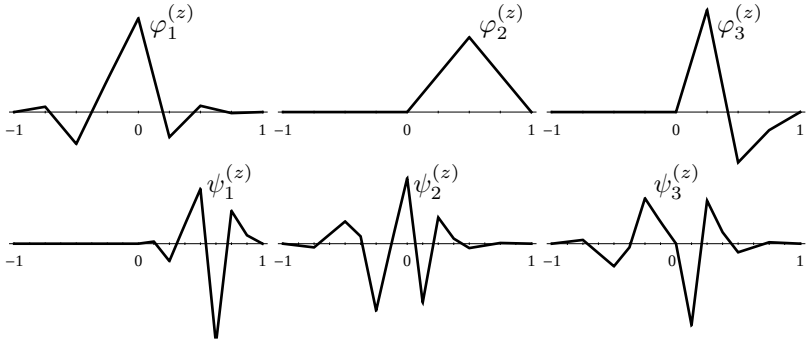

Figure 5.1: $L_2(\mathbb{R})$-orthonormal, continuous piecewise linear scaling functions and wavelets. Their values in $\frac{1}{4}\mathbb{Z}$ or $\frac{1}{8}\mathbb{Z}$ can be found in [DGH96]

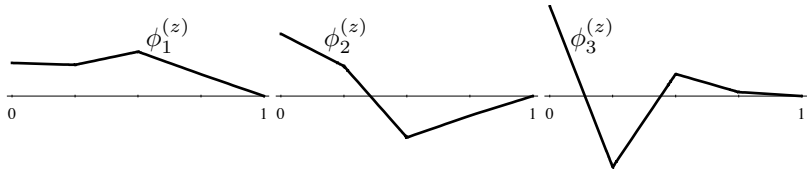

Figure 5.2: The scaling functions on the lowest level, for the case $z = \{1\}$.

illustrated in Figure 5.2, and

$$\{\psi_{1,\ell,i}\colon 0 \le i \le 2^{\ell-1}-1\} \bigcup \{\psi_{j,\ell,i}\colon 1 \le i \le 2^{\ell-1}-1,\ j = 2,3\} \bigcup \Big\{\frac{\psi_{2,\ell,0}|_{[0,1]}}{\|\psi_2|_{[0,1]}\|_{L_2(0,1)}}\Big\} \bigcup \Big\{\frac{\psi_{3,\ell,2^{\ell-1}}|_{[0,1]}}{\|\psi_3|_{[-1,0]}\|_{L_2(-1,0)}}\Big\},$$

respectively.

The collection $\{\varphi_1^{(z)}, \varphi_2^{(z)}, \varphi_3^{(z)}\}$ was constructed as follows: As initial choice for a basis for $\breve{V}_0^{(z)}$, we took the orthonormal collection $\{\frac{\varphi_1|_{[0,1]}}{\|\varphi_1|_{[0,1]}\|_{L_2(0,1)}}, \varphi_2, \varphi_3\}$. By applying suitable rotations to the pairs of the first and the second and the first and the third basis functions, the resulting modified second and third basis functions were given one vanishing moment. By again applying a suitable rotation to these modified second and third basis functions, the resulting final third basis function got two vanishing moments.

Our experiments, reported on in Section 5.6, are carried out with these wavelets. That is, we took $\Psi^{(z)} = \{\psi_\lambda^{(z)}\colon \lambda \in \Lambda_z\}$ to be the union of the basis for $\breve{V}_0^{(z)}$ and that for $\breve{V}_\ell^{(z)} \ominus^{\perp_{L_2(0,1)}} \breve{V}_{\ell-1}^{(z)}$ for all $\ell \in \mathbb{N}$, where, as usual, we define the level $|\lambda|$ of $\psi_\lambda^{(z)}$ to be 0 or ℓ, respectively. Since these wavelets satisfy appropriate Jackson and Bernstein estimates, $\Psi^{(z)}$ and $\{2^{-|\lambda|}\psi_\lambda^{(z)}\colon \lambda \in \nabla_z\}$ are Riesz bases for $L_2(0,1)$ and $H^1_{0,z}(0,1)$, respectively. Only one scaling function and, on each level $\ell > 0$, the rightmost wavelet of type 3 have no vanishing moments.

For other choices of $z \subseteq \{0,1\}$, the adaptation of the bases from [DGH99] on the line to the interval can follow similar lines.

5.3 Near sparsity of A

For a class of univariate wavelet bases that contains those discussed above, in this section, we investigate how well the stiffness matrix **A** with respect to the resulting tensor product basis can be approximated by sparse matrices. As outlined in the introduction, near sparsity of **A** is an essential ingredient of an adaptive wavelet method.

We consider $\Psi^{(z)} = \{\psi_\lambda^{(z)} : \lambda \in \nabla_z\}$ to be an orthonormal basis for $L_2(0,1)$, such that $\{2^{-|\lambda|}\psi_\lambda^{(z)} : \lambda \in \nabla_z\}$ is a Riesz basis for $H^1_{0,z}(0,1)$. Apart from that, we assume that

i. $\operatorname{diam}(\operatorname{supp}\psi_\lambda^{(z)}) \eqsim 2^{-|\lambda|}$.
ii. For some $d \in \mathbb{N}$, each wavelet $\psi_\lambda^{(z)}$ is piecewise polynomial of order d, that
iii. has a singular support that consists of a bounded number of points, uniformly in λ.
iv. Each point in $[0,1]$ is contained in the interior of the convex hull of the support of at most a bounded number of $\psi_\lambda^{(z)}$ with $|\lambda| = \ell$, uniformly in $\ell \in \mathbb{N}_0$.
v. $\|\psi_\lambda^{(z)}\|_{L_\infty} \lesssim 2^{\frac{1}{2}|\lambda|}$, $\|\dot\psi_\lambda^{(z)}\|_{L_\infty} \lesssim 2^{\frac{3}{2}|\lambda|}$.
vi. Wavelets on levels larger than 0 whose supports have empty intersection with z have $d-2$ vanishing moments.

Remark 5.3.1. By the above assumptions we have $\#\{\lambda \in \nabla_z : |\lambda| = \ell\} \lesssim 2^\ell$. Actually, for Ψ being a basis for $L_2(0,1)$, it is also needed that $\#\{\lambda \in \nabla_z : |\lambda| = \ell\} \gtrsim 2^\ell$.

Remark 5.3.2. Thinking of a wavelet basis of order d, i.e. a basis that locally reproduces any polynomial of order d that vanishes at the Dirichlet boundary, the orthogonality of the basis implies assumption vi with $d-2$ reading as d.

Because of the form of the bilinear form (5.1), and the use of tensor product wavelets, the stiffness matrix **A** will be a sum of tensor product operators involving factors that are stiffness matrices of one-dimensional Laplacians in wavelet coordinates. The following result concerns near-sparsity of these matrices.

Proposition 5.3.3. *Let* $\vec{A}_z = \left[\frac{\int_0^1 \dot\psi_\mu^{(z)}\dot\psi_\lambda^{(z)}}{\|\dot\psi_\mu^{(z)}\|\|\dot\psi_\lambda^{(z)}\|}\right]_{\lambda,\mu\in\nabla_z}$, *and for* $j \in \mathbb{N}$, *let* $\vec{A}_z^{(j)}$ *be constructed from* $\vec{A}_z$ *by dropping all entries* $(\vec{A}_z)_{\lambda,\mu}$ *with* $||\lambda|-|\mu|| \geq j$. *Then the number of non-zero entries in each row or column of* $\vec{A}_z^{(j)}$ *is* $\mathcal{O}(j)$, *and*

$$\|\vec{A}_z - \vec{A}_z^{(j)}\| \leq C_{z,\mathrm{sp}} 2^{-j/2},$$

for some constant $C_{z,\mathrm{sp}}$.

Proof. If $\operatorname{supp}\psi_\mu^{(z)} \subset (0,1)$, and the interior of the convex hull of $\operatorname{supp}\psi_\mu^{(z)}$ has empty intersection with sing. supp. $\psi_\lambda^{(z)}$, then $\int_0^1 \dot\psi_\mu^{(z)}\dot\psi_\lambda^{(z)} = -\int_0^1 \psi_\mu^{(z)}\ddot\psi_\lambda^{(z)} = 0$ by ii and vi. By iii and iv, we conclude that the number of non-zero entries $(\vec{A}_z)_{\lambda,\mu}$ for $|\mu| = \ell$ is bounded uniformly in λ and ℓ. By symmetry, the first statement follows.

From

$$\begin{aligned}|\int_0^1 \dot\psi_\mu^{(z)}\dot\psi_\lambda^{(z)}| &\le \operatorname{diam}(\operatorname{supp}\psi_\mu^{(z)}\cap\operatorname{supp}\psi_\lambda^{(z)})\|\dot\psi_\mu^{(z)}\|_{L_\infty}\|\dot\psi_\lambda^{(z)}\|_{L_\infty}\\ &\lesssim 2^{-\max(|\mu|,|\lambda|)}2^{\frac{3}{2}|\mu|}2^{\frac{3}{2}|\lambda|}\eqsim 2^{-\frac{1}{2}||\lambda|-|\mu||}\|\dot\psi_\mu^{(z)}\|\|\dot\psi_\lambda^{(z)}\|\end{aligned}$$

by v and vi, together with the previous observation, the second statement follows by an application of the Schur lemma. ◊

Remark 5.3.4. If $z=\{0,1\}$ and the wavelets satisfy the additional smoothness condition $\|\ddot\psi_\lambda^{(z)}\|_{L_\infty}\lesssim 2^{|\lambda|\frac{5}{2}}$, then from the property $|\int_0^1\dot\psi_\mu^{(z)}\dot\psi_\lambda^{(z)}|=|\int_0^1\psi_\mu^{(z)}\ddot\psi_\lambda^{(z)}|\le \operatorname{diam}(\operatorname{supp}\psi_\mu^{(z)})\times\|\psi_\mu^{(z)}\|_{L_\infty}\|\ddot\psi_\lambda^{(z)}\|_{L_\infty}\lesssim 2^{\frac{3}{2}(|\lambda|-|\mu|)}2^{|\lambda|+|\mu|}$, one infers that even the estimate $\|\vec A-\vec A^{(j)}\|\lesssim 2^{-3j/2}$ holds. Even $\|\vec A-\vec A^{(j)}\|\lesssim 2^{-5j/2}$ could be obtained when additionally $\|\dddot\psi_\lambda^{(z)}\|_{L_\infty}\lesssim 2^{|\lambda|\frac{7}{2}}$ and all wavelets on positive levels have at least one vanishing moment. For orthogonal wavelets, however, the last requirement is in conflict with $z=\{0,1\}$ that was used for the integration by parts.

Using the above univariate wavelets, let $\boldsymbol\Psi:=\{\boldsymbol\psi_{\boldsymbol\lambda}\colon\boldsymbol\lambda\in\boldsymbol\nabla\}$ be defined as in (5.3).

Theorem 5.3.5. *For $j\in\mathbb{N}$, let $\mathbf{A}^{(j)}$ be the matrix created from $\mathbf{A}=a(\boldsymbol\psi_{\boldsymbol\mu},\boldsymbol\psi_{\boldsymbol\lambda})_{\boldsymbol\lambda,\boldsymbol\mu\in\boldsymbol\nabla}$ with $a(\cdot,\cdot)$ from* (5.1) *by dropping all entries $\mathbf{A}_{\boldsymbol\lambda,\boldsymbol\mu}$ for which $\||\boldsymbol\lambda|-|\boldsymbol\mu|\|_\infty\ge j$. Then the number of non-zero entries in each row or column of $\mathbf{A}^{(j)}$ is bounded by some absolute multiple of jn, and*

$$\|\mathbf{A}-\mathbf{A}^{(j)}\|\le\max_z\|\vec A_z-\vec A_z^{(j)}\|\ \ (\le\max_z C_{z,\mathrm{sp}}2^{-j/2}).$$

Proof. In view of Proposition 5.3.3, we only have to prove the first inequality. Let $\vec B_z:=[\int_0^1\dot\psi_\mu^{(z)}\dot\psi_\lambda^{(z)}]_{\lambda,\mu\in\nabla_z}$, $\vec D_z:=\operatorname{diag}(\vec B_z)$, and let $\vec B_z^{(j)}$ be constructed from $\vec B_z$ by dropping all entries $(\vec B_z)_{\lambda,\mu}$ with $||\lambda|-|\mu||\ge j$. From $\vec A_z:=\vec D_z^{-\frac12}\vec B_z\vec D_z^{-\frac12}$, $\vec A_z^{(j)}:=\vec D_z^{-\frac12}\vec B_z^{(j)}\vec D_z^{-\frac12}$, and since $\vec A_z-\vec A_z^{(j)}$ is symmetric, we have

$$-\|\vec A_z-\vec A_z^{(j)}\|\vec D_z\le\vec B_z-\vec B_z^{(j)}\le\|\vec A_z-\vec A_z^{(j)}\|\vec D_z. \tag{5.9}$$

(Since these inequalities concern unbounded matrices, they should be interpreted as inequalities between scalar products involving any finitely supported vector.)

Let

$$\begin{aligned}\mathbf{B}&:=[a(\otimes_{m=1}^n\psi_{\mu_m}^{(z_m)},\otimes_{m=1}^n\psi_{\lambda_m}^{(z_m)})]_{\boldsymbol\lambda,\boldsymbol\mu\in\boldsymbol\nabla}\\ &=c_0+c_1\vec B_{z_1}\otimes I\otimes\cdots\otimes I+\ldots+c_nI\otimes\cdots\otimes I\otimes\vec B_{z_n},\\ \mathbf{D}&:=c_0+c_1\vec D_{z_1}\otimes I\otimes\cdots\otimes I+\cdots+c_nI\otimes\cdots\otimes I\otimes\vec D_{z_n},\\ \mathbf{B}^{(j)}&:=c_0+c_1\vec B_{z_1}^{(j)}\otimes I\otimes\cdots\otimes I+\cdots+c_nI\otimes\cdots\otimes I\otimes\vec B_{z_n}^{(j)}.\end{aligned}$$

Then $\mathbf{A}=\mathbf{D}^{-\frac12}\mathbf{B}\mathbf{D}^{-\frac12}$ and $\mathbf{A}^{(j)}=\mathbf{D}^{-\frac12}\mathbf{B}^{(j)}\mathbf{D}^{-\frac12}$. By applying (5.9) n times, we infer that

$$-\max_z\|\vec A_z-\vec A_z^{(j)}\|(\mathbf{D}-c_0)\le\mathbf{B}-\mathbf{B}^{(j)}\le\max_z\|\vec A_z-\vec A_z^{(j)}\|(\mathbf{D}-c_0),$$

and so by $\mathbf{D}-c_0\le\mathbf{D}$ that $\|\mathbf{A}-\mathbf{A}^{(j)}\|\le\max_z\|\vec A_z-\vec A_z^{(j)}\|$. ◊

Remark 5.3.6. For $n > 1$, the matrix $\mathbf{A}^{(j)}$ still has many entries that can be dropped without significantly increasing the error. Indeed, $\mathbf{A}_{\boldsymbol{\lambda},\boldsymbol{\mu}}$ and so $\mathbf{A}^{(j)}_{\boldsymbol{\lambda},\boldsymbol{\mu}}$ can only be non-zero when $\boldsymbol{\lambda}$ and $\boldsymbol{\mu}$ differ in at most one coordinate, say the i-th one. Then $\mathbf{A}^{(j)}_{\boldsymbol{\lambda},\boldsymbol{\mu}} = \frac{\|\psi^{(z_i)}_{\lambda_i}\|}{\|\boldsymbol{\psi}_{\boldsymbol{\lambda}}\|}\vec{A}^{(j)}_{\lambda_i,\mu_i}\frac{\|\psi^{(z_i)}_{\mu_i}\|}{\|\boldsymbol{\psi}_{\boldsymbol{\mu}}\|}$, where the pre- and post factor are of the order $\frac{2^{|\lambda_i|}}{\sqrt{\sum_{m=1}^n 4^{|\lambda_m|}}}$ and $\frac{2^{|\mu_i|}}{\sqrt{\sum_{m=1}^n 4^{|\mu_m|}}}$, respectively, which can be very small. Using the Schur lemma one can show that in any case elements with modulus less than some multiple of $\frac{2^{-j/2}}{(j+1)n}$ can be dropped from $\mathbf{A}^{(j)}$ while keeping the error on the same level.

We recall the following definition from [GS06]:

> *A matrix* $\mathbf{E}$ *is called to be* s^*-computable *when for some constant* C *and any* $j \in \mathbb{N}_0$, *there exists a matrix* $\mathbf{E}^{(j)}$ *having in each column not more than* Cj *non-zero entries, whose joint computation takes not more than* Cj *operations, such that for any* $\bar{s} < s^*$, *there exists a constant* $D_{\bar{s}}$ *such that* $\|\mathbf{E} - \mathbf{E}^{(j)}\| \leq D_{\bar{s}} j^{-\bar{s}}$.

Theorem 5.3.5 shows that $\mathbf{A}$ is s^*-computable for $s^* = \infty$ with $C \eqsim n$ and, for any $\bar{s}$, with $D_{\bar{s}}$ being an absolute constant (the spectral argument applied in the proof of Theorem 5.3.5 prevents that also $D_{\bar{s}}$ grows linearly with n, which would be the case if simply a repeated triangle inequality was applied). In the next sections, it will not be essential that $s^* = \infty$, but it suffices that it is larger than $d-1$, being the maximum rate of best N-term approximation that can be expected.

Remark 5.3.7. We discuss some generalizations of Theorem 5.3.5. Instead of (5.1), let

$$a(u,v) = \int_\Omega c_0 uv + \sum_{i,j=1}^n d_{ij}\partial_j u \partial_i v$$

where the d_{ij} are constants such that for some constants $Q \geq q > 0$,

$$q \leq \sum_{i,j=1}^n d_{ij}\xi_i\xi_j \Big/ \sum_{m=1}^n c_m \xi_m^2 \leq Q, \quad (\xi \in \mathbb{R}^n).$$

From $\frac{|\int_0^1 \psi^{(z)}_\mu \psi^{(z)}_\lambda|}{\sqrt{\|\psi^{(z)}_\mu\|\|\psi^{(z)}_\lambda\|}} \lesssim 2^{||\lambda|-|\mu||}$, and, with $\triangle^{(i,j)}_k := \vec{D}^{\frac{1}{2}}_{z_k}$ for $k \in \{i,j\}$ and $\triangle^{(i,j)}_k := I$ otherwise, from $\sum_{i,j=1}^n d_{ij}\bigotimes_{k=1}^n \triangle^{(i,j)}_k \leq Q(\mathbf{D} - c_0)$, one may verify that with $m(n) := \#\{d_{ij} \neq 0\}$, there exist $\mathbf{A}^{(j)}$ having $\mathcal{O}(jm(n))$ non-zeros in each column with $\|\mathbf{A} - \mathbf{A}_j\| \leq 2^{-j/2}$.

By additionally using results from [SS08], for variable, sufficiently smooth coefficients d_{ij} that each depend on at most a uniformly bounded number of space variables x_k, one can show that $\mathbf{A}$ is s^*-computable for some $s^* > d-1$ with $C \eqsim m(n)$ and, for any $\bar{s} < s^*$, with $D_{\bar{s}}$ being an absolute constant. Concluding we can say that in these generalized settings the results of this chapter are still valid with the factor n showing up in the operation count of the adaptive wavelet algorithm now reading as $m(n) \in [n, n^2]$.

5.4 The adaptive wavelet scheme

5.4.1 Underlying principles

We recall the main ideas behind the adaptive wavelet method introduced in [GHS07]. It is a modification of the scheme by Cohen, Dahmen and DeVore from [CDD01], in which the recurrent coarsening of the iterands is avoided. This modification results in a quantitatively better performing method, which was confirmed in numerical experiments [DHS06, GHS07].

Throughout this Section 5.4, $\mathbf{A}\colon \ell_2(\boldsymbol{\Lambda}) \to \ell_2(\boldsymbol{\Lambda})$ is some general bounded, symmetric and positive definite operator that is s^*-computable, where $\boldsymbol{\Lambda}$ is some countable index set. Not before the next section, we return to our particular matrix $\mathbf{A}$, and investigate the issue of the dependence of constants on the space dimension.

For any $\boldsymbol{\Lambda} \subset \boldsymbol{\nabla}$, with $\ell_2(\boldsymbol{\Lambda})$ we will mean the subspace of $\mathbf{v} \in \ell_2(\boldsymbol{\nabla})$ with supports in $\boldsymbol{\Lambda}$. The trivial embedding of $\ell_2(\boldsymbol{\Lambda})$ into $\ell_2(\boldsymbol{\nabla})$ will be denoted by $\mathbf{I}_{\boldsymbol{\Lambda}}$, and its adjoint with respect to $\langle \cdot, \cdot \rangle$, i.e., the operator that replaces coefficients outside $\boldsymbol{\Lambda}$ by zeros, will be denoted by $\mathbf{P}_{\boldsymbol{\Lambda}}$. We set $\mathbf{A}_{\boldsymbol{\Lambda}} = \mathbf{P}_{\boldsymbol{\Lambda}}\mathbf{A}\mathbf{I}_{\boldsymbol{\Lambda}}$. Using that $\mathbf{A}$ is symmetric and positive definite, one verifies that for $\mathbf{v} \in \ell_2(\boldsymbol{\nabla})$ and $\mathbf{v}_{\boldsymbol{\Lambda}} \in \ell_2(\boldsymbol{\Lambda})$,

$$\|\mathbf{A}^{-1}\|^{-\frac{1}{2}}\|\mathbf{v}\| \le |||\mathbf{v}||| \le \|\mathbf{A}\|^{\frac{1}{2}}\|\mathbf{v}\|,\ \|\mathbf{A}\mathbf{v}\| \le \|\mathbf{A}\|^{\frac{1}{2}}|||\mathbf{v}|||,\ \|\mathbf{A}^{-1}\|^{-\frac{1}{2}}|||\mathbf{v}_{\boldsymbol{\Lambda}}||| \le \|\mathbf{A}_{\boldsymbol{\Lambda}}\mathbf{v}_{\boldsymbol{\Lambda}}\|,$$

which properties will be used often in the following. The solution $\mathbf{u}_{\boldsymbol{\Lambda}} \in \ell_2(\boldsymbol{\Lambda})$ of $\mathbf{A}_{\boldsymbol{\Lambda}}\mathbf{u}_{\boldsymbol{\Lambda}} = \mathbf{P}_{\boldsymbol{\Lambda}}\mathbf{f}$ is the *Galerkin approximation* to $\mathbf{u}$ from $\ell_2(\boldsymbol{\Lambda})$. With respect to $|||\cdot|||$, it is the best approximation to $\mathbf{u}$ from this subspace.

The methods from [CDD01, GHS07] generate a sequence of (approximate) Galerkin solutions with respect to a sequence of nested subspaces of $\ell_2(\boldsymbol{\nabla})$. In part (a) of the following lemma, which is [CDD01, Lemma 4.1], it is shown how a given subspace can be enlarged such that the error in the Galerkin solution is reduced by a constant factor. In part (b), from [GHS07], and in the discussion following this lemma, it is shown that if one is not too greedy, i.e., if one is content with a moderate error reduction, then besides having convergence, one keeps quasi-optimal control over the dimensions of the subspaces. Although $\mathbf{w}$ in this lemma can be any element of $\ell_2(\boldsymbol{\Lambda}_0)$, one may think of it as being (an approximation to) the Galerkin solution from $\ell_2(\boldsymbol{\Lambda}_0)$. For convenience we recall the short proof.

Lemma 5.4.1. *Let $\mu \in (0,1]$, $\boldsymbol{\Lambda}_0 \subset \boldsymbol{\Lambda}_1 \subset \boldsymbol{\nabla}$, $\mathbf{w} \in \ell_2(\boldsymbol{\Lambda}_0)$ such that*

$$\|\mathbf{P}_{\boldsymbol{\Lambda}_1}(\mathbf{f} - \mathbf{A}\mathbf{w})\| \ge \mu\|\mathbf{f} - \mathbf{A}\mathbf{w}\|. \tag{5.10}$$

(a) Then, for $\mathbf{u}_{\boldsymbol{\Lambda}_1} \in \ell_2(\boldsymbol{\Lambda}_1)$ being the solution of $\mathbf{A}_{\boldsymbol{\Lambda}_1}\mathbf{u}_{\boldsymbol{\Lambda}_1} = \mathbf{P}_{\boldsymbol{\Lambda}_1}\mathbf{f}$, we have

$$|||\mathbf{u} - \mathbf{u}_{\boldsymbol{\Lambda}_1}||| \le \rho|||\mathbf{u} - \mathbf{w}|||,$$

where $\rho = \rho(\mathbf{A}, \mu) := [1 - \kappa(\mathbf{A})^{-1}\mu^2]^{\frac{1}{2}} < 1$.

(b) If $\mu < \kappa(\mathbf{A})^{-\frac{1}{2}}$ and $\boldsymbol{\Lambda}_1$ is the smallest *set satisfying* (5.10)*, then*

$$\#(\boldsymbol{\Lambda}_1 \backslash \boldsymbol{\Lambda}_0) \le \min\{N\colon |||\mathbf{u} - \mathbf{u}_N||| \le \sigma|||\mathbf{u} - \mathbf{w}|||\}, \tag{5.11}$$

where $\sigma = \sigma(\mathbf{A}, \mu) := [1 - \mu^2\kappa(\mathbf{A})]^{\frac{1}{2}} > 0$.

Proof. (a) We have

$$\begin{aligned}\|\!|\mathbf{u}_{\mathbf{\Lambda}_1}-\mathbf{w}|\!\| &\geq \|\mathbf{A}\|^{-\frac{1}{2}}\|\mathbf{A}(\mathbf{u}_{\mathbf{\Lambda}_1}-\mathbf{w})\| \geq \|\mathbf{A}\|^{-\frac{1}{2}}\|\mathbf{P}_{\mathbf{\Lambda}_1}(\mathbf{f}-\mathbf{A}\mathbf{w})\| \\ &\geq \|\mathbf{A}\|^{-\frac{1}{2}}\mu\|\mathbf{f}-\mathbf{A}\mathbf{w}\| \geq \kappa(\mathbf{A})^{-\frac{1}{2}}\mu\|\!|\mathbf{u}-\mathbf{w}|\!\|.\end{aligned}$$

The proof of (a) is completed by using the Galerkin orthogonality

$$\|\!|\mathbf{u}-\mathbf{w}|\!\|^2 = \|\!|\mathbf{u}-\mathbf{u}_{\mathbf{\Lambda}_1}|\!\|^2 + \|\!|\mathbf{u}_{\mathbf{\Lambda}_1}-\mathbf{w}|\!\|^2.$$

(b) For an N as in the right-hand side of (5.11), let $\breve{\mathbf{\Lambda}} := \mathbf{\Lambda}_0 \cup \operatorname{supp}\mathbf{u}_N$. Then, for the solution of $\mathbf{A}_{\breve{\mathbf{\Lambda}}}\mathbf{u}_{\breve{\mathbf{\Lambda}}} = \mathbf{P}_{\breve{\mathbf{\Lambda}}}\mathbf{f}$, we have $\|\!|\mathbf{u}-\mathbf{u}_{\breve{\mathbf{\Lambda}}}|\!\| \leq \|\!|\mathbf{u}-\mathbf{u}_N|\!\|$, and so by Galerkin orthogonality

$$\|\!|\mathbf{u}_{\breve{\mathbf{\Lambda}}}-\mathbf{w}|\!\| \geq \mu\kappa(\mathbf{A})^{\frac{1}{2}}\|\!|\mathbf{u}-\mathbf{w}|\!\|,$$

giving

$$\begin{aligned}\|\mathbf{P}_{\breve{\mathbf{\Lambda}}}(\mathbf{f}-\mathbf{A}\mathbf{w})\| &= \|\mathbf{A}_{\breve{\mathbf{\Lambda}}}(\mathbf{u}_{\breve{\mathbf{\Lambda}}}-\mathbf{w})\| \geq \|\mathbf{A}^{-1}\|^{-\frac{1}{2}}\|\!|\mathbf{u}_{\breve{\mathbf{\Lambda}}}-\mathbf{w}|\!\| \\ &\geq \|\mathbf{A}^{-1}\|^{-\frac{1}{2}}\mu\kappa(\mathbf{A})^{\frac{1}{2}}\|\!|\mathbf{u}-\mathbf{w}|\!\| \geq \mu\|\mathbf{f}-\mathbf{A}\mathbf{w}\|.\end{aligned}$$

By our assumption on $\mathbf{\Lambda}_1$, we conclude that $\#(\mathbf{\Lambda}_1\backslash\mathbf{\Lambda}_0) \leq \#(\breve{\mathbf{\Lambda}}\backslash\mathbf{\Lambda}_0) \leq N$. ◊

Let us think of $\mathbf{w}$ in Lemma 5.4.1 as the exact Galerkin solution on $\mathbf{\Lambda}_0$. Then starting with $\mathbf{\Lambda}_0 = \varnothing$, a repeated application of part (a) gives a sequence $\mathbf{\Lambda}_0 \subset \mathbf{\Lambda}_1 \subset \cdots$, and corresponding Galerkin solutions $\mathbf{u}_{\mathbf{\Lambda}_0}, \mathbf{u}_{\mathbf{\Lambda}_1}, \ldots$ with $\|\!|\mathbf{u}-\mathbf{u}_{\mathbf{\Lambda}_k}|\!\| \leq \rho\|\!|\mathbf{u}-\mathbf{u}_{\mathbf{\Lambda}_{k-1}}|\!\|$. This is the idealized version of the adaptive wavelet method we are going to apply. Note that generally the residuals $\mathbf{f}-\mathbf{A}\mathbf{u}_{\mathbf{\Lambda}_k}$ are infinitely supported vectors, so that this algorithm cannot be performed in practice. For the moment ignoring this fact, let us take $\mu < \kappa(\mathbf{A})^{-\frac{1}{2}}$. Then, assuming that $\mathbf{u} \in \mathcal{A}^s_\infty$ for some $s > 0$, part (b) shows that

$$\begin{aligned}\#(\mathbf{\Lambda}_k\backslash\mathbf{\Lambda}_{k-1}) &\leq \min\{N\colon \|\!|\mathbf{u}-\mathbf{u}_N|\!\| \leq \sigma\|\!|\mathbf{u}-\mathbf{u}_{\mathbf{\Lambda}_{k-1}}|\!\|\} \\ &\leq [\|\mathbf{A}\|^{-\frac{1}{2}}\sigma\|\!|\mathbf{u}-\mathbf{u}_{\mathbf{\Lambda}_{k-1}}|\!\|]^{-1/s}\|\mathbf{u}\|^{1/s}_{\mathcal{A}^s_\infty},\end{aligned}$$

by $\|\!|\cdot|\!\| \leq \|\mathbf{A}\|^{\frac{1}{2}}\|\cdot\|$ and the definition of $\|\cdot\|_{\mathcal{A}^s_\infty}$. By combining both estimates, for $\ell \in \mathbb{N}$ we have

$$\begin{aligned}\#\mathbf{\Lambda}_\ell = \sum_{k=1}^{\ell}\#(\mathbf{\Lambda}_k\backslash\mathbf{\Lambda}_{k-1}) &\leq \|\mathbf{A}\|^{1/2s}\sigma^{-1/s}\|\mathbf{u}\|^{1/s}_{\mathcal{A}^s_\infty}\sum_{k=1}^{\ell}\|\!|\mathbf{u}-\mathbf{u}_{\mathbf{\Lambda}_{k-1}}|\!\|^{-1/s} \\ &\leq \|\mathbf{A}\|^{1/2s}\sigma^{-1/s}\|\mathbf{u}\|^{1/s}_{\mathcal{A}^s_\infty}\|\!|\mathbf{u}-\mathbf{u}_{\mathbf{\Lambda}_\ell}|\!\|^{-1/s}\sum_{k=1}^{\ell}(\rho^{\ell-k+1})^{1/s} \\ &\leq \|\mathbf{A}\|^{1/s}\frac{(\rho/\sigma)^{1/s}}{1-\rho^{1/s}}\|\mathbf{f}-\mathbf{A}\mathbf{u}_{\mathbf{\Lambda}_\ell}\|^{-1/s}\|\mathbf{u}\|^{1/s}_{\mathcal{A}^s_\infty}. \qquad (5.12)\end{aligned}$$

In view of $\mathbf{u} \in \mathcal{A}^s_\infty$, generally the support of any approximation to $\mathbf{u}$ with an $\|\!|\cdot|\!\|$-error equal to that of $\mathbf{u}_{\mathbf{\Lambda}_\ell}$ can generally not be expected to be smaller than $\|\!|\mathbf{u}-\mathbf{u}_{\mathbf{\Lambda}_\ell}|\!\|^{-1/s}\|\mathbf{u}\|^{1/s}_{\mathcal{A}^s_\infty} \geq \|\mathbf{A}^{-1}\|^{-1/s}\|\mathbf{f}-\mathbf{A}\mathbf{u}_{\mathbf{\Lambda}_\ell}\|^{-1/s}\|\mathbf{u}\|^{1/s}_{\mathcal{A}^s_\infty}$. Comparing this lower bound with the upper bound from (5.12), we conclude that up to the factor $\frac{(\rho/\sigma)^{1/s}}{1-\rho^{1/s}}\kappa(\mathbf{A})^{1/s}$, generally the cardinality of the set $\mathbf{\Lambda}_\ell$ produced by the algorithm is the smallest that can be expected.

Remark 5.4.2. Thinking of $\mu = \beta\kappa(\boldsymbol{A})^{-\frac{1}{2}}$ for some fixed $\beta < 1$, $\frac{(\rho/\sigma)^{1/s}}{1-\rho^{1/s}}\kappa(\mathbf{A})^{1/s}$ is a bounded function of $(s, \kappa(\boldsymbol{A}))$ on any compact subset of $(0,\infty)\times[1,\infty)$. For any s, $\frac{(\rho/\sigma)^{1/s}}{1-\rho^{1/s}}\kappa(\mathbf{A})^{1/s}$ tends to infinity when $\kappa(\mathbf{A})$ does, underlining the importance of using $L_2(0,1)$-orthonormal univariate wavelets in our application of solving elliptic PDEs in high space dimensions.

5.4.2 Practical scheme and rates

As we said, the algorithm from the previous subsection is not feasible in practice, because it uses the generally infinitely supported residuals. Apart from stopping the iteration, which we did not discuss so far, these residuals are only used to indicate in which way the current subspace has to be enlarged. For a proper enlargement it is, however, sufficient to know where the largest entries of the residual are located, and for that goal it suffices to use an approximate residual with a sufficiently small relative error.

We will assume the availability of the following routines. Realizations will be discussed in the forthcoming subsections.

APPLY$[\boldsymbol{\Lambda}, \mathbf{w}, \varepsilon] \to \mathbf{z}$: *For $\varepsilon > 0$, $\boldsymbol{\Lambda} \subset \boldsymbol{\nabla}$, and a finitely supported $\mathbf{w} \in \ell_2(\boldsymbol{\Lambda})$, it yields a finitely supported $\mathbf{z} \in \ell_2(\boldsymbol{\Lambda})$ with $\|\mathbf{A}_{\boldsymbol{\Lambda}}\mathbf{w} - \mathbf{z}\| \le \varepsilon$.*

RHS$[\boldsymbol{\Lambda}, \varepsilon] \to \mathbf{g}$: *For $\varepsilon > 0$, $\boldsymbol{\Lambda} \subset \boldsymbol{\nabla}$, it yields a finitely supported $\mathbf{g} \in \ell_2(\boldsymbol{\Lambda})$ with $\|\mathbf{P}_{\boldsymbol{\Lambda}}\mathbf{f} - \mathbf{g}\| \le \varepsilon$.*

Furthermore, in view of minimizing the computational complexity, we will not solve the Galerkin systems $\mathbf{A}_{\boldsymbol{\Lambda}_k}\mathbf{u}_{\boldsymbol{\Lambda}_k} = \mathbf{P}_{\boldsymbol{\Lambda}_k}\mathbf{f}$ exactly. Instead, we solve them using an iterative method starting with the previous iterand, and with a tolerance being a sufficiently small multiple of the error in that iterand. Moreover, we will allow that instead of the exact right-hand side $\mathbf{P}_{\boldsymbol{\Lambda}_k}\mathbf{f}$, we only have a sufficiently accurate approximation to it available. We assume the availability of the following routine, whose realization will be discussed in the next subsection.

GALSOLVE$[\boldsymbol{\Lambda}, \mathbf{g}_{\boldsymbol{\Lambda}}, \mathbf{w}_{\boldsymbol{\Lambda}}^{(0)}, \delta, \varepsilon] \to \mathbf{w}_{\boldsymbol{\Lambda}}$: *For $\delta \ge \varepsilon > 0$, $\boldsymbol{\Lambda} \subset \boldsymbol{\nabla}$, $\mathbf{g}_{\boldsymbol{\Lambda}}, \mathbf{w}_{\boldsymbol{\Lambda}}^{(0)} \in \ell_2(\boldsymbol{\Lambda})$ with $\|\mathbf{g}_{\boldsymbol{\Lambda}} - \mathbf{A}_{\boldsymbol{\Lambda}}\mathbf{w}_{\boldsymbol{\Lambda}}^{(0)}\| \le \delta$, it yields a $\mathbf{w}_{\boldsymbol{\Lambda}} \in \ell_2(\boldsymbol{\Lambda})$ with $\|\mathbf{g}_{\boldsymbol{\Lambda}} - \mathbf{A}_{\boldsymbol{\Lambda}}\mathbf{w}_{\boldsymbol{\Lambda}}\| \le \varepsilon$.*

Now suppose that we have available an approximation $\mathbf{w}$ to $\mathbf{u}$, with support contained in some finite $\boldsymbol{\Lambda}_0 \subset \boldsymbol{\nabla}$, as well as an approximation $\mathbf{r}$ to $\mathbf{f} - \mathbf{A}\mathbf{w}$ with $\|(\mathbf{f} - \mathbf{A}\mathbf{w}) - \mathbf{r}\| \le \omega\|\mathbf{r}\|$ for some constant $\omega > 0$. Then our task will be to enlarge $\boldsymbol{\Lambda}_0$ to some $\boldsymbol{\Lambda}_1 \subset \boldsymbol{\nabla}$ such that for some constant $\alpha > \omega$,

$$\|\mathbf{P}_{\boldsymbol{\Lambda}_1}\mathbf{r}\| \ge \alpha\|\mathbf{r}\|. \tag{5.13}$$

Indeed, then $\|\mathbf{P}_{\boldsymbol{\Lambda}_1}(\mathbf{f} - \mathbf{A}\mathbf{w})\| \ge \|\mathbf{P}_{\boldsymbol{\Lambda}_1}\mathbf{r}\| - \omega\|\mathbf{r}\| \ge (\alpha - \omega)\|\mathbf{r}\| \ge \frac{\alpha-\omega}{1+\omega}\|\mathbf{f} - \mathbf{A}\mathbf{w}\|$, and so an application of Lemma 5.4.1(a) shows that the error in the Galerkin solution from $\ell_2(\boldsymbol{\Lambda}_1)$ is strictly less than that in $\mathbf{w}$.

Moreover, with $\mu := \frac{\alpha+\omega}{1-\omega}$, and $\boldsymbol{\nabla} \supset \hat{\boldsymbol{\Lambda}} \supset \boldsymbol{\Lambda}_0$ being *any* set with $\|\mathbf{P}_{\hat{\boldsymbol{\Lambda}}}(\mathbf{f} - \mathbf{A}\mathbf{w})\| \ge \mu\|\mathbf{f} - \mathbf{A}\mathbf{w}\|$, we have $\mu\|\mathbf{r}\| \le \mu\|\mathbf{f} - \mathbf{A}\mathbf{w}\| + \mu\omega\|\mathbf{r}\| \le \|\mathbf{P}_{\hat{\boldsymbol{\Lambda}}}(\mathbf{f} - \mathbf{A}\mathbf{w})\| + \mu\omega\|\mathbf{r}\| \le \|\mathbf{P}_{\hat{\boldsymbol{\Lambda}}}\mathbf{r}\| + (1+\mu)\omega\|\mathbf{r}\|$, or $\|\mathbf{P}_{\hat{\boldsymbol{\Lambda}}}\mathbf{r}\| \ge \alpha\|\mathbf{r}\|$. So if we would select $\boldsymbol{\Lambda}_1 \supset \boldsymbol{\Lambda}_0$ satisfying (5.13) with *minimal* cardinality, then $\#(\boldsymbol{\Lambda}_1\backslash\boldsymbol{\Lambda}_0) \le \#(\hat{\boldsymbol{\Lambda}}\backslash\boldsymbol{\Lambda}_0)$, and

if additionally $\mu < \kappa(\mathbf{A})^{-\frac{1}{2}}$, then using Lemma 5.4.1(b) we would have quasi optimal control over the cardinality of this set.

Remark 5.4.3. The cost of our adaptive wavelet algorithm will be dominated by that of the computation of the approximate residuals. Assuming $\mathbf{u} \in \mathcal{A}^s_\infty$, (the upper bound for) the latter will scale as the prescribed tolerance to the power $-1/s$. So in particular for relatively small values of s, it will be beneficial if we could reduce the prescribed tolerances by some factor. In above lines, we estimated $\|\mathbf{P}_{\hat{\mathbf{\Lambda}}}(\mathbf{f}-\mathbf{A}\mathbf{w})\| \le \|\mathbf{P}_{\hat{\mathbf{\Lambda}}}\mathbf{r}\| + \omega\|\mathbf{r}\|$ for $\hat{\mathbf{\Lambda}} \supset \mathbf{\Lambda}_0$ being the smallest set with $\|\mathbf{P}_{\hat{\mathbf{\Lambda}}}(\mathbf{f}-\mathbf{A}\mathbf{w})\| \ge \mu\|\mathbf{f}-\mathbf{A}\mathbf{w}\|$, and we applied similar steps with interchanged roles of $\mathbf{r}$ and $\mathbf{f}-\mathbf{A}\mathbf{w}$. The first estimate can only be sharp when the error $(\mathbf{f}-\mathbf{A}\mathbf{w})-\mathbf{r}$ is fully supported in $\hat{\mathbf{\Lambda}}$, which is unlikely. Making the assumption that the error is more equally distributed in the sense that $\|\mathbf{P}_{\hat{\mathbf{\Lambda}}}(\mathbf{f}-\mathbf{A}\mathbf{w})\| \le \|\mathbf{P}_{\hat{\mathbf{\Lambda}}}\mathbf{r}\| + \omega\mu\|\mathbf{r}\|$, (and similarly $\|\mathbf{P}_{\mathbf{\Lambda}_1}\mathbf{r}\| \le \|\mathbf{r}\| + \alpha\omega\|\mathbf{r}\|$), instead of $\omega < \alpha$ and $\mu := \frac{\alpha+\omega}{1-\omega} < \kappa(\mathbf{A})^{-\frac{1}{2}}$, we end up with the relaxed conditions $\omega < \frac{1}{2}$, and $\mu := \frac{\alpha}{1-2\omega} < \kappa(\mathbf{A})^{-\frac{1}{2}}$.

Also the upper bound $\kappa(\mathbf{A})^{-\frac{1}{2}}$ for μ derived in Lemma 5.4.1(b) is the result of a succession of two worst case analyses that unlikely or even impossibly can occur at the same time. So although we have no rigorous proof for this, we expect that in practice the conditions on the parameters α, ω, μ can be violated to some unfortunately unknown extent, by that improving the quantitative behavior of the algorithm. The same comment applies to the forthcoming parameter γ for the calls of GALSOLVE.

Finding the *smallest* $\mathbf{\Lambda}_1 \supset \mathbf{\Lambda}_0$ for which (5.13), or equivalently,

$$\|\mathbf{r}|_{\mathbf{\nabla}\setminus\mathbf{\Lambda}_0} - \mathbf{r}|_{\mathbf{\Lambda}_1\setminus\mathbf{\Lambda}_0}\| \le \sqrt{1-\alpha^2}\,\|\mathbf{r}\|$$

is valid, requires the sorting of all coefficients of $\mathbf{r}_{\mathbf{\nabla}\setminus\mathbf{\Lambda}_0}$ by their modulus, which, with $L := \#\operatorname{supp}\mathbf{r}|_{\mathbf{\nabla}\setminus\mathbf{\Lambda}_0}$, already takes the order of $L\log L$ operations. In order to avoid the log-factor, we realize that it is not essential that $\#(\mathbf{\Lambda}_1\setminus\mathbf{\Lambda}_0)$ be truly minimal. Sufficient is that it is minimal up to some constant factor, that for convenience will be fixed to be 2. It requires an approximate sorting of the coefficients of $\mathbf{r}_{\mathbf{\nabla}\setminus\mathbf{\Lambda}_0}$ by their modulus, that will be performed by a call of the following routine. This routine will also be used for the implementation of the APPLY routine, in which setting the idea of performing an approximate ordering was introduced in [Bar05, Met02].

BUCKETSORT$[\mathbf{v},\varepsilon] \to [(\mathbf{v}_{[p]})_{1\le p\le P},\Pi]$: *The input $\mathbf{v} \in \ell_2(\mathbf{\Lambda})$ should be finitely supported, and $\varepsilon > 0$. Let P be the smallest integer with $2^{-P/2}\|\mathbf{v}\|_\infty\sqrt{\#\operatorname{supp}\mathbf{v}} \le \varepsilon$. Store the indices of $\mathbf{v}$ in P buckets, depending on the modulus of the corresponding coefficient to be in one of the P intervals $(\frac{1}{\sqrt{2}}\|\mathbf{v}\|_\infty, \|\mathbf{v}\|_\infty]$, $(\frac{1}{2}\|\mathbf{v}\|_\infty, \frac{1}{\sqrt{2}}\|\mathbf{v}\|_\infty]$, …, or $(2^{-P/2}\|\mathbf{v}\|_\infty, 2^{-(P-1)/2}\|\mathbf{v}\|_\infty]$, and discard them otherwise. For $1 \le p \le P$, define $\mathbf{v}_{[p]}$ as the restriction of $\mathbf{v}$ to the indices from the p-th bucket. Define $\Pi\colon \mathbb{N} \to \mathbf{\nabla}$ by numbering the indices in the buckets from the first to the last, and within each bucket in arbitrary order. The definition of Π beyond the last numbered index is irrelevant.*

Note that the number of buckets P is $\max(0, \lceil 2\log_2(\|\mathbf{v}\|_\infty\sqrt{\#\operatorname{supp}\mathbf{v}}/\varepsilon)\rceil)$. This P is taken such that the squared sum of the coefficients corresponding to the indices not stored in any bucket is not larger than ε^2. This means that for the

task of finding a (quasi) minimal Λ such that $\|\mathbf{v} - \mathbf{v}|_\Lambda\| \le \varepsilon$ these coefficients can be discarded anyway. By furthermore using that the squared coefficients corresponding to indices within one bucket differ at most a factor 2, one arrives at the following result (cf. [GHS07, Remark 2.3]).

Proposition 5.4.4. *The number of operations required by a call of the routine* $[\,\cdot\,,\Pi] := \textsc{bucketsort}[\mathbf{v},\varepsilon]$ *is bounded by some absolute multiple of*

$$\#\operatorname{supp}\mathbf{v} + \max(1, \lceil \log(\|\mathbf{v}\|_\infty \sqrt{\#\operatorname{supp}\mathbf{v}}/\varepsilon)\rceil).$$

For any $\delta \ge \varepsilon$*, the smallest number* $K \in \mathbb{N}_0$ *with* $\|\mathbf{v} - \mathbf{v}|_{\Pi(\{1,\dots,K\})}\| \le \delta$ *satisfies* $K \le 2\min\{N \in \mathbb{N}_0 \colon \|\mathbf{v} - \mathbf{v}_N\| \le \delta\}$.

Above considerations lead to the following practical variant of the scheme from the previous subsection.

$\textsc{solve}[\nu_{-1},\varepsilon] \to \mathbf{w}_k$:
% *Let* $\alpha,\omega,\gamma,\theta$ *be constants with* $\omega \in (0,\alpha)$, $\frac{\alpha+\omega}{1-\omega} < \kappa(\mathbf{A})^{-\frac{1}{2}}$, $\theta > 0$ *and*
% $\gamma \in \big(0, \frac{1}{6}\kappa(\mathbf{A})^{-\frac{1}{2}}\frac{\alpha-\omega}{1+\omega}\big)$. *The parameter* ν_{-1} *is an estimate for the norm of the*
% *initial residual* $\mathbf{f}$.

$k := 0$, $\mathbf{w}_k := 0$, $\mathbf{\Lambda}_k := \varnothing$
`do` $\zeta := \theta\nu_{k-1}$
  `do` $\zeta := \zeta/2$, $\mathbf{r}_k := \textsc{rhs}[\boldsymbol{\nabla},\zeta/2] - \textsc{apply}[\boldsymbol{\nabla},\mathbf{w}_k,\zeta/2]$
    `if` $\nu_k := \|\mathbf{r}_k\| + \zeta \le \varepsilon$ `then stop endif`
  `until` $\zeta \le \omega\|\mathbf{r}_k\|$
  $[\,\cdot\,,\Pi] := \textsc{bucketsort}[\mathbf{r}_k|_{\boldsymbol{\nabla}\setminus\mathbf{\Lambda}_k}, \sqrt{1-\alpha^2}\,\|\mathbf{r}_k\|]$
  determine the smallest $K \in \mathbb{N}_0$ *with* $\|\mathbf{r}_k|_{\boldsymbol{\nabla}\setminus\mathbf{\Lambda}_k} - \mathbf{r}_k|_{\Pi(\{1,\dots,K\})}\| \le \sqrt{1-\alpha^2}\,\|\mathbf{r}_k\|$
  $\mathbf{\Lambda}_{k+1} := \mathbf{\Lambda}_k \cup \Pi(\{1,\dots,K\})$
  $\mathbf{g}_{k+1} := \textsc{rhs}[\mathbf{\Lambda}_{k+1},\gamma\nu_k]$
  $\mathbf{w}_{k+1} := \textsc{galsolve}[\mathbf{\Lambda}_{k+1},\mathbf{g}_{k+1},\mathbf{w}_k,(1+\gamma)\nu_k,\gamma\nu_k]$
  $k := k+1$
`enddo`

In the inner loop of this adaptive wavelet algorithm **solve**, an approximate residual $\mathbf{r}_k$ of the current iterand $\mathbf{w}_k$ is determined with $\|\mathbf{r}_k^* - \mathbf{r}_k\| \le \omega\|\mathbf{r}_k\|$, with $\mathbf{r}_k^*$ denoting the exact residual. This is done by computing approximate residuals with geometrically decreasing tolerances ζ until either this condition is met, or $\|\mathbf{r}_k^*\| \le \|\mathbf{r}_k\| + \|\mathbf{r}_k^* - \mathbf{r}_k\| \le \|\mathbf{r}_k\| + \zeta =: \nu_k \le \varepsilon$, in which case the algorithm stops.

Because of the geometrical decrease of the tolerances, the cost of this inner loop is always dominated by the cost of its last iteration. From a quantitative point of view, however, it is useful to tune the constant θ to be as large as possible such that the inner loop "usually" terminates in the first iteration. When the $\|\mathbf{r}_k\|$ exhibit a linear decrease as function of k, which is generally the best that can be expected, a selection of θ to be (slightly smaller than) $\frac{2\omega}{1+\omega}$ times

the rate seems to be a sensible choice. Indeed, if $\nu_{k-1} = (1+\omega)\|\mathbf{r}_{k-1}\|$, then $\frac{1}{2}\frac{2\omega}{1+\omega}\frac{\|\mathbf{r}_k\|}{\|\mathbf{r}_{k-1}\|}\nu_{k-1} = \omega\|\mathbf{r}_k\|$.

By adding perturbation arguments to the analysis from the previous subsection, we end up with the following result. For details we refer to [GHS07]. Inspection of the proof shows that a constant that is unspecified there is actually of the form $D_4\|\mathbf{A}\|^{1/s}$, with D_4 as given in the current theorem.

Theorem 5.4.5. *For any ε, $\nu_{-1} > 0$, $\mathbf{w} := \textsc{solve}[\nu_{-1}, \varepsilon]$ terminates with*

$$\|\mathbf{f} - \mathbf{A}\mathbf{w}\| \le \varepsilon.$$

If, for some $s > 0$, $\mathbf{u} \in \mathcal{A}^s_\infty$, then

$$\#\operatorname{supp}\mathbf{w} \le D_4\|\mathbf{A}\|^{1/s}\varepsilon^{-1/s}\|\mathbf{u}\|^{1/s}_{\mathcal{A}^s_\infty}$$

for some constant $D_4 > 0$, only dependent on $\kappa(\mathbf{A})$ when it tends to ∞, s when it tends to 0 or ∞, and ω, α and γ when they approach the boundaries of their domains of definition.

5.4.3 Cost of SOLVE

Using that $\max_{\boldsymbol{\lambda}\in\boldsymbol{\nabla}\setminus\boldsymbol{\Lambda}_k}|(\mathbf{r}_k)_{\boldsymbol{\lambda}}| \le \|\mathbf{r}_k\|$, Proposition 5.4.4 shows that the cost of a call $[\,\cdot\,,\Pi] := \textsc{bucketsort}[\mathbf{r}_k|_{\boldsymbol{\nabla}\setminus\boldsymbol{\Lambda}_k}, \sqrt{1-\alpha^2}\,\|\mathbf{r}_k\|]$ in **SOLVE** can be bounded by some absolute multiple of $\#\operatorname{supp}\mathbf{r}_k$. The same holds for the cost of evaluating the next line in the algorithm. Since the preceding computation of $\mathbf{r}_k$ requires in any case the order of $\#\operatorname{supp}\mathbf{r}_k$ operations, the cost of the call of **SOLVE** will be determined by that of the calls of **RHS**, **APPLY** and **GALSOLVE**.

The realization and cost of the routines **APPLY** and **GALSOLVE** will be discussed in this subsection. A realization of a routine **RHS** will be specific for the problem at hand, and will be discussed in Section 5.5.

The proof of Theorem 5.4.5 from [GHS07] shows that whenever $\mathbf{u} \in \mathcal{A}^s_\infty$ for some $s > 0$, then any $\mathbf{w}_k$ computed inside **SOLVE** satisfies

$$\#\operatorname{supp}\mathbf{w}_k \le D_5\|\mathbf{u} - \mathbf{w}_k\|^{-1/s}\|\mathbf{u}\|^{1/s}_{\mathcal{A}^s_\infty}$$

for a constant $D_5 > 0$, only dependent on $\kappa(\mathbf{A})$, s, ω, α and γ in the way indicated in Theorem 5.4.5. Putting $d := D_5^{-1} + 1$, and, for tolerances $\varepsilon \ge d\|\mathbf{u} - \mathbf{w}_k\|$, by approximating $\mathbf{w}_k$ by $\mathbf{u}_N$ with $\|\mathbf{u}-\mathbf{u}_N\| \le (1-\frac{1}{d})\varepsilon$, so that indeed $\|\mathbf{w}_k-\mathbf{u}_N\| \le \varepsilon$, or by $\mathbf{w}_k$ itself otherwise, one easily verifies that

$$\|\mathbf{w}_k\|_{\mathcal{A}^s_\infty} = \sup_{\varepsilon>0}\ \varepsilon \min_{\{N\in\mathbb{N}_0:\ \|\mathbf{w}_k-(\mathbf{w}_k)_N\|\le\varepsilon\}} N^s \le (1+D_5)\|\mathbf{u}\|_{\mathcal{A}^s_\infty}. \tag{5.14}$$

This uniform boundedness of the iterands in $\|\cdot\|_{\mathcal{A}^s_\infty}$ is the key to the design of suitable routines **APPLY** and **GALSOLVE**.

The idea behind the approximate application of $\mathbf{A}$ introduced in [CDD01] is as follows: Chop the input vector $\mathbf{w} = \mathbf{w}_k$ into $j := \lceil \log_2(\#\operatorname{supp}\mathbf{w} + 1) - 1\rceil$ pieces

$$\mathbf{w} = \mathbf{w}_1 + [\mathbf{w}_3 - \mathbf{w}_1] + \ldots + [\mathbf{w}_{2^{j+1}-1} - \mathbf{w}_{2^j-1}],$$

where $\mathbf{w}_{2^{p+1}-1}$ is the best $2^{p+1}-1$ approximation to $\mathbf{w}$, and approximate the application of $\mathbf{A}$ to each of the pieces separately. We have $\|\mathbf{w}_{2^{p+1}-1} - \mathbf{w}_{2^p-1}\| \le$

$\|\mathbf{w} - \mathbf{w}_{2^p-1}\| \lesssim 2^{-sp}\|\mathbf{w}\|_{\mathcal{A}^s_\infty}$ (cf. footnote 1). So the larger is $\#\operatorname{supp}[\mathbf{w}_{2^{p+1}-1} - \mathbf{w}_{2^p-1}] = 2^p$, and so the more columns of the approximation of $\mathbf{A}$ are needed, the smaller is $\|\mathbf{w}_{2^{p+1}-1} - \mathbf{w}_{2^p-1}\|$, and so the less accurate this approximation can be. So this approximate matrix vector product uses both the near sparsity of the matrix and that of the vector.

The following routine **APPLY** is based on a variation of the above principle. There will be the following differences with the original routine from [CDD01] aiming at increasing the efficiency:

- In order to avoid suboptimal log-factors due to sorting needed to determine best N-term approximations, the approximate sorting routine **BUCKETSORT** is applied.
- Since there is little to be gained by approximating columns of $\mathbf{A}$ corresponding to indices inside one bucket with different accuracies, we will chop $\mathbf{w}$ in pieces corresponding to the subdivision of the indices over the buckets. These pieces do not have a prescribed cardinality, but instead have a prescribed range of values. A similar idea was applied in [DHS06], with ranges that depend on some upper bound for the value of s for which $\mathbf{u} \in \mathcal{A}^s$ can be expected. The **APPLY** routine below is universal in the sense that no prior knowledge about the value of s is needed.
- Instead of using a priori fixed accuracies of the approximate matrix vector product on each of the pieces, to minimize the cost for achieving a prescribed tolerance, we use an optimization strategy based on a posteriori information.

APPLY$[\mathbf{\Lambda}, \mathbf{w}, \varepsilon] \to \mathbf{z}$:
% $\mathbf{w} \in \ell_2(\mathbf{\Lambda})$ *is finitely supported,* $\varepsilon > 0$.
% *For* $j \in \mathbb{N}_0$, *let* $\mathbf{A}^{(j)}$ *and* $\overline{e}_j$ *be matrices and constants such that* $\mathbf{A}^{(0)} := 0$,
% $\|\mathbf{A} - \mathbf{A}^{(j)}\| \le \overline{e}_j$ *and* $\lim_{j\to\infty} \overline{e}_j = 0$.
% *For* $j \in \mathbb{N}_0$, *let* c_j *be an upperbound for both the number of non-zero entries*
% *in each column of* $\mathbf{A}^{(j)}$, *and for the number of arithmetic operations needed*
% *for their joint computation, where* $\sup_{j\in\mathbb{N}} \frac{c_{j+1}}{c_j} < \infty$ *and* $c_0 := 0$.

$[(\mathbf{w}_{[p]})_p, \cdot\,] :=$ **BUCKETSORT**$[\mathbf{w}, \varepsilon/(2\overline{e}_0)]$
Compute the smallest $\ell \in \mathbb{N}_0$ *with*

$$\delta := \overline{e}_0 \,\|\mathbf{w} - \sum_{p=1}^{\ell} \mathbf{w}_{[p]}\| \le \varepsilon/2.$$

Determine, in $\mathcal{O}(\#\operatorname{supp}\mathbf{w})$ *operations,* $\mathbf{j} \in \mathbb{N}_0^\ell$ *such that* $\sum_{p=1}^{\ell} \overline{e}_{\mathbf{j}_p} \|\mathbf{w}_{[p]}\| \le \varepsilon - \delta$ *and* $c_{\mathbf{j}_p} \lesssim c_{\tilde{\mathbf{j}}_p}$ $(p = 1, \dots, \ell)$, *where* $\tilde{\mathbf{j}} \in \mathbb{N}_0^\ell$ *is the solution of*

$$\sum_{p=1}^{\ell} c_{\tilde{\mathbf{j}}_p} \#\operatorname{supp}\mathbf{w}_{[p]} \to \min!, \quad \sum_{p=1}^{\ell} \overline{e}_{\tilde{\mathbf{j}}_p} \|\mathbf{w}_{[p]}\| \le \varepsilon - \delta. \tag{5.15}$$

Compute

$$z := \mathbf{P}_{\mathbf{\Lambda}} \sum_{p=1}^{\ell} \mathbf{A}^{(\mathbf{j}_p)} \mathbf{w}_{[p]}.$$

Theorem 5.4.6. *For* $\mathbf{z} \coloneqq \textsc{apply}[\Lambda, \mathbf{w}, \varepsilon]$, *we have* $\|\mathbf{P}_\Lambda \mathbf{A}\mathbf{w} - \mathbf{z}\| \le \varepsilon$. *If for some* $s^* > 0$, *for any* $\bar{s} < s^*$, $\sup_{j\in\mathbb{N}} e_j c_j^{\bar{s}} < \infty$, *i.e., if* $\mathbf{A}$ *is* s^*-computable, *then for any* $s \in (0, s^*)$,

$$\#\operatorname{supp}\mathbf{z} \lesssim \varepsilon^{-1/s}\|\mathbf{w}\|_{\mathcal{A}^s_\infty}^{1/s}, \tag{5.16}$$

and the number of operations required by the call can be bounded by some absolute multiple of

$$1 + \#\operatorname{supp}\mathbf{w} + \varepsilon^{-1/s}\|\mathbf{w}\|_{\mathcal{A}^s_\infty}^{1/s}, \tag{5.17}$$

both estimates only dependent on s *when it tends to* 0 *or to* s^*, *and on* $\bar{e}_0$, *being an upper bound for* $\|\mathbf{A}\|$.

Before proving this theorem, we discuss how to determine valid values of $\mathbf{j}$ in the **apply** routine in two common situations. If for some constants C and D, $c_j = Cj$ and $\bar{e}_j = Dj^{-s^*}$, so that $\mathbf{A}$ is s^*-computable, then

$$\tilde{\mathbf{j}}_p = \left(\frac{\|\mathbf{w}_{[p]}\|}{\#\operatorname{supp}\mathbf{w}_{[p]}}\right)^{\frac{1}{s^*+1}} \left(\frac{\sum_{q=1}^{\ell}\|\mathbf{w}_{[q]}\|^{\frac{1}{s^*+1}}(\#\operatorname{supp}\mathbf{w}_{[q]})^{\frac{s^*}{1+s^*}}}{(\varepsilon-\delta)/D}\right)^{\frac{1}{s^*}}$$

is the solution of (5.15) when minimization is performed over $\mathbb{R}^\ell$. If for some constants C, D and $\varrho > 0$, $c_j = Cj$ and $\bar{e}_j = D2^{-\varrho j}$, so that $\mathbf{A}$ is even ∞-computable, then

$$\tilde{\mathbf{j}}_p = \log_2\left(\frac{\|\mathbf{w}_{[p]}\|\sum_{q=1}^{\ell}\#\operatorname{supp}\mathbf{w}_{[q]}}{\#\operatorname{supp}\mathbf{w}_{[p]}(\varepsilon-\delta)/D}\right)\Big/\varrho$$

is the solution of (5.15) when minimization is performed over $\mathbb{R}^\ell$. Assuming these $\tilde{\mathbf{j}}_p$ are non-negative, by rounding them up to the nearest value in $\mathbb{N}_0$ one obtains a valid $\mathbf{j}$.

Proof of Theorem 5.4.6. Let $s \in (0, s^*)$ and $s < \bar{s}_1 < \bar{s}_2 < s^*$. The first statement follows from $\|\mathbf{A}\|\|\mathbf{w} - \sum_{p=1}^{\ell}\mathbf{w}_{[p]}\| \le \delta$ and $\sum_{p=1}^{\ell}\|\mathbf{A} - \mathbf{A}^{(\mathbf{j}_p)}\|\|\mathbf{w}_{[p]}\| \le \varepsilon - \delta$.

By Proposition 5.4.4, the cost of a call $[(\mathbf{w}_{[p]})_p, \cdot\,] = \textsc{bucketsort}[\mathbf{w}, \varepsilon/(2\bar{e}_0)]$ is bounded by some absolute multiple of

$$\begin{aligned}
&\#\operatorname{supp}\mathbf{w} + \max(1, \lceil\log(\#\operatorname{supp}\mathbf{w}) + \log(\|\mathbf{w}\|_\infty/(\varepsilon/2\bar{e}_0))\rceil)\\
&\lesssim \#\operatorname{supp}\mathbf{w} + \max(1, \log(\varepsilon^{-1}\|\mathbf{w}\|))\\
&\lesssim \#\operatorname{supp}\mathbf{w} + 1 + \varepsilon^{-1/s}\|\mathbf{w}\|_{\mathcal{A}^s_\infty}^{1/s}.
\end{aligned}$$

With $\tau \coloneqq (\frac{1}{2} + s)^{-1} > 2$, it is known (see e.g. [DeV98]) that

$$\#\{\boldsymbol{\lambda} \in \boldsymbol{\nabla} : |\mathbf{w}_{\boldsymbol{\lambda}}| > \eta\} \lesssim \eta^{-\tau}\|\mathbf{w}\|_{\mathcal{A}^s_\infty}^{\tau} \quad (\eta > 0).$$

As a consequence, we have

$$\#\operatorname{supp}\mathbf{w}_{[p]} \lesssim 2^{p\tau/2}\|\mathbf{w}\|_\infty^{-\tau}\|\mathbf{w}\|_{\mathcal{A}^s_\infty}^{\tau}$$

and

$$\|\mathbf{w}_{[p]}\| \lesssim 2^{-p/2}\|\mathbf{w}\|_\infty\sqrt{\#\operatorname{supp}\mathbf{w}_{[p]}} \lesssim 2^{-ps\tau/2}\|\mathbf{w}\|_\infty^{1-\tau/2}\|\mathbf{w}\|_{\mathcal{A}^s_\infty}^{\tau/2}.$$

The proof will be completed once we have shown that there exists a $\mathbf{j} \in \mathbb{N}_0^\ell$ with $\sum_{p=1}^{\ell}\bar{e}_{\mathbf{j}_p}\|\mathbf{w}_{[p]}\| \le \varepsilon - \delta$ and $\sum_{p=1}^{\ell} c_{\mathbf{j}_p}\operatorname{supp}\mathbf{w}_{[p]} \lesssim \varepsilon^{-1/s}\|\mathbf{w}\|_{\mathcal{A}^s_\infty}^{1/s}$. For $\ell = 0$ there is nothing to prove, so we assume that $\ell > 0$.

By definition of ℓ, we have

$$\varepsilon/2 < \overline{e}_0\|\mathbf{w} - \sum_{p=1}^{\ell-1}\mathbf{w}_{[p]}\| = \overline{e}_0\sqrt{\sum_{p=\ell}^{\infty}\|\mathbf{w}_{[p]}\|^2} \lesssim \overline{e}_0 2^{-\ell s\tau/2}\|\mathbf{w}\|_\infty^{1-\tau/2}\|\mathbf{w}\|_{\mathcal{A}^s_\infty}^{\tau/2},$$

or

$$2^{\ell\tau/2}\|\mathbf{w}\|_\infty^{-\tau}\|\mathbf{w}\|_{\mathcal{A}^s_\infty}^{\tau} \lesssim \varepsilon^{-1/s}\|\mathbf{w}\|_{\mathcal{A}^s_\infty}^{1/s}. \tag{5.18}$$

Note that here we used the notation $\mathbf{w}_{[p]}$ also to denote the restriction of $\mathbf{w}$ to indices from buckets that actually were not generated in **BUCKETSORT**.

Let $J \geq \ell$ be the smallest integer such that $\sum_{p=1}^{\ell} 2^{-(J-p)\bar{s}_1\tau/2}\|\mathbf{w}_{[p]}\| \leq \varepsilon - \delta$. So when $J > \ell$, from $\bar{s}_1 > s$ we have

$$\begin{aligned}
\varepsilon/2 \leq \varepsilon - \delta &< \sum_{p=1}^{\ell} 2^{-(J-1-p)\bar{s}_1\tau/2}\|\mathbf{w}_{[p]}\| \\
&< \sum_{p=1}^{\ell} 2^{-(J-1-p)\bar{s}_1\tau/2}2^{-ps\tau/2}\|\mathbf{w}\|_\infty^{1-\tau/2}\|\mathbf{w}\|_{\mathcal{A}^s_\infty}^{\tau/2} \\
&\lesssim 2^{-(J-1-\ell)\bar{s}_1\tau/2}2^{-\ell s\tau/2}\|\mathbf{w}\|_\infty^{1-\tau/2}\|\mathbf{w}\|_{\mathcal{A}^s_\infty}^{\tau/2} \\
&\leq 2^{-(J-1)s\tau/2}\|\mathbf{w}\|_\infty^{1-\tau/2}\|\mathbf{w}\|_{\mathcal{A}^s_\infty}^{\tau/2}
\end{aligned}$$

or

$$2^{J\tau/2}\|\mathbf{w}\|_\infty^{-\tau}\|\mathbf{w}\|_{\mathcal{A}^s_\infty}^{\tau} \lesssim \varepsilon^{-1/s}\|\mathbf{w}\|_{\mathcal{A}^s_\infty}^{1/s}, \tag{5.19}$$

which by (5.18) is also valid when $J = \ell$.

Now select $\mathbf{j}_p$ to be the smallest integer such that $\overline{e}_{\mathbf{j}_p} \leq 2^{-(J-p)\bar{s}_1\tau/2}$. Then indeed $\sum_{p=1}^{\ell}\overline{e}_{\mathbf{j}_p}\|\mathbf{w}_{[p]}\| \leq \varepsilon - \delta$, and by $\overline{e}_{j-1}c_{j-1}^{\bar{s}_2} \lesssim 1$ and $c_j \lesssim c_{j-1}$, we have $c_{\mathbf{j}_p} \lesssim 2^{(J-p)(\bar{s}_1/\bar{s}_2)\tau/2}$. From (5.19) we conclude that

$$\begin{aligned}
\sum_{p=1}^{\ell} c_{\mathbf{j}_p}\operatorname{supp}\mathbf{w}_{[p]} &\lesssim \sum_{p=1}^{\ell} 2^{(J-p)(\bar{s}_1/\bar{s}_2)\tau/2}2^{p\tau/2}\|\mathbf{w}\|_\infty^{-\tau}\|\mathbf{w}\|_{\mathcal{A}^s_\infty}^{\tau} \\
&\lesssim 2^{(J-\ell)(\bar{s}_1/\bar{s}_2)\tau/2}2^{\ell\tau/2}\|\mathbf{w}\|_\infty^{-\tau}\|\mathbf{w}\|_{\mathcal{A}^s_\infty}^{\tau} \\
&\lesssim 2^{J\tau/2}\|\mathbf{w}\|_\infty^{-\tau}\|\mathbf{w}\|_{\mathcal{A}^s_\infty}^{\tau} \lesssim \varepsilon^{-1/s}\|\mathbf{w}\|_{\mathcal{A}^s_\infty}^{1/s}
\end{aligned}$$

which completes the proof. ◊

Next we present a realization of the routine **GALSOLVE**. Given $\mathbf{\Lambda} \subset \mathbf{\nabla}$, $\mathbf{g}_{\mathbf{\Lambda}}, \mathbf{w}_{\mathbf{\Lambda}}^{(0)} \in \ell_2(\mathbf{\Lambda})$, and $\delta \geq \varepsilon > 0$ with $\|\mathbf{g}_{\mathbf{\Lambda}} - \mathbf{A}_{\mathbf{\Lambda}}\mathbf{w}_{\mathbf{\Lambda}}^{(0)}\| \leq \delta$, it should produce a $\mathbf{w}_{\mathbf{\Lambda}} \in \ell_2(\mathbf{\Lambda})$ with $\|\mathbf{g}_{\mathbf{\Lambda}} - \mathbf{A}_{\mathbf{\Lambda}}\mathbf{w}_{\mathbf{\Lambda}}\| \leq \varepsilon$. **GALSOLVE** will only be called for $\mathbf{w}_{\mathbf{\Lambda}}^{(0)}$ being the previous iterand produced inside **SOLVE**, and for δ/ε being uniformly bounded, the latter meaning that only a fixed reduction of the initial error has to be achieved.

An obvious approach is to apply a fixed number of iterations of some iterative method. A problem, however, is that generally $\mathbf{A}_{\mathbf{\Lambda}}$ is not truly sparse, in the sense that its number of non-zero entries is not of the order of $\#\mathbf{\Lambda}$. The approach we follow is based on the observation that if for some constant $\mu < 1$, a fixed, sufficiently large j is chosen such that with $\mathbf{A}_{\mathbf{\Lambda}}^{(j)} := \mathbf{P}_{\mathbf{\Lambda}}\mathbf{A}^{(j)}\mathbf{I}_{\mathbf{\Lambda}}$, $\|\mathbf{I} - \mathbf{A}_{\mathbf{\Lambda}}(\mathbf{A}_{\mathbf{\Lambda}}^{(j)})^{-1}\| \leq \frac{\mu\varepsilon}{\delta}$, then $\|\mathbf{g}_{\mathbf{\Lambda}} - \mathbf{A}_{\mathbf{\Lambda}}[\mathbf{w}_{\mathbf{\Lambda}}^{(0)} + (\mathbf{A}_{\mathbf{\Lambda}}^{(j)})^{-1}(\mathbf{g}_{\mathbf{\Lambda}} - \mathbf{A}_{\mathbf{\Lambda}}\mathbf{w}_{\mathbf{\Lambda}}^{(0)})]\| \leq \mu\varepsilon$. Having chosen μ being

strictly less than one, room is left to approximate the application of $(\mathbf{A}_\Lambda^{(j)})^{-1}$ by an iterative method ($\mathbf{A}^{(j)}$ is sparse), and to replace the initial residual $\mathbf{g}_\Lambda - \mathbf{A}_\Lambda \mathbf{w}_\Lambda^{(0)}$ by an approximation. Concerning the latter, we approximate $\mathbf{A}_\Lambda \mathbf{w}_\Lambda^{(0)}$ by a call of APPLY. Its cost are controlled in terms of $\#\Lambda$ and $\|\mathbf{w}_\Lambda^{(0)}\|_{\mathcal{A}_\infty^s}$, the latter known to be bounded (cf. (5.14)).

The *defect correction* procedure outlined above is an alternative for the approximate application of Richardson's iteration to $\mathbf{A}_\Lambda \mathbf{w}_\Lambda = \mathbf{g}_\Lambda$ starting with $\mathbf{w}_\Lambda^{(0)}$ as proposed in [CDD01], where in *each* iteration the application of $\mathbf{A}_\Lambda$ is approximated by a call of APPLY. Since, due to the built-in adaptivity, calls of APPLY are quantitatively demanding, whereas furthermore within our defect correction method the iterative method can be chosen to be of optimal Krylov type, we expect the latter method to have better quantitative properties.

GALSOLVE$[\Lambda, \mathbf{g}_\Lambda, \mathbf{w}_\Lambda^{(0)}, \delta, \varepsilon] \to \mathbf{w}_\Lambda$:
% The input satisfies $\delta \geq \varepsilon > 0$, $\Lambda \subset \nabla$, $\mathbf{g}_\Lambda$, $\mathbf{w}_\Lambda^{(0)} \in \ell_2(\Lambda)$ *with* $\|\mathbf{g}_\Lambda - \mathbf{A}_\Lambda \mathbf{w}_\Lambda^{(0)}\| \leq \delta$.
% Let $(\overline{e}_j)_j$, $(c_j)_j$ *be defined as in the* APPLY *routine, and let* $\underline{e}_0^{-1}$ *be an upper*
% bound for $\|\mathbf{A}^{-1}\|$.

Compute the smallest $j \in \mathbb{N}_0$ *with* $\overline{e}_j(\underline{e}_0)^{-1} \leq \frac{\varepsilon}{3\varepsilon+3\delta}$
$\mathbf{r}_\Lambda^{(0)} := \mathbf{g}_\Lambda -$ APPLY$[\Lambda, \mathbf{w}_\Lambda^{(0)}, \frac{\varepsilon}{3}]$
With $\mathbf{A}_\Lambda^{(j)} := \mathbf{P}_\Lambda \mathbf{A}^{(j)} \mathbf{I}_\Lambda$, *approximate* $(\mathbf{A}_\Lambda^{(j)})^{-1}\mathbf{r}_\Lambda^{(0)}$ *using the Conjugate Residuals method starting with zero until the current iterand* $\mathbf{e}_\Lambda$ *satisfies* $\|\mathbf{r}_\Lambda^{(0)} - \mathbf{A}_\Lambda^{(j)}\mathbf{e}_\Lambda\| \leq \frac{\varepsilon}{3}$
$\mathbf{w}_\Lambda := \mathbf{w}_\Lambda^{(0)} + \mathbf{e}_\Lambda$

Theorem 5.4.7. $\mathbf{w}_\Lambda :=$ GALSOLVE$[\Lambda, \mathbf{g}_\Lambda, \mathbf{w}_\Lambda^{(0)}, \delta, \varepsilon]$ *satisfies* $\|\mathbf{g}_\Lambda - \mathbf{A}_\Lambda \mathbf{w}_\Lambda\| \leq \varepsilon$. *If for any* $\bar{s} < s^*$, $\sup_{j\in\mathbb{N}} \overline{e}_j c_j^{\bar{s}} < \infty$, *i.e., if* $\mathbf{A}$ *is* s^**-computable, then for any* $s < s^*$, *for some increasing function* η, *the number of operations required by the call can be bounded by some absolute multiple of*

$$\varepsilon^{-1/s}\|\mathbf{w}_\Lambda^{(0)}\|_{\mathcal{A}_\infty^s}^{1/s} + \eta(\delta/\varepsilon))\#\Lambda + 1, \tag{5.20}$$

only dependent on s *when it tends to* 0 *or to* s^*, *and on* $\overline{e}_0$ *and* $\underline{e}_0$.

Proof. The selection of j implies that $\|\mathbf{A}_\Lambda - \mathbf{A}_\Lambda^{(j)}\|\|\mathbf{A}^{-1}\| \leq \frac{\varepsilon}{3\varepsilon+3\delta}$. So writing $\langle \mathbf{A}_\Lambda^{(j)}\mathbf{v}_\Lambda, \mathbf{v}_\Lambda\rangle = \langle \mathbf{A}_\Lambda \mathbf{v}_\Lambda, \mathbf{v}_\Lambda\rangle - \langle (\mathbf{A}_\Lambda - \mathbf{A}_\Lambda^{(j)})\mathbf{v}_\Lambda, \mathbf{v}_\Lambda\rangle$, we find

$$(1 - \tfrac{\varepsilon}{3\varepsilon+3\delta})\|\mathbf{A}^{-1}\|^{-1}\|\mathbf{v}_\Lambda\|^2 \leq \langle \mathbf{A}_\Lambda^{(j)}\mathbf{v}_\Lambda, \mathbf{v}_\Lambda\rangle \leq \|\mathbf{A}\|\|\mathbf{v}_\Lambda\|^2 + \tfrac{\varepsilon}{3\varepsilon+3\delta}\|\mathbf{A}^{-1}\|^{-1}\|\mathbf{v}_\Lambda\|^2.$$

We infer that $\|\mathbf{A}_\Lambda - \mathbf{A}_\Lambda^{(j)}\|\|(\mathbf{A}_\Lambda^{(j)})^{-1}\| \leq \frac{\frac{\varepsilon}{3\varepsilon+3\delta}}{1-\frac{\varepsilon}{3\varepsilon+3\delta}} = \frac{\varepsilon}{2\varepsilon+3\delta}$, and by $\frac{\varepsilon}{3\varepsilon+3\delta} \leq \frac{1}{6}$, that $\kappa(\mathbf{A}_\Lambda^{(j)}) \leq \frac{1}{5} + \frac{6}{5}\kappa(\mathbf{A})$. Writing

$$\begin{aligned}\mathbf{g}_\Lambda - \mathbf{A}_\Lambda \mathbf{w}_\Lambda =& (\mathbf{g}_\Lambda - \mathbf{A}_\Lambda \mathbf{w}_\Lambda^{(0)} - \mathbf{r}_\Lambda^{(0)}) + (\mathbf{r}_\Lambda^{(0)} - \mathbf{A}_\Lambda^{(j)}\mathbf{e}_\Lambda) \\ &+ (\mathbf{I} - \mathbf{A}_\Lambda(\mathbf{A}_\Lambda^{(j)})^{-1})(\mathbf{r}_\Lambda^{(0)} + \mathbf{A}_\Lambda^{(j)}\mathbf{e}_\Lambda - \mathbf{r}_\Lambda^{(0)}),\end{aligned}$$

and using $\|\mathbf{r}_\Lambda^{(0)}\| \leq \delta + \frac{\varepsilon}{3}$, we find $\|\mathbf{g}_\Lambda - \mathbf{A}_\Lambda \mathbf{w}_\Lambda\| \leq \frac{\varepsilon}{3} + \frac{\varepsilon}{3} + \frac{\varepsilon}{2\varepsilon+3\delta}(\delta + \frac{\varepsilon}{3} + \frac{\varepsilon}{3}) \leq \varepsilon$.

By Theorem 5.4.6, for any $s \in (0, s^*)$ the number of operations needed for the call APPLY$[\Lambda, \mathbf{w}_\Lambda^{(0)}, \frac{\varepsilon}{3}]$ can be bounded by some absolute multiple of $1 + \#\Lambda + \varepsilon^{-1/s}\|\mathbf{w}_\Lambda^{(0)}\|_{\mathcal{A}_\infty^s}^{1/s}$, dependent on s when it tends to 0 or to s^*, and on $\overline{e}_0$. For each $\bar{s} < s^*$, the number of non-zero entries in each column of $\mathbf{A}_\Lambda^{(j)}$ as well

as the number of operations needed for their joint computation is bounded by a multiple of $((3+\frac{3\delta}{\varepsilon})/\underline{e}_0)^{1/\bar{s}}$. Each iteration of Conjugate Residuals therefore requires not more than a multiple of $(1+((3+\frac{3\delta}{\varepsilon})/\underline{e}_0)^{1/\bar{s}})\#\mathbf{\Lambda}$ operations. The number of iterations is bounded by the smallest $\ell\in\mathbb{N}$ for which $\frac{2c^\ell}{1+c^{2\ell}}\geq\frac{\varepsilon/3}{\delta+\varepsilon/3}$ where $c=\big(\sqrt{\kappa(\mathbf{A}_{\mathbf{\Lambda}}^{(j)})}-1\big)/\big(\sqrt{\kappa(\mathbf{A}_{\mathbf{\Lambda}}^{(j)})}+1\big)$ (see e.g. [Hac94]). Since $\frac{2c^\ell}{1+c^{2\ell}}\leq 2c^\ell$, this number is not larger than $\lceil\log(2(3\delta/\varepsilon+1)/\log(1/c)\rceil$. Using that $\log(1/c)^{-1}\lesssim\sqrt{\kappa(\mathbf{A})}\leq\sqrt{\bar{e}_0/\underline{e}_0}$, the proof is completed. ◊

Using that the tolerances for calls of **apply** and **rhs** inside **solve** are geometrically decreasing, that for $\mathbf{u}\in\mathcal{A}^s_\infty$ the iterands $\mathbf{w}_k$ in **solve** satisfy $\|\mathbf{w}_k\|_{\mathcal{A}^s_\infty}\lesssim\|\mathbf{u}\|_{\mathcal{A}^s_\infty}$ (cf. (5.14)), and finally that calls of **galsolve**$[\cdot,\cdot,\cdot,\delta,\varepsilon]$ are only made for $\delta/\varepsilon\lesssim 1$, using Theorem 5.4.6 and Theorem 5.4.7 we end up with the following result. Details can be verified by substituting the bounds from Theorem 5.4.6 and Theorem 5.4.7 into the corresponding proof from [GHS07].

Theorem 5.4.8. *If $\nu_{-1}\eqsim\|\mathbf{f}\|\gtrsim\varepsilon$, and for some $0<s<s^*$, $\mathbf{u}\in\mathcal{A}^s_\infty$ and $\mathbf{rhs}_s<\infty$ (cf. (5.6)), then the number of operations required by the call* **solve**$[\nu_{-1},\varepsilon]$ *is bounded by a multiple of*

$$\varepsilon^{-1/s}[\|\mathbf{u}\|^{1/s}_{\mathcal{A}^s_\infty}+\mathbf{rhs}_s^{1/s}], \tag{5.21}$$

only dependent on s when it tends to 0 or to s^*, on $\bar{e}_0$ and $\underline{e}_0$, and on the parameters α, ω, γ, θ when they approach the boundaries of their domains of definition.

Remark 5.4.9. The expression (5.21) is also an upper bound for the sum of the lengths of all vectors that were generated by the call **solve**$[\nu_{-1},\varepsilon]$.

5.5 Application to high dimensional elliptic PDEs

We are going to apply **solve** to systems $\mathbf{Au}=\mathbf{f}$ that result from the boundary value problems (5.1) written in the tensor product wavelet basis (5.3) with univariate wavelet bases $\Psi^{(z)}$ as in Section 5.3. With $\bar{e}_0$, $\underline{e}_0$ being available upper or lower bounds for $\max_z\lambda^{(1,z)}_{\max}$ or $\min_z\lambda^{(1,z)}_{\min}$ from (5.7), respectively, we have that $\|\mathbf{A}\|\leq\bar{e}_0$ and $\|\mathbf{A}^{-1}\|\leq\underline{e}_0^{-1}$ uniformly in n, $c_0\geq 0$ and $c_m>0$ $(1\leq m\leq n)$. With C_{sp} being some available upper bound for $\max_z\sup_j 2^{j/2}\|\vec{A}_z-\vec{A}_z^{(j)}\|$ (cf. Proposition 5.3.3), we know how to construct a matrix $\mathbf{A}^{(j)}$ having a multiple of jn non-zeros in each row and column with $\|\mathbf{A}-\mathbf{A}^{(j)}\|\leq C_{\mathrm{sp}}2^{-j/2}$ uniformly in n, $c_0\geq 0$ and $c_m>0$ $(1\leq m\leq n)$. So on the one hand, for any fixed n, $\mathbf{A}$ is ∞-computable, but on the other hand, the number of non-zeros in each row and column of $\mathbf{A}^{(j)}$ grows linearly with n.

Taking the latter into account within the preceding analysis, the expressions (5.16), (5.17) and (5.20) read as

$$\#\operatorname{supp}\mathbf{z}\lesssim n\varepsilon^{-1/s}\|\mathbf{w}\|^{1/s}_{\mathcal{A}^s_\infty}, \tag{5.22}$$

$$1+\#\operatorname{supp}\mathbf{w}+n\varepsilon^{-1/s}\|\mathbf{w}\|^{1/s}_{\mathcal{A}^s_\infty},$$

and

$$n\varepsilon^{-1/s}\|\mathbf{w}^{(0)}_{\mathbf{\Lambda}}\|^{1/s}_{\mathcal{A}^s_\infty}+\eta(\delta/\varepsilon)n\#\mathbf{\Lambda}+1,$$

respectively, only dependent on s when it tends to 0 or ∞. This leads to the following version of Theorem 5.4.5 and Theorem 5.4.8 when specialized to these systems resulting from high dimensional elliptic equations.

Theorem 5.5.1. *For any $\varepsilon, \nu_{-1} > 0$, $\mathbf{w} \coloneqq \textsc{solve}[\nu_{-1}, \varepsilon]$ terminates with $\|\mathbf{f} - \mathbf{A}\mathbf{w}\| \le \varepsilon$, so that $|||u - \sum_{\boldsymbol{\lambda}\in\boldsymbol{\nabla}} \mathbf{w}_{\boldsymbol{\lambda}}\psi_{\boldsymbol{\lambda}}||| = |||\mathbf{u} - \mathbf{w}||| \le \underline{c}_0^{-\frac{1}{2}}\varepsilon$. If, for some $s > 0$, $\mathbf{u} \in \mathcal{A}^s_\infty$, then*

$$\operatorname{supp}\mathbf{w} \lesssim \varepsilon^{-1/s}\|\mathbf{u}\|^{1/s}_{\mathcal{A}^s_\infty}.$$

If $\nu_{-1} \eqsim \|\mathbf{f}\| \gtrsim \varepsilon$, and $\mathbf{rhs}_s < \infty$ (cf. (5.6)), then the number of operations required by the call is bounded by a multiple of

$$\varepsilon^{-1/s}[n\|\mathbf{u}\|^{1/s}_{\mathcal{A}^s_\infty} + \mathbf{rhs}_s^{1/s}], \tag{5.23}$$

everything uniformly in n, $c_0 \ge 0$, and $c_m > 0$ $(1 \le m \le n)$, and only dependent on s when it tends to 0 or to ∞, and on the parameters $\alpha, \omega, \gamma, \theta$ when they approach the boundaries of their domains of definition.

What is left is the discussion of *a valid routine* **rhs**. As a consequence of Theorem 5.4.6, for any $s > 0$, $\mathbf{A}\colon \mathcal{A}^s_\infty \to \mathcal{A}^s_\infty$ is bounded with $\|\mathbf{A}\mathbf{v}\|_{\mathcal{A}^s_\infty} \lesssim n\|\mathbf{v}\|_{\mathcal{A}^s_\infty}$. Indeed, for $\mathbf{v} \in \mathcal{A}^s_\infty$ and $\varepsilon > 0$, let $N \in \mathbb{N}$ be such that $\|\mathbf{v} - \mathbf{v}_N\| \le \varepsilon/(2\|\mathbf{A}\|)$. Put $\mathbf{z} \coloneqq \textsc{apply}[\boldsymbol{\nabla}, \mathbf{v}_N, \varepsilon/2]$. Then $\#\operatorname{supp}\mathbf{z} \lesssim n(\varepsilon/2)^{-1/s}\|\mathbf{v}_N\|^{1/s}_{\mathcal{A}^s_\infty}$ (here we applied (5.22) replacing (5.16)). Now the statement follows from $\|\mathbf{v}_N\|_{\mathcal{A}^s_\infty} \le \|\mathbf{v}\|_{\mathcal{A}^s_\infty}$, $\|\mathbf{A}\mathbf{v} - \mathbf{z}\| \le \|\mathbf{A}\|\|\mathbf{v} - \mathbf{v}_N\| + \|\mathbf{A}\mathbf{v}_N - \mathbf{z}\| \le \varepsilon$ and the definition of $\mathcal{A}^s_\infty$.

As a consequence, if the right hand side vector $\mathbf{f}$ is such that we can realize its (quasi) best N-term approximations in $\mathcal{O}(N)$ operations, uniformly in n, then assuming $\mathbf{u} \in \mathcal{A}^s_\infty$, the resulting routine **rhs** satisfies $\mathbf{rhs}_s \lesssim n\|\mathbf{u}\|_{\mathcal{A}^s_\infty}$. In this situation, the upper bound (5.23) for the cost of **solve** is never dominated by the term $\varepsilon^{-1/s}\mathbf{rhs}_s^{1/s}$. Unfortunately, even for a family over n of smooth right hand sides f, it seems hard to guarantee these conditions uniformly in n. On the other hand, the estimate $\|\mathbf{f}\|_{\mathcal{A}^s_\infty} \le \|\mathbf{A}\|_{\mathcal{A}^s_\infty \to \mathcal{A}^s_\infty}\|\mathbf{u}\|_{\mathcal{A}^s_\infty}$ might be very crude, so that quasi-optimal approximations, uniformly in n, are actually not needed to arrive at $\mathbf{rhs}_s \lesssim n\|\mathbf{u}\|_{\mathcal{A}^s_\infty}$.

In the following, we will focus on the situation that for some $\bar{s} > s$, $\mathbf{rhs}_{\bar{s}} < \infty$, however generally dependent on n and on $c_0 \ge 0$ and $c_m > 0$ $(1 \le m \le n)$. In this situation, the bound (5.23) may be read as $\varepsilon^{-1/s}n\|\mathbf{u}\|^{1/s}_{\mathcal{A}^s_\infty} + \varepsilon^{-1/\bar{s}}\mathbf{rhs}_{\bar{s}}^{1/\bar{s}}$, meaning that in any case for any *fixed* n and c_m $(0 \le m \le n)$, the cost of approximating the right hand side is *asymptotically* negligible, i.e., when ε tends to zero.

Let us start with assuming that *all* univariate wavelets $\psi^{(z)}_\lambda$ on positive levels have d vanishing moments (cf. Remark 5.3.2), for the moment ignoring that this is not true for wavelets whose supports have non-empty intersection with a Dirichlet boundary. Then from $|\int_0^1 v\psi^{(z)}_\lambda| = \inf_{p\in P_{d-1}}|\int_0^1 (v-p)\psi^{(z)}_\lambda| \lesssim 2^{-(d+\frac{1}{2})|\lambda|}|v|_{W^d_\infty(0,1)}$, a tensor product argument, and taking into account the normalization of the product wavelets, for smooth f we infer that

$$\big|f(\psi_{\boldsymbol{\lambda}})\big| = \Big|\int_{(0,1)^n} f\psi_{\boldsymbol{\lambda}}\Big| \lesssim \frac{2^{-(\frac{1}{2}+d)|||\boldsymbol{\lambda}|||_1}}{\sqrt{c_0 + \sum_{m=1}^n c_m 4^{|\lambda_m|}}} \lesssim 2^{-((\frac{1}{2}+d)|||\boldsymbol{\lambda}|||_1 + |||\boldsymbol{\lambda}|||_\infty)}. \tag{5.24}$$

In view of this estimate, it is natural to consider approximations to $\mathbf{f}$ by, for some parameter ℓ, dropping all entries $f(\psi_{\boldsymbol{\lambda}})$ with indices $\boldsymbol{\lambda}$ outside

$$\boldsymbol{\nabla}^{(\mathrm{optsp})}_\ell \coloneqq \{\boldsymbol{\lambda} \in \boldsymbol{\nabla}\colon (\tfrac{1}{2}+d)|||\boldsymbol{\lambda}|||_1 + |||\boldsymbol{\lambda}|||_\infty \le (\tfrac{1}{2}+d+\tfrac{1}{n})\ell\}. \tag{5.25}$$

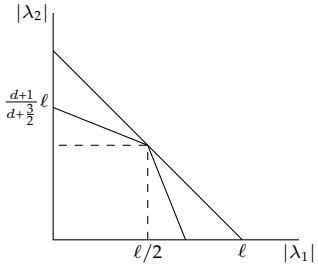

Figure 5.3: Standard and optimized sparse grid space in two space dimensions for the approximation of the right-hand side.

Using that $\#\{\lambda \in \boldsymbol{\nabla}_z : |\lambda| \le k\} \eqsim 2^k$ (Remark 5.3.1), one may verify[2] that $\#\boldsymbol{\nabla}_\ell^{(\mathrm{optsp})} \eqsim 2^\ell$ with a constant factor that depends on n though. The error in this approximation can therefore be bounded by a multiple of $\big(\sum_{k>\ell} 2^k 4^{-(\frac{1}{2}+d+\frac{1}{n})k}\big)^{\frac{1}{2}} \eqsim 2^{-(d+\frac{1}{n})\ell}$. So with an approximation having support length N, the error is not larger than $CN^{-(d+\frac{1}{n})}$, for some constant C that may depend on n though (and on the coefficients c_m and f).

Remark 5.5.2. Following [GK00], we call $\mathrm{span}\{\boldsymbol{\psi}_{\boldsymbol{\lambda}} : \boldsymbol{\lambda} \in \boldsymbol{\nabla}_\ell^{(\mathrm{optsp})}\}$ an *optimized sparse grid* space. With the standard sparse grid space $\mathrm{span}\{\boldsymbol{\psi}_{\boldsymbol{\lambda}} : \boldsymbol{\lambda} \in \boldsymbol{\nabla},\ \||\boldsymbol{\lambda}|\|_1 \le \ell\}$, one would need $N(\log N)^{n-1}$ unknowns to guarantee an error $\mathcal{O}(N^{-(d+\frac{1}{n})})$, or equivalently, with N unknowns the error is $\mathcal{O}(N^{-(d+\frac{1}{n})}(\log N)^{(n-1)(d+\frac{1}{n})})$. See Figure 5.3 for an illustration.

Remark 5.5.3. Using $\|\mathbf{f}-\mathbf{g}\| \eqsim \|f - \sum_{\boldsymbol{\lambda}\in\boldsymbol{\nabla}} \mathbf{g}_{\boldsymbol{\lambda}}\boldsymbol{\psi}_{\boldsymbol{\lambda}}\|_{H^{-1}(0,1)^n}$, one might have expected that with a $\mathbf{g}$ of length N an error $N^{-(d+1)}$ should be realizable. Above analysis shows, however, that generally the rate $d+\frac{1}{n}$ cannot be improved, and more generally, that when errors are measured in negative norms a mild deterioration of the rate as n increases cannot be avoided. Yet, in view of our aim to approximate the right hand side with a rate better than that for the solution, note that for any n, $d+\frac{1}{n}$ is safely larger than the generally best possible rate $d-1$ for approximating u.

The fact that for $z \neq \varnothing$, on all levels there are univariate wavelets having no vanishing moments is a price that has to be paid for the use of orthonormal wavelets. Indeed, considering biorthogonal wavelets, one could select dual spaces that do not incorporate Dirichlet boundary conditions, so that all primal wavelets on positive levels have vanishing moments.

For $\lambda \in \nabla$, let $d(\lambda)$ denote the number of vanishing moments of $\psi_\lambda^{(z)}$, now being either d or 0. Then $|\int_0^1 v\psi_\lambda^{(z)}| \lesssim 2^{-(d(\lambda)+\frac{1}{2})|\lambda|}|v|_{W_\infty^{d(\lambda)}(0,1)}$, and instead of (5.24), we obtain

$$|f(\boldsymbol{\psi}_{\boldsymbol{\lambda}})| = \Big|\int_{(0,1)^n} f\boldsymbol{\psi}_{\boldsymbol{\lambda}}\Big| \lesssim 2^{-[\||\boldsymbol{\lambda}|\|_\infty + \sum_{m=1}^n (d(\lambda_m)+\frac{1}{2})|\lambda_m|]}.$$

[2]Indeed, this follows from Proposition 3.3.4 in Chapter 3 with $\gamma = -\frac{1}{\frac{1}{2}+d}$.

In view of this estimate, we construct approximations to $\mathbf{f}$ by dropping all entries $\mathbf{f}(\psi_{\boldsymbol{\lambda}})$ with $\||\boldsymbol{\lambda}|\|_\infty + \sum_{m=1}^n (\frac{1}{2} + d(\lambda_m))|\lambda_m| > (\frac{1}{2} + d + \frac{1}{n})\ell$ for some parameter ℓ. Using that for any $c > 0$,

$$\#\{\lambda \in \nabla\colon |\lambda| \le k \text{ and } d(\lambda) = d, \text{ or } |\lambda| \le ck \text{ and } d(\lambda) = 0\} \eqsim 2^k + c(k+1) \eqsim 2^k,$$

dependent on c but uniform in k, we obtain that

$$\#\{\boldsymbol{\lambda} \in \boldsymbol{\nabla}\colon \||\boldsymbol{\lambda}|\|_\infty + \sum_{m=1}^n (\tfrac{1}{2} + d(\lambda_m))|\lambda_m| \le (\tfrac{1}{2} + d + \tfrac{1}{n})k\} \eqsim 2^k.$$

As above, we conclude that with an approximation having support length N, the error is $\mathcal{O}(N^{-(d+\frac{1}{n})})$, for some constant C that may depend on n though (and on the coefficients c_m and f).

In general, entries $f(\psi_{\boldsymbol{\lambda}})$ have to be approximated by the application of a suitable *quadrature rule*. For simplicity, here we discuss this issue only in the situation that $z = \varnothing$ so that (5.24) is valid for all wavelets. In [SS08], we studied quadrature rules for approximating the entries of the stiffness matrix for high dimensional PDEs having non-constant but smooth coefficients. From the analysis there, we deduce that, for sufficiently smooth f, the application of a product composite quadrature rule taking N function evaluations yields an approximation $\widetilde{f(\psi_{\boldsymbol{\lambda}})}$ with

$$|f(\psi_{\boldsymbol{\lambda}}) - \widetilde{f(\psi_{\boldsymbol{\lambda}})}| \lesssim N^{-\alpha} 2^{-((\frac{1}{2}+d)\||\boldsymbol{\lambda}|\|_1 + \||\boldsymbol{\lambda}|\|_\infty)},$$

where α is proportional to the *order* of the one-dimensional composite rule, and inversely proportional to n. This dependence of α on n can be (nearly) removed by applying sparse product rules. This gives the advantage that the order of the rule can be chosen to be (nearly) independent of n, and with that so are the smoothness requirements on f.

Let us now select $\alpha > d + \frac{1}{n}$ and a parameter $\sigma \in (d + \frac{1}{n}, \alpha)$. Then given $\boldsymbol{\nabla}_\ell^{(\mathrm{optsp})}$, for approximating $f(\psi_{\boldsymbol{\lambda}})$ we take the rule with $N = N_{\boldsymbol{\lambda}} \eqsim 2^{(\ell-k)\frac{\sigma}{\alpha}}$ when $\boldsymbol{\lambda} \in \boldsymbol{\nabla}_k^{(\mathrm{optsp})} \setminus \boldsymbol{\nabla}_{k-1}^{(\mathrm{optsp})}$ ($\boldsymbol{\nabla}_{-1}^{(\mathrm{optsp})} := \varnothing$). Assuming each evaluation of f to take $\mathcal{O}(1)$ operations, the total work for approximating $[f(\psi_{\boldsymbol{\lambda}})]_{\boldsymbol{\lambda} \in \boldsymbol{\nabla}_\ell^{(\mathrm{optsp})}}$ is then bounded by some multiple of $\sum_{k=0}^\ell 2^k 2^{(\ell-k)\frac{\sigma}{\alpha}} \eqsim 2^\ell$, whereas the $\ell_2(\boldsymbol{\nabla})$-norm of the quadrature error can be bounded by some multiple of $\sqrt{\sum_{k=0}^\ell 2^k 4^{(k-\ell)\sigma} 4^{-(\frac{1}{2}+d+\frac{1}{n})k}} \eqsim 2^{-(d+\frac{1}{n})\ell}$. We conclude that for sufficiently smooth f, $\mathbf{rhs}_{d+\frac{1}{n}} < \infty$ (generally depending on n, the coefficients c_m and on f).

5.6 Implementation and numerical results

For some general, fixed symmetric positive definite bi-infinite matrix $\mathbf{A}$, our considerations in Section 5.4 concerning the operation count of **SOLVE** apply under the assumption that any entry of any vector that is generated inside this routine can be stored in or fetched from memory in $\mathcal{O}(1)$ operations. This assumption is valid in the unrealistic situation that we have an unlimited amount of memory at our disposal, where each location can be accessed in $\mathcal{O}(1)$ operations. Indeed, in that case, using some ordering on the index set $\boldsymbol{\nabla}$ to store any vector

from $\ell_2(\boldsymbol{\nabla})$ as an infinite array, we have direct access to each of its entries. If, instead of assuming an infinite memory, we restrict ourselves to wavelet indices up to a certain high level, and allocate arrays for corresponding vectors, then we see that adaptivity does not result in a reduction of memory requirements compared to non-adaptive schemes.

Therefore, let us consider the storage of any finitely supported $\mathbf{v} \in \ell_2(\boldsymbol{\nabla})$ as a *linked list* of its non-zero entries ordered by their indices, which requires an amount of memory that is proportional to its support length. Here we make the assumption that the amount of memory needed to store any index $\boldsymbol{\lambda} \in \boldsymbol{\nabla}$ that is encountered is fixed. Then in view of Remark 5.4.9, the total *amount of memory* needed for a call $\textsc{solve}[\cdot\,,\varepsilon]$ is bounded by an absolute multiple of

$$\varepsilon^{-1/s}\big[\|\mathbf{u}\|_{\mathcal{A}^s_\infty}^{1/s} + \mathbf{rhs}_s^{1/s}\big].$$

With this data structure, the addition of two vectors requires a number of operations that is proportional to the *sum* of their lengths. This has an unfortunate consequence for the cost of a call $\textsc{apply}[\boldsymbol{\nabla},\mathbf{w},\varepsilon]$. In this routine the sum is computed of a number of vectors, each of them being an approximate column of $\mathbf{A}$ multiplied by the corresponding coefficient from the input vector (from which very small coefficients were removed beforehand). The number of vectors K and the sum of their lengths L, and with that the maximal possible length of the output vector, are all bounded by some absolute multiple of $\varepsilon^{-1/s}\|\mathbf{w}\|_{\mathcal{A}^s_\infty}^{1/s}$. If one would add the second until the K-th vector to the first one, then one could end up with a complexity that is quadratic in L. Instead, if one adds pairwise vectors 1 and 2, 3 and 4, etc., and proceeds similarly with the set of $\lceil K/2\rceil$ resulting vectors, until finally one vector is left being thus the output vector, the total complexity is $(\log K)L$. Indeed, the cost of each step of summing all pairs of current vectors is proportional to the total sum of their lengths, which is never larger than L, whereas the number of these steps is $\lceil \log_2 K\rceil$. Realizing that the indices in the output vector are ordered, one infers that such a log-factor cannot be avoided. By substituting the bounds for K and L, we conclude that with the storage of a vector as a linked list, the cost of this call of $\textsc{apply}$ is bounded by a multiple of $1 + \#\operatorname{supp}\mathbf{w} + \log(\varepsilon^{-1/s}\|\mathbf{w}\|_{\mathcal{A}^s_\infty}^{1/s})\varepsilon^{-1/s}\|\mathbf{w}\|_{\mathcal{A}^s_\infty}^{1/s}$. With that we find that the *number of operations* needed for a call $\textsc{solve}[\cdot\,,\varepsilon]$ is bounded by a constant multiple of

$$\log\big(\varepsilon^{-1/s}\|\mathbf{u}\|_{\mathcal{A}^s_\infty}^{1/s}\big)\varepsilon^{-1/s}\|\mathbf{u}\|_{\mathcal{A}^s_\infty}^{1/s} + \varepsilon^{-1/s}\mathbf{rhs}_s^{1/s},$$

so that we end up with suboptimal computational complexity. So far this phenomenon seems to have been ignored in the literature on adaptive wavelet methods.

Specializing the discussion to the solution of elliptic boundary value problems in high space dimensions using tensor product wavelet bases, we have to take into account that an index is an n-tuple. In view of the bound (5.23), the storage requirements are therefore of the order

$$n\varepsilon^{-1/s}\big[n\|\mathbf{u}\|_{\mathcal{A}^s_\infty}^{1/s} + \mathbf{rhs}_s^{1/s}\big].$$

Since comparing two indices now requires $\mathcal{O}(n)$ operations, the cost of the addition of two vectors stored as ordered linked lists is now proportional to n times

the sum of their lengths. We end up with a total computational complexity of the order

$$n\big[\log\big(n\varepsilon^{-1/s}\|\mathbf{u}\|_{\mathcal{A}^s_\infty}^{1/s}\big)n\varepsilon^{-1/s}\|\mathbf{u}\|_{\mathcal{A}^s_\infty}^{1/s}+\varepsilon^{-1/s}\mathbf{rhs}_s^{1/s}\big].$$

In our actual implementation, we have not used linked lists but *hash tables* to store the vectors. We chose this mainly because of the convenience of programming, but also since we expect that *usually* it results in faster code. Clearly, given any hash function $\boldsymbol{\nabla}\to\{1,\dots,M\}$, with M being the size of the hash table, one can always construct $\boldsymbol{\Lambda}\subset\boldsymbol{\nabla}$ whose elements are all mapped onto a single entry in the hash table (collision), in which case the hash-based implementation will be very slow. In our tests, the cost of storing vectors was proportional to their length.

For our *numerical tests*, we considered the Laplace operator, i.e., $c_0=0$ and $c_1=\ldots=c_n=1$. We took $\Gamma_D=\overline{\partial\Omega\cap\mathbb{R}^n_{>0}}$, i.e, homogeneous Dirichlet boundary conditions at the right boundary point in each coordinate direction ($z_m\equiv z=\{1\}$). We used the univariate $L_2(0,1)$-orthonormal continuous piecewise linear (multi-) wavelets discussed in Section 5.2 as building block for the tensor product wavelet basis for $H^1_{0,\Gamma_D}(0,1)^n$. Numerically, we estimated the extremal eigenvalues $\lambda^{(1,z)}_{\min}\approx 0.19$ and $\lambda^{(1,z)}_{\max}\approx 2.8$ of the one-dimensional Laplace operator in wavelet coordinates $\vec{A}_z$, being also lower or upper bounds for the extremal eigenvalues of the n-dimensional Laplace operator in tensor product wavelet coordinates $\mathbf{A}$ (see (5.8)). These bounds are used in the routines **apply** and **galsolve**.

Sparse approximations to $\mathbf{A}$ are constructed from sparse approximations to $\vec{A}$. In Section 5.3, we considered $\vec{A}^{(j)}_z$ by dropping all entries $(\vec{A}_z)_{\lambda,\mu}$ with $||\lambda|-|\mu||>j$. It turns out that this $\vec{A}^{(j)}_z$ contains entries that are much smaller in modulus than some of those that were dropped. Therefore, in order to improve quantitative properties of the algorithm, in our experiments we used approximations to $\vec{A}$ by dropping all entries with modulus below some given tolerance. For the resulting approximation with a maximal number of j nonzero entries per row and column, which we again denote as $\vec{A}^{(j)}_z$, we found numerically that $\|\vec{A}_z-\vec{A}^{(j)}_z\|\lessapprox 0.45\times 2^{-0.05\times j}$. Using notations as in the proof of Theorem 5.3.5, with $\vec{B}^{(j)}_z:=\vec{D}_z^{1/2}\vec{A}^{(j)}_z\vec{D}_z^{1/2}$, the maximal number of non-zeros per row and column of $\mathbf{A}^{(j)}:=\mathbf{D}^{\frac12}(\vec{B}^{(j)}_z\otimes I\otimes\cdots\otimes I+\cdots+I\otimes\cdots\otimes I\otimes\vec{B}^{(j)}_z)\mathbf{D}^{\frac12}$ is nj (or actually $n(j-1)+1$), where $\|\mathbf{A}-\mathbf{A}^{(j)}\|\lessapprox 0.45\times 2^{-0.05\times j}$. This estimate was used to perform the optimization in the **apply** routine as discussed following Theorem 5.4.6. The use of these modified sparse approximations reduced the cost of a call of **solve** by approximately 30%.

Additionally, we applied an extra dropping in the spirit of Remark 5.3.6. When $\vec{A}^{(j)}_z$ was constructed by dropping all elements in $\vec{A}_z$ with modulus less than ε, we dropped all elements from the resulting $\mathbf{A}^{(j)}$ with modulus less than ε. We observed that this additional dropping hardly influences the accuracies of the approximate matrix vector multiplications, whereas, for $n>1$, the cost of calls of **solve** was reduced by approximately a factor 2.

For our convenience, we took as right hand side $f=1$. In this case, the solution u is the restriction to $(0,1)^n$ of $\tilde{u}$ solving $-\boldsymbol{\Delta}\tilde{u}=1$ on $\tilde{\Omega}=(0,2)^n$, $\tilde{u}=0$ on $\partial\tilde{\Omega}$. For any $\ell\in\mathbb{N}_0$, there exists one $\lambda\in\nabla_z$ with $|\lambda|=\ell$ and

$\int_0^1 \psi_\lambda^{(z)} \neq 0$, and so for any $\boldsymbol{\ell} \in \mathbb{N}_0^n$, there exists one $\boldsymbol{\lambda} \in \boldsymbol{\nabla}$ with $|\boldsymbol{\lambda}| = \boldsymbol{\ell}$ and $\mathbf{f}_{\boldsymbol{\lambda}} = \int_{(0,1)^n} \boldsymbol{\psi}_{\boldsymbol{\lambda}} \neq 0$. Based on the estimate $|\mathbf{f}_{\boldsymbol{\lambda}}| \lesssim 2^{-(\|\|\boldsymbol{\lambda}\|\|_\infty + \frac{1}{2}\|\|\boldsymbol{\lambda}\|\|_1)}$, we considered optimized sparse grid approximations $[\mathbf{f}_{\boldsymbol{\lambda}}]_{\boldsymbol{\lambda} \in \boldsymbol{\nabla}_\ell^{(\mathrm{optsp})}}$ with $\boldsymbol{\nabla}_\ell^{(\mathrm{optsp})}$ from (5.25) with $d = 0$. We simply estimated the error in this approximation by the $\ell_2(\boldsymbol{\nabla})$-norm of $[\mathbf{f}_{\boldsymbol{\lambda}}]_{\boldsymbol{\lambda} \in \boldsymbol{\nabla}_{\ell+1}^{(\mathrm{optsp})} \setminus \boldsymbol{\nabla}_\ell^{(\mathrm{optsp})}}$, and took the smallest ℓ for which this norm is less than the given tolerance. Using that $\mathbf{f}$ is exceptionally sparse, one easily verifies that $\mathbf{rhs}_s < \infty$ for any s (dependent on n though).

Concerning the parameters in **solve**, some testing indicated that the best results are obtained with approximately $\alpha = 0.6$ $\omega = 0.4$, $\gamma = 0.2$, $\theta = 2\omega/(1+\omega)$ Not very surprisingly (cf. Remark 5.4.3), these values are actually outside the ranges for which the algorithm was proven to be optimal. For 'admissible' parameter values, however, we obtained similar approximate solutions at higher cost though.

Numerical results obtained with **solve** are given in Figure 5.4.

For any n, we know that $\mathbf{u} \in \mathcal{A}_\infty^1$ (see Section 5.1). As shown by Theorem 5.5.1, as a consequence, the approximations $\widetilde{\mathbf{u}_N}$ produced by **solve** also convergence with asymptotic rate 1. With $\tilde{\mathbf{f}} - \tilde{\mathbf{A}}\widetilde{\mathbf{u}_N}$ denoting the approximate residual of $\widetilde{\mathbf{u}_N}$ computed inside **solve** with small relative error, moreover we have the estimates $\sup_N N\|\tilde{\mathbf{f}} - \tilde{\mathbf{A}}\widetilde{\mathbf{u}_N}\| \eqsim \sup_N N\|\mathbf{u} - \widetilde{\mathbf{u}_N}\| \eqsim \sup_N N\|\mathbf{u} - \mathbf{u}_N\| \eqsim \sup_N N \inf_{\mathbf{v} \in \ell_2(\boldsymbol{\nabla})} \|\|u - \sum_{\boldsymbol{\lambda} \in \boldsymbol{\nabla}} \mathbf{v}_{\boldsymbol{\lambda}} \boldsymbol{\psi}_{\boldsymbol{\lambda}}\|\|$ ($\eqsim \|\mathbf{u}\|_{\mathcal{A}_\infty^1}$) with constant(s) that are *independent of* n. In view of Figure 5.4, we conclude that for this family of solutions with right hand sides $f = 1$, apparently $\|\mathbf{u}\|_{\mathcal{A}_\infty^1}/\|\mathbf{u}\|$ is increasing as function of n, so that, as a consequence, the larger n is, the later the asymptotic rate shows up. Better results as function of n will be obtained with coordinate directions with two Neumann boundaries, since for $f = 1$, the solution in those directions will be constant. For one Dirichlet and one Neumann boundary condition in each coordinate direction as we considered, for $n \geq 2$ the rate with (optimized) sparse grid approximation will be $\frac{1}{2} + \frac{1}{n}$ (see Section 5.1).

Finally, in Figure 5.5, for $n \in \{1, 2, \ldots, 10\}$, we show the support size of the approximate residual computed inside **solve** divided by n times the support size of the corresponding approximate solution. As predicted by Theorem 5.4.8, this quotient is bounded uniformly in n. The fact that it behaves like a constant shows that the cost of a call of **solve** that produces an approximate solution of length N, being up to a constant multiple as good as a best N-term approximation, is proportional to n times N.

Remark 5.6.1. Our solution method did not make of use of the symmetry in the right hand function $f = 1$ and thus in the solution. It also did not use the fact that this f is a separable function so that its representation is a rank 1 tensor. In this sense we expect that the results we obtained are representative for general moderately smooth f that do not vanish at the Dirichlet boundary. Methods that do exploit the property of the right hand side vector being a low rank tensor search an approximate solution in data sparse, low rank format, see [Gra04, GHK05]. It would be interesting to see whether such methods can be combined with adaptivity.

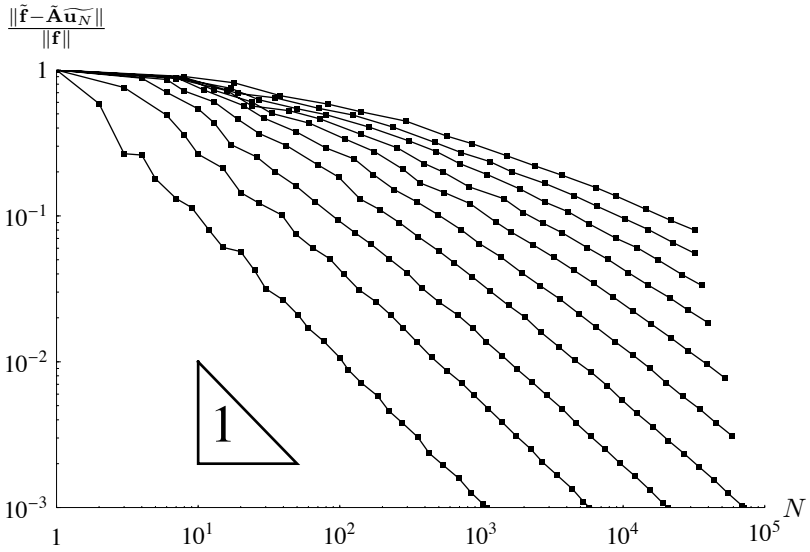

Figure 5.4: $\frac{\|\tilde{\mathbf{f}}-\tilde{\mathbf{A}}\widetilde{\mathbf{u}_N}\|}{\|\mathbf{f}\|}$ for $n \in \{1, 2, \ldots, 10\}$, where $\tilde{\mathbf{f}} - \tilde{\mathbf{A}}\widetilde{\mathbf{u}_N}$ denotes an approximate residual, with a small relative error, of the approximate solution $\widetilde{\mathbf{u}_N}$ produced by **SOLVE** with support length N

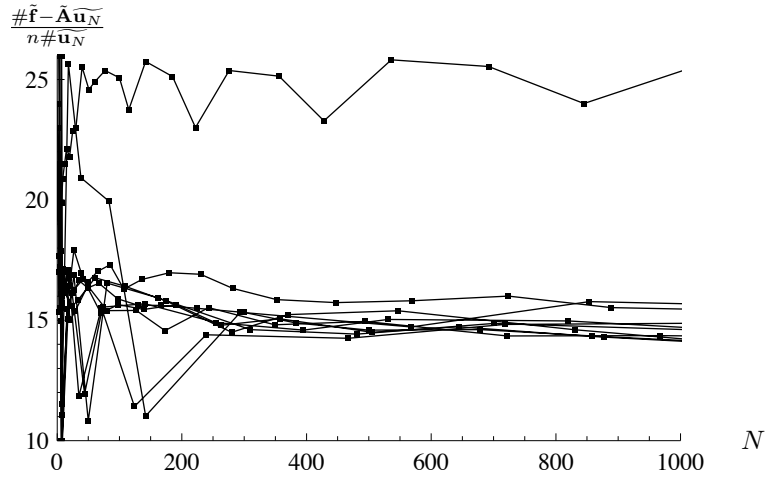

Figure 5.5: Support size of the approximate residual computed inside **SOLVE** divided by n times the support size of the corresponding approximate solution for $n \in \{1, 2, \ldots, 10\}$. The line on top corresponds to $n = 1$.

Chapter 6
A sparse Laplacian in tensor product wavelet coordinates

We construct a wavelet basis on the unit interval with respect to which *both* the (infinite) mass and stiffness matrix corresponding to the one-dimensional Laplacian are (truly) sparse and boundedly invertible. As a consequence, the (infinite) stiffness matrix corresponding to the Laplacian on the n-dimensional unit box with respect to the n-fold tensor product wavelet basis is also sparse and boundedly invertible. This greatly simplifies the implementation and improves the quantitative properties of an adaptive wavelet scheme to solve the multi-dimensional Poisson equation. The results extend to any second order partial differential operator with constant coefficients that defines a boundedly invertible operator.

6.1 Introduction

Let us denote $\mathrm{I} := (0,1)$ and $\square := \mathrm{I}^n$. In Chapter 5, we developed an adaptive tensor product wavelet method that for given $f \in H^{-1}(\square)$ solves the problem of finding $u \in H_0^1(\square)$ such that

$$a(u,v) := \int_{\square} c_0 uv + \sum_{m=1}^{n} c_m \partial_m u \partial_m v = f(v) \qquad (v \in H_0^1(\square)), \tag{6.1}$$

where $c_0 \geq 0$ and $c_m > 0$ $(m = 1, \ldots, n)$ are constants. Actually, there we allowed homogeneous Dirichlet boundary conditions on only part of the boundary, but, as we will see, in this chapter we need them on the whole of the boundary. General, possibly non-symmetric second order partial differential operators with constant coefficients will be considered at the end of Section 6.3.

Using that

$$H_0^1(\square) = H_0^1(\mathrm{I}) \otimes L_2(\mathrm{I}) \otimes \cdots \otimes L_2(\mathrm{I}) \;\cap\; \ldots \;\cap\; L_2(\mathrm{I}) \otimes \cdots \otimes L_2(\mathrm{I}) \otimes H_0^1(\mathrm{I}),$$

we constructed a Riesz basis for $H_0^1(\square)$ by tensorizing univariate Riesz bases of wavelet type. Indeed, if $\Psi = \{\psi_\lambda \colon \lambda \in \nabla\}$ is a Riesz basis for $L_2(\mathrm{I})$ that, when normalized in $H^1(\mathrm{I})$, is a Riesz basis for $H_0^1(\mathrm{I})$, then, when normalized in $H^1(\square)$, $\Psi \otimes \cdots \otimes \Psi$ is a Riesz basis for $H_0^1(\square)$. This holds true with Riesz constants that are bounded uniformly in $c_0 \geq 0$ and $c_m > 0$ $(m = 1, \ldots, n)$, when we equip $H_0^1(\square)$

with the energy norm $\|\!|\!| \cdot |\!|\!| = a(\cdot\,,\cdot)^{\frac{1}{2}}$. These Riesz constants are even bounded uniformly in the space dimension n if (and only if) Ψ is an orthonormal basis for $L_2(\mathrm{I})$.

Denoting the resulting Riesz basis for $H_0^1(\square)$ as

$$\boldsymbol{\Psi} := \{\psi_{\boldsymbol{\lambda}} := \otimes_{m=1}^n \psi_{\lambda_m} / |\!|\!| \otimes_{m=1}^n \psi_{\lambda_m} |\!|\!| \colon \boldsymbol{\lambda} \in \boldsymbol{\nabla} := \nabla^n\},$$

by writing $u = \mathbf{u}^\mathsf{T}\boldsymbol{\Psi} := \sum_{\boldsymbol{\lambda}\in\boldsymbol{\nabla}} \mathbf{u}_{\boldsymbol{\lambda}}\psi_{\boldsymbol{\lambda}}$, and with $\mathbf{f} := (f(\psi_{\boldsymbol{\lambda}}))_{\boldsymbol{\lambda}\in\boldsymbol{\nabla}}$, an equivalent formulation of (6.1) is

$$\mathbf{A}\mathbf{u} = \mathbf{f}. \tag{6.2}$$

The stiffness matrix $\mathbf{A}$ with respect to $\boldsymbol{\Psi}$ reads as

$$\mathbf{A} = \mathbf{D}^{-1}(c_0\vec{M}\otimes\cdots\otimes\vec{M} + c_1\vec{A}\otimes\vec{M}\otimes\cdots\otimes\vec{M} + \cdots + c_n\vec{M}\otimes\cdots\otimes\vec{M}\otimes\vec{A})\mathbf{D}^{-1},$$

where $\mathbf{D} := \operatorname{diag}(|\!|\!|\psi_{\boldsymbol{\lambda}}|\!|\!| \colon \boldsymbol{\lambda} \in \boldsymbol{\nabla})$, and

$$\vec{A} := \left(\int_{\mathrm{I}} \dot{\psi}_\mu \dot{\psi}_\lambda\right)_{\lambda,\mu\in\nabla} \quad \text{and} \quad \vec{M} := \left(\int_{\mathrm{I}} \psi_\mu \psi_\lambda\right)_{\lambda,\mu\in\nabla}$$

are the one-dimensional (unnormalized) stiffness and mass matrices, respectively. Here, and on other places, a (double) dot on top of a univariate function denotes its (second) derivative. A (double) dot on top of a linear space of univariate functions will denote the linear space of (second) derivatives of these functions. The aforementioned results about $\boldsymbol{\Psi}$ being a Riesz basis for $H_0^1(\square)$ equipped with $|\!|\!| \cdot |\!|\!|$ are equivalent to the matrix $\mathbf{A}$ defining a boundedly invertible mapping on $\ell_2(\boldsymbol{\nabla})$, with a condition number that is bounded uniformly in $c_0 \geq 0$ and $c_m > 0$ $(m = 1,\dots,n)$ (and in n iff Ψ is $L_2(\mathrm{I})$-orthonormal). Another equivalent property is that for $\mathbf{v} \in \ell_2(\boldsymbol{\nabla})$ being an approximation to $\mathbf{u}$, it holds that

$$|\!|\!| u - \mathbf{v}^\mathsf{T}\boldsymbol{\Psi} |\!|\!| \eqsim \|\mathbf{u} - \mathbf{v}\|_{\ell_2(\boldsymbol{\nabla})}.$$

Here and in the remainder, with $C \lesssim D$ we will mean that C can be bounded by a multiple of D, independently of parameters on which C and D may depend, possibly with the exception of the space dimension n. Obviously, $C \gtrsim D$ is defined as $D \lesssim C$, and $C \eqsim D$ as $C \lesssim D$ and $C \gtrsim D$.

In Chapter 5, we solved (6.2) with an adaptive wavelet Galerkin method introduced in [CDD01] and later modified in [GHS07]. Given a finite set $\boldsymbol{\Lambda} \subset \boldsymbol{\nabla}$, let $\mathbf{I}_{\boldsymbol{\Lambda}} \colon \ell_2(\boldsymbol{\Lambda}) \to \ell_2(\boldsymbol{\nabla})$ denote the trivial embedding, so that its adjoint $\mathbf{P}_{\boldsymbol{\Lambda}} \colon \ell_2(\boldsymbol{\nabla}) \to \ell_2(\boldsymbol{\Lambda})$ is the restriction of a vector to its indices in $\boldsymbol{\Lambda}$. With $\mathbf{A}_{\boldsymbol{\Lambda}} := \mathbf{P}_{\boldsymbol{\Lambda}}\mathbf{A}\mathbf{I}_{\boldsymbol{\Lambda}}$ and $\mathbf{f}_{\boldsymbol{\Lambda}} := \mathbf{P}_{\boldsymbol{\Lambda}}\mathbf{f}$, the solution of $\mathbf{A}_{\boldsymbol{\Lambda}}\mathbf{u}_{\boldsymbol{\Lambda}} = \mathbf{f}_{\boldsymbol{\Lambda}}$ is known as the Galerkin approximation to $\mathbf{u}$ from $\ell_2(\boldsymbol{\Lambda})$. The ideal adaptive wavelet Galerkin scheme reads as follows:

% Let $\mu \in (0,1)$ be a sufficiently small parameter

$\boldsymbol{\Lambda}_0 := \varnothing$, $\mathbf{u}_{\boldsymbol{\Lambda}_0} := 0$,
`for` $i = 1, 2, \dots$ `do`
  find the smallest $\boldsymbol{\Lambda}_{i+1} \supset \boldsymbol{\Lambda}_i$ *with* $\|\mathbf{P}_{\boldsymbol{\Lambda}_{i+1}}(\mathbf{f} - \mathbf{A}\mathbf{u}_{\boldsymbol{\Lambda}_i})\| \geq \mu\|\mathbf{f} - \mathbf{A}\mathbf{u}_{\boldsymbol{\Lambda}_i}\|$
  solve $\mathbf{A}_{\boldsymbol{\Lambda}_{i+1}}\mathbf{u}_{\boldsymbol{\Lambda}_{i+1}} = \mathbf{f}_{\boldsymbol{\Lambda}_{i+1}}$
`enddo`

Note that the residual $\mathbf{f} - \mathbf{A}\mathbf{u}_{\mathbf{\Lambda}_i}$ plays the role of an a posteriori error estimator to guide a proper expansion of the set $\mathbf{\Lambda}_i$.

The above scheme cannot be performed exactly. First of all, generally $\mathbf{f}$ will be infinitely supported and thus has to be approximated. Secondly, with the available univariate wavelet bases, either $\vec{M}$ or $\vec{A}$ or both are not sparse, and so generally any column of $\mathbf{A}$ has infinitely many non-zeros. Thanks to the properties of wavelets, however, as being smooth and having vanishing moments, the sizes of the entries of $\vec{M}$ and $\vec{A}$, and thus of $\mathbf{A}$ do decay rapidly away from the diagonal. This property has been used to design an adaptive approximate matrix-vector multiplication routine APPLY in which the accuracy with which any column is approximated increases with the modulus of the corresponding entry in the vector. This APPLY routine is used both for approximate computation of the residual $\mathbf{f} - \mathbf{A}\mathbf{u}_{\mathbf{\Lambda}_i}$ and for the approximate multiplication with $\mathbf{A}_{\mathbf{\Lambda}_{i+1}}$ for the iterative solution of the Galerkin problem $\mathbf{A}_{\mathbf{\Lambda}_{i+1}}\mathbf{u}_{\mathbf{\Lambda}_{i+1}} = \mathbf{f}_{\mathbf{\Lambda}_{i+1}}$. Concerning the latter, note that generally the number of non-zero entries in $\mathbf{A}_{\mathbf{\Lambda}_{i+1}}$ is not of the order of $\#\mathbf{\Lambda}_{i+1}$.

The resulting practical scheme was shown to converge with the *best possible rate* in *linear complexity*. Moreover, since tensor product wavelets are applied, this rate is *independent of the space dimension* ([DS09]). If (and only if) Ψ is L_2(I)-orthonormal, even the constant factor in the error bound that the adaptive scheme may lose compared to the corresponding best N-term approximations is independent of n. In future work, we will generalize the approach to non-product domains using domain decomposition techniques.

Although the scheme has optimal computational complexity, quantitatively the application of the APPLY routine is very demanding, where this routine is also not easy to implement. This is the motivation to develop in this chapter a univariate wavelet basis Ψ such that *both* $\vec{A}$ and $\vec{M}$, and thus $\mathbf{A}$ are sparse. In this case, $\mathbf{A}$ can be applied *exactly* to a (finitely supported) vector at a cost that is linear in its support length. Since Ψ will be a Riesz basis for L_2(I) and, when normalized in H^1(I), a Riesz basis for H^1_0(I), the bi-infinite matrix $\mathbf{A}$, i.e., the representation of the operator defined in (6.1) with respect to the normalized tensor product basis, will be a boundedly invertible mapping, uniformly in $c_0 \geq 0$ and $c_m > 0$ $(m = 1, \ldots, n)$. Since Ψ, however, will not be L_2(I)-orthonormal, the condition number of $\mathbf{A}$ will grow with the space dimension n.

In view of applications in sparse grid algorithms (e.g. see [BG04]), for completeness we emphasize that for any subset $\mathbf{\Lambda} \subset \boldsymbol{\nabla}$, $\mathbf{A}|_{\mathbf{\Lambda}\times\mathbf{\Lambda}}$ is sparse and well-conditioned, with a condition number not larger than that of $\mathbf{A}$.

Remark 6.1.1. When having univariate wavelets that lead to sparse $\vec{A}$ and $\vec{M}$, the stiffness matrix $\mathbf{A}$ corresponding to (6.1) is sparse because the coefficients c_i are constants. For smooth, non-constant coefficients, the additional non-zeros outside the sparsity pattern of a constant coefficient operator will be much smaller, depending on the levels of the wavelets involved. For the residual computation inside the adaptive wavelet scheme, it can be envisaged that they can be ignored, possibly apart from those corresponding to some coarsest levels.

Remark 6.1.2. Instead of being satisfied with a stiffness matrix $\mathbf{A}$ that is sparse,

one may think of searching a wavelet basis of $H_0^1(\square)$ such that the stiffness matrix is diagonal. This would mean that if $\mathbf{f}$ has a finite support $\mathbf{\Lambda} \subset \mathbf{\nabla}$, then the exact solution of (6.1) is in the span of the wavelets with indices in $\mathbf{\Lambda}$. This seems hard, or perhaps impossible to realize on a bounded domain and for dimensions $n \geq 2$. We refer to [DW93] for a discussion of related issues on the domain $\mathbb{R}^2$.

Of course, in order to end up with a diagonal stiffness matrix, one can tensorize the univariate basis $\{\sqrt{2}\sin(k\pi x)\colon k \in \mathbb{N}_0\}$. As shown in Chapter 3, with this approach, however, even for smooth f generally only low convergence rates are possible.

6.2 A first attempt: Continuous piecewise smooth wavelets?

We will search a collection of univariate wavelets $\Psi = \{\psi_\lambda\colon \lambda \in \nabla\}$ such that, with $|\lambda| \in \mathbb{N}_0$ denoting the level of ψ_λ or that of λ,

C1. $\operatorname{diam}\operatorname{supp}\psi_\lambda \lesssim 2^{-|\lambda|}$,
C2. $\sup_{j,k\in\mathbb{N}_0} \#\{|\lambda| = j\colon [k2^{-j}, (k+1)2^{-j}] \cap \operatorname{supp}\psi_\lambda \neq \varnothing\} < \infty$,
C3. Ψ is Riesz basis for $L_2(\mathrm{I})$,
C4. $\{\psi_\lambda/\|\dot{\psi}_\lambda\|_{L_2(\mathrm{I})}\colon \lambda \in \nabla\}$ is a Riesz basis for $H_0^1(\mathrm{I})$,
C5. $\int_\mathrm{I} \dot{\psi}_\lambda\dot{\psi}_\mu = 0$ when $||\lambda| - |\mu|| > M$,
C6. $\int_\mathrm{I} \psi_\lambda\psi_\mu = 0$ when $||\lambda| - |\mu|| > M$,

where $M \in N_0$ is some constant, that later will be chosen to be 1. As a consequence, with respect to a level-wise partition of the wavelets, $\vec{A}$ and $\vec{M}$ will be block tridiagonal with, because of C1 and C2, sparse non-zero blocks. Note that under the assumptions C1 and C2, $\vec{A}$ and $\vec{M}$ are sparse if and only if C5 and C6, respectively, are valid. We will refer to the properties C1 and C2 by saying that the wavelets are (uniformly) local and that the collection of wavelets on each level is (uniformly) locally finite, respectively.

Proposition 6.2.1. *If, in addition to* C1 – C4*, each wavelet is piecewise smooth with a bounded derivative, then* C5 *requires that they are in* C^1.

Proof. Suppose the statement is wrong. For some $\mu \in \nabla$, let $\dot{\psi}_\mu$ have a jump in some $y \in \mathrm{I}$. Then there exists a $K = K(\mu) \geq M + |\mu|$ such that for all $\lambda \in \nabla$ with $|\lambda| > K$ and $\psi_\lambda(y) \neq 0$, it holds that $\operatorname{supp}\psi_\lambda \subset \mathrm{I}$ and ψ_μ is smooth on $\operatorname{supp}\psi_\lambda\backslash\{y\}$, where we used that ψ_μ is piecewise smooth. Then by C5, for those λ we have

$$0 = \int_\mathrm{I} \dot{\psi}_\lambda\dot{\psi}_\mu = \big(\dot{\psi}_\mu(y^-) - \dot{\psi}_\mu(y^+)\big)\psi_\lambda(y) - \int_\mathrm{I} \ddot{\psi}_\mu\psi_\lambda,$$

and so (μ is fixed),

$$|\psi_\lambda(y)| \lesssim \int_\mathrm{I} |\psi_\lambda| \lesssim \sqrt{2^{-|\lambda|}}. \tag{6.3}$$

Writing $u \in L_2(\mathrm{I})$ as $u = \sum_{\lambda\in\nabla} c_\lambda\psi_\lambda$, C3 shows that $\|u\|_{L_2(\mathrm{I})}^2 \eqsim \sum_{\lambda\in\nabla} |c_\lambda|^2$. When $u \in H_0^1(\mathrm{I})$, then C4 shows that this expansion converges also in $H^1(\mathrm{I})$, and thus

in $L_\infty(\mathrm{I})$, i.e., that

$$u(y) = \sum_{\{\lambda\in\nabla\colon\, \psi_\lambda(y)\neq 0\}} c_\lambda \psi_\lambda(y).$$

Now by using (6.3) for $|\lambda| > K$, and the fact that $|\psi_\lambda(y)| < \infty$ for each of the finitely many other $\lambda \in \nabla$, an application of the Cauchy-Schwarz inequality shows that $|u(y)| \lesssim \|u\|_{L_2(\mathrm{I})}$, which inequality, however, is not valid on $H^1_0(\mathrm{I})$. We conclude that the wavelets have to be in C^1. ◊

Remark 6.2.2. Proposition 6.2.1 confirms the well-known fact that the hierarchical basis is not a Riesz basis for $L_2(\mathrm{I})$. Indeed, this basis of continuous piecewise linears satisfies C1, C2, C4 and C5, where $\vec{A}$ is even diagonal, and thus it cannot satisfy C3.

Remark 6.2.3. The above proof also shows that, assuming C1, C2, C3, C5 and that each wavelet is piecewise smooth with a bounded derivative, the collection $\{\psi_\lambda/\|\psi_\lambda\|_{H^1(\mathrm{I})}\colon \lambda\in\nabla\}$ can be a Riesz basis for $H^1(\mathrm{I})$ (instead of $H^1_0(\mathrm{I})$) only if $\dot\psi_\mu(0) = \dot\psi_\mu(1) = 0$ for all $\mu \in \nabla$. Indeed, suppose $\dot\psi_\mu$ does not vanish at the boundary, say at 0. Then there exists a $K \geq M + |\mu|$ such that for all $\lambda \in \nabla$ with $|\lambda| > K$ and $\psi_\lambda(0) \neq 0$, it holds that $\operatorname{supp}\psi_\lambda \subset [0,1)$ and ψ_μ is smooth on $\operatorname{supp}\psi_\lambda$. Then by C5, for those λ we have

$$0 = \int_{\mathrm{I}} \dot\psi_\lambda\dot\psi_\mu = -\dot\psi_\mu(0)\psi_\lambda(0) - \int_{\mathrm{I}} \ddot\psi_\mu\psi_\lambda,$$

and the same arguments as in the proof of Proposition 6.2.1 lead to a contradiction.

In view of having a rapidly converging wavelet expansion, for a wavelet basis for $H^1(\mathrm{I})$ the conditions $\dot\psi_\mu(0) = \dot\psi_\mu(1) = 0$ are in any case undesirable. Actually, we expect that such a basis even does not exist.

In view of this, we restrict ourselves to the task of constructing a collection Ψ such that C1 – C5 are valid, i.e., in particular such that $\{\psi_\lambda/\|\dot\psi_\lambda\|_{L_2(\mathrm{I})}\colon \lambda\in\nabla\}$ is a Riesz basis for $H^1_0(\mathrm{I})$.

6.3 Biorthogonal cubic Hermite wavelets

In order to construct wavelets that, properly scaled, generate Riesz bases for a range of Sobolev spaces, in particular for $L_2(\mathrm{I})$ and $H^1_0(\mathrm{I})$ (cf. C3 and C4), we will use the following well-known theorem (cf. [Dah96, DS99c, Coh03]).

Theorem 6.3.1 (Biorthogonal space decompositions)**.** *Let*

$$V_0 \subset V_1 \subset \cdots \subset L_2(\mathrm{I}), \qquad \tilde V_0 \subset \tilde V_1 \subset \cdots \subset L_2(\mathrm{I})$$

be sequences of primal and dual spaces such that

$$\dim V_j = \dim \tilde V_j < \infty \quad \textit{and} \quad \alpha_j := \inf_{0\neq\tilde v_j\in\tilde V_j} \sup_{0\neq v_j\in V_j} \frac{|\langle \tilde v_j, v_j\rangle_{L_2(\mathrm{I})}|}{\|\tilde v_j\|_{L_2(\mathrm{I})}\|v_j\|_{L_2(\mathrm{I})}} \gtrsim 1. \quad (6.4)$$

In addition, for some $0 < \gamma < d$*, let*

$$\inf_{v_j\in V_j} \|v - v_j\|_{L_2(\mathrm{I})} \lesssim 2^{-jd}\|v\|_{\mathcal{H}^d(\mathrm{I})} \quad (v \in \mathcal{H}^d(\mathrm{I}))$$

(Jackson estimate), *and*

$$\|v_j\|_{\mathcal{H}^s(\mathrm{I})} \lesssim 2^{js}\|v_j\|_{L_2(\mathrm{I})} \quad (v_j \in V_j,\ s \in [0,\gamma))$$

(Bernstein estimate), *where* $\mathcal{H}^s(\mathrm{I})$ ($s \in [0,d]$) *are Hilbert spaces such that* $\mathcal{H}^s(\mathrm{I}) = [L_2(\mathrm{I}), \mathcal{H}^d(\mathrm{I})]_{s/d}$, *and let similar estimates be valid at the dual side with* $((V_j)_j, d, \gamma, \mathcal{H}^s(\mathrm{I}))$ *reading as* $((\tilde{V}_j)_j, \tilde{d}, \tilde{\gamma}, \tilde{\mathcal{H}}^s(\mathrm{I}))$.

Then, with $\Phi_0 = \{\varphi_{0,k}\colon k \in I_0\}$ *being a basis for* V_0 (*scaling functions*) *and* $\Psi_j = \{\psi_{j,k}\colon k \in J_j\}$ ($j \in \mathbb{N}$) *being uniform* $L_2(\mathrm{I})$*-Riesz bases for* $W_j := V_j \cap \tilde{V}_{j-1}^{\perp_{L_2(\mathrm{I})}}$ (*wavelets*), *for* $s \in (-\tilde{\gamma}, \gamma)$ *the collection*

$$\Phi_0 \cup \bigcup\nolimits_{j\in\mathbb{N}} 2^{-sj}\Psi_j$$

is a Riesz basis for $\mathcal{H}^s(\mathrm{I})$, *where* $\mathcal{H}^s(\mathrm{I}) := (\tilde{\mathcal{H}}^{-s}(\mathrm{I}))'$ *for* $s < 0$.

In view of the notations introduced earlier, we denote (j,k) also as λ, where $|\lambda| = j$, $\varphi_{0,k}$ as $\psi_{0,k}$ and $I_0 \cup \cup_{j\in\mathbb{N}} J_j$ as ∇.

Remark 6.3.2. Assume that for any $j \in \mathbb{N}_0$, $\dim V_j = \dim \tilde{V}_j < \infty$. Then $\alpha_j > 0$ in (6.4) is equivalent to the existence of a bounded projector $Q_j\colon L_2(\mathrm{I}) \to L_2(\mathrm{I})$ with $\operatorname{Im} Q_j = V_j$ and $\operatorname{Im}(I - Q_j) = \tilde{V}_j^{\perp_{L_2(\mathrm{I})}}$, where $\|Q_j\|_{L_2(\mathrm{I})\to L_2(\mathrm{I})} = \alpha_j^{-1}$. So, $\alpha_j \gtrsim 1$ is equivalent to the existence of a sequence of such biorthogonal projectors that are bounded uniformly in j (cf. [Ste03]).

The nesting of primal and dual sequences implies that $Q_{j+1}Q_j = Q_j = Q_jQ_{j+1}$, from which it follows that $V_j = Q_jV_{j+1}$ and $W_j = (I - Q_j)V_{j+1} = \operatorname{Im}(Q_{j+1} - Q_j)$. In particular, it holds that $V_j = V_0 \oplus W_1 \oplus \cdots \oplus W_j$.

Still assuming $\dim V_j = \dim \tilde{V}_j < \infty$, $\alpha_j \gtrsim 1$ in (6.4) is also equivalent to the property that for uniform $L_2(\mathrm{I})$-Riesz bases Φ_j and $\tilde{\Phi}_j$ for V_j and $\tilde{V}_j$, respectively, $\langle \Phi_j, \tilde{\Phi}_j\rangle_{L_2(\mathrm{I})}^{-1}$ exists with a uniformly bounded spectral norm, or, equivalently, that V_j and $\tilde{V}_j$ can be equipped with biorthogonal uniform $L_2(\mathrm{I})$-Riesz bases. In cases where these biorthogonal bases can be chosen to be both uniformly local, then under some mild additional condition, both the (primal) wavelets and the corresponding dual wavelets can be selected to be uniformly local (cf. e.g. [Dah97, Ste03]). In the application of Theorem 6.3.1 that we study in this chapter, only the primal scaling functions and wavelets will be uniformly local.

We are going to apply Theorem 6.3.1 for V_j being the space of *cubic Hermite splines* satisfying first order homogeneous Dirichlet boundary conditions with respect to the $j+1$ times dyadically refined interval $\mathrm{I} = (0,1)$, and with $\tilde{V}_j$ being the space of piecewise cubics with respect to the j times dyadically refined I, i.e.,

$$V_j := \prod_{k=0}^{2^{j+1}-1} P_3(k2^{-(j+1)}, (k+1)2^{-(j+1)}) \cap C^1(\mathrm{I}) \cap H_0^1(\mathrm{I}), \tag{6.5}$$

$$\tilde{V}_j := \prod_{k=0}^{2^{j}-1} P_3(k2^{-j}, (k+1)2^{-j}). \tag{6.6}$$

Theorem 6.3.3. *It holds that* $\dim V_j = \dim \tilde{V}_j$ *and*

$$\inf_{j\in\mathbb{N}_0} \inf_{0\neq\tilde{v}_j\in\tilde{V}_j} \sup_{0\neq v_j\in V_j} \frac{|\langle \tilde{v}_j, v_j\rangle_{L_2(\mathrm{I})}|}{\|\tilde{v}_j\|_{L_2(\mathrm{I})}\|v_j\|_{L_2(\mathrm{I})}} > 0.$$

The dimension of V_j is $4\times 2^{j+1} - (2^{j+1}-1)2 - 2 = 2^{j+2} = 4\times 2^j$, being the dimension of $\tilde{V}_j$. We postpone the proof of the second statement of this theorem to Section 6.6.

We will construct uniform $L_2(\mathrm{I})$-Riesz bases Ψ_j for $W_j = V_j \cap \tilde{V}_{j-1}^{\perp_{L_2(\mathrm{I})}}$ in Section 6.4. Note that due to the absence of boundary conditions incorporated in the definition of $\tilde{V}_j$, all wavelets, i.e., any element of Ψ_j, has 4 vanishing moments. This is very convenient for constructing sparse approximations to $\mathbf{f} = (f(\psi_{\boldsymbol{\lambda}}))_{\boldsymbol{\lambda}\in\boldsymbol{\nabla}}$.

With Φ_0 being some basis for V_0, an application of Theorems 6.3.1 and 6.3.3 yields the following result.

Corollary 6.3.4. *Let* $\mathcal{H}^s(\mathrm{I}) := [L_2(\mathrm{I}), H^4(\mathrm{I})\cap H_0^1(\mathrm{I})]_{s/4}$ *for* $s\in[0,4]$ *and* $\mathcal{H}^s(\mathrm{I}) := (H^{-s}(\mathrm{I}))'$ *for* $s<0$. *Then for* $s\in(-\frac{1}{2},\frac{5}{2})$, *the collection* $\Phi_0\cup\cup_{j\in\mathbb{N}} 2^{-sj}\Psi_j$ *is a Riesz basis for* $\mathcal{H}^s(\mathrm{I})$.

Remark 6.3.5. It is known (e.g. see [LM72]) that for $s\in[1,4]$, $\mathcal{H}^s(\mathrm{I}) = H^s(\mathrm{I})\cap H_0^1(\mathrm{I})$ and that for $s\in[0,1]\backslash\{\frac{1}{2}\}$, $\mathcal{H}^s(\mathrm{I}) = H_0^s(\mathrm{I})$, the latter space being equal to $H^s(\mathrm{I})$ for $s\in[0,\frac{1}{2})$.

The wavelets that we construct in Section 6.4 will be uniformly local and will be such that the collections Ψ_j that span the spaces $W_j = V_j\cap\tilde{V}_{j-1}^{\perp_{L_2(I)}}$ are uniformly locally finite, i.e., the conditions C1 and C2 formulated in the previous section are valid. The conditions C3 and C4 are special cases of Corollary 6.3.4. Finally, as is demonstrated in the following proposition, by the choice of the sequence of dual spaces $(\tilde{V}_j)_j$ also the remaining conditions C5 and C6 are valid with $M=1$.

Proposition 6.3.6. *For all* $j\in\mathbb{N}_0$, *it holds that* $\dot{W}_{j+2}\perp_{L_2(\mathrm{I})}\dot{V}_j$ *and* $W_{j+2}\perp_{L_2(\mathrm{I})} V_j$.

Proof. Since for $w_{j+2}\in W_{j+2}$ and $v_j\in V_j$, $\langle \dot{w}_{j+2}, \dot{v}_j\rangle_{L_2(\mathrm{I})} = -\langle w_{j+2}, \ddot{v}_j\rangle_{L_2(\mathrm{I})}$, the first statement is equivalent to $W_{j+2}\perp_{L_2(\mathrm{I})}\ddot{V}_j$.

For $v_j\in V_j$, let $\ddot{v}_j = 0$. Then v_j is a piecewise polynomial of degree 1. Since additionally $v_j\in C^1(\mathrm{I})\cap H_0^1(\mathrm{I})$, we infer that $v_j = 0$, and thus that $\dim\ddot{V}_j = \dim V_j$. Clearly $\ddot{V}_j\subset\prod_{k=0}^{2^{j+1}-1} P_1(k2^{-(j+1)},(k+1)2^{-(j+1)})$, the latter being a space of dimension 2^{j+2}, and so both spaces are equal.

For $v_j\in V_j$ and $z_j\in\ddot{V}_j$, let $v_j+z_j=0$. Then $z_j\in\ddot{V}_j\cap C^1(\mathrm{I})\cap H_0^1(\mathrm{I})$, and thus $z_j=0$, meaning that $V_j\cap\ddot{V}_j = \{0\}$. Clearly $V_j+\ddot{V}_j\subset\tilde{V}_{j+1}$. Since $\dim(V_j+\ddot{V}_j) = \dim V_j + \dim\ddot{V}_j = 2^{j+3} = \dim\tilde{V}_{j+1}$, we conclude that $V_j+\ddot{V}_j = \tilde{V}_{j+1}$, and thus that the statements of the proposition are equivalent to $W_{j+2}\perp_{L_2(\mathrm{I})}\tilde{V}_{j+1}$. ♢

Remark 6.3.7. Besides the cubic Hermite splines, we also tried the following maximally smooth spline options for the sequence $(V_j)_j$:

a. $V_j := \prod_{k=0}^{2^{j+1}-1} P_2(k2^{-(j+1)},(k+1)2^{-(j+1)})\cap C^1(\mathrm{I})\cap H_0^1(\mathrm{I})$,

b. $V_j := \prod_{k=0}^{2^{j+1}-1} P_3(k2^{-(j+1)}, (k+1)2^{-(j+1)}) \cap C^2(\mathrm{I}) \cap H_0^1(\mathrm{I})$,

c. $V_j := \prod_{k=0}^{2^{j+1}-1} P_4(k2^{-(j+1)}, (k+1)2^{-(j+1)}) \cap C^3(\mathrm{I}) \cap H_0^2(\mathrm{I})$.

With $W_j := \operatorname{span} \Psi_j$, also in these cases the conditions $\dot{W}_{j+2} \perp_{L_2(\mathrm{I})} \dot{V}_j$ and $W_{j+2} \perp_{L_2(\mathrm{I})} V_j$ are equivalent to $W_{j+2} \perp_{L_2(\mathrm{I})} (\ddot{V}_j + V_j)$, and $\dim \ddot{V}_j = \dim V_j$.

In case a, we have that $\ddot{V}_j = \prod_{k=0}^{2^{j+1}-1} P_0(k2^{-(j+1)}, (k+1)2^{-(j+1)})$ and $V_j \cap \ddot{V}_j = \{0\}$. So the appropriate choice for $\tilde{V}_{j+1}$ is $V_j + \ddot{V}_j$. It holds that $\dim V_j = 2^{j+1} = \dim \tilde{V}_j$, but as one may verify, α_j from (6.4) is zero for any $j \in \mathbb{N}_0$. Since $\alpha_j \gtrsim 1$ is a necessary condition for the wavelets to generate a Riesz basis for $L_2(\mathrm{I})$, with this choice C1 – C5 cannot be realized.

In case b, we have that $\ddot{V}_j = \prod_{k=0}^{2^{j+1}-1} P_1(k2^{-(j+1)}, (k+1)2^{-(j+1)}) \cap C(\mathrm{I})$ and $V_j \cap gV_j = \{0\}$. When choosing $\tilde{V}_{j+1} = V_j + \ddot{V}_j$, we have $\dim \tilde{V}_j = 2(2^j + 1) = \dim V_j + 1$, and Theorem 6.3.1 cannot be applied.

In case c, we have that $\ddot{V}_j \subsetneq Z_j := \prod_{k=0}^{2^{j+1}-1} P_2(k2^{-(j+1)}, (k+1)2^{-(j+1)}) \cap C^1(\mathrm{I})$ and $V_j \cap \ddot{V}_j \subset V_j \cap Z_j = \{0\}$. Choosing $\tilde{V}_{j+1} = V_j + \ddot{V}_j$, we have $\dim V_j = 2^{j+1} = \dim \tilde{V}_j$, but, as we verified numerically, $\alpha_j \downarrow 0$ for $j \to 0$.

Returning to the spaces V_j and $\tilde{V}_j$ from (6.5) and (6.6), and with $\Psi = \{\psi_\lambda : \lambda \in \nabla\} = \Phi_0 \cup \cup_{j \in \mathbb{N}} \Psi_j$ being the collection of wavelets that will be constructed in Section 6.4, i.e., Ψ_j spans $W_j = V_j \cap \tilde{V}_j^{\perp_{L_2(\mathrm{I})}}$, in addition to C5 and C6 we have

$$\int_{\mathrm{I}} \psi_\lambda \dot{\psi}_\mu = 0 \quad \text{when } ||\lambda| - |\mu|| > 1. \tag{6.7}$$

For $|\lambda| - |\mu| > 1$, this follows from the fact that

$$\dot{V}_j \subset \prod_{k=0}^{2^{j+1}-1} P_2(k2^{-(j+1)}, (k+1)2^{-(j+1)}) \cap C(\mathrm{I}) \subset \tilde{V}_{j+1} \quad (= V_j + \ddot{V}_j),$$

and for $|\mu| - |\lambda| > 1$ by additionally using integration by parts and the first order homogeneous Dirichlet boundary conditions.

Note that $\dot{V}_j \subset V_j + \ddot{V}_j$ is *not* valid for the spaces V_j from Remark 6.3.7, so we got (6.7) "coincidentally". A consequence is that for *any* constants $(a_{\alpha,\beta})_{|\alpha|,|\beta| \le 1}$, the representation, with respect to the properly scaled wavelet basis Ψ, of the problem of finding $u \in H_0^1(\square)$ such that for given $f \in H^{-1}(\square)$,

$$\int_\square \sum_{|\alpha|,|\beta| \le 1} a_{\alpha,\beta} \partial^\alpha u \partial^\beta v = f(v) \quad (v \in H_0^1(\square)), \tag{6.8}$$

is of the form

$$\mathbf{A}\mathbf{u} = \mathbf{f}, \tag{6.9}$$

where $\mathbf{A}$ is sparse. Indeed, also first order partial derivatives or mixed second order partial derivatives lead to a tensor product of sparse matrices. The matrix $\mathbf{A}$ is boundedly invertible whenever the constants $(a_{\alpha,\beta})_{|\alpha|,|\beta| \le 1}$ are such that (6.8) defines a boundedly invertible operator between $H_0^1(\square)$ and $H^{-1}(\square)$. For cases where $\mathbf{A}$ is not symmetric positive definite, a possibility to solve (6.9) is to apply the adaptive wavelet Galerkin scheme to the normal equations.

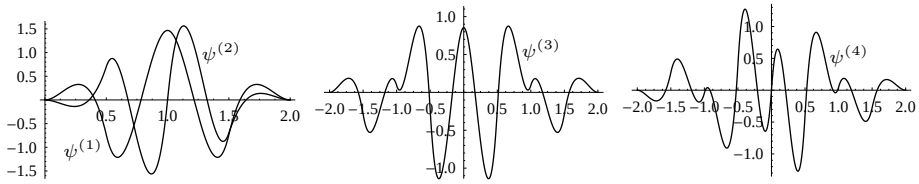

Figure 6.1: The wavelets $\psi^{(1)}$, $\psi^{(2)}$, $\psi^{(3)}$ and $\psi^{(4)}$, normalized in L_2.

6.4 Construction of the wavelets

With V_j and $\tilde{V}_j$ from (6.5) and (6.6), we construct uniform $L_2(\mathrm{I})$-Riesz bases Ψ_{j+1} for $V_{j+1} \cap \tilde{V}_j^{\perp_{L_2(\mathrm{I})}}$, which are also uniformly local and uniformly locally finite.

Let $\varphi^{(1)}, \varphi^{(2)} \in P_3(-1,0) \times P_3(0,1) \cap C^1(-1,1)$ be defined by

$$\begin{aligned} \varphi^{(1)}(\pm 1) &= 0, & (\varphi^{(2)})'(\pm 1) &= 0, \\ \varphi^{(1)}(0) &= 1, & (\varphi^{(2)})'(0) &= 1, \\ (\varphi^{(1)})'(0) = (\varphi^{(1)})'(\pm 1) &= 0, & \varphi^{(2)}(0) = \varphi^{(2)}(\pm 1) &= 0. \end{aligned} \tag{6.10}$$

Integer translates of $\varphi^{(1)}$, $\varphi^{(2)}$ span the space of C^1 piecewise cubics with respect to the pieces $[k, k+1]$ ($k \in \mathbb{Z}$). With

$$\varphi_{j,k}^{(i)} := \sqrt{2^{j+1}}\, \varphi^{(i)}(2^{j+1} \cdot - k),$$

the collection

$$\Phi_j := \{\varphi_{j,k}^{(1)} \colon k \in \{1, 2, \dots, 2^{j+1} - 1\}\} \cup \{\varphi_{j,k}^{(2)}|_{\mathrm{I}} \colon k \in \{0, 1, \dots, 2^{j+1}\}\} \tag{6.11}$$

is a uniform $L_2(\mathrm{I})$-Riesz basis for V_j from (6.5).

We construct 4 types of "mother wavelets". These functions are C^1 piecewise cubics w.r.t. the pieces $[k, k+\frac{1}{2}]$ ($k \in \frac{1}{2}\mathbb{Z}$), i.e., they are in the span of $\{\varphi^{(i)}(2\cdot - k) \colon i \in \{1,2\}, k \in \mathbb{Z}\}$, and they are $L_2(\mathbb{R})$-orthogonal to $\prod_{k \in 2\mathbb{Z}} P_3(k, k+2)$.

We seek the first two types of the form

$$\begin{aligned} \psi^{(1)} &:= \sum_{k=1}^{3} a_k^{(1)} \varphi^{(1)}(2\cdot - k) + \sum_{k=1}^{3} b_k^{(1)} \varphi^{(2)}(2\cdot - k), \\ \psi^{(2)} &:= \sum_{k=1}^{3} a_k^{(2)} \varphi^{(1)}(2\cdot - k) + \sum_{k=1}^{3} b_k^{(2)} \varphi^{(2)}(2\cdot - k), \end{aligned}$$

meaning that their support is $[0,2]$. Up to a scaling, these functions are uniquely determined by imposing that they are orthogonal to $P_3(0,2)$ and that $\psi^{(1)}(\cdot - 1)$ is even and $\psi^{(2)}(\cdot - 1)$ is odd. The coefficients $a_k^{(i)}$, $b_k^{(i)}$ ($i \in \{1,2\}$) can be found in Table 6.1.

We seek the third and fourth type of the form

$$\begin{aligned} \psi^{(3)} &:= \sum_{k=-3}^{3} a_k^{(3)} \varphi^{(1)}(2\cdot - k) + \sum_{k=-3}^{3} b_k^{(3)} \varphi^{(2)}(2\cdot - k), \\ \psi^{(4)} &:= \sum_{k=-3}^{3} a_k^{(4)} \varphi^{(1)}(2\cdot - k) + \sum_{k=-3}^{3} b_k^{(4)} \varphi^{(2)}(2\cdot - k), \end{aligned}$$

meaning that their support is $[-2,2]$. Up to a scaling, these functions are uniquely determined by imposing that they are orthogonal to $P_3(-2,0) \times P_3(0,2)$,

k	-3	-2	-1	0	1	2	3
$a_k^{(1)}$	$-$	$-$	$-$	$-$	$-\frac{2}{15}$	$\frac{4}{15}$	$-\frac{2}{15}$
$b_k^{(1)}$	$-$	$-$	$-$	$-$	-1	0	1
$a_k^{(2)}$	$-$	$-$	$-$	$-$	$\frac{7}{39}$	0	$-\frac{7}{39}$
$b_k^{(2)}$	$-$	$-$	$-$	$-$	1	$\frac{44}{13}$	1
$a_k^{(3)}$	$-\frac{4595}{13728}$	$\frac{7}{65}$	$-\frac{18737}{68640}$	1	$-\frac{18737}{68640}$	$\frac{7}{65}$	$-\frac{4595}{13728}$
$b_k^{(3)}$	$-\frac{68741}{22880}$	$-\frac{69}{40}$	$-\frac{204701}{22880}$	0	$\frac{204701}{22880}$	$\frac{69}{40}$	$\frac{68741}{22880}$
$a_k^{(4)}$	$\frac{417}{22880}$	$-\frac{7}{2340}$	$\frac{5443}{205920}$	0	$-\frac{5443}{205920}$	$\frac{7}{2340}$	$-\frac{417}{22880}$
$b_k^{(4)}$	$\frac{723}{4576}$	$\frac{1}{8}$	$\frac{8153}{13728}$	$\frac{1}{2}$	$\frac{8153}{13728}$	$\frac{1}{8}$	$\frac{723}{4576}$

Table 6.1: Coefficients for the construction of wavelets.

that $\psi^{(3)}$ is even and $\psi^{(4)}$ is odd and, in order to create a more sparse mass matrix, that they are orthogonal to $\psi^{(1)}(\cdot - k)$ and $\psi^{(2)}(\cdot - k)$ ($k \in 2\mathbb{Z}$). The coefficients $a_k^{(i)}$, $b_k^{(i)}$ ($i \in \{3,4\}$) can be found in Table 6.1.

With

$$\psi_{j+1,k}^{(i)} := \sqrt{2^{j+1}}\,\psi^{(i)}(2^{j+1}\cdot - k),$$

by construction, the collection

$$\begin{aligned}\Psi_{j+1} := {} & \{\psi_{j+1,k}^{(i)} \colon i \in \{1,2\},\ k \in \{0,2,\dots,2^{j+1}-2\}\} \\ & \cup \{\psi_{j+1,k}^{(3)} \colon k \in \{2,4,\dots,2^{j+1}-2\}\} \cup \{\psi_{j+1,k}^{(4)}|_{\mathrm{I}} \colon k \in \{0,2,\dots,2^{j+1}\}\} \quad (6.12)\end{aligned}$$

is contained in $W_{j+1} = V_{j+1} \cap \tilde{V}_j^{\perp_{L_2(\mathrm{I})}}$, where its cardinality, being 2^{j+2}, is equal to the dimension of this space, i.e., the collection spans W_{j+1}.

With $\bar{\psi}_1 := \psi_1$, $\bar{\psi}_2 := \psi_2$, $\bar{\psi}_3 := \psi_3|_{[0,2]}$, $\bar{\psi}_4 := \psi_4|_{[0,2]}$, $\bar{\psi}_5 := \psi_3(\cdot - 2)|_{[0,2]}$ and $\bar{\psi}_6 := \psi_4(\cdot - 2)|_{[0,2]}$, a numerical calculation reveals that the "element mass matrix"

$$\left(\langle \bar{\psi}_i, \bar{\psi}_j \rangle_{L_2(0,2)}\right)_{1\le i,j\le 6} = \begin{pmatrix} \frac{2467613}{3603600} & \frac{400733}{10810800} & 0 & 0 & -\frac{923411}{3603600} & \frac{137987}{10810800} \\ \frac{400733}{10810800} & \frac{7841}{3603600} & 0 & 0 & -\frac{137987}{10810800} & \frac{20431}{32432400} \\ 0 & 0 & \frac{52}{1575} & 0 & 0 & 0 \\ 0 & 0 & 0 & \frac{704}{10647} & 0 & 0 \\ -\frac{923411}{3603600} & -\frac{137987}{10810800} & 0 & 0 & \frac{2467613}{3603600} & -\frac{400733}{10810800} \\ \frac{137987}{10810800} & \frac{20431}{32432400} & 0 & 0 & -\frac{400733}{10810800} & \frac{7841}{3603600} \end{pmatrix}$$

is positive definite. As a consequence, for any $B \subset 2\mathbb{Z}$, and any subset

$$\Sigma \subset \{\psi^{(i)}(\cdot - k) \colon i \in \{1,\dots,4\},\ k \in 2\mathbb{Z}\}$$

of functions that do not identically vanish on $G := \cup_{k\in B}(k, k+2)$, $\{\sigma|_G \colon \sigma \in \Sigma\}$ is a $L_2(G)$-Riesz basis of its span with a condition number that can be bounded on an absolute multiple of the condition number of $\left[\langle \bar{\psi}_i, \bar{\psi}_j \rangle_{L_2(0,2)}\right]_{1\le i,j\le 6}$. This follows from the observation that

$$\Big\langle \sum_{\sigma\in\Sigma} c_\sigma \sigma, \sum_{\tau\in\Sigma} c_\tau \tau \Big\rangle_{L_2(G)} = \sum_{k\in B} \Big\langle \sum_{\sigma\in\Sigma} c_\sigma \sigma|_{(k,k+2)}, \sum_{\tau\in\Sigma} c_\tau \tau|_{(k,k+2)} \Big\rangle_{L_2(k,k+2)}.$$

Since the same holds true for the dilated functions, we conclude that (6.12) defines a uniform $L_2(\mathrm{I})$-Riesz basis for $V_{j+1} \cap \tilde{V}_j^{\perp_{L_2(\mathrm{I})}}$.

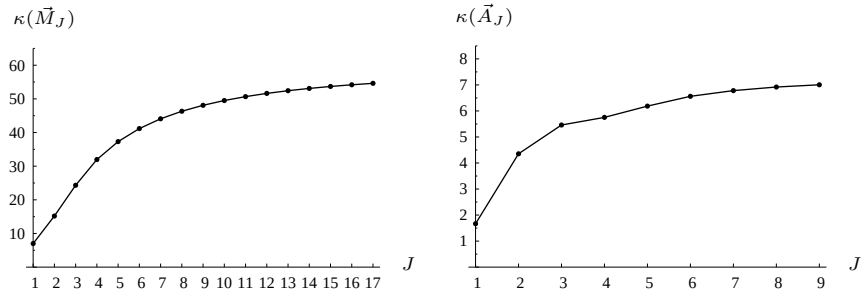

Figure 6.2: Condition number of the mass matrix $\vec{M}_j$ (left) and the stiffness matrix $\vec{A}_j$ (right).

6.5 Condition numbers

A result of Corollary 6.3.4 is that $\Phi_0 \cup \cup_{j\in\mathbb{N}}\Psi_j$, where Φ_0 and Ψ_j are as in (6.11) and (6.12), respectively, forms, when normalized in $L_2(\mathrm{I})$ or $H^1(\mathrm{I})$, a Riesz basis for $L_2(\mathrm{I})$ and $H^1_0(\mathrm{I})$, respectively. In particular, this shows that the condition numbers of the mass matrix and the normalized stiffness matrix are bounded. In various estimates, the values of these condition numbers play a role. Since it is not feasible to compute the actual condition numbers of the infinite dimensional matrices, instead we computed those of

$$\vec{A}_J := \left(\frac{\int_{\mathrm{I}} \dot{\psi}_\mu \dot{\psi}_\lambda}{\|\dot{\psi}_\mu\|_{L_2(\mathrm{I})}\|\dot{\psi}_\lambda\|_{L_2(\mathrm{I})}}\right)_{\substack{\lambda,\mu\in\nabla\\ |\lambda|,|\mu|\le J}} \quad \text{and} \quad \vec{M}_J := \left(\int_{\mathrm{I}} \psi_\mu\psi_\lambda\right)_{\substack{\lambda,\mu\in\nabla\\ |\lambda|,|\mu|\le J}}.$$

The condition numbers of these matrices, which are bounded uniformly in J, are shown in Figure 6.2.

Also, we computed the condition number of the mass matrix of wavelets on one level, i.e., the condition number of the matrix $\left(\int_{\mathrm{I}} \psi_\mu\psi_\lambda\right)_{\lambda,\mu\in\nabla,|\lambda|=|\mu|=J}$. Numerical results show that the value of this condition number is bounded by 2.2 uniformly in J.

6.6 Proof of Theorem 6.3.3

In view of Remark 6.3.2, it suffices to construct uniform $L_2(\mathrm{I})$-Riesz bases Φ_j and $\tilde{\Phi}_j$ for V_j from (6.5) and $\tilde{V}_j$ from (6.6), respectively, such that $\langle\Phi_j, \tilde{\Phi}_j\rangle_{L_2(\mathrm{I})}$ is invertible, with an inverse that is bounded uniformly in j.

With $\varphi^{(1)}$ and $\varphi^{(2)}$ from (6.10), and $\varphi^{(3)} := \varphi^{(1)}(\cdot - 1)$ and $\varphi^{(4)} := \varphi^{(2)}(\cdot - 1)$,

$$\{\varphi^{(i)}(\cdot - k)\colon i \in \{1,\dots,4\},\ k \in 2\mathbb{Z}\} \tag{6.13}$$

spans the space of C^1 piecewise cubics with respect to the pieces $[k, k{+}1]$ ($k \in \mathbb{Z}$), see Figure 6.3(a). With $\tilde{\varphi}^{(i)}(x) := (x-1)^{i-1}|_{[0,2]}$, obviously

$$\{\tilde{\varphi}^{(i)}(\cdot - k)\colon i \in \{1,\dots,4\},\ k \in 2\mathbb{Z}\} \tag{6.14}$$

spans $\prod_{k\in 2\mathbb{Z}} P_3(k, k+2)$, see Figure 6.3(b).

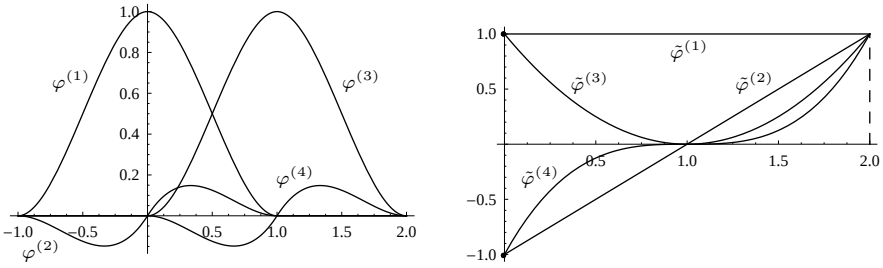

(a) $\{\varphi^{(1)}, \varphi^{(2)}, \varphi^{(3)}, \varphi^{(4)}\}$ from (6.13) (b) $\{\tilde{\varphi}^{(1)}, \tilde{\varphi}^{(2)}, \tilde{\varphi}^{(3)}, \tilde{\varphi}^{(4)}\}$ from (6.14)

Figure 6.3: Initial primal and dual scaling functions.

We apply a number of basis transformation at the primal and dual side. First we update $\varphi^{(1)}$, $\varphi^{(2)}$ with multiples of $\varphi^{(3)}$, $\varphi^{(3)}(\cdot + 2)$, $\varphi^{(4)}$, $\varphi^{(4)}(\cdot + 2)$, and $\tilde{\varphi}^{(1)}$, $\tilde{\varphi}^{(2)}$ with multiples of $\tilde{\varphi}^{(3)}$ and $\tilde{\varphi}^{(4)}$ in such a way that the new $\varphi^{(1)}$, $\varphi^{(2)}$ are orthogonal to $\tilde{\varphi}^{(3)}(\cdot - k)$ and $\tilde{\varphi}^{(4)}(\cdot - k)$ ($k \in 2\mathbb{Z}$), and the new $\tilde{\varphi}^{(1)}$, $\tilde{\varphi}^{(2)}$ are orthogonal to $\varphi^{(3)}$ and $\varphi^{(4)}$. In particular, we redefine

$$\begin{pmatrix} \varphi^{(1)} \\ \varphi^{(2)} \end{pmatrix} := \begin{pmatrix} \varphi^{(1)} \\ \varphi^{(2)} \end{pmatrix} + \begin{pmatrix} -2 & -2 & -\frac{45}{4} & \frac{45}{4} \\ -\frac{1}{4} & \frac{1}{4} & \frac{5}{4} & \frac{5}{4} \end{pmatrix} \begin{pmatrix} \varphi^{(3)} \\ \varphi^{(3)}(\cdot + 2) \\ \varphi^{(4)} \\ \varphi^{(4)}(\cdot + 2) \end{pmatrix},$$

$$\begin{pmatrix} \tilde{\varphi}^{(1)} \\ \tilde{\varphi}^{(2)} \end{pmatrix} := \begin{pmatrix} \tilde{\varphi}^{(1)} \\ \tilde{\varphi}^{(2)} \end{pmatrix} + \begin{pmatrix} -\frac{15}{2} & 0 \\ 0 & -\frac{7}{2} \end{pmatrix} \begin{pmatrix} \tilde{\varphi}^{(3)} \\ \tilde{\varphi}^{(4)} \end{pmatrix}.$$

To make two more inner products between local primal and dual functions zero, next we redefine

$$\begin{pmatrix} \tilde{\varphi}^{(1)} \\ \tilde{\varphi}^{(2)} \end{pmatrix} := \begin{pmatrix} -\frac{1}{4} & \frac{15}{16} \\ -\frac{1}{4} & -\frac{15}{16} \end{pmatrix} \begin{pmatrix} \tilde{\varphi}^{(1)} \\ \tilde{\varphi}^{(2)} \end{pmatrix}.$$

Furthermore, we multiply $\varphi^{(1)}$ with $\frac{2}{3}$ and $\varphi^{(2)}$ with $\frac{48}{7}$. Finally, we redefine

$$\begin{pmatrix} \tilde{\varphi}^{(1)} \\ \tilde{\varphi}^{(2)} \end{pmatrix} := \begin{pmatrix} 1 & 1 \\ 1 & -1 \end{pmatrix} \begin{pmatrix} \tilde{\varphi}^{(1)} \\ \tilde{\varphi}^{(2)}(\cdot + 2) \end{pmatrix}.$$

By the last transformation, as $\varphi^{(1)}$ ($\varphi^{(2)}$) the function $\tilde{\varphi}^{(1)}$ ($\tilde{\varphi}^{(2)}$) is even (odd).

The newly defined primal and dual scaling functions are illustrated in Figures 6.4(a) and 6.4(b), respectively. Note that our transformations did not change the spans of the collections (6.13) and (6.14).

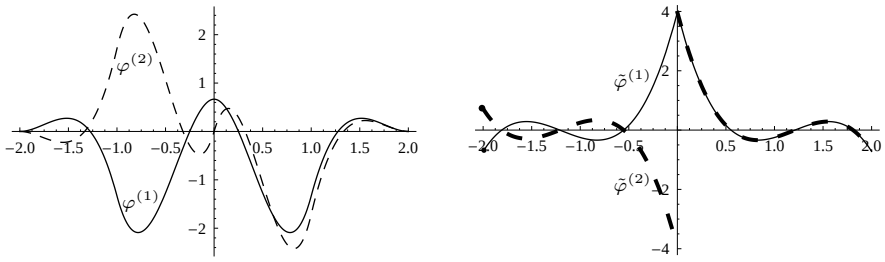

(a) $\{\varphi^{(1)}, \varphi^{(2)}\}$ (b) $\{\tilde{\varphi}^{(1)}, \tilde{\varphi}^{(2)}\}$

Figure 6.4: New primal and dual scaling functions.

A direct computation shows that

$$\left\langle \begin{pmatrix} \varphi^{(1)} \\ \varphi^{(2)} \\ \varphi^{(1)}(\cdot - 2) \\ \varphi^{(2)}(\cdot - 2) \\ \varphi^{(3)} \\ \varphi^{(4)} \end{pmatrix}, \begin{pmatrix} \tilde{\varphi}^{(1)} \\ \tilde{\varphi}^{(2)} \\ \tilde{\varphi}^{(1)}(\cdot - 2) \\ \tilde{\varphi}^{(2)}(\cdot - 2) \\ \tilde{\varphi}^{(3)} \\ \tilde{\varphi}^{(4)} \end{pmatrix} \right\rangle_{L_2(0,2)} = \left(\begin{array}{cccc|cc} \frac{1}{2} & \frac{1}{2} & 0 & 0 & 0 & 0 \\ \frac{1}{2} & \frac{1}{2} & \frac{1}{14} & -\frac{1}{14} & 0 & 0 \\ 0 & 0 & \frac{1}{2} & -\frac{1}{2} & 0 & 0 \\ -\frac{1}{14} & -\frac{1}{14} & -\frac{1}{2} & \frac{1}{2} & 0 & 0 \\ \hline 0 & 0 & 0 & 0 & \frac{2}{15} & 0 \\ 0 & 0 & 0 & 0 & 0 & \frac{2}{105} \end{array}\right). \quad (6.15)$$

With

$$\varphi_{j,k}^{(i)} := \sqrt{2^{j+1}}\, \varphi^{(i)}(2^{j+1} \cdot - k), \qquad \tilde{\varphi}_{j,k}^{(i)} := \sqrt{2^{j+1}}\, \tilde{\varphi}^{(i)}(2^{j+1} \cdot - k)$$

and

$$\begin{aligned} \Phi_j^{(1)} &:= \{\varphi_{j,k}^{(1)} \colon k \in \{2, \dots, 2^{j+1} - 2\}\} \cup \{\varphi_{j,k}^{(2)}|_{\mathrm{I}} \colon k \in \{0, 2, \dots, 2^{j+1}\}\}, \\ \Phi_j^{(2)} &:= \{\varphi_{j,k}^{(i)} \colon i \in \{3, 4\},\ k \in \{0, 2, \dots, 2^{j+1} - 2\}\}, \\ \tilde{\Phi}_j^{(1)} &:= \{\tilde{\varphi}_{j,k}^{(1)} \colon k \in \{2, \dots, 2^{j+1} - 2\}\} \cup \{\tilde{\varphi}_{j,k}^{(2)}|_{\mathrm{I}} \colon k \in \{0, 2, \dots, 2^{j+1}\}\}, \\ \tilde{\Phi}_j^{(2)} &:= \{\tilde{\varphi}_{j,k}^{(i)} \colon i \in \{3, 4\},\ k \in \{0, 2, \dots, 2^{j+1} - 2\}\}, \end{aligned}$$

the collections $\Phi_j := \Phi_j^{(1)} \cup \Phi_j^{(2)}$ and $\tilde{\Phi}_j := \tilde{\Phi}_j^{(1)} \cup \tilde{\Phi}_j^{(2)}$ are uniform $L_2(\mathrm{I})$-Riesz bases for V_j and $\tilde{V}_j$, respectively. Indeed, one verifies that $\operatorname{span} \Phi_j \subset V_j$, $\operatorname{span} \tilde{\Phi}_j \subset \tilde{V}_j$ and that $\#\Phi_j = \dim V_j = 2^{j+1} = \dim \tilde{V}_j = \#\tilde{\Phi}_j$. From the local supports and the proper normalization of the basis functions, one also easily verifies that for any coefficient vector $\mathbf{c}_j$ of the appropriate size, $\|\mathbf{c}_j^{\mathsf{T}} \Phi_j\|_{L_2(\mathrm{I})} \lesssim \|\mathbf{c}_j\|_{\ell_2}$ and $\|\mathbf{c}_j^{\mathsf{T}} \tilde{\Phi}_j\|_{L_2(\mathrm{I})} \lesssim \|\mathbf{c}_j\|_{\ell_2}$. Instead of a direct verification that also $\|\mathbf{c}_j^{\mathsf{T}} \Phi_j\|_{L_2(\mathrm{I})} \gtrsim \|\mathbf{c}_j\|_{\ell_2}$ and $\|\mathbf{c}_j^{\mathsf{T}} \tilde{\Phi}_j\|_{L_2(\mathrm{I})} \gtrsim \|\mathbf{c}_j\|_{\ell_2}$ are valid, i.e., that Φ_j and $\tilde{\Phi}_j$ are uniform $L_2(\mathrm{I})$-Riesz bases for their spans, it suffices to verify that $\langle \Phi_j, \tilde{\Phi}_j \rangle_{L_2(\mathrm{I})}$ is invertible, with an inverse that is bounded uniformly in j, which we will do below. Indeed, from

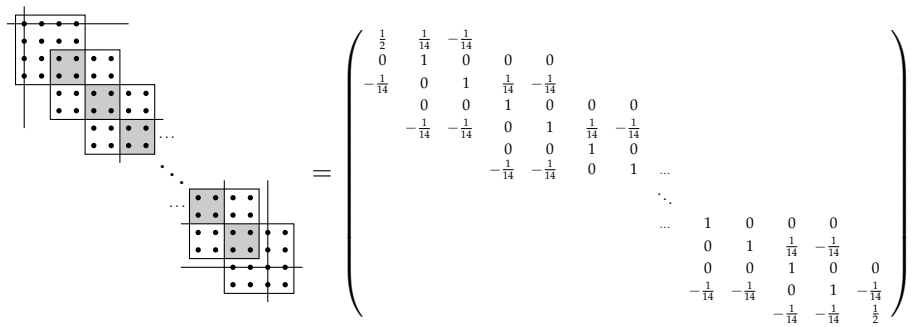

Figure 6.5: The assembling of $\langle \Phi_j^{(1)}, \tilde{\Phi}_j^{(1)} \rangle_{L_2(\mathrm{I})}$ from the 4×4 left upper block from (6.10).

this property and $\|\mathbf{c}_j^{\mathsf{T}} \Phi_j\|_{L_2(\mathrm{I})} \lesssim \|\mathbf{c}_j\|_{\ell_2}$, we obtain

$$\|\tilde{\mathbf{c}}_j\|_{\ell_2} \lesssim \|\langle \Phi_j, \tilde{\Phi}_j \rangle_{L_2(\mathrm{I})} \tilde{\mathbf{c}}_j\|_{\ell_2} = \sup_{\mathbf{c}_j \neq 0} \frac{|\langle \mathbf{c}_j, \langle \Phi_j, \tilde{\Phi}_j \rangle_{L_2(\mathrm{I})} \tilde{\mathbf{c}}_j \rangle_{\ell_2}|}{\|\mathbf{c}_j\|_{\ell_2}} = \sup_{\mathbf{c}_j \neq 0} \frac{|\langle \mathbf{c}_j^{\mathsf{T}} \Phi_j, \tilde{\mathbf{c}}_j^{\mathsf{T}} \tilde{\Phi}_j \rangle_{L_2(\mathrm{I})}|}{\|\mathbf{c}_j\|_{\ell_2}}$$

$$\lesssim \|\tilde{\mathbf{c}}_j^{\mathsf{T}} \tilde{\Phi}_j\|_{L_2(\mathrm{I})} \sup_{\mathbf{c}_j \neq 0} \frac{\|\mathbf{c}_j^{\mathsf{T}} \Phi_j\|_{L_2(\mathrm{I})}}{\|\mathbf{c}_j\|_{\ell_2}} \lesssim \|\tilde{\mathbf{c}}_j^{\mathsf{T}} \tilde{\Phi}_j\|_{L_2(\mathrm{I})},$$

and similarly, using $\|\tilde{\mathbf{c}}_j^{\mathsf{T}} \tilde{\Phi}_j\|_{L_2(\mathrm{I})} \lesssim \|\tilde{\mathbf{c}}_j\|_{\ell_2}$, that $\|\mathbf{c}_j\|_{\ell_2} \lesssim \|\mathbf{c}_j^{\mathsf{T}} \Phi_j\|_{L_2(\mathrm{I})}$.

For $i \neq i'$, $\langle \Phi_j^{(i)}, \tilde{\Phi}_j^{(i')} \rangle_{L_2(\mathrm{I})} = 0$, and $\langle \Phi_j^{(2)}, \tilde{\Phi}_j^{(2)} \rangle_{L_2(\mathrm{I})}$ is a diagonal matrix that is uniformly spectrally equivalent to the identity matrix. The matrix $\langle \Phi_j^{(1)}, \tilde{\Phi}_j^{(1)} \rangle_{L_2(\mathrm{I})}$ is assembled from the 4×4 left upper block from (6.15) as indicated in Figure 6.5, where in the overlays the matrices should be added. The striking out of the first and the one but last rows and columns corresponds to the fact that for $k \in \{0, 2^{j+2}\}$, the functions $\varphi_{j,k}^{(1)}$ and $\tilde{\varphi}_{j,k}^{(1)}$ are not in Φ_j and $\tilde{\Phi}_j$, respectively. By multiplying the first and last rows and columns of $\langle \Phi_j^{(1)}, \tilde{\Phi}_j^{(1)} \rangle_{L_2(\mathrm{I})}$ with $\sqrt{2}$, a matrix of the form $I - B_j$ is obtained, where $\|B_j\| \leq \sqrt{\|B_j\|_1 \|B_j\|_\infty} \leq \rho$ for some $\rho < 1$ independent of j. Such a matrix is invertible, with a uniformly bounded inverse, with which the proof of Theorem 6.3.3 is completed. $\Diamond$

Bibliography

[Bar01] Titus Barsch. *Adaptive Multiskalenverfahren für elliptische partielle Differentialgleichungen—Realisierung, Umsetzung un numerische Ergebnisse*. PhD thesis, RWTH Aachen, Aachen, 2001. Referenced on page 29.

[Bar05] Arne Barinka. *Fast Evaluation Tools for Adaptive Wavelet Schemes*. PhD thesis, RTWH Aachen, March 2005. Referenced on page 89.

[BDM00] Arne Barinka, Stephan Dahlke, and Nicole Mulders. The IGPM Villemoes machine. Technical Report 184, IGPM, RWTH Aachen, 2000. Referenced on page 17.

[BF03] Silvia Bertoluzza and Silvia Falletta. Building wavelets on $]0,1[$ at large scales. *J. Fourier Anal. Appl.*, 9(3):261–288, 2003. Referenced on page 21.
doi:10.1007/s00041-003-0014-0

[BG04] Hans-Joachim Bungartz and Michael Griebel. Sparse grids. *Acta Numer.*, 13:147–269, 2004. Referenced on pages 45, 76 and 107.
doi:10.1017/S0962492904000182

[Bit05] Kai Bittner. A new view on biorthogonal spline wavelets. Preprint, Universität Ulm, 2005. Referenced on page 37.

[Bit06] Kai Bittner. Biorthogonal spline wavelets on the interval. In *Wavelets and Splines: Athens 2005*, pages 93–104. Nashboro Press, Brentwood, TN, 2006. Referenced on page 7.

[Bur05] Carsten Burstedde. *Fast Optimised Wavelet Methods for Control Problems Constrained by Elliptic PDEs*. PhD thesis, Rheinischen Friedrich-Wilhelms-Universität Bonn, 2005. Referenced on page 21.

[CDD01] Albert Cohen, Wolfgang Dahmen, and Ronald DeVore. Adaptive wavelet methods for elliptic operator equations: convergence rates. *Math. Comp.*, 70(233):27–75, 2001. Referenced on pages 2, 78, 79, 86, 91, 92, 95 and 106.
doi:10.1090/S0025-5718-00-01252-7

[CDD02] Albert Cohen, Wolfgang Dahmen, and Ronald DeVore. Adaptive wavelet methods. II. Beyond the elliptic case. *Found. Comput. Math.*, 2(3):203–245, 2002. Referenced on page 78.
doi:10.1007/s102080010027

[CDF92] Albert Cohen, Ingrid Daubechies, and Jean-Christophe Feauveau. Biorthogonal bases of compactly supported wavelets. *Comm. Pure Appl. Math.*, 45(5):485–560, 1992. Referenced on pages 7, 16, 17, 18, 19, 20, 26 and 29.
doi:10.1002/cpa.3160450502

[Coh03] Albert Cohen. *Numerical analysis of wavelet methods*, volume 32 of *Studies in Mathematics and its Applications*. North-Holland Publishing Co., Amsterdam, 2003. Referenced on pages 46, 77 and 109.

[CT99] Claudio Canuto and Anita Tabacco. *Ondine Biortogonali: teoria e applicazioni*, volume 46 of *Quaderni dell'Unione Matematica Italiana*. Pitagora Editrice, Bologna, 1999. Referenced on page 16.

[Dah95] Wolfgang Dahmen. Multiscale analysis, approximation, and interpolation spaces. In *Approximation theory VIII, Vol. 2 (College Station, TX, 1995)*, volume 6 of *Ser. Approx. Decompos.*, pages 47–88. World Sci. Publ., River Edge, NJ, 1995. Referenced on page 17.

[Dah96] Wolfgang Dahmen. Stability of multiscale transformations. *J. Fourier Anal. Appl.*, 2(4):314–361, 1996. Referenced on page 109.

[Dah97] Wolfgang Dahmen. Wavelet and multiscale methods for operator equations. In *Acta numerica, 1997*, volume 6 of *Acta Numer.*, pages 55–228. Cambridge Univ. Press, Cambridge, 1997. Referenced on page 110.

[Dau88a] Ingrid Daubechies. Orthonormal bases of compactly supported wavelets. *Comm. Pure Appl. Math.*, 41(7):909–996, 1988. Referenced on page 81.
doi:10.1002/cpa.3160410705

[Dau88b] Monique Dauge. *Elliptic boundary value problems on corner domains*, volume 1341 of *Lecture Notes in Mathematics*. Springer-Verlag, Berlin, 1988. Smoothness and asymptotics of solutions. Referenced on page 77.

[dB01] Carl de Boor. *A practical guide to splines*, volume 27 of *Applied Mathematical Sciences*. Springer-Verlag, New York, revised edition, 2001. Referenced on pages 15, 16 and 19.

[DeV98] Ronald A. DeVore. Nonlinear approximation. In *Acta numerica, 1998*, volume 7 of *Acta Numer.*, pages 51–150. Cambridge Univ. Press, Cambridge, 1998. Referenced on pages 77 and 93.

[DGH96] George C. Donovan, Jeffrey S. Geronimo, and Douglas P. Hardin. Intertwining multiresolution analyses and the construction of piecewise-polynomial wavelets. *SIAM J. Math. Anal.*, 27(6):1791–1815, 1996. Referenced on pages 79, 81 and 82.
doi:10.1137/S0036141094276160

[DGH99] George C. Donovan, Jeffrey S. Geronimo, and Douglas P. Hardin. Orthogonal polynomials and the construction of piecewise polynomial smooth wavelets. *SIAM J. Math. Anal.*, 30(5):1029–1056, 1999. Referenced on pages 79, 81 and 82.
doi:10.1137/S0036141096313112

[DHS06] Wolfgang Dahmen, Helmut Harbrecht, and Reinhold Schneider. Compression techniques for boundary integral equations—asymptotically optimal complexity estimates. *SIAM J. Numer. Anal.*, 43(6):2251–2271, 2006. Referenced on pages 86 and 92.
doi:10.1137/S0036142903428852

[DKU97] Wolfgang Dahmen, Angela Kunoth, and Karsten Urban. Wavelets in numerical analysis and their quantitative properties. In *Surface fitting and multiresolution methods (Chamonix–Mont-Blanc, 1996)*, pages 93–130. Vanderbilt Univ. Press, Nashville, TN, 1997. Referenced on pages 7 and 31.

[DKU99] Wolfgang Dahmen, Angela Kunoth, and Karsten Urban. Biorthogonal spline wavelets on the interval—stability and moment conditions. *Appl. Comput. Harmon. Anal.*, 6(2):132–196, 1999. Referenced on pages 3, 5, 7, 8, 19, 21, 23, 24, 29, 30 and 31.
doi:10.1006/acha.1998.0247

[DM93a] Wolfgang Dahmen and Charles A. Micchelli. Banded matrices with banded inverses. II. Locally finite decomposition of spline spaces. *Constr. Approx.*, 9(2-3):263–281, 1993. Referenced on pages 26, 27 and 28.
doi:10.1007/BF01198006

[DM93b] Wolfgang Dahmen and Charles A. Micchelli. Using the refinement equation for evaluating integrals of wavelets. *SIAM J. Numer. Anal.*, 30(2):507–537, 1993. Referenced on pages 13 and 30.
doi:10.1137/0730024

[DP06] Erwan Deriaz and Valérie Perrier. Divergence-free and curl-free wavelets in two dimensions and three dimensions: application to turbulent flows. *J. Turbul.*, 7:1–37, 2006. Referenced on pages 65 and 66.
doi:10.1080/14685240500260547

[DS98] Wolfgang Dahmen and Reinhold Schneider. Wavelets with complementary boundary conditions—function spaces on the cube. *Results Math.*, 34(3-4):255–293, 1998. Referenced on page 34.

[DS99a] Wolfgang Dahmen and Reinhold Schneider. Composite wavelet bases for operator equations. *Math. Comp.*, 68(228):1533–1567, 1999. Referenced on page 3.
doi:10.1090/S0025-5718-99-01092-3

[DS99b] Wolfgang Dahmen and Reinhold Schneider. Wavelets on manifolds. I. Construction and domain decomposition. *SIAM J. Math. Anal.*, 31(1):184–230, 1999. Referenced on page 3.
doi:10.1137/S0036141098333451

[DS99c] Wolfgang Dahmen and Rob Stevenson. Element-by-element construction of wavelets satisfying stability and moment conditions. *SIAM J. Numer. Anal.*, 37(1):319–352, 1999. Referenced on pages 9 and 109.
doi:10.1137/S0036142997330949

[DS09] Monique Dauge and Rob Stevenson. Sparse tensor product wavelet approximation of singular functions. Draft, 2009. Referenced on pages 4, 61, 77 and 107.

[DSS09] Tammo Jan Dijkema, Christoph Schwab, and Rob Stevenson. An adaptive wavelet method for solving high-dimensional elliptic PDEs. *Constr. Approx.*, 2009. Accepted for publication. Referenced on page 5.

[DW93] Stephan Dahlke and Ilona Weinreich. Wavelet-Galerkin methods: an adapted biorthogonal wavelet basis. *Constr. Approx.*, 9(2-3):237–262, 1993. Referenced on page 108.
doi:10.1007/BF01198005

[FH65] Richard P. Feynman and Albert R. Hibbs. *Quantum Mechanics and Path Integrals*. McGraw-Hill Companies, 1965. Referenced on page 75.

[Fre85] Mark I. Freidlin. *Functional integration and partial differential equations*, volume 109 of *Annals of Mathematics Studies*. Princeton University Press, Princeton, NJ, 1985. Referenced on page 75.

[GHK05] Ivan P. Gavrilyuk, Wolfgang Hackbusch, and Boris N. Khoromskij. Hierarchical tensor-product approximation to the inverse and related operators for high-dimensional elliptic problems. *Computing*, 74(2):131–157, 2005. Referenced on page 102.
doi:10.1007/s00607-004-0086-y

[GHS07] Tsogtgerel Gantumur, Helmut Harbrecht, and Rob Stevenson. An optimal adaptive wavelet method without coarsening of the iterands. *Math. Comp.*, 76(258):615–629, 2007. Referenced on pages 2, 79, 86, 90, 91, 96 and 106.
doi:10.1090/S0025-5718-06-01917-X

[GK00] Michael Griebel and Stephan Knapek. Optimized tensor-product approximation spaces. *Constr. Approx.*, 16(4):525–540, 2000. Referenced on pages 4, 45, 53, 76 and 98.
doi:10.1007/s003650010010

[GK08] Michael Griebel and Stephan Knapek. Optimized general sparse grid approximation spaces for operator equations. *Math. Comp.*, 2008. Referenced on page 45.

[GO95] Michael Griebel and Peter Oswald. Tensor product type subspace splittings and multilevel iterative methods for anisotropic problems. *Adv. Comput. Math.*, 4(1-2):171–206, 1995. Referenced on pages 48 and 81.
doi:10.1007/BF02123478

[Goo03] Tim N. T. Goodman. A class of orthogonal refinable functions and wavelets. *Constr. Approx.*, 19(4):525–540, 2003. Referenced on pages 79 and 81.
doi:10.1007/s00365-003-0535-4

[Gra04] Lars Grasedyck. Existence and computation of low Kronecker-rank approximations for large linear systems of tensor product structure. *Computing*, 72(3-4):247–265, 2004. Referenced on page 102.
doi:10.1007/s00607-003-0037-z

[GS06] Tsogtgerel Gantumur and Rob Stevenson. Computation of differential operators in wavelet coordinates. *Math. Comp.*, 75(254):697–709, 2006. Referenced on page 85.
doi:10.1090/S0025-5718-06-01917-X

[Hac94] Wolfgang Hackbusch. *Iterative solution of large sparse systems of equations*, volume 95 of *Applied Mathematical Sciences*. Springer-Verlag, New York, 1994. Translated and revised from the 1991 German original. Referenced on page 96.

[Har01] Helmut Harbrecht. *Wavelet Galerkin schemes for the boundary element method in three dimensions*. PhD thesis, Technische Universität Chemnitz, 2001. Referenced on pages 27, 28 and 29.

[HKZ00] Reinhard Hochmuth, Stephan Knapek, and Gerhard Zumbusch. Tensor products of Sobolev spaces, approximation spaces and applications. SFB 256 685, Universität Bonn, 2000. Referenced on page 59.

[HS05] Viet Ha Hoang and Christoph Schwab. High-dimensional finite elements for elliptic problems with multiple scales. *Multiscale Model. Simul.*, 3(1):168–194, 2004/05. Referenced on page 75.
doi:10.1137/030601077

[LC85] Ward A. Light and E. Will Cheney. *Approximation theory in tensor product spaces*, volume 1169 of *Lecture Notes in Mathematics*. Springer-Verlag, Berlin, 1985. Referenced on page 47.

[LM72] Jacques-Louis Lions and Enrico Magenes. *Non-homogeneous boundary value problems and applications. Vol. II*, volume 182 of *Die Grundlehren der mathematischen Wissenschaften*. Springer-Verlag, New York, 1972. Translated from the French by P. Kenneth. Referenced on pages 46 and 111.

[LR91] Pierre Gilles Lemarié-Rieusset. Fonctions à support compact dans les analyses multi-résolutions. *Rev. Mat. Iberoamericana*, 7(2):157–182, 1991. Referenced on page 20.

[LR92] Pierre Gilles Lemarié-Rieusset. Analyses multi-résolutions non orthogonales, commutation entre projecteurs et derivation et ondelettes vecteurs à divergence nulle. *Rev. Mat. Iberoamericana*, 8:221–237, 1992. Referenced on page 66.

[Met02] Arnold Metselaar. *Handling Wavelet Expansions in Numerical Methods*. PhD thesis, University of Twente, 2002. Referenced on pages 17 and 89.

[Mey91] Yves Meyer. Ondelettes sur l'intervalle. *Rev. Mat. Iberoamericana*, 7(2):115–133, 1991. Referenced on page 20.

[Ngu05] Hoang Nguyen. *Finite element wavelets for solving partial differential equations*. PhD thesis, Universiteit Utrecht, 2005. Referenced on page 10.

[Nit05] Pál-Andrej Nitsche. Sparse approximation of singularity functions. *Constr. Approx.*, 21(1):63–81, 2005. Referenced on pages 4, 61 and 77.
doi:10.1007/s00365-004-0559-4

[Nit06] Pál-Andrej Nitsche. Best N-term approximation spaces for tensor product wavelet bases. *Constructive Approximation*, 24(1):49–70, 2006. Referenced on pages 4 and 77.
doi:10.1007/s00365-005-0609-6

[Pri06] Miriam Primbs. *Stabile biorthogonale Spline-Waveletbasen auf dem Intervall*. PhD thesis, Universität Duisburg-Essen, 2006. Referenced on pages 5, 7, 8, 17, 21, 24, 29, 35, 36 and 135.

[Pri08] Miriam Primbs. On the computation of Gramian matrices for refinable bases on the interval. *Int. J. Wavelets Multiresolut. Inf. Process.*, 6(3):459–479, 2008. Referenced on page 30.
doi:10.1142/S0219691308002422

[SF98] Kai Schneider and Marie Farge. Wavelet approach for modelling and computing turbulence. In *Advances in turbulence modelling*, Lecture Series 1998-5. Von Karman Institute for Fluid Dynamics, Brussels, 1998. Referenced on page 65.

[SS08] Christoph Schwab and Rob Stevenson. Adaptive wavelet algorithms for elliptic PDE's on product domains. *Math. Comp.*, 77(261):71–92, 2008. Referenced on pages 78, 85 and 99.
doi:10.1090/S0025-5718-07-02019-4

[SSZ99] Gilbert Strang, Vasily Strela, and Ding-Xuan Zhou. Compactly supported refinable functions with infinite masks. In *The functional and harmonic analysis of wavelets and frames (San Antonio, TX, 1999)*, volume 247 of *Contemp. Math.*, pages 285–296. Amer. Math. Soc., Providence, RI, 1999. Referenced on page 13.

[Ste03] Rob Stevenson. Locally supported, piecewise polynomial biorthogonal wavelets on nonuniform meshes. *Constr. Approx.*, 19(4):477–508, 2003. Referenced on pages 10 and 110.
doi:10.1007/s00365-003-0545-2

[Ste08] Rob Stevenson. Divergence-free wavelet bases on the hypercube. Preprint. University of Amsterdam, October 2008. Referenced on pages 65, 72 and 73.

[Sun91] Qiyu Sun. Two-scale difference equation: local and global linear independence. Manuscript, 1991. Referenced on page 17.

[Thi04] Henning Thielemann. Bounds for smoothness of refinable functions. *Linear Algebra Appl.*, 391:245–260, 2004. Referenced on page 17.
doi:10.1016/j.laa.2004.03.037

[Tod09] Radu Alexandru Todor. A new approach to energy-based sparse finite-element spaces. *IMA J. Numer. Anal.*, 29(1):72–85, 2009. Referenced on page 45.
doi:10.1093/imanum/drm041

[TS07] Radu Alexandru Todor and Christoph Schwab. Convergence rates for sparse chaos approximations of elliptic problems with stochastic coefficients. *IMA J. Numer. Anal.*, 27(2):232–261, 2007. Referenced on page 75.
doi:10.1093/imanum/drl025

[TtMvD00] Cees Traas, Hennie ter Morsche, and Ruud van Damme. *Splines en wavelets*. Epsilon Uitgaven, Utrecht, 2000. Referenced on page 16.

[Urb02] Karsten Urban. *Wavelets in numerical simulation: Problem adapted construction and applications*, volume 22 of *Lecture Notes in Computational Science and Engineering*. Springer-Verlag, Berlin, 2002. Referenced on page 65.

[Vil94] Lars F. Villemoes. Wavelet analysis of refinement equations. *SIAM J. Math. Anal.*, 25(5):1433–1460, 1994. Referenced on page 17.
doi:10.1137/S0036141092228179

[Yse05] Harry Yserentant. Sparse grid spaces for the numerical solution of the electronic Schrödinger equation. *Numer. Math.*, 101(2):381–389, 2005. Referenced on page 75.
doi:10.1007/s00211-005-0581-x

[Zen91] Christoph Zenger. Sparse grids. In *Parallel algorithms for partial differential equations (Kiel, 1990)*, volume 31 of *Notes Numer. Fluid Mech.*, pages 241–251. Vieweg, Braunschweig, 1991. Referenced on pages 4, 45 and 76.

List of symbols

$\eqsim$	equivalent ... 8
$\lesssim$	smaller than, up to some constant factor ... 8
$\gtrsim$	greater than, up to some constant factor ... 8
$\square$	the unit n-cube I^n ... 47
$\boldsymbol{\Delta}$	Laplace operator ... 73, 101, 105
∇	index set ... 7
$\boldsymbol{\nabla}$	index set ∇^n ... 48
$\boldsymbol{\nabla}_J^{\text{full}}$	full grid index set ... 49
$\boldsymbol{\nabla}_J^{(\gamma)}$	sparse grid index set $\gamma = 0$: normal sparse grid index set ... 50 $\gamma > 0$: concave sparse grid index set ... 54 $\gamma < 0$: convex sparse grid index set ... 56
$(a_k)_k$	mask of ${}_d\varphi$ ... 16
$(\tilde{a}_k)_k$	mask of ${}_{d,\tilde{d}}\tilde{\varphi}$ ... 17
$\vec{A}$	one-dimensional stiffness matrix ... 83, 106
$\vec{A}^{(j)}$	sparse approximation to $\vec{A}$ ... 83
$\mathbf{A}$	stiffness matrix ... 78, 106
$\mathbf{A}^{(j)}$	sparse approximation to $\mathbf{A}$ ... 84
$\mathcal{A}_\tau^s$	approximation space ... 77
$B_{d,\mathbf{t}}^k$	k-th B-spline of order d w.r.t. $\mathbf{t}$ ... 15
γ	Bernstein estimate ... 9
$\tilde{\gamma}$	dual Bernstein estimate ... 10, 17
Γ, Γ_D	Dirichlet boundary ... 70, 73, 76
$\tilde{\Gamma}$	Neumann boundary ... 70, 73
$\mathbf{c}$	vector in ℓ_2 ... 7
C_1, C_2	Riesz constants ... 7
$\check{\mathbf{C}}^L$, $\check{\mathbf{C}}^R$	boundary blocks of $\tilde{\mathbf{R}}_j^{\text{init}}$ ... 22
d	order of Jackson estimate ... 9, 46

$\tilde{d}$	order of dual Jackson estimate ... 10
φ	mother scaling function ... 14
$\varphi_{j,k}$	scaling function ... 19
$\varphi_{[j,k]}$	scaling function on $\mathbb{R}$ ... 14, 66
${}_d\varphi$	CDF scaling function of order d ... 16
φ_ℓ	Fourier basis function $\sqrt{2}\sin(\ell\pi\cdot)$ ... 58
$\tilde{\varphi}$	dual mother scaling function ... 14
$\tilde{\varphi}_{j,k}$	dual scaling function ... 20
$\tilde{\varphi}_{[j,k]}$	dual scaling function on $\mathbb{R}$ ... 14, 66
${}_{d,\tilde{d}}\tilde{\varphi}$	dual CDF scaling function of orders d, $\tilde{d}$ ... 17
$\boldsymbol{\Phi}_j$	collection of scaling functions ... 9, 18
$\boldsymbol{\Phi}_{[j]}$	collection of scaling functions on $\mathbb{R}$ ... 14
$\tilde{\boldsymbol{\Phi}}_j$	collection of dual scaling functions ... 9, 21
$\tilde{\boldsymbol{\Phi}}_{[j]}$	collection of dual scaling functions on $\mathbb{R}$ ... 14, 20
H	separable Hilbert space ... 7
H^s	Sobolev space (for integer s) ... 8, 33, 46, 111
$\mathcal{H}^s$	Sobolev space (for fractional s) ... 8, 33, 46, 110
$\mathcal{H}^{\boldsymbol{s}}(\square)$	$\mathcal{H}^{s_1}(\mathrm{I})\otimes\cdots\otimes\mathcal{H}^{s_n}(\mathrm{I})$ ... 49
$\mathscr{H}_{s,t}(\square)$	$\mathcal{H}^{(s,t,\ldots,t)}(\square)\cap\cdots\cap\mathcal{H}^{(t,\ldots,t,s)}(\square)$ ... 49
$\mathbf{H}(\operatorname{div}0;\mathbb{R}^n)$	the space $\{\mathbf{u}\in\mathbf{H}(\operatorname{div};\mathbb{R}^n)\colon \operatorname{div}\mathbf{u}=0\}$ ... 65
$\mathbf{H}(\operatorname{div};\mathbb{R}^n)$	the space $\{\mathbf{u}\in L_2(\mathbb{R}^n)^n\colon \operatorname{div}\mathbf{u}\in L_2(\mathbb{R}^n)\}$ ... 65
$\mathbf{H}_{0,\Gamma}(\operatorname{div};\square)$	$\mathbf{H}(\operatorname{div};\square)$ with Dirichlet boundaries Γ ... 70
$\mathbf{H}_{0,\Gamma}(\operatorname{div}0;\square)$	$\mathbf{H}(\operatorname{div}0;\square)$ with Dirichlet boundaries Γ ... 70
I	the interval $(0,1)$ ... 18
I_j	index set ... 18, 50, 54, 56
$\mathbf{I}$	identity matrix ... 8
j_0	lowest level ... 21
$j_{\min}$	reduced lowest level ... 31
$\kappa(\Sigma)$	condition number of Σ ... 7
λ	index in ∇ ... 7, 46
$\boldsymbol{\lambda}$	index in $\boldsymbol{\nabla}$ ... 48
$[\ell_1,\ell_2]$	support of ${}_d\varphi$ ... 16
$[\tilde{\ell}_1,\tilde{\ell}_2]$	support of ${}_{d,\tilde{d}}\tilde{\varphi}$ ... 17
$\mu(d)$	d mod 2 ... 17
m_L, m_R	order of boundary conditions ... 16, 33
$\tilde{m}_L, \tilde{m}_R$	order of dual boundary conditions ... 33
$\mathbf{M}_j$	two-scale matrix ... 12
$\mathbf{M}_{j,0}$	refinement matrix ... 9
$\mathbf{M}_{j,1}$	wavelet matrix ... 11

Index

Samenvatting

In deze samenvatting zal ik proberen iets van de inhoud van dit proefschrift zodanig uit te leggen, dat de meerderheid van de lezers het kan volgen. Hier zal de wiskundige grondigheid onder lijden, maar ik hoop dat de rest van dit proefschrift dat compenseert.

Veel verschijnselen, bijvoorbeeld het weer, of de beurskoersen, kunnen worden beschreven met differentiaalvergelijkingen. Daarin speelt de 'helling' van een grootheid op oneindig kleine gebiedjes een rol. Laten we die onbekende grootheid, die bijvoorbeeld de temperatuur op een bepaalde plaats kan voorstellen, u noemen. Zie figuur 1 voor een illustratie.

In veel realistische gevallen kunnen differentiaalvergelijkingen niet opgelost worden: er is wel een oplossing, maar daar kun je geen functievoorschrift voor vinden. Om toch een idee te krijgen van de oplossing, kun je die alleen zoeken op een beperkt aantal punten (zie figuur 1). Door deze zogenaamde discretisatie kan een benaderde oplossing $\tilde{u}$ op de roosterpunten worden gevonden. De benaderde oplossing $\tilde{u}$ is in het algemeen niet gelijk aan de echte oplossing u, zelfs niet op de roosterpunten. Dit komt doordat je in plaats van naar de helling op oneindig kleine gebiedjes nu slechts nog kijkt naar de gemiddelde helling op 'erg kleine' gebiedjes. Hoe kleiner je die gebiedjes neemt, des te beter $\tilde{u}$ op u zal lijken. Voor zogenaamde eersteordemethoden halveert de fout $\tilde{u} - u$ als de afstand tussen de roosterpunten halveert.

Het halveren van de afstand tussen roosterpunten brengt met zich mee dat er meer roosterpunten genomen moeten worden. En hoe meer roosterpunten er zijn, hoe langer een computer zal moeten rekenen om $\tilde{u}$ te vinden. De toename van het aantal roosterpunten hangt af van de dimensie van het definitiegebied van de differentiaalvergelijking. In één dimensie, op een lijnstuk, moet je het aantal punten verdubbelen om de afstand te halveren. In twee dimensies moet je om diezelfde halvering te bereiken, al vier keer zo veel punten nemen. In het algemeen moet je voor een halvering van de afstand tussen roosterpunten 2^n keer zo veel punten nemen, waarin n de dimensie van het probleem is.

Het feit dat het rekenwerk toeneemt met een factor 2^n terwijl de fout maar met een factor 2 afneemt, wordt de 'dimensievloek' (*curse of dimensionality*) genoemd: bij grotere dimensies wordt de hoeveelheid rekenwerk zo groot, dat het niet meer haalbaar is om een goede benadering te vinden binnen redelijke tijd.

In dit proefschrift wordt aangetoond dat deze dimensievloek omzeild kan worden voor problemen die zich afspelen op 'vierkante' gebieden, bijvoorbeeld

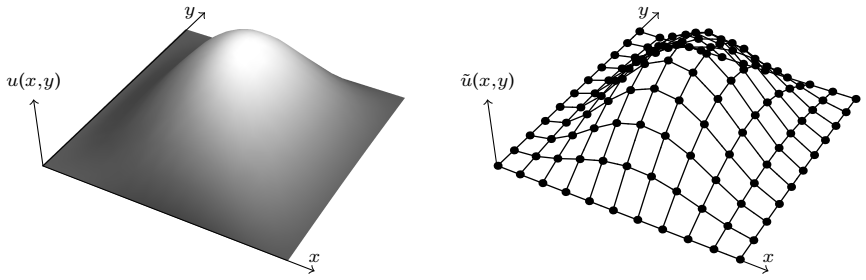

Figuur 1: Een functie op een tweedimensionaal gebied (links) en haar discretisatie (rechts).

vierkanten, kubussen en analoga in hogere dimensies. Laten we ons voor het moment even beperken tot twee dimensies. Voor dit soort problemen kun je de nog onbekende oplossing u schrijven als een gewogen som van bekende 'basisfuncties':

$$u(x,y) = c_1 \cdot \psi_1(x,y) + c_2 \cdot \psi_2(x,y) + c_3 \cdot \psi_3(x,y) + \ldots$$

Hierin zijn alleen de getallen c_1, c_2, ... nog onbekend. De oorspronkelijke differentiaalvergelijking kan nu worden geschreven als een probleem waarin alleen deze getallen een rol spelen. Heb je de getallen c_i gevonden, dan is volgens bovenstaande formule ook u te berekenen.

Een probleem is wel dat je in het algemeen oneindig veel basisfuncties nodig hebt om de exacte oplossing u te vinden. Het is zaak om de basisfuncties ψ_i zo te kiezen, dat met een beperkt aantal basisfuncties uit die oneindige verzameling al een redelijke benadering van de oplossing kan worden gemaakt. Dat is het geval voor 'wavelets' (letterlijk 'kleine golfjes'). De fout, die gemaakt wordt door maar een beperkt aantal basisfuncties te nemen, hangt af van de grootte van de getallen c_i die horen bij de basisfuncties die niet meegenomen worden. Het liefst zouden we dus de basisfuncties kiezen op volgorde van afnemende c_i. Maar daarvoor zouden we alle (oneindig veel) c_i's eerst moeten uitrekenen, en dat is ondoenlijk.

Bij waveletbases in één dimensie is er een logische volgorde om de basisfuncties te kiezen, namelijk op volgorde van kleiner wordende 'drager' (het gebied waarop ze niet nul zijn). In hoofdstuk 2 wordt een waveletbasis in één dimensie geconstrueerd.

In meer dimensies kunnen basisfuncties gemaakt worden door het product te nemen van wavelets in elke richting (zie figuur 2). Dit zorgt voor langgerekte functies, bijvoorbeeld bij het product van een wavelet met een grote drager in de x-richting en een erg kleine drager in de y-richting. De c_i's die horen bij functies die in alle richtingen kleine dragers hebben, zijn extra klein. Het blijkt dat de oppervlakte van de drager van $\psi_i(x,y)$ bepalend is voor de grootte van

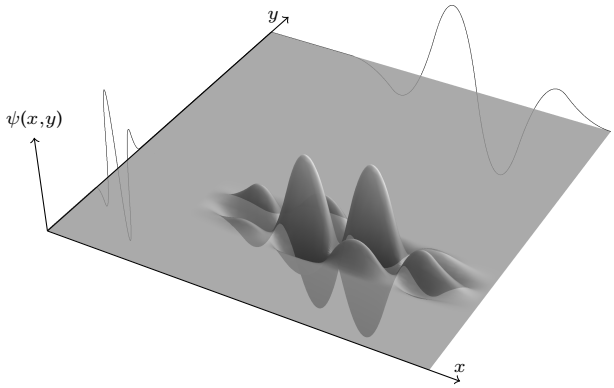

Figuur 2: Een tensorproductwavelet. De drager van de wavelet in de x-richting is groot, en die van de wavelet in de y-richting is klein. Daardoor ontstaat een langgerekte functie.

de coëfficiënt c_i. Als de wavelets in volgorde van afnemende drageroppervlakte worden genomen, blijkt dat de afname van de fout, naar mate er meer wavelets genomen worden, niet meer afhankelijk is van de dimensie. Dit is het idee achter zogenaamde 'sparse grids', die in hoofdstuk 3 worden behandeld. Hiermee is de dimensievloek in principe opgelost.

De voorgaande analyse gaat alleen op als de functie u niet al te grillig is. Als u in een bepaald gebied erg steil is, of rare pieken heeft, werken sparse grids niet meer optimaal. Aan het eind van hoofdstuk 3 toon ik aan dat dit al vrij snel het geval is, en dat de mate van toepasbaarheid van sparse grids dus beperkt is. Voor functies die wel steil zijn, kunnen adaptieve methoden gebruikt worden. In een adaptieve methode worden steeds betere benaderingen van de functie u gemaakt, waarbij steeds meer basisfuncties ψ_i gebruikt worden. Welke basisfuncties er extra genomen moeten worden, wordt bepaald aan de hand van de vorige benadering $\tilde{u}$. Het blijkt dat de adaptieve methode uit hoofdstuk 5 optimaal convergeert, d.w.z. de dimensievloek oplost, voor veel meer functies dan sparse grids. Ik heb dit voor functies tot in tien dimensies numeriek uitgerekend.

In hoofdstuk 6 wordt een waveletbasis geconstrueerd waarmee de genoemde adaptieve methode veel makkelijker wordt.

Waveletmethoden kunnen ook gebruikt worden om stromingsproblemen op te lossen. Bij dit soort problemen heeft de onbekende functie u niet alleen een waarde, maar ook een richting. Voor veel problemen met waterstromingen is het belangrijk dat er geen water ontstaat of verdwijnt. Dit geldt voor de basis in hoofdstuk 4.

Dankwoord

Tijdens de totstandkoming van dit proefschrift ben ik door veel mensen geholpen, die ik hier hartelijk wil bedanken.

Ten eerste ben ik mijn promotor Rob Stevenson veel dank verschuldigd voor zijn begeleiding. Zonder zijn toewijding, geduld en enthousiasme was dit proefschrift er niet geweest. Ik heb veel van hem geleerd en kijk met plezier terug op de prettige samenwerking. Henk van der Vorst bedank ik voor het waarnemen van de rol van promotor namens de Universiteit Utrecht.

Verder dank ik de leden van de leescommissie, Helmut Harbrecht, Tom Koornwinder, Kees Oosterlee en Christoph Schwab, voor de tijd die zij hebben gestoken in het proeflezen van dit proefschrift.

Ik heb tien jaar doorgebracht aan het Mathematisch Instituut van de Universiteit Utrecht. Mede dankzij alle leuke medewerkers is die tijd omgevlogen. Tijdens de beginperiode van mijn aio-tijd werkten verschillende personen in Utrecht aan waveletmethoden. Ik mocht profiteren van de ervaring van Gantumur, Helmut, Mario, Yaroslav en Hoang.

De afgelopen twee jaar heb ik ook regelmatig in Amsterdam gewerkt, omdat Rob Stevenson een hoogleraarspost aan de Universiteit van Amsterdam had geaccepteerd. Ik bedank het Korteweg-de Vries Instituut voor Wiskunde voor zijn gastvrijheid.

Manuel Werner en Thorsten Raasch (Philips-Universität Marburg) leverden gegevens over [Pri06] die ik heb gebruikt voor tabel 2.3 en tabel 2.4. Dit scheelde een hoop programmeerwerk.

En natuurlijk waren er veel leuke collega-aio's, met wie ik veel lol heb gehad, zowel binnen de wiskunde als erbuiten. In het bijzonder wil ik Charlene, Maarten, Arthur, Jeroen, Job, Sander, Vincent, Alex, Rogier, Bas, Arno en Joost noemen.

Mijn kamergenoot Arthur ben ik ook dank verschuldigd voor zijn hulp bij de vele praktische problemen met LaTeX, C++, koffie zetten en dergelijke. En Vincent, ook deeltijdkamergenoot, heeft me met zijn aanstekelijke enthousiasme vaak het leuke van lastige problemen doen inzien.

Verder bedank ik mijn familie en vrienden voor hun belangstelling en enorme geduld. Mijn broers Jaap en Pieter waren zo vriendelijk de rol van paranimf op zich te nemen.

Tot slot: Brenda, dankjewel dat je er bent. Zonder jou was het een stuk minder gezellig geweest.

Curriculum vitae

Tammo Jan Dijkema werd op 4 januari 1981 geboren in het Drentse Oosterhesselen. Hij behaalde in 1999 zijn vwo-diploma aan het Esdal College in Emmen. Aansluitend begon hij aan een bachelorstudie wiskunde aan de Universiteit Utrecht, die hij in 2003 afrondde (met minors Computational Science en Natuurkunde). Hij besloot zijn studie in 2004 met een Master in Scientific Computing. In het kader daarvan heeft hij gewerkt aan een model voor de menselijke bloedsomloop bij reanimatie. Het werk hieraan zette hij, na het behalen van zijn diploma, nog enkele maanden voort in Philadelphia (VS).

In 2005 startte hij zijn promotie aan de Universiteit Utrecht, onder begeleiding van Rob Stevenson, in de vakgroep Numerieke Analyse van Henk van der Vorst. In het kader van deze promotie deed hij onderzoek naar adaptieve waveletmethoden, wat heeft geresulteerd in dit proefschrift.